Alpine River Ecosystem Response to Glacier Retreat

Sarah Catherine Fell

Submitted in accordance with the requirements for the degree of
Doctor of Philosophy

The University of Leeds
School of Geography

June 2019

Declarations

The candidate confirms that the work submitted is her own, except where work which has formed part of jointly authored publications has been included. The contribution of the candidate and the other authors to this work has been explicitly indicated below. The candidate confirms that appropriate credit has been given within the thesis where reference has been made to the work of others.

Chapter Two

The work in Chapter Two has appeared in publication as:

Fell, S. C., Carrivick, J. L. and Brown, L. E. 2017. The multitrophic effects of climate change and glacier retreat in mountain rivers. *BioScience.* **67**(10), pp. 897-911.

Contributions: SCF and LEB jointly developed the concept of this article. SCF synthesised the literature, led the writing, produced the figures and reviewed the manuscript. LEB contributed to the design of the figures and revised the text. JLC conceptualised and created Figure 2.2 and commented upon manuscript drafts.

Chapter Three

The work in Chapter Three has appeared in publication as:

Fell, S. C., Carrivick, J. L., Kelly, M. G., Füreder, L. and Brown, L. E. 2018. Declining glacier cover threatens the biodiversity of alpine river diatom assemblages. *Global Change Biology*. **24**(12), pp. 5828-5840.

Contributions: The concept of this paper was developed by SCF and LEB. Fieldwork was conducted by SCF, LEB and JLC and all laboratory work was performed by SCF. In addition, SCF led the writing and LEB revised the manuscript and contributed to the development of figures. MGK advised upon methodological approaches, assisted in diatom identification, provided reference materials and commented on multiple drafts of the text. LF organised field site access and himself and JLC reviewed the manuscript.

Chapter Four

Although currently unpublished, Chapter Four benefited from advice pertaining to both laboratory methods and data analysis from Eoin O'Gorman of the University of Essex and Guy Woodward of Imperial College London.

Chapter Five

For Chapter Five, components of the fieldwork were conducted by Sophie Cauvy-Fraunié (Ecuador, France) (IRSTEA), Verónica Crespo-Pérez (Ecuador) (Museo de Zoologia, Quito) and Eran Hood (Alaska) (University of Alaska Southeast). Molecular sequencing, qPCR analysis and formatting of the resulting data was performed by Alex Dumbrell, Kate Randall and Kirsty Matthews Nicholass at the University of Essex, with SCF assisting in sample preparation.

For Chapters Three, Four and Five, laboratory analysis of water samples (dissolved carbon and nutrients) was performed by David Ashley at the University of Leeds.

Copyright declaration

Acknowledgements

I am incredibly grateful to many people who have supported me throughout my PhD. Firstly, I would like to thank my supervisors Lee Brown and Jonathan Carrivick. Their enthusiasm, creativity, guidance and humour has been invaluable to me throughout this project, and I am thankful to them for providing me with opportunities that I could only have dreamed of at its beginning.

My PhD was made possible by a Natural Environment Research Council Scholarship (no. NE/L002574/1) as part of the Leeds-York Doctoral Training Partnership. An additional grant was obtained from the International Network for Terrestrial Research and Monitoring in the Arctic under the European Union H2020 (Grant Agreement No. 730938) for fieldwork in Norway. The University of Leeds River Basin Processes and Management Cluster considerately supported laboratory work conducted at the University of Essex.

This thesis has enabled me to collaborate with many experienced and inspiring co-authors and colleagues. For their meticulous field observations, I thank Eran Hood, Sophie Cauvy-Fraunié and Verónica Crespo-Pérez. My molecular laboratory work benefited from the expertise of Alex Dumbrell, Kate Randall and Kirsty Matthews Nicholass. Guy Woodward, Eoin O'Gorman, Kieran Khamis, Kirsty Scott, Leopold Füreder and Scott Tiegs provided advice upon the development of methodological approaches which added great value to my work. Assistance in biota identification was patiently provided by Francois Edwards, Martyn Kelly and Steve Brooks. I also appreciate the time of my Research Support Group, Chris Hassall who gave interesting ideas, and Duncan Quincey who provided reassurance.

For their support in the field I thank my supervisors, Jenna Sutherland, Joseph Bamforth, Joseph Mallalieu and particularly my parents, Neil and Catherine Fell. I am grateful for the assistance of Rüdiger Kaufmann of the Obergurgl Alpine Research Centre and Erika Leslie of the Finse Alpine Research Centre. My field site access was kindly assisted by Leopold Füreder (Austria), the Department of Conservation (New Zealand), Ulvik Fjellstyre, Trond Buttingsrud and Nikolai Friberg (Norway). For their proficiency and assistance in the laboratory I thank Emma Davie, David Ashley, Dave Wilson, Jianguo Qu and Rachel Gasior. I also appreciate the time of my mum, Catherine, who diligently proof-read drafts.

The company of my friends has been of great support throughout my time at Leeds, with particular gratitude to Alice Butler, Annie Connolly, James Bell, Jess Baker, Joseph Mallalieu, Luca Budello, Samuel Eze, Sarah Letsinger and Suad Almanji.

My greatest thanks to my family, for their constant support throughout my PhD and all other aspects of my life. I am forever thankful for my parents Neil and Catherine, my brother Joseph and my husband Ben, alongside my grandparents, who are dearly missed. If I achieve, it will be because of their unconditional love. You are my everything, and I love you all to the moon and back. Finally, I dedicate this thesis to the memory of my granda Joseph Fell, who was the inspiration for it all.

Abstract

Climate change is accelerating glacier retreat across mountain regions globally. Reductions in ice melt inputs are rapidly altering the geomorphology, flow regime and physicochemistry of rivers, modifying their habitats and ecological communities. These changes will influence the biodiversity and ecosystem service provision of alpine rivers. The responses of many taxonomic groups remain undescribed, with implications for freshwater networks and their functions not fully assessed. This thesis used chronosequences of sites representative of reducing catchment glacier cover to investigate the response of alpine river ecosystem structure and functioning to glacier retreat. A new literature-derived conceptual model was developed to synthesise the multitrophic responses of taxonomic groups to declining glacier cover and identify research gaps for this study. Focus was then placed upon benthic diatoms, a less studied group which drive primary production in alpine rivers. Observations in the Austrian Alps provided first evidence of their increased alpha- but reduced beta-diversity as glacier cover was lost. To consider concurrent taxonomic responses, nine new river food webs were constructed using gut contents analysis, for the natural successional gradient imposed by glacier retreat. Significant rewiring of food webs occurred along the chronosequence, with absence of species loss and network collapse indicating robustness to deglaciation. A global-scale field experiment revealed the structure of mountain river ecological communities to be associated significantly with their ecosystem functioning. Ice loss increased the abundance of aquatic fungi and a cellulolytic gene, which were correlated to accelerated decomposition of cellulose, the principal component of riparian vegetation. Findings were used to revise ecological models and propose future research. The identification of clear links between decreasing glacier cover and freshwater biodiversity, food webs and functioning suggests that glacier retreat will drive major alterations in alpine river ecosystems.

Table of Contents

List of Tables

List of Figures

List of Appendices

List of Abbreviations

16S	16S ribosomal RNA sequences
α-diversity	Alpha (local) diversity
β-diversity	Beta (site) diversity
γ- diversity	Gamma (regional) diversity
AASER	Arctic and Alpine Stream Ecosystem Research (Program)
AFDM	Ash free dry mass
AIC	Akaike information criterion
ArcGIS	Aeronautical reconnaissance coverage geographic information system
ASTER	Advanced spaceborne thermal emission and reflection radiometer
B	Basal node
BMNT	Bundesministerium Nachhaltigkeit und Tourismus (Federal Ministry of Sustainability and Tourism - Austria)
BSA	Bovine serum albumin
C	Directed connectance
^{14}C	Radiocarbon
cbhI	Cellobiohydrolase I gene
CELLDEX	CELLulose DEcomposition EXperiment
CEN	Comité Européen de Normalisation (European Committee for Standardisation)
cf.	Compare
Con	Consumer
CPOM	Coarse particulate organic matter
DC	Dissolved carbon
DD	Degree-day
DEM	Digital elevation model
DNA	Deoxyribonucleic acid
DOC	Dissolved organic carbon
EC	Electrical conductivity
EEA	European Environment Agency
F	*F*-test statistic
GAM	Generalised additive model
GAMM	Generalised additive mixed model
GCA	Gut contents analysis
GIS	Geographic information system

GLM	Generalised linear model
GLMM	Generalised linear mixed model
gr.	Group (species-group)
H_x	Hypothesis
I	Intermediate node
IPCC	Intergovernmental Panel on Climate Change
ITS	Internal transcribed spacer (region)
IUCN	International Union for Conservation of Nature
juv.	Juvenile
K	Kelvin
k_B	Boltzmann constant
k_D	Daily cellulose decomposition rate (non-temperature-adjusted)
M	Biomass
max.	Maximum
MCL	Mean chain length
min.	Minimum
N	Abundance (population density)
n	Number (samples/sites/replicates)
NGS	Next-generation sequencing
NMDS	Non-metric multidimensional scaling
NTU	Nephelometric turbidity units
O_x	Objective
OLS	Ordinary least squares
OTU	Operational taxonomic unit
PCR	Polymerase chain reaction
qPCR	Quantitative polymerase chain reaction
Res	Resource
rho	Spearman’s rank correlation coefficient
RNA	Ribonucleic acid
S	Node (species)
SD	Standard deviation
SE	Standard error
SIA	Stable isotope analysis
SNSB	Staatliche Naturwissenschaftliche Sammlungen Bayerns (Bavarian State Scientific Collections)
sp. (spp.)	Species (multiple)

SSC	Suspended sediment concentration
T	Top node
t	*T*-test statistic
Temp	Mean river water temperature (°C)
T_{max}	Maximum river water temperature (°C)
TN	Total nitrogen
TP	Total phosphorous
TS	Tensile strength
USGS	United States Geological Survey
v.	Version
var.	Variety
vs.	Versus
WGS	World geodetic system
WWF	World Wide Fund for Nature

Chapter One: Introduction

1.1 Research context and rationale

Anthropogenically forced climate change is driving unprecedented twenty-first century increases in near-surface temperatures globally (Pepin et al., 2015). This warming is of greatest rate and magnitude in alpine and Arctic regions, which are also experiencing altered patterns of precipitation (Huss, 2012; Gobiet et al., 2014). Consequently, many mountain catchments are characterised by pervasive and accelerating glacier thinning and retreat (Huss et al., 2017; Beniston et al., 2018), with the European Alps predicted to lose up to 89 % of their glacier volume by 2100 (EEA, 2016). Alterations to the rate, timing and volume of ice melt contributions to alpine rivers may modify their geomorphic stability, physicochemistry and temperature dynamics (Milner and Petts, 1994; Milner et al., 2009; Bliss et al., 2014; Huss and Hock, 2018), with significant implications for river habitats and their associated biodiversity (Brown et al., 2007a). This climatic sensitivity, coupled with potential for glacier-fed headwaters to influence community assembly and ecosystem functioning in freshwaters downstream (Milner et al., 2017), makes alpine rivers critically important places to study the influence of climatic change upon ecological systems (Hannah et al., 2007).

Following attainment of peak flow, sustained glacier retreat will reduce ice melt inputs to proglacial mountain rivers, altering the proportional contribution of snowpack melt, precipitation and groundwater flow (Brown et al., 2007a; Huss et al., 2008; Bliss et al., 2014). Each water source has discrete physicochemical and discharge characteristics, with rivers dominated by glacier meltwaters hosting significantly lower mean water temperature, channel stability and electrical conductivity than groundwater-fed reaches but higher suspended sediment concentrations and greater diel and seasonal discharge variability (Milner and Petts, 1994; Milner et al., 2001; Brown et al., 2007b). This abiotic environment influences how macroinvertebrates and microbenthos assemble as communities, many of which support rare, endemic and threatened species (Ilg and Castella, 2006; Falasco and Bona, 2011; Jacobsen et al., 2012). Concurrent biotic influences of predation, competition, parasitism and dispersal may also be important drivers of community succession but remain less studied in alpine rivers (Brown and Milner, 2012; Brown et al., 2018). The heterogeneity of aquatic habitat is thought to be responsible for high biodiversity in mountain river systems yet as glacier retreat modifies water source contributions, it will alter the extent, distribution

and persistence of their associated habitats and ecological interactions (Milner et al., 2017).

While the response of river macroinvertebrate communities to deglaciation is well described (Milner et al., 2001; Jacobsen et al., 2012; Brown et al., 2018), impacts upon freshwater meiofauna and microbenthic species remain less understood. For example, few studies have investigated the sensitivity of benthic diatoms to glacier retreat despite their important functional role as the principal primary producers in alpine river systems (Rott et al., 2006; Gesierich and Rott, 2012). Collating the simultaneous, interactive and cumulative responses of populations across multiple taxonomic groups will improve prediction of whole aquatic ecosystem alterations following glacier retreat (Woodward et al., 2010a). Food web modifications cannot be extrapolated from species responses as emergent properties characterise these complex systems and a network-scale approach is required as individuals will never be impacted by glacier retreat in isolation (Woodward, 2009). In turn, investigation of structural and allometric (size-based) food web responses are critical to understanding the implications of ice loss for river community succession. As high-alpine rivers lie above the treeline, energy availability to their food webs is driven primarily by decomposition of autochthonous resources, with inputs of terrestrial litter typically constrained to wind-blown materials and local inputs of alpine herbs and grasses (Gessner et al., 1998; Zah and Uehlinger, 2001). These detrital sources are composed predominantly of cellulose, the most abundant organic polymer on Earth (Tiegs et al., 2019). There is a critical requirement to consider if and how river microbial assemblages process this material as glaciers retreat, given that its decomposition may account for significant fluxes of carbon into the atmosphere, downstream sediments and through aquatic trophic levels (Aufdenkampe et al., 2011; Singer et al., 2012).

Enhanced understanding of the response of whole alpine river communities and their ecosystem functioning to glacier retreat can identify a wide range of imperilled species, potentially informing alpine freshwater conservation strategies, which rarely consider benthic taxa (Hannah et al., 2007; Khamis et al., 2014a). It also permits broader application as alpine rivers can act as model systems for understanding ecological succession given the range of water sources, morphologies and thermal characteristics of these systems. Due to the strong sensitivity of atmosphere-cryosphere linkages, studies of alpine rivers could provide early warning insights into future alterations of running water ecosystems at lower-altitude and -latitude (Woodward et al., 2010a;

Beniston et al., 2018). This approach could facilitate global-scale understanding of aquatic responses to a changing climate, a recent focus of multi-regional studies investigating the geographic variability of alpine watershed processes (Jacobsen et al., 2012; Brown et al., 2018). This is critical given that the global rate of species loss in freshwaters exceeds that of all other habitat types (WWF, 2018). As much of the current understanding of river ecosystem structure and functioning, particularly regarding implications for food webs and decomposition rates, has predominantly been developed in temperate freshwaters, this thesis tests the generality of this knowledge and associated concepts to determine its application in comparatively extreme alpine environments.

1.2 Aim, objectives and research approach

This thesis aimed to determine how the structure and functioning of alpine river ecosystems respond to the alterations in catchment glacier cover induced by glacier retreat. This research focus was underpinned by four principal objectives: (O_1) to develop, test and refine a conceptual model to describe the influence of reducing catchment glacier cover upon alpine freshwater biota spanning multiple trophic groups; (O_2) to quantify the response of alpine benthic diatom assemblage biodiversity to a gradient of declining glacier cover in the European Alps; (O_3) to investigate alterations to the structure and allometry of alpine river food webs along a glacier cover gradient in the European Alps, and (O_4) to determine how cellulose decomposition rates and river microbial communities vary along chronosequences of catchment glacier cover across multiple mountain regions globally. O_2 to O_4 were investigated in the Hohe Tauern region of the central Austrian Alps, selected as its closely located alpine catchments hosted a broad spectrum of permanent ice cover and minimal anthropogenic influence, while reducing variability in meteorological and geological characteristics (Robson et al., 2016). These criteria were also employed to select sites in five additional glacierised mountain regions to address O_4.

Glacier retreat was characterised throughout this thesis in a space-for-time manner using chronosequences of quantified catchment glacier cover (Pickett, 1989). This approach was selected in preference to methods which represent glacier influence through qualitative water source categories (e.g., kryal, rhithral, krenal) (Hieber et al., 2001; Rott et al., 2006) or sampling site distance from glacier margins (Milner and Petts, 1994; Gesierich and Rott, 2012), as they do not capture the spectrum of intermediate glacier retreat stages and can be disrupted by spatial (lakes, tributaries,

aquifer upwelling) and temporal (diurnal flood peaks, storm events) discontinuities (Milner et al., 2001; Huss et al., 2008). Unlike other quantitative proxies of glacier influence, including a multivariate glaciality index (Ilg and Castella, 2006), discharge wavelet patterns (Cauvy-Fraunié et al., 2014) and water source chemistry analysis (Brown et al., 2009a), this gradient of catchment glacier cover could be determined remotely through spatial analysis (ArcGIS). This enabled site selection prior to fieldwork, which was vital given the remote positioning of study locations. Previous research has shown that chronosequences representative of reducing glacier influence capture the alterations to river communities noted in response to real-time glacier retreat (Jacobsen et al., 2012; Brown et al., 2018).

1.3 Research originality

This thesis hosted theoretical novelty through its development of a conceptual model which synthesised published literature and original data to inform predictions of multiple alpine river taxonomic group responses to reducing catchment glacier cover. It provided novelty in research approach as few published studies have used fully quantified chronosequences to represent glacier retreat, when investigating biotic community responses (Rott et al., 2006; Brown et al., 2007a; Wilhelm et al., 2013; Ren et al., 2017a). While the specific research methods are well established, the originality of this research lay in their application in alpine catchments and along gradients of glacier cover. No previous research has investigated alterations to benthic diatom community assemblages, food web structure or cellulose decomposition along quantified spectrums of reducing catchment glacier cover. To date, only three studies have constructed gut contents analysis derived food webs in glacial streams and only at sites with high ice or snow melt inputs (Lavandier and Décamps, 1983; Clitherow et al., 2013; Parker and Huryn, 2013). Cellulose decomposition rates have not previously been identified in glacier-fed mountain rivers, despite its potential ecological relevance in comparison to traditional leaf based approaches, at sites above the treeline (Zah and Uehlinger, 2001). Originality and significance of the research undertaken was validated by publication of work for Chapter Two in *BioScience* (Fell et al., 2017) and Chapter Three in *Global Change Biology* (Fell et al., 2018).

1.4 Thesis synopsis

Through literature synthesis, this thesis developed a conceptual model of alpine river biota responses to reducing catchment glacier cover (Chapter Two). Data were then collated through spatial analysis (ArcGIS), fieldwork and laboratory investigations to

test these model predictions and investigate alterations to river ecosystem structure and functioning, in response to glacier retreat (Chapter Three, Four, Five). Findings were used to refine the initial theoretical conceptions and in turn, develop understanding of the ecological response of alpine river systems to a shrinking cryosphere (Chapter Six). To holistically investigate these responses, observations were conducted across a range of geographical scales, from singular (Chapter Three, Four) to multiple (Chapter Five) glacierised regions and simultaneously across a range of biological scales, from genes (Chapter Five), to individual populations (Chapter Three), to whole community networks (Chapter Four) and finally the ecosystem functioning of these communities (Chapter Five). Thesis structure is displayed in Figure 1.1 and methodological approaches taken to investigate different biological scales displayed in Figure 1.2.

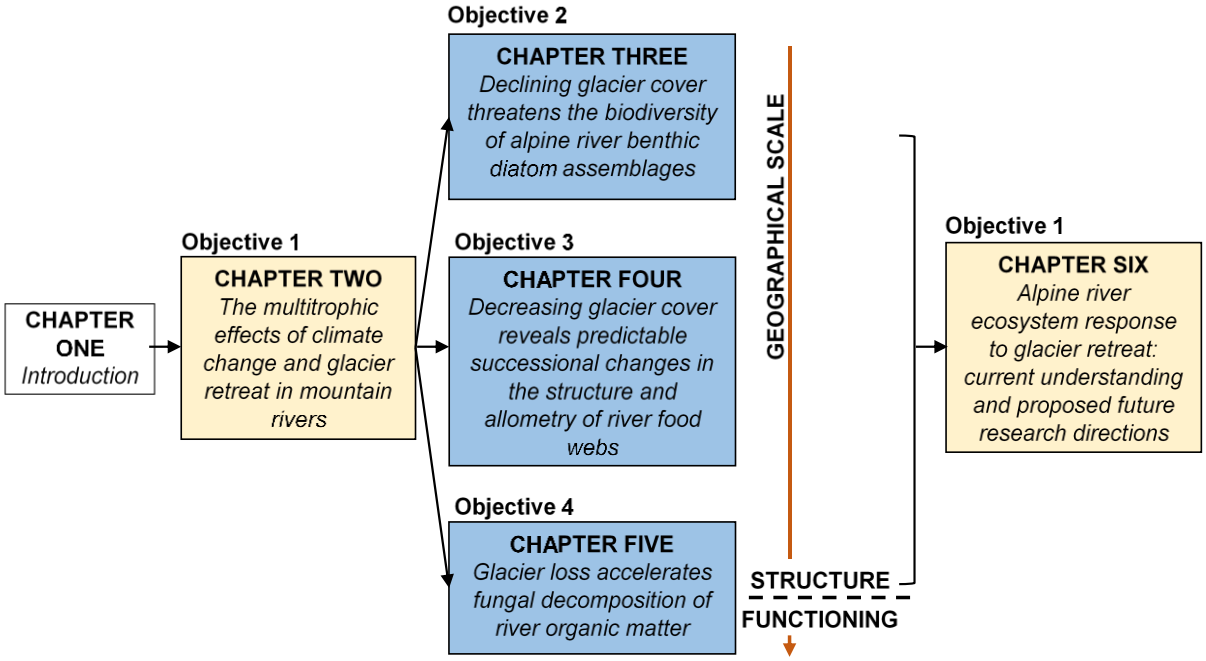

Figure 1.1 Schematic representation of thesis structure. Box colour reflected the predominant focus of each chapter as theoretical (yellow) or observational (blue).

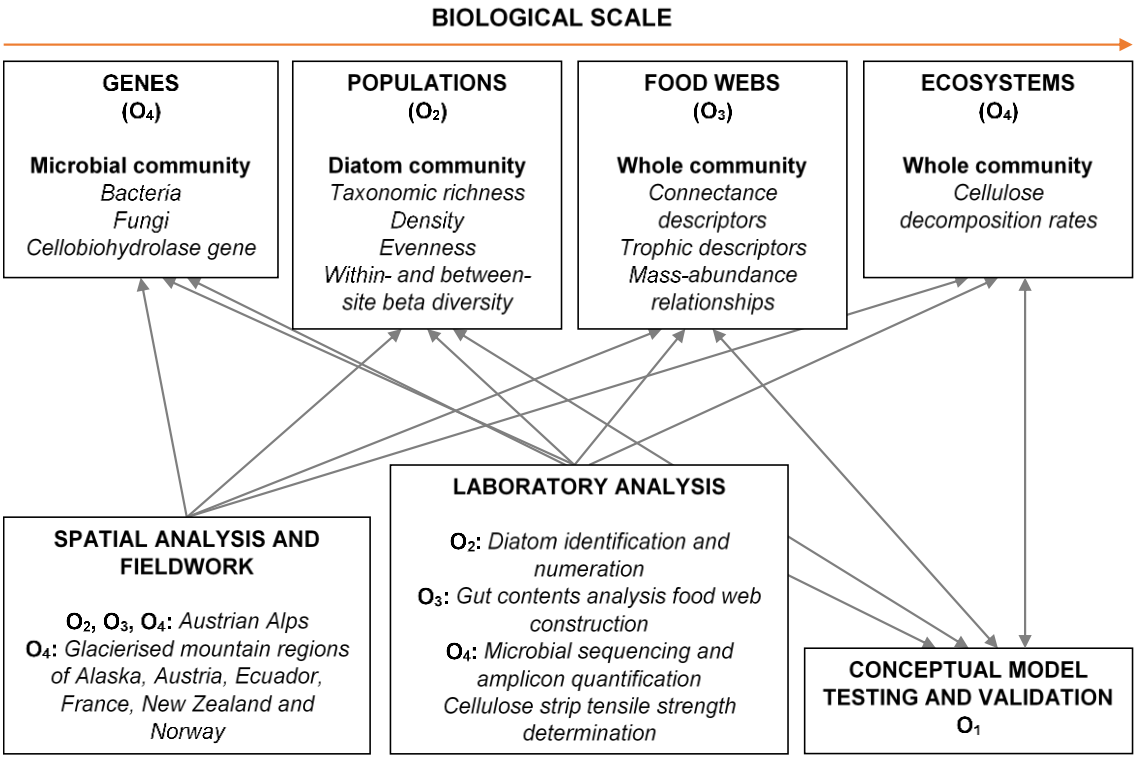

Figure 1.2 Methodological approaches adopted to investigate different levels of biological organisation with regard to alpine river biotic communities. O = research objective.

Chapter Two synthesised current understanding of climate-hydrology-ecology interactions in mountain rivers, providing a rationale for research focus upon river ecosystems in deglaciating catchments. New conceptualisations of how reducing catchment glacier cover influences alpine stream biota were presented for multiple taxonomic groups. Chapter Three provided a population-scale investigation of benthic diatom assemblage responses to reducing catchment glacier cover before Chapter Four identified alterations to the structure and allometry of food webs along this gradient. Chapter Five investigated decomposition rates of cellulose in mountain rivers and documented, through genetic analysis, the microbial community associated with this process across six glacierised regions. The final chapter collated key findings from previous chapters and described revision of the original conceptual model. Applications of this thesis to research and conservation were considered before limitations and recommendations for future research directions were discussed.

Chapter Two: The multitrophic effects of climate change and glacier retreat in mountain rivers

2.1 Introduction

The sustained dependency of human society on hydrocarbons is predicted to increase global near-surface temperatures, particularly across the second half of the twenty-first century (IPCC, 2013). Warming will be most pervasive in high-altitude (alpine) and -latitude (Arctic) regions and will be coupled with changing precipitation patterns (Gobiet et al., 2014). Significant climatic changes are already occurring in these environments, reducing the distribution, thickness and permanency of ice sheets and driving the thinning and retreat of many mountain glaciers (Zemp et al., 2015). Continued retreat will alter the proportional contribution of ice melt, snow melt and groundwater to proglacial mountain river systems (Brown et al., 2007a). Each of these water sources has a unique physicochemical signature and flow regime, which influences the assembly of river communities (Milner et al., 2009). Glacier retreat and loss will therefore alter the mosaic of aquatic habitats across glacier floodplains, threatening multiple endemic and rare species that often exist at their tolerance limits (Wrona et al., 2006; Brown et al., 2009b; Jacobsen et al., 2012; Giersch et al., 2016). Wider alterations to the persistence, density and distribution of species will combine to drive major biological reorganisation of mountain river ecosystems (Brown and Milner, 2012; Jacobsen et al., 2012).

Most ecological research in proglacial river systems has focused predominantly on populations or communities of specific taxonomic groups, particularly macroinvertebrates (Figure 2.1). To move forward understanding of how climate change and glacier retreat are reshaping whole aquatic ecosystems, there is a need to develop an integrated understanding spanning multiple taxonomic groups and trophic levels in glacier-fed rivers (e.g., bacteria, protists, fungi, algae, diatoms, invertebrates, mammals, amphibians and fish; Clitherow et al., 2013). Individual to population-level responses cannot always be extrapolated easily to predict links at a network-level, given that emergent properties are characteristic of complex systems (Woodward et al., 2010a). One means of integrating the interactions among species that are responding in unison to environmental change is within the context of food web ecology.

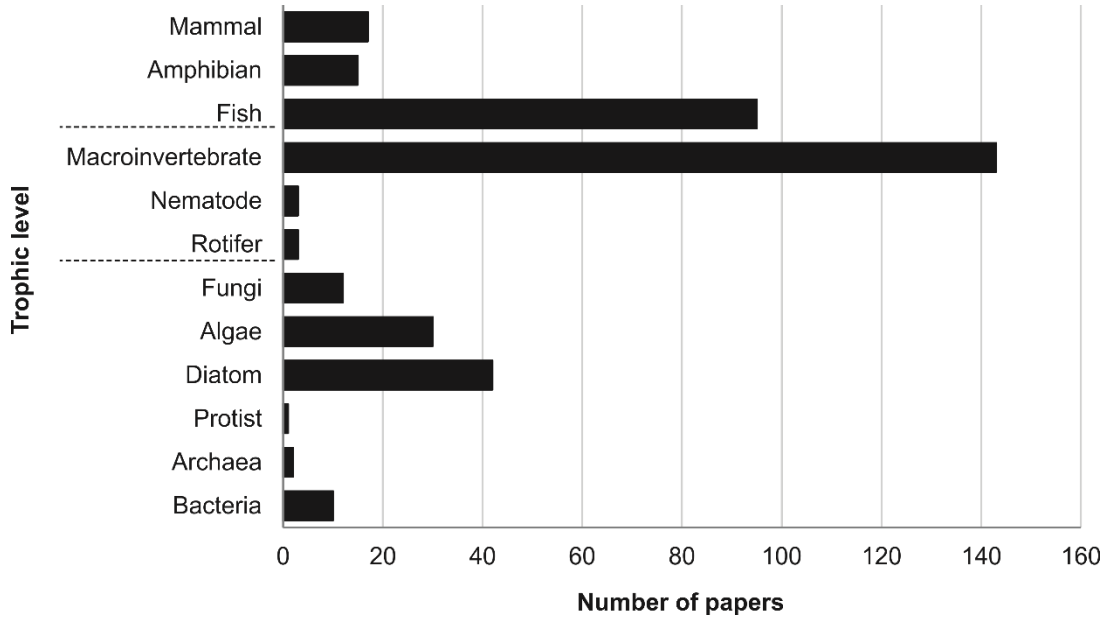

Figure 2.1 A summary of published literature regarding alpine stream taxonomic groups and food webs in glacier-fed rivers from 1976 to 2017. Data were extracted from the Web of Science (3 March 2017) and based on the following search criteria and mixtures thereof: taxa, alpine, river, stream, food web and glacier. These search combinations identified research within glacier-fed rivers, even if they were not identified as such within publication titles.

This chapter provided an overview of global-scale patterns of glacier retreat and effects on mountain river hydrological and physicochemical environments. It then synthesised the existing knowledge of how different groups of freshwater taxa (biofilm, invertebrates and vertebrates) respond to glacier retreat, predominantly with a Northern Hemisphere focus because this is where most of the relevant research has been undertaken. This knowledge was then integrated within a new conceptual framework that considered simultaneous responses of biota to shrinking glaciers as part of multitrophic river ecosystems. This new multitaxonomic response framework was used subsequently to explore the consequences for how whole river food webs can be expected to respond to ongoing glacier retreat. Such an approach is required to inform alpine conservation strategies by providing a holistic food web context for the multiple cold environment endemic species that are found in glacier-fed rivers around the world (e.g., Brown et al., 2009b; Giersch et al., 2016). These often rare species are potentially sensitive and vulnerable to climate change and their successful conservation will require detailed consideration of their links within river assemblages. As glacier-fed river systems will respond rapidly to climate change, any reassembly of food webs could help to identify structural and functional changes that could be monitored in running waters across other biogeographical regions (Woodward et al., 2010a).

2.2 Climate change induced glacier retreat in the twenty-first century

Arctic and alpine zones are experiencing pervasive increases in near-surface temperatures and altered patterns of precipitation (Gobiet et al., 2014), leading to the thinning and retreat of many glaciers (IPCC, 2013). The magnitude of these changes is amplified within alpine regions as decreases in snow accumulation, earlier spring melt and prolonged summer ice melt are altering surface albedo and lengthening the melt season. This increases energy absorption and sustains negative glacier mass balances (Gobiet et al., 2014). These positive feedback mechanisms are accelerating alpine glacier shrinkage in many regions (Figure 2.2; Zemp et al., 2015). For large glaciers and ice sheets, such as those in parts of Iceland and Greenland, this ice melt will initially increase river discharge, scouring and exposing new channels as their margins recede. Smaller glaciers will see consistent reductions in runoff and eventually complete loss (Gobiet et al., 2014).

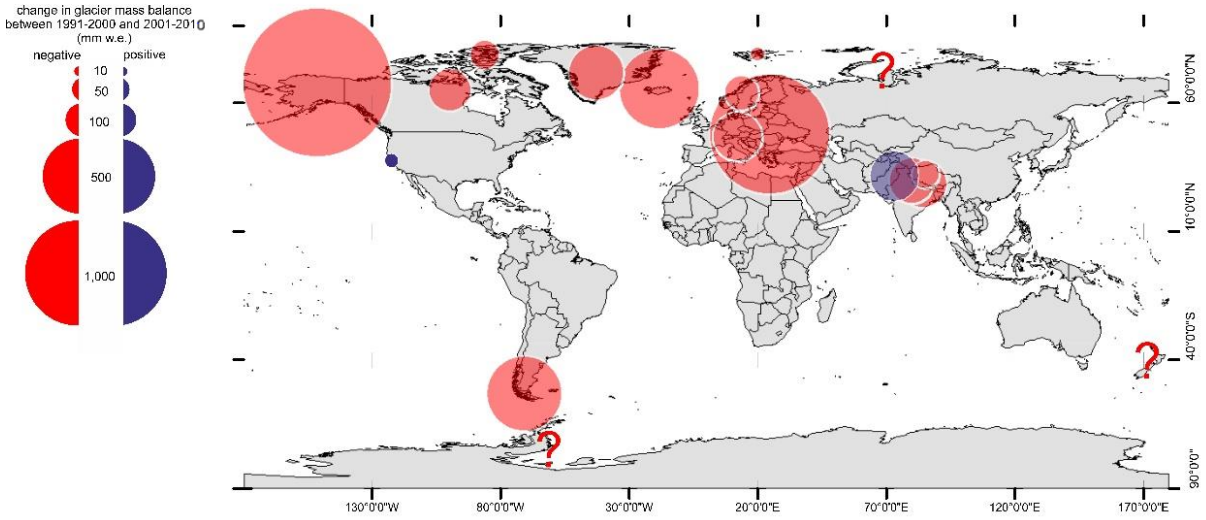

Figure 2.2 Global glacier mass balance alterations (1991 to 2000 and 2001 to 2010), adapted from Zemp et al. (2015). The question marks represent the absence of comparable data sets.

2.3 Hydrology and physicochemistry of mountain rivers in a changing climate

In addition to glacier ice melt, mountain rivers are supplied by runoff from snowpack ablation and groundwater. As described by Brown et al. (2003), these water sources have distinct physicochemical compositions and discharge patterns. River reaches dominated by ice melt have significantly lower mean water temperatures, electrical conductivity and channel stability and higher suspended sediment concentrations and greater discharge fluctuations than groundwater reaches (Figure 2.3). Ice melt inputs

reduce and groundwater influence increases with downstream distance from glacier margins, reflecting reducing catchment glacier cover (Brown et al., 2003). Temporal variability within water source contributions is sustained by diel and seasonal ice melt cycles, interannual alteration to snowpack accumulation and intense storm events (Milner et al., 2009; Cauvy-Fraunié et al., 2013).

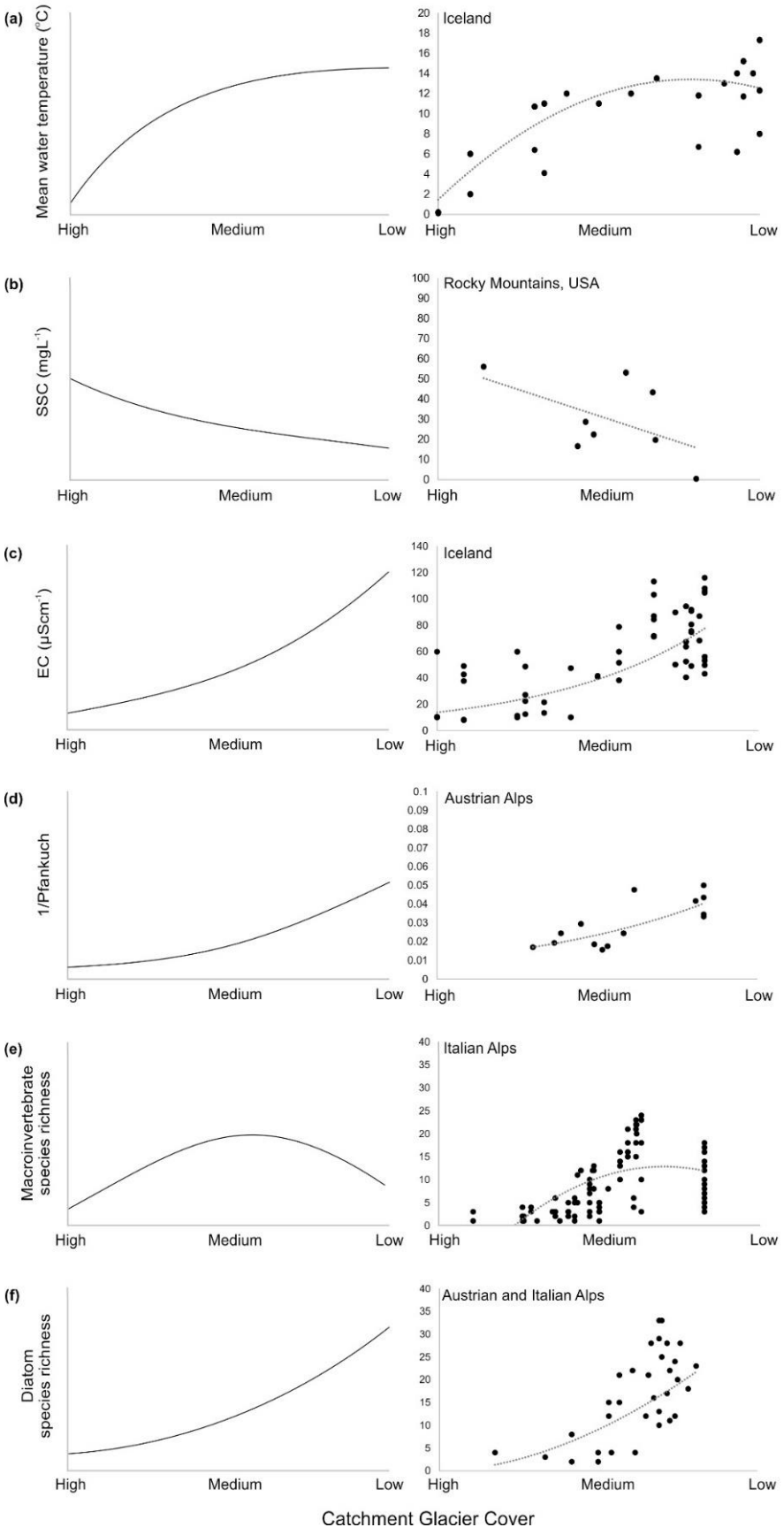

Figure 2.3 Theoretical predictions (left) and empirical data (right) for physicochemical parameter responses to reducing catchment glacier cover across the Northern Hemisphere.

Data adapted from (a) Gíslason et al. (2001), (b) Thompson et al. (2013), (c) Gíslason et al. (2001), (d) Khamis et al. (2016), (e) Maiolini and Lencioni, (2001) and (f) Rott et al. (2006).

Mountain catchments are particularly vulnerable to climate change because glacier runoff significantly influences the source, rate and timing of water directed to river networks (Brown et al., 2003; Jansson et al., 2003). Subsequently, prolonged glacier retreat will add further spatiotemporal variability to water source patterns. Reducing ice melt inputs will increase the proportional contribution of snow melt, rain and groundwater (Brown et al., 2003), completely reworking the mosaic of channel environments present in glacier-fed river floodplains (Malard et al., 2006; Brown et al., 2015) and inducing significant reorganisation of river biotic communities.

2.4 Biotic responses to glacier retreat

Mountain river ecosystems host a range of taxa, which play varied trophic roles. Primary producers include bacteria, soft-bodied algae and diatoms, whereas other bacteria, fungi and protists play important roles as microbial decomposers and consumers of particulate and dissolved organic matter (Battin et al., 2016). Benthic rotifers feed on primary producers (bacteria and algae) and detritus alongside protozoans (Schmid-Araya and Schmid, 2000). Free-living nematodes also consume these groups, with some species predating rotifers and other meiofauna (Schmid-Araya and Schmid, 2000). Multiple trophic roles are also spanned by macroinvertebrates, with grazers and scrapers feeding on biofilm species, detritivorous shredders, collectors and filter feeders consuming dead organic matter and predators selecting adult and larval invertebrates (Woodward, 2009). Fish, primarily salmonids, are often the top predators of glacier-fed river systems and although diet is species, life stage and region specific, components include smaller fish, macroinvertebrates and freshwater zooplankton (Sinnatamby et al., 2012). Some fish species also feed on the eggs of amphibians, which can be insectivorous or predatory (Arntzen et al., 2009; Kuzmin et al., 2009). Where present, semi-aquatic mammals such as desman species (Talpidae) predate many trophic levels with diets spanning macrophytes, insects, fish and amphibians (Biffi et al., 2016).

Aquatic taxa within mountain rivers will respond simultaneously to water source alterations imposed by glacier retreat (Brown and Milner, 2012; Eisendle-Flöckner et al., 2013; Battin et al., 2016). It is important to review contemporary knowledge of these responses before attempting to understand holistically the reshaping of glacier-fed river

ecosystems during deglaciation. Disparate literature considering biofilm, invertebrates and vertebrates was collated here because despite a recent proliferation of studies considering trophic groups of alpine river ecosystems, they are rarely considered collectively. Particular focus was given to less studied groups that contribute to community response and encompass a broad range of endemism, rarity and vulnerability to climate change.

2.4.1 Bacteria and Archaea

Genetically diverse bacterial communities persist within alpine rivers, with Cyanobacteria (*Homeothrix, Clastidium*) dominating biofilm formation (Kawecka et al., 1971; Battin et al., 2001; Rott et al., 2006). Glacially influenced rivers support *Bacteroidetes, Proteobacteria, Actinobacteria* and *Nitrospira*, with species that adhere to subglacial ice surfaces contributing to river community composition following spring basal floods (Battin et al., 2001; Wilhelm et al., 2013). Archaea also inhabit glacier ice, entering stream biofilm communities during intensive melting events and reducing in density with increasing distance from the glacier terminus (Battin et al., 2001). Although reducing glacier influence increases bacterial biomass, Wilhelm et al. (2013) noted reductions in bacterial α- and β-diversity as cold stenothermic species were replaced by generalist taxa (Freimann et al., 2013). However, this remains contested given that Battin et al. (2016) found α-diversity to increase as ice melt exposed rock and soil habitats, which provided a greater diversity of microbe sources.

Glacial rivers are dominated by bacterial specialists, with groundwater species expressing greater metabolic redundancy and environmental plasticity (Freimann et al., 2013; Battin et al., 2016). This gradient of specialisation is correlated with suspended sediment concentration and highly glacial sites host taxa adapted to reduced light penetration and greater abrasion (Peter and Sommaruga, 2016). Glacier margin habitats are also susceptible to spring melt flood pulses, which constrain bacterial cell density through scouring, sheer stress and fine sediment abrasion of biofilm architecture (Blenkinsopp and Lock, 1994). Reducing glacier influence may diminish this habitat heterogeneity, favouring a more generalist bacterial community (Freimann et al., 2013). Response to catchment-scale variability in electrical conductivity and pH can further influence local species dominance (Wilhelm et al., 2013; Battin et al., 2016).

2.4.2 Fungi

Aquatic hyphomycetes dominate alpine river fungal communities and are the principal microbial decomposers of allochthonous organic matter inputs (Gessner and Robinson, 2003). Specialist species are relatively unconstrained by cold temperatures and high suspended sediment concentrations, with fungal biomass, taxonomic richness, sporulation rate and diversity at glacial sites reduced but comparable to those of temperate rivers (Gessner and Robinson, 2003). Decomposition rates were reduced 20 to 60 % at temperatures approaching zero degrees Celsius, but it has been argued that this stemmed from a limited supply of organic matter rather than from physicochemical constraints on metabolism (Robinson et al., 1998). Reduced glacier influence may alter species dominance within fungal communities favouring those adapted to warmer waters, although this response will be mediated by local factors including nutrient supply and disturbance regime (Battin et al., 2016).

2.4.3 Protists

The influence of glacier retreat on protists remains poorly understood (Rott et al., 2006; Battin et al., 2016). Eisendle-Flöckner et al. (2013) found a 35 % reduction in catchment ice coverage in the Austrian Alps to double algal (minus diatom) abundance and increase protist abundance threefold, suggesting a stronger relationship with deglaciation than for other biofilm taxa. However, the absence of species-level identification and comparative studies hinders a more detailed analysis of this response. Low protist abundance where glacier influence is high may result from predation by meiofaunal invertebrates (Hakenkamp and Morin, 2000), which can remain relatively abundant within cold conditions. Some protists (e.g., larger amoeba) can reach sizes that justify classification as meiofauna, and their preferential grazing of benthic bacteria and algae (Hakenkamp and Morin, 2000) may limit the density of these taxa at less glacial sites.

2.4.4 Soft-bodied algae

Filamentous algae, particularly *Hydrurus foetidus*, dominates high-altitude river biofilm (Kawecka et al., 1971; Hieber et al., 2001). Although extensive catchment glaciation dramatically reduces algal species richness, density and diversity, cold stenotherms adapt to variability in flow and nutrient pulses through alterations to cell physiology, life-cycle length and preferential use of stable microhabitats (Kawecka et al., 1971; Rott et al., 2006). Sessile algae are influenced by seasonal variability in light availability, disturbance and temperature (Kawecka et al., 1971). Hieber et al. (2001) described the

resulting proliferation of algal growth and chlorophyll production during spring and autumn: times of reduced suspended sediment concentrations, increased solar radiation and nutrient influx from snowpack melt. These blooms overlay a general increase in algal biomass with reducing glacier influence, a trend driven in part by groundwater blooms extending through summer (Lavandier and Décamps, 1983; Rott et al., 2006). Glacial river algae contribute significantly to the Red Lists of threatened algae across Europe (Ludwig and Schnittler, 1996; Gesierich and Rott, 2012).

2.4.5 Diatoms

Unlike other algae, diatom species richness remains high until within very close proximity to glacier margins and they form the principal food source of cold-adapted macroinvertebrates (Rott et al., 2006; Clitherow et al., 2013). As was shown by Gesierich and Rott (2012), *Hannaea arcus*, *Achnanthes* spp., *Odontidium* spp. and *Fragilaria* spp. consistently dominate glacial sites across Europe, North America and the Himalaya (Hieber et al., 2001; Antoniades and Douglas, 2002; Rott et al., 2006). These pioneer species are small and non-mobile and resist abrasion in turbid glacial rivers through strong adhesion to substrates at the benthic interface (Hieber et al., 2001; Gesierich and Rott, 2012). Antoniades and Douglas (2002) identified the specialist adaptions of *H. arcus* to cold waters and subsequent intolerance of groundwater. In contrast, species including *Odontidium mesodon* demonstrate greater environmental plasticity, occurring within subalpine and lower-altitude rivers. Total diatom biomass increases as ice melt inputs are reduced, but this proliferation may be constrained by herbivory, because grazing macroinvertebrates are more abundant within warmer, more stable rivers (Milner et al., 2009). The strong attachment capability of small epilithic diatoms may limit their consumption at glacial sites, increasing densities relative to other biofilm taxa (Gesierich and Rott, 2012).

2.4.6 Invertebrates

Although understanding of microinvertebrates (e.g., nematodes and rotifers) remains limited in comparison with that of macroinvertebrates (Thorp and Rogers, 2011), Eisendle-Flöckner et al. (2013) studied these groups in detail across the Möll catchment, Austrian Alps, where they dominated the invertebrate community. Taxonomic richness increased with decreasing glacier influence, but density and abundance did not do so consistently, showing limited seasonal variability. This relationship requires further investigation, but elevated biomass despite harsh environmental conditions may be explained by the resilience traits of these pioneer

taxa (Eisendle-Flöckner et al., 2013; Robertson et al., 2015). At highly glacial sites, nematodes were more diverse but less abundant than rotifers, and their maturity was constrained, suggesting a strong negative relationship with glacial influence (Eisendle-Flöckner et al., 2013). Despite this, some meiofauna may be resilient to the high flows associated with large glaciers yet to reach peak retreat rates, because although Robertson et al. (2015) identified meiofaunal taxonomic abundance and richness to decline following an extreme rainfall event, they returned to preflood values for some rivers within two years. Protozoan responses to glacier retreat should be coupled with meiofaunal responses, because they feed on rotifers and are consumed by nematodes and microinvertebrates (Schmid-Araya and Schmid, 2000).

The relationship between alpine water sources and the macroinvertebrate component of river communities is well documented (Milner and Petts, 1994; Castella et al., 2001; Jacobsen et al., 2012; Cauvy-Fraunié et al., 2015). Strong responses of macroinvertebrate α- and β-diversity to glacier retreat have been linked to changes in water temperature and channel stability in many studies (Milner et al., 2001; Brown et al., 2007a; Finn et al., 2013). Milner and Petts (1994) and then Milner et al. (2001) developed a conceptual model to include water temperature and channel stability as critical drivers of macroinvertebrate assembly in glacially influenced rivers (Figure 2.4). This illustrated the reorganisation of macroinvertebrate communities in response to reducing glacial influence (Milner and Petts, 1994), embodying the individualistic concept (Gleason, 1926), by attributing ecological communities to particular positions along natural gradients in response to their tolerances.

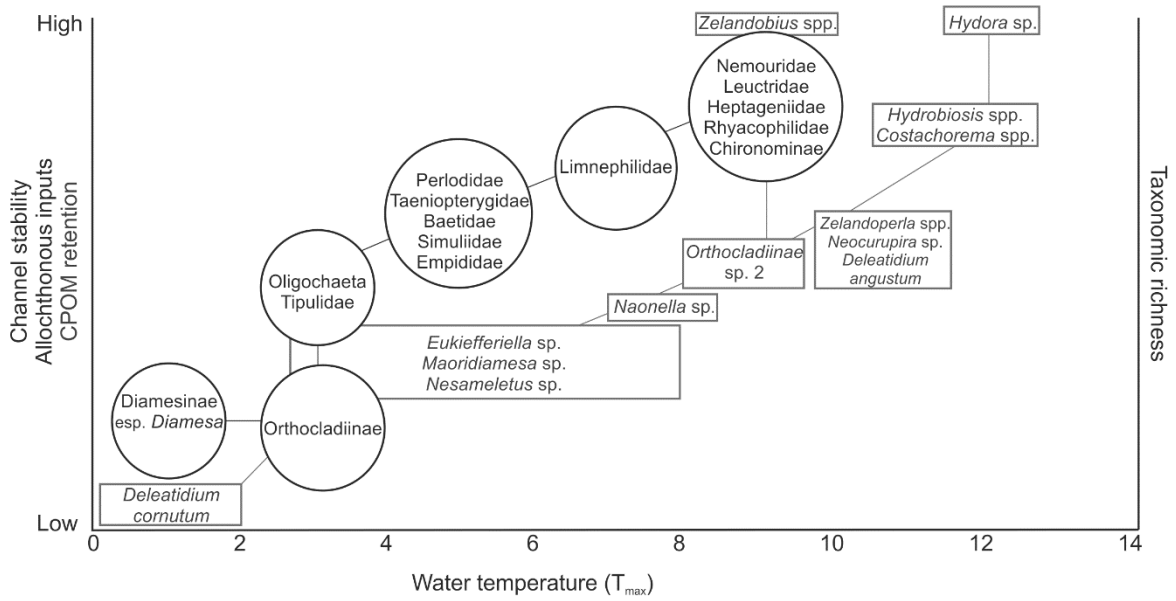

Figure 2.4 A composite figure based on the conceptual models of Milner et al. (2001) (black text, circles) and Cadbury et al. (2011) (grey text, squares) to illustrate the influence of water temperature and channel stability on macroinvertebrate community composition in Northern and Southern Hemisphere (New Zealand) sites respectively.

Milner et al.'s (2001) revised model used information from the Arctic and Alpine Stream Ecosystem Research Program (AASER; Figure 2.4). This conceptual synthesis incorporated information from a large number of European study sites and accounted for serial discontinuities by removing reliance on previous assumptions that confined low water temperature and channel stability to close glacial proximity (Milner et al., 2001; Milner, 2016). Jacobsen et al. (2014) also identified temporal shifts in the distribution of glacier influence, with diurnal flood pulses altering downstream physicochemistry gradients and leading to the subsequent reorganisation of macroinvertebrate communities. Figure 2.4 highlights the first occurrence of *Diamesa* in highly glacial sites and an increase in other macroinvertebrate groups, and therefore taxonomic richness, density and biomass, with reducing glacier influence. Castella et al. (2001) demonstrated the pervasiveness of this pattern across Europe, identifying links between macroinvertebrate community structure, substrate stability and water temperature in glacial rivers within five biogeographical regions across the Northern Hemisphere. Cadbury et al. (2011) later refined this model for Southern Hemisphere species, using data collected in alpine New Zealand (Figure 2.4). Despite increases in macroinvertebrate richness and biomass, glacier retreat is reducing the β- and γ-diversity of alpine rivers globally (Brown et al., 2007a; Jacobsen et al., 2012; Finn et al., 2013). This is driven by the extirpation of cold stenothermic

species dependent on the physicochemical environment provided by ice melt inputs (Giersch et al., 2016). This conceptual model has proven very successful in explaining macroinvertebrate community structure patterns in many glacier-fed river environments (Milner, 2016). It therefore has significant potential for being developed more widely to incorporate other taxonomic groups, something that to date has not been attempted.

2.4.7 Mammals

Although few semi-aquatic mammals inhabit alpine rivers, isolated species of Talpidae (desman) and Soricinae (water shrew) are found in localised populations (Queiroz et al., 1996; Hutterer et al., 2016). The Iberian desman (*Galemys pyrenaicus*) shelter within the riparian vegetation and rocky banks of glacier-fed rivers, across the Pyrenean Region (Biffi et al., 2016). This species is indicative of low mean water temperatures and preferentially feeds within rapid, highly oxygenated riffles (Biffi et al., 2016). Their range is dictated by the presence of prey (Trichoptera, Plecoptera, Ephemeroptera) and the absence of predators, including American mink (*Neovison vison*; Biffi et al., 2016). The semi-aquatic Eurasian water shrew (*Neomys fodiens*) mirrors the dependency of the Iberian desman for cold running waters, hunting insects, crustaceans, frogs and fish below 2500 m altitude (Hutterer et al., 2016). In contrast, the larger Russian desman (*Desmana moschata*) inhabits slow flowing rivers and lakes of forested alpine floodplains (Ponomarev et al., 2015). Distributed across Russia, Belarus, Ukraine and Kazakhstan, this species feeds omnivorously on macroinvertebrates, amphibians, fish and plant detritus (Queiroz et al., 1996; Ponomarev et al., 2015). Both desman species are IUCN Red List vulnerable species, and reducing glacier influence may particularly threaten the Iberian desman (*G. pyrenaicus*), which is more heavily dependent on diminishing ice melt reaches (Biffi et al., 2016).

2.4.8 Amphibians

Salamandridae encompasses a number of amphibious species that rely on European mountain rivers. The common fire salamander (*Salamandra salamandra*) and alpine newt (*Ichthyosaura alpestris*) favour zones of reduced glacier influence, including alpine woodland rivers below 2500 m (Kuzmin et al., 2009; Arntzen et al., 2009). In contrast, the Pyrenean brook newt (*Calotriton asper*) requires fast flowing, highly oxygenated, cobbled river reaches for larval development (Comas and Ribas, 2015). The common frog (*Rana temporaria*) persists within mountain woodlands and meadows below 2300 m, using rivers and lakes for larval development and

overwintering in open water to avoid freezing conditions (Ludwig et al., 2015). Glacier retreat may alter the behaviour of these species (e.g., abandonment of freeze-avoidance strategies) but not their persistence, because they also inhabit many non-glacierised mountain catchments (Ludwig et al., 2015). Glacier retreat therefore has the potential to create much more suitable river environments, aiding the spread of these large bodied aquatic predators.

2.4.9 Fish

Fish are often absent from highly glacial rivers, in which low water temperature constrains growth rates or fails to meet the optima required for particular life-cycle stages (Fleming, 2005). Waterfalls and steep channel gradients may also limit their dispersal within mountain rivers. For many species, spawning is constrained in braided channel systems because of high suspended sediment concentrations and an absence of stable pool environments (Milner et al., 2009). Despite this, large glacier-fed river systems in Alaska and the Rocky Mountains are able to support salmonid populations, because ice melt increases summer flow rates relative to clear water tributaries, facilitating upstream migration and elevating nutrient and oxygen availability (Dorava and Milner, 2000). These systems also host slow flowing side channels and pools suitable for rearing and juvenile overwintering, where high suspended sediment conditions provide cover from aerial predators (Milner et al., 2011). Arctic charr (*Salvelinus alpinus*) have also colonised low velocity proximal glacial streams in Arctic Canada and Norway, particularly where they are warmed by upstream glacial lakes (Witkowski et al., 2008; Sinnatamby et al., 2012).

A reduction of glacier ice melt could limit channel discharge, restricting salmonid migration and disconnecting channel marginal habitats. However, flow compensation from snow melt and groundwater sources could maintain high, less turbid discharge, aiding migration and spawning (Fleming, 2005; Milner et al., 2009). Reducing glacier influence and subsequent increases in mean water temperatures may facilitate upstream dispersal of fish species as they track expansion of their thermal optima (Hari et al., 2005). Milner et al. (2011) found salmonids were able to rapidly recolonise proglacial channels within ten years of their exposure from ice cover. This dispersal may be limited by anthropogenic barriers, including hydroelectric dams (Hari et al., 2005). Biological constraints include the comparatively reduced oxygen concentrations of warmer waters, novel predation pressures as communities reassemble and the potential increase of temperature dependent disease (Hari et

al., 2005). Periods of high velocity flow following intense ice melt periods could act as physical barriers to fish dispersal within alpine streams (Sinnatamby et al., 2012).

2.5 Synthesising freshwater ecosystem responses to glacier retreat

Changes to alpine river water sourcing driven by glacier retreat will clearly influence the processes of mountain river ecosystem assembly for all trophic groups (Ilg and Castella, 2006; Brown and Milner, 2012). The discrete physicochemical and flow regime characteristics of ice melt, snowpack melt and groundwater act as strong abiotic filters in proglacial rivers, enabling only species with traits and behaviours adapted to these particular conditions to persist (Milner et al., 2001; Ilg and Castella, 2006; Brown and Milner, 2012). Although the majority of studies focusing on community assembly in glacier-fed river systems have worked with macroinvertebrates (Figure 2.1; Ilg and Castella, 2006; Brown and Milner, 2012; Cauvy-Fraunié et al., 2015), evidence from other groups such as bacteria and protists also suggest a strong abiotic influence on assembly (Eisendle-Flöckner et al., 2013; Wilhelm et al., 2013). Species richness and density are reduced heavily in glacial rivers, but cold stenothermic species have adapted to persist within turbid conditions close to freezing (Wilhelm et al., 2013; Peter and Sommaruga, 2016). In contrast, diatom and aquatic hyphomycetes communities are relatively unconstrained by harsh conditions (Gessner and Robinson 2003; Rott et al., 2006).

As environmental harshness declines with glacier retreat, there is expected to be a strong reduction in the influence of deterministic, abiotic control of community composition and subsequently a greater importance of stochastic and competition driven assembly processes (Milner et al., 2011; Brown and Milner, 2012; Jacobsen and Dangles, 2012). This effect has been noted for macroinvertebrates but may be altered with detailed consideration of assembly processes that consider interactions among multiple biological groups, many of which have been less well studied. Furthermore, the relative importance of biotic interactions and dispersal processes is still considered as a secondary effect in comparison with abiotic controls, despite recent observations of strong predation, omnivory and cannibalism in glacially influenced rivers (Füreder et al., 2003; Clitherow et al., 2013; Khamis et al., 2015). Reductions in ice melt inputs are already driving the reassembly of aquatic ecosystems, because species colonisation is mediated by the efficacy of physiological and behavioural adaptions to imposed conditions (Ilg and Castella, 2006; Milner et al., 2011; Brown and Milner, 2012; Eisendle-Flöckner et al., 2013). There is therefore a pressing need to develop an

understanding of the importance of whole ecosystem interactions in these reassembly processes.

This literature synthesis has informed the development of a new conceptual framework that advances the widely accepted model of Milner et al. (2001) for macroinvertebrates (Figure 2.4) to predict multitrophic responses to reducing glacier influence (Figure 2.5). The first appearances of all biological groups considered in this synthesis were mapped simultaneously to a gradient of reducing catchment glacier cover. The purpose of this model was to inform holistic predictions of whole alpine river community reassembly and potential food web restructuring in response to glacier retreat. Therefore, it can serve as a focus for moving alpine river science, conservation and management beyond current paradigms that typically focus on single taxonomic groups.

Vertebrates


Calotriton sp.
Lee Brown, 2017


Salvelinus malma
Lee Brown, 2017

Fish
(North America, Scandinavia)
Fish
(all other river systems)
Mammals
Amphibians

Salmo sp.
Salvelinus alpinus

Salmo trutta
Cottus gobio
Salmo salar
Salvelinus malma

Thymallus thymallus
Phoxinus phoxinus
Squalius cephalus

Barbus barbus
Rutilus rutilus

Talpidae
(*Galemys pyrenaicus*)

Neomys fodiens

Talpidae
(*Desmana moschata*)

Calotriton asper
Hynodiidae

Salamandra salamandra
Ichthyosaura alpestris

Rana temporaria

Invertebrates
(predators)


Rhyacophila sp.
Centre for Biodiversity Genomics 2010

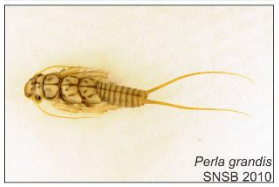
Perla grandis
SNSB 2010

Diamesa
Encentrum sp.

Perlodidae
Empididae
Cephalodella sp.
Mononchus

Rhyacophilidae
(*Rhyacophila angelieri*)

Chloroperlidae

Hirudinea

Invertebrates
(detritivores)


Hydropsychidae sp.
Centre for Biodoversity Genomics 2016


Leptophlebiidae sp.
Centre for Biodiversity Genomics 2011

Bdelloidea
Colurella sp.
Hofmanneria sp.
(*Hazenesis*)

Tipulidae

Taeniopterygidae
Oligochata
Lecane sp.
Lepadella sp.

Leuctridae
Nemouridae
(*Lednia tumana*)
Limnephilidae

Leptophlebiidae
Ephemeridae
Hydropsychidae

Invertebrates
(herbivores)


Diamesa
Sarah Fell, 2017


Simuliidae
Lee Brown, 2017

Eumonhystera sp.
Diamesa

Simuliidae

Orthocladiinae
Baetidae
(*Baetis alpinus*)

Heptageniidae

Glossosomatidae
Dissotrocha sp.

Planorbidae
Lymnaeidae

Biofilm


Euglena sp.
Deuterostome 2011


Odontidium mesodon
Sarah Fell, 2017

Odontidium sp.
Fragilaria sp.
Achnanthes sp.
Hannaea arcus

Encyonema minutum
Odontidium mesodon
Meridion circulare
Odontidium hyemale

Chrysophyta
(*Hydrurus foetidus*)

Cyanophyta
(*Chamaesiphon*)

Chlorophyta
(*Microspora*)

Cyanobacteria
(*Homeothrix, Clastidium*)

Bacteroidetes
Proteobacteria
Actinobacteria
Nitrospira

Aquatic hyphomycetes

Ciliates
Pompholyxophrys sp.

Astasia sp.
Euglena sp.

Verrucomicrobia
Firmicutes

Hypotrichida
Trachelomonas

Cocconeis sp.

Deinococcus
Eubacteria

Amoeba sp.
Colpoda sp.
Halteria sp.
Heliozoa
Vorticella sp.

Diatoms
Algae
Bacteria
Fungi
Protists

Taxon biomass

High — Medium — Low

Catchment Glacier Cover

◄ **Figure 2.5** A conceptual model of the first appearance of key alpine river taxa along a gradient of reducing catchment glacier cover across the Northern Hemisphere. The lines denote expected changes in individual biomass along the glacial gradient. Information regarding bacteria, protists, fungi, algae, diatoms, microinvertebrates, macroinvertebrates, mammals, amphibians and fish was synthesised to predict biofilm, invertebrate and vertebrate responses to reducing glacier influence.

This conceptual model was derived from the literature synthesis described above and therefore requires broader geographic validation and refinement to assess its general applicability, in a similar manner to which the model of Milner and Petts (1994) was revised by the coordinated European studies (AASER) described by Milner et al. (2001). Data were predominantly from the Northern Hemisphere and although some studies demonstrate a global generality of macroinvertebrate responses to glacier retreat (Castella et al., 2001; Jacobsen et al., 2012), species assemblages require adjustment to reflect glacier-fed river ecosystems in the Southern Hemisphere (Cadbury et al., 2011; Jacobsen et al., 2012; Cauvy-Fraunié et al., 2015). The model has a temporal focus toward data collected during summer months and therefore might not adequately capture the seasonal biomass and diversity fluctuations of specific taxa (e.g., macroinvertebrates and non-diatom algae). Protist, nematode and rotifer components in particular need more focus than other groups, because fewer studies were available to detail their responses (Eisendle-Flöckner et al., 2013; Robertson et al., 2015).

2.6 Freshwater biodiversity responses to glacier retreat: model application

From the multitrophic synthesis of population responses to glacier retreat, a number of general trends can be hypothesised that transcend most taxa. Figure 2.5 suggested both an increase in the biomass of most groups with reducing glacier influence, as well as a shift toward the introduction of more large bodied predators (invertebrates, mammals and amphibians) as glacier cover declines. This whole food web response is likely to underpin the decreasing part of the unimodal response of macroinvertebrate taxonomic richness and density at low glacier cover (Jacobsen et al., 2012). Although macroinvertebrate α-diversity has been shown to peak at intermediate stages of glacier influence (Jacobsen et al., 2012; Brown et al., 2015), this synthesis suggested that the response might not be generalisable to other groups. Vertebrates, for example, provided an exception to these trends, because desman species (*G. pyrenaicus*) and the Pyrenean brook newt (*C. asper*) preferentially occupied high velocity mountain

rivers in the Pyrenees, increasing their density and in turn biomass with reducing glacier influence (Comas and Ribas, 2015; Biffi et al., 2016). Notably, they appeared first at intermediate levels of glacier catchment cover (Figure 2.5), in contrast to ubiquitous macroinvertebrates. They then continued to benefit from their improved habitat conditions, few if any larger predators and abundant food sources as glaciers were lost.

For some biofilm groups (Archaea, bacteria, algae, fungi and protists) and meiofauna (rotifers and nematodes), the relationship between taxonomic richness and reducing glacier influence appeared to be linear, resulting in increases in biomass with glacier retreat (Figure 2.5). However, a relative lack of research focusing on the biomass of these groups along comprehensive gradients of glacier influence may mask a unimodal response as this linear trend is adjusted for groups including diatoms and protists (Figure 2.5). Here, densities were relatively suppressed by intensified grazing pressures as meiofauna and macroinvertebrate densities increased (Hakenkamp and Morin, 2000; Gesierich and Rott, 2012). The additive influence of these varied, multiple taxa group responses needs to be explored in more detail, but the cumulative effect can be hypothesised as an increase in community biomass in response to glacier retreat, reaching some form of asymptote at low or no glacier cover. However, the presence of subsidies from terrestrial systems may alter the nature of the total biomass response, especially at low or no glacier cover, or in locations such as southeast Alaska and New Zealand, where glaciers often terminate in close proximity to forests.

Figure 2.5 illustrated a further trend that transcends most taxa: for the first appearing species, there was a transition from specialists to omnivorous generalists with higher trophic roles as glacier influence was reduced. Many cold-adapted species are recognised as threatened or endangered primarily because of climate induced habitat contraction, which for fully aquatic taxa is compounded by limited dispersal opportunity when large mountain ranges isolate proglacial river systems (Wrona et al., 2006; Brown et al., 2009b; Giersch et al., 2016). These species include macroinvertebrates (*Baetis alpinus, Lednia tumana*, and *Rhyacophila angelieri*) but can be found at multiple trophic levels within diatoms (*O. mesodon* and *Odontidium hyemale*), algae (Red List algae species), and vertebrates (*G. pyrenaicus* and *C. asper*) (Ludwig and Schnittler, 1996, Brown et al., 2007a; Finn et al., 2013; Comas and Ribas, 2015; Biffi et al., 2016; Giersch et al., 2016). The extirpation of macroinvertebrate stenotherms drives a reduction in γ-diversity across formally glacierised catchments (Jacobsen et

al., 2012), a trend that will be exacerbated through the loss of cold stenotherms at additional trophic levels (Figure 2.5).

2.7 Food web responses to glacier retreat

Although it is important to determine the responses of particular trophic groups to glacier retreat and climate change generally, constituent taxa will never be affected independently because of the diversity of feeding and competitive interactions. This means that extrapolating out to community or whole ecosystem responses from population-level studies is likely to fail to capture the emergent properties that characterise complex ecological networks (Woodward et al., 2010a). This multitaxa response framework enabled explorations of how whole mountain river food webs will respond to deglaciation. Despite the significant contribution of network theory to freshwater science (Thompson et al., 2012), still only a few food webs have been constructed for proglacial river systems. Most researchers have employed stable isotope analysis to map energy flow through benthic communities (Zah et al., 2001; Fellman et al., 2015) highlighting, for example, the importance of dissolved organic matter consumption by microbial groups supporting wider food webs. However, further comparison of food webs is required to compare different mountain water sources. More studies of species-level interactions using connectance food webs are crucial to investigation of the direct and indirect cascades that will occur through entire river ecosystems with decreasing glacier influence (Clitherow et al., 2013).

In a detailed mountain river food web study, Clitherow et al. (2013) used gut content analysis to produce connectance and trivariate food webs for the river within 100 m of the Ödenwinkelkees glacier, Austrian Alps (Figure 2.6). Food webs were characterised by the highest connectance values (0.05 to 0.19) obtained for running waters, primarily because of generalist, opportunistic and omnivorous macroinvertebrate feeding strategies in response to low primary production (Clitherow et al., 2013). Mean chain lengths were very short (2 to 2.27) because large predators were absent, given the cold-water temperature constraints on body size (Ilg and Castella, 2006; Clitherow et al., 2013). This diminished the size structuring usually prevalent within freshwaters (Woodward, 2009). The webs supported few nodes and links, reflecting the low densities and biomass of taxa illustrated in Figure 2.5. Feeding links were predominantly between macroinvertebrates (Chironomidae, *Diamesa*) and both epilithic diatoms and detritus (Clitherow et al., 2013), as was noted in other studies (Zah et al., 2001; Füreder et al., 2003). Although unable to identify species-level connections,

stable isotope analyses from other river systems have confirmed that the short mean chain lengths and low numbers of nodes and links in glacier margin food webs result from macroinvertebrate feeding plasticity in response to an annually sustained autochthonous energy base (Fellman et al., 2015). Isotope methods can be particularly useful for detecting links not easily observed using gut content approaches. For example, whereas Clitherow et al. (2013) inferred the importance of microbial subsidies of carbon and other nutrients in the Ödenwinkelkees food web, Fellman et al. (2015) were able to use ^{14}C signatures to confirm that this was the case in other glacial rivers, where ancient carbon (hundreds of years old) released from the glacier was probably consumed by microbes and then assimilated by macroinvertebrates.

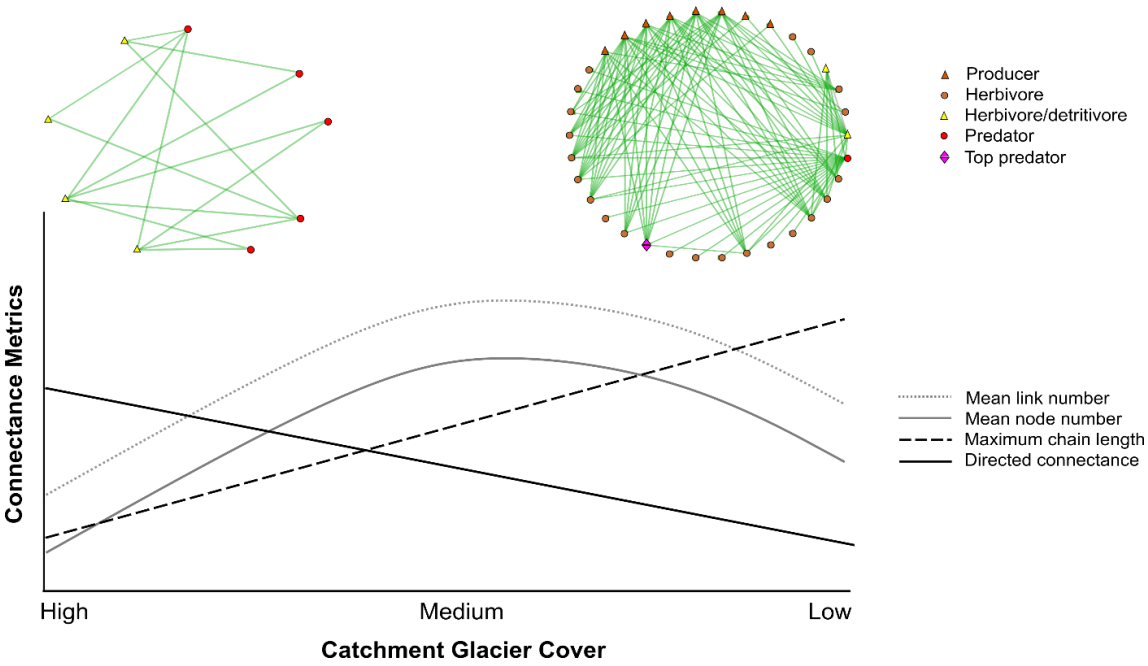

Figure 2.6 The predicted response of river food web connectance metrics to reducing catchment glacier cover. Observed connectance food webs are displayed for sites of high (adapted from Clitherow et al., 2013) and low (adapted from Parker and Huryn, 2006) glacier influence.

Parker and Huryn (2006) constructed connectance food webs for an Arctic mountain river lacking glacier influence (Figure 2.6), which provided an indication of the changes that can be expected following glacier loss. A spring-fed food web supported slightly lower connectance (0.165 to 0.188) and longer mean chain lengths (2.98 to 3.10; Parker and Huryn, 2006) than those documented in the study by Clitherow et al. (2013). They also encompassed on average a further 14.5 nodes and 62.5 links (Parker and Huryn, 2006; Clitherow et al., 2013). Although an absolute comparison was affected by differences in sampling effort and taxonomy between the two studies,

some general patterns were deduced from this approach. The Arctic food webs were influenced primarily by the addition of top predators, Dolly Varden trout (*Salvelinus malma*) and America dipper (*Cinclus mexicanus*), absent from the Austrian glacial food webs. In addition, Khamis et al. (2015) investigated the influence of increased macroinvertebrate predator abundance (*Perla grandis*) in spring-fed, in-situ experimental mesocosm channels. Their results suggested that the future range expansion of this species (into streams that are currently highly glacial and therefore are unsuitable habitat) will increase trophic height (and therefore food chain length) and body-size spectrums through invasion, intraguild predation, and interference competition (Khamis et al., 2015).

As prolonged glacier retreat will lead to ice melt influenced river reaches becoming dominated by groundwaters, it could be expected that their food webs will adopt the structural characteristics of spring-fed community networks (Lavandier and Décamps, 1983). On the basis of this concept, Figure 2.6 illustrated predicted changes to connectance food web metrics with reducing catchment glacier cover. Construction of alpine river food webs along gradients of glacier influence, using standardised methods and analysis techniques, is required to test these predictions further. In their absence, research investigating food web responses to increasing water temperatures may be drawn on to explain this structural reassembly. Warming increases cold water productivity, and more nutrient rich waters may reduce directed connectivity by abating the requirement for flexible, opportunistic feeding strategies and diminishing the omnivory and cannibalism adopted to survive on a limited food supply (Lavandier and Décamps, 1983; Friberg et al., 2009, Clitherow et al., 2013). Warmer waters will also reduce constraints on body mass and metabolic rates, hosting a greater abundance of larger individuals and supporting increased predator densities (Parker and Huryn, 2006; Woodward et al., 2010a). This, together with the upstream migration of ectothermic species following the expanding range of a particular life stage thermal optimum, will increase food chain lengths and the number of nodes (species) and links (Lavandier and Décamps, 1983; Brown et al., 2007a). The spectra of body sizes will also increase, strengthening size structuring, which can promote web stability (Woodward, 2009).

Lavandier and Décamps (1983) identified connectance food webs to increase community abundance and the diversity of species along a gradient of increasing maximum water temperature within the snow melt-fed Estaragne Basin, French

Pyrenees. However, this proliferation may be constrained because novel species colonisation can introduce increased or additional predation pressures, interference competition and preferential suppression of particular prey (Parker and Huryn, 2006; Wrona et al., 2006; Khamis et al., 2015). Nodes and link numbers may also be reduced by the extirpation of cold stenotherms through competition and habitat contraction (Hari et al., 2005; Wrona et al., 2006; Brown et al., 2007a; Khamis et al., 2015).

Reducing glacier influence comprises more than an increase in river water temperature, with reducing suspended sediment concentrations, discharge variability and channel instability also influencing food web structure (Parker and Huryn, 2006; Dekar et al., 2009). Parker and Huryn (2006) found spring-fed rivers supporting these conditions to facilitate significantly increased bryophyte growth and persistence, in comparison with more unstable, dynamic channels. Bryophyte and epilithon communities provide structurally complex habitat refugia and food sources for macroinvertebrate larvae and meiofauna (Battin et al., 2016). Turbidity gradients also exert strong control on the density of bacteria (Peter and Sommaruga, 2016). In turn, reduced disturbance regimes may provide a mechanism for increasing productivity, biomass and species densities in mountain river food webs, independently of mean water temperature.

Glacier retreat may further influence food web structure indirectly, acting beyond water source alteration. Prolonged retreat and the subsequent extension of the ice-free period will reduce the seasonality of river ecosystems, ensuring that production and reproduction become less confined to a short summer phase (Malard et al., 2006; Durant et al., 2007). This may increase energy availability to food webs, particularly through algal blooming, or uncouple the timing of consumer requirement from prey availability, reducing food web links and potentially taxon survival (Durant et al., 2007). Significant ice loss could also lead to intermittency or cessation of flow (Robinson et al., 2016). Periods of low or no flow could introduce trophic cascades of variable magnitude and may induce the compensatory reorganisation of whole food web cores, influencing all species within a community both directly and indirectly (Ledger et al., 2013; Lu et al., 2016).

2.8 Conclusions

This synthesis chapter presented a novel conceptual framework that collated the simultaneous responses of multitrophic river ecosystems to glacier retreat (Figure 2.5).

Knowledge of biofilm, invertebrate and vertebrate responses from individual studies can inform holistic predictions of the rapid reshaping of mountain river ecosystems in response to climate change. Although the responses of certain taxa remain poorly resolved, general predictions from the best studied groups can nevertheless guide understanding of food web responses to deglaciation. Glacial reaches are expected to shift over time to develop the structural characteristics of contemporary rain and groundwater-fed food webs (Figure 2.6). Increases in mean water temperature and channel stability will drive reduced directed connectance and increased mean chain lengths, predator densities, energy availability, size structuring and the relative contribution of biotic (particularly competition) influences on community assembly (Parker and Huryn, 2006; Woodward et al., 2010a; Brown and Milner, 2012). Mean numbers of nodes and links may initially increase as more and larger generalist species proliferate, broadening the spectrum of body sizes (Friberg et al., 2009). However, the potential extinction of some cold specialist species due to novel predation pressure and habitat reduction may constrain these metrics (Hari et al., 2005; Wrona et al., 2006; Brown et al., 2007a; Giersch et al., 2016). Ice melt could induce further structural reorganisation as reduced seasonality, periodic drought and potential flow cessation alter energy production rates and network stability (Durant et al., 2007, Lu et al., 2016). The scientific community places ‘high confidence’ in the accelerating and pervasive nature of worldwide glacial shrinkage (IPCC, 2013, p. 4). The associated threats to mountain river biodiversity (Jacobsen et al., 2012) highlight the urgent need for an improved understanding of these predicted responses.

Future research should investigate protist, nematode, rotifer, virus and protozoa communities in much more detail, given that less is known regarding the response of these groups to glacier retreat and especially their role within food webs, which often reveal vertebrate-macroinvertebrate-algal links. Protist species should receive particular focus because their densities appear to be more sensitive to deglaciation than those of other freshwater taxa (Eisendle-Flöckner et al., 2013). Species whose density and richness are influenced minimally by glacial conditions (e.g., aquatic hyphomycetes, diatoms and rotifers) should be highlighted as potential conservation priorities, because intensive specialisation may increase their vulnerability to water source alterations (Wrona et al., 2006). Comparative studies are required to determine food web structure both at the extremes of glacier influence and along a quantified spectrum of intermediary stages to investigate the ecosystem-level effects of glacier retreat (Clitherow et al., 2013). There is also requirement for more winter sampling

(Brown et al., 2015) to determine the influence of seasonal variability in biomass (macroinvertebrate, non-diatom algae) on ecosystem structure and food web dynamics.

Despite the need for further validation, this new conceptual framework offered immediate potential to inform conservation management strategies by highlighting that cold stenothermic species are found beyond the macroinvertebrate component of river communities (e.g., algae, diatoms and vertebrates) and that other taxonomic groups can serve as differential indicators of climate change in mountain river systems. It also holds value beyond alpine rivers because the reorganisation of communities within glacierised headwaters will intrinsically influence the species pools available to colonise downstream reaches, potentially reshaping their assembly processes (Brown and Milner, 2012). The often strong deterministic effects of habitat on alpine river biological communities mean that they are valuable model systems for understanding ecosystem responses to environmental change. Coupled with the potential for species interactions to be investigated and manipulated easily and comprehensively (e.g., Khamis et al., 2015; Cauvy-Fraunié et al., 2016), glacier-fed rivers offer significant potential to inform mechanistic predictions in other river systems that will be modified by environmental change.

Chapter Three: Declining glacier cover threatens the biodiversity of alpine river diatom assemblages

3.1 Introduction

Pervasive and accelerated glacier retreat in alpine regions worldwide is predicted to intensify throughout the twenty-first century (IPCC, 2013). This diminishing ice cover will ultimately reduce the contribution of ice melt to rivers, subsequently increasing the relative contributions of snow melt, groundwater streams and precipitation (Brown et al., 2003; Milner et al., 2017; Huss and Hock, 2018). Alteration to meltwater sourcing will physically modify channel geomorphology as diurnal and seasonal ice melt discharge peaks are attenuated, reducing erosion and reworking of proglacial sediments (Carrivick and Heckmann, 2017). Each water source also generates discrete physicochemical conditions, forming the habitat template upon aquatic communities and acting as an environmental filter to taxa which do not possess the morphological and behavioural trait combinations required to survive (Brown et al., 2018). Spatiotemporal mixing of water sources creates further diversity of habitat conditions within alpine rivers. Whilst there has been a major research focus upon the impact of glacier retreat on macroinvertebrate communities, far less is understood of how other aquatic groups will respond (Fell et al., 2017).

The sensitivity of freshwater benthic diatoms to environmental change has led to their use as a representative indicator taxa in the assessment of water quality globally (Wang et al., 2014; Lobo et al., 2016). Diatom assemblages possess a diverse spectrum of ecological optima and tolerances and they reassemble in response to alterations in physicochemical environment, which underpins their use in assessment of the condition of freshwater ecosystems required by the European Water Framework Directive (Kelly et al., 2008; Lobo et al., 2016). However, there remains a clear need for knowledge of diatom assemblage responses to natural and indirect anthropogenic change, such as glacier retreat.

Benthic diatoms, alongside additional biofilm components including cyanobacteria and other algae, play a major role in primary production within alpine rivers (Rott et al., 2006; Battin et al., 2016). This autochthonous input is critical to these above treeline systems which receive minimal energy subsidy from the riparian zone (Zah and Uehlinger, 2001). Alpine rivers, particularly springs, have been identified as potential

hotspots of benthic diatom biodiversity, hosting rare and threatened taxa, often in high abundance (Rott et al., 2006; Cantonati et al., 2012). *Hannaea arcus* and the genera *Achnanthidium*, *Fragilaria and Odontidium* are consistently the most abundant taxa within diatom assemblages across the European Alps, Himalaya and Rocky Mountains, with new species belonging to the latter recently identified in mountain streams (Hieber et al., 2001; Gesierich and Rott, 2012; Nautiyal et al., 2015; Jüttner et al., 2015, 2017). However, a more complete consideration of benthic diatoms is needed to inform understanding of alpine river biodiversity responses to glacier retreat, given their role as a principal food source for invertebrate primary consumers in glacier-fed rivers (Clitherow et al., 2013).

Previous research investigating river diatom assemblages within mountain catchments has considered glacial influence with regard to distance from ice margins (Nautiyal et al., 2015) and water source origins (Hieber et al., 2001). However, holistic predictions of aquatic community response to future glacier retreat require approaches that identify alterations to alpine freshwater biodiversity along a quantified spectrum of glacial influence (Brown et al., 2007a). While such chronosequence approaches have been used recently to determine the response of macroinvertebrate, algae (excluding diatoms) and microbial prokaryote communities to deglaciation (Rott et al., 2006; Brown et al., 2007a; Ren et al., 2017a), they are yet to be applied to benthic diatom assemblages. The efficacy of alpine freshwater conservation strategy is critically dependent upon understanding these responses, particularly for taxa that are vulnerable to extirpation due to limited motility and dispersal capacity (Liu et al., 2013).

This study examined diatom assemblage structure and the abundance of individual species in rivers draining the eastern European Alps. Although proglacial regions of the Alps host high aquatic alpine biodiversity, glaciers are in long-term retreat, with approximately two-thirds of total glacier volume lost since 1850 (Zemp et al., 2006), and a further 4 to 18 % reduction of the 2003 ice area predicted by 2100 (Huss, 2012). This study adopted a chronosequence approach, sampling river sites in watersheds hosting different percentages of permanent ice cover, to provide a gradient of catchment glacier cover and in turn, a proxy for the stages of glacier retreat. This study aimed to (a) quantify the biodiversity of diatom assemblages present in alpine rivers along the catchment glacier cover gradient, (b) determine taxon-level responses to glacier cover and (c) investigate the environmental drivers underpinning glacier influence upon alpine river benthic diatoms. This research design facilitated novel

investigation of diatom assemblage response to decreases in glacier cover within the European Alps.

3.2 Materials and methods

3.2.1 Study area

Field observations were made in the central Austrian Alps during June and July of 2015 and 2016 (Figure 3.1; Appendix 1). Variability of glacier coverage within a small geographical region provided a broad spectrum of glacier cover whilst minimising large-scale differences due to climate or other catchment characteristics (Robson et al., 2016). Thirteen river sites spanning a gradient of catchment glacier cover (0 to 64 % permanent ice cover) were identified throughout the Eisboden, Obersulzbach and Rotmoos valleys (Table 3.1). Sites were selected with minimal direct anthropogenic influence and where sampling was possible at locations above the treeline. Sites included streams predominantly fed by glacial meltwaters (> 50 % catchment glacier cover) (O1, R1), mixed streams draining melt, springs and aquifer upwelling (25 to 50 % catchment glacier cover) (E2, E3, O3, R2, R3, R4, U1) and those sourced predominantly (1 to 25 % catchment glacier cover) (E1, U2) and entirely by groundwater flow (0 % catchment glacier cover) (E4, O2), to represent varying glacier cover (Table 3.1).

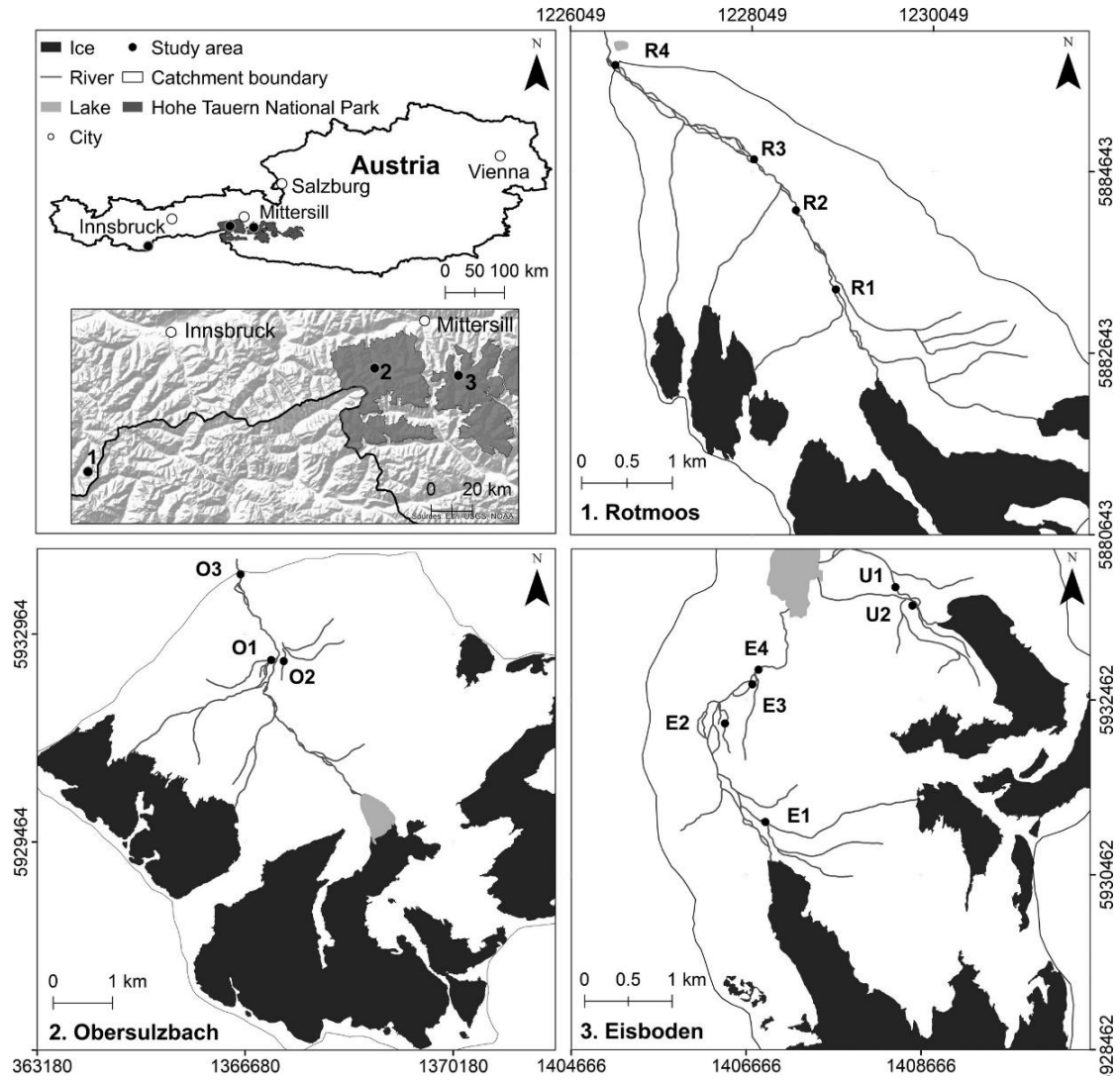

Figure 3.1 Schematic diagrams illustrating the position of sampling sites within multiple glacierised valleys of the Austrian Alps. WGS 1984 World Mercator projection. Diagrams are derived from the ArcMap™ World Imagery Basemap (Land Salzburg 07/11/15 and Land Tyrol 08/03/15) with glacier outlines sourced from the Glaciology Commission (2015). Source credits: Esri, DigitalGlobe, GeoEye, i-cubed, USDA, USGS, AEX, Getmapping, Aerogrid, IGN, IGP, swisstopo and the GIS User Community.

Table 3.1 Sampling site information.

Valley	Date	Aspect	Geology	Site Code	Coordinates (N, E)	Altitude (m)	Area (km^2)	Glacier cover (%)
Rotmoos	June 2016	N	Mica schists, Gneisses, Marble	R1	46.83104, 11.04022	2351	4.0	64
				R2	46.83633, 11.03612	2310	7.1	41
				R3	46.83981, 11.03206	2290	8.3	38
				R4	46.84623, 11.01827	2253	10.8	30
Obersulzbach	June 2015	NNW	Muscovite schists, Quartzites	O1	47.13371, 12.28085	1948	19.3	52
				O2	47.13319, 12.28296	1942	1.2	0
				O3	47.14214, 12.27648	1746	29.2	42
Eisboden	June/ July 2015	N	Mica schists, Feldspar, Gneisses	E1	47.12436, 12.63836	2129	0.5	3
				E2	47.13125, 12.63408	2074	8.6	26
				E3	47.13413, 12.63749	2052	8.5	28
				E4	47.13477, 12.63710	2056	0.02	0
				U1	47.14075, 12.65157	2275	2.1	46
				U2	47.13979, 12.65328	2286	0.04	1

Permanent ice cover of discrete catchments pertaining to individual river sampling sites was determined using the watershed analysis function of ArcMap™ 10.4. Flow direction and accumulation models were applied to a filled 10 m ASTER Digital Elevation Model (DEM) (GitHub, 2016), to determine downslope water flow direction based upon local topography. Automated watershed delineation followed river network boundaries and were then checked manually using high-resolution aerial photography, to avoid error induced by DEM resolution and to achieve the most accurate representation of local geomorphology. Regional ice extents (Glaciology Commission, 2015) were constrained to watershed boundaries to calculate the percentage of catchment area covered by ice (Table 3.1).

3.2.2 Field sampling

Water temperature, electrical conductivity (EC) and pH were measured in-situ at each site using Hanna Instruments (Woonsocket, RI, USA) H19063, HI9033 and HI98130 meters, respectively. Pfankuch Index bottom component estimates were collected (Pfankuch, 1975) as a proxy for channel geomorphological stability, with lower values representing more stable riverbeds. Reciprocal values (1/Pfankuch Index scores) were used in statistical analyses so that larger values represented higher stability. River water (100 mL) was collected for ex-situ optical turbidity analysis using a Hanna Instrument HI93703 meter and then filtered (0.2 µm mesh) for nutrient analysis. This included the detection of dissolved organic carbon (DOC) using an Analytik Jena Multi N/C 2100 elemental thermal oxidation analyser, whereas phosphate (PO_4^{3-}), nitrate

(NO_3^-) and total nitrogen (TN) concentrations were analysed using a Two Skalar San ++ Continuous flow auto-analyser.

Benthic biofilms were sampled following the CEN (2014) protocol. At each site, five submerged cobbles were selected randomly from riffles to represent a diversity of river site microhabitats. For sites O2 and O3, only three and four replicates were available respectively, due to sample damage during transportation (total *n* = 62 replicates). Benthic algae were scrubbed from a 9 cm^2 area of the upper surface of each cobble, using a plastic template and sterile toothbrush. Cobbles potentially exposed during prolonged periods of low flow were avoided. Samples were preserved within 70 % methylated spirits and stored at 4 °C prior to analysis.

3.2.3 Laboratory analysis

To prepare samples for microscopic analysis, organic material was removed to enable the unobstructed observation of diatom valves (CEN, 2014). The hot hydrogen peroxide (H_2O_2) method (CEN, 2014) was used to reduce reaction times between H_2O_2 and organic matter. Samples were homogenised and 20 mL of 30 % H_2O_2 added to a 5 mL subsample, which was heated in a water bath at 90 °C (± 5° C) for 3 hr. The remaining H_2O_2 was neutralised with 50 % hydrochloric acid (HCL) and subsamples suspended within distilled water and centrifuged at 1,200 rpm for 4 min, four times. The remaining 5 mL pellet was diluted by adding 5 to 20 mL of distilled water, depending upon diatom concentration. The solutions were then homogenised with a vortex mixer (Stuart SA8) and 0.5 mL pipetted onto the centre of a 19 mm circular coverslip, which had been cleaned with ethanol. Coverslips were covered and air dried overnight. They were mounted using Naphrax®, as its high refractive index (> 1.6) facilitated the clear examination of diatoms (CEN, 2014). The initial volume of each biofilm cobble sample and any dilutions was recorded and accounted for in subsequent volumetric calculations.

Diatom valves were counted and identified using light microscopy (Leica DM 2000), at × 1,000 magnification (N Plan lens, 100 ×/1.25 oil PH3) in brightfield view. A minimum of 500 complete, individual diatom valves were identified to the highest resolution possible, to reflect the species composition of each replicate. For replicates with fewer than 500, all valves were counted. A single researcher performed all microscopy to prevent inter-analyst variance (Culverhouse et al., 2014). Identification followed Kelly (2000), Krammer and Lange-Bertalot (2004, 2007a, 2007b, 2008), and Spaulding

(2018), with taxonomic nomenclature following Lange-Bertalot et al. (2017). Characterisation of variation within the *Achnanthidium minutissimum* complex followed Potapova and Hamilton (2007).

To determine estimates of absolute diatom abundance, or valve density, the number of valves counted within coverslip transects was used to estimate the total number present upon the whole coverslip (0.5 mL) and then multiplied to m^{-2} based on sample volume and rock area sampled (Scott et al., 2014). These extrapolations were averaged across rock scrub replicates for each river site, with mean valves m^{-2} underpinning all diatom abundance analysis. As a minimum, half of each coverslip was screened, with transects encompassing both the coverslip centre and edges. Repeat counts of 20 % of all replicates identified an average estimated absolute abundance error of ± 3 %. This approach was adopted in preference to microsphere analysis given the significant and unpredictable variability of diatom concentrations between replicates hindering estimates of suitable microsphere to diatom ratios (Battarbee and Kneen, 1982).

3.2.4 Data analysis

The diatom species × abundance matrix was used to calculate summary metrics describing biodiversity at each river sampling site: (a) taxonomic richness (b) density of valves m^{-2}, (c) Pielou's evenness (Oksanen, 2019), (d) Shannon diversity index (Oksanen, 2019) and (e) taxonomic richness of taxa classified on the Red List of Algae for Germany (Lange-Bertalot and Steindorf, 1996). The Red List was collated to identify taxa of algal conservation priority, and despite development from research solely within German freshwaters, it was applied within this study given the absence of comparable data sets for Austrian rivers and the geographical proximity of their alpine regions. Changes to taxonomic nomenclature since Red List publication were identified following Guiry (2018). As the diatom assemblages hosted many taxa only identified at single sites in low abundance, Shannon diversity index was adopted as it does not weight common species over rare ones (Morris et al., 2014). Relationships between these indices and glacier cover were tested using generalised linear models (GLM) or generalised additive models (GAM) for data showing pronounced non-linear relationships, with the latter constructed using the *mgcv* package in R (Wood, 2011). Akaike information criterion values were used to determine best fit, with Negative binomial and Gaussian distributions specified. Smoothing parameters for GAM were selected following the procedures outlined by Wood (2004). Model performance was

evaluated using the percentage of deviance explained. GAMs and GLMs were also used to determine the relationship between catchment glacier cover and site-specific environmental parameters (mean water temperature, EC, turbidity, pH, 1/Pfankuch Index scores, nutrient concentrations).

Within-site β-diversity was calculated from the abundance of diatom valves identified in the replicate biofilm cobble scrub samples collected from individual river sites. Components of β-diversity (total dissimilarity (Sørensen), turnover (Simpson) and nestedness (Nestedness) were calculated for each river site using the *betapart* package of R (Baselga et al., 2017) and GLM used to describe the relationship between average beta component values and catchment glacier cover per site. Between-site β-diversity was determined by amalgamating average diatom valve abundances from replicates to determine a singular valve abundance value for each river site. Sørensen, Simpson and Nestedness indices were calculated for the species × abundance matrix. These components were related to pairwise differences (Bray-Curtis dissimilarity index) in catchment glacier cover between all river sites. Mantel tests (*vegan* R package) were used to determine the significance of correlation between these dissimilarity matrices.

Ordination analysis was performed to investigate diatom assemblage composition and taxon-level responses along the gradient of glacier cover. Prior to analysis, the estimated average abundance (valves m^{-2}) of identified diatom taxa at each site was $\log_{10}(\times + 1)$ transformed to constrain the influence of disparate records upon outcomes for data containing zero values (Khamis et al., 2014b). Non-metric multidimensional scaling (NMDS) was applied to a Bray-Curtis dissimilarity matrix using the *vegan* package of R (Oksanen et al., 2017). Significantly correlated ($p < 0.05$) scaled (*mean* = 0, *SD* = 1) physicochemical and nutrient vectors were fitted to the resulting configuration using the *envfit* procedure. Both NMDS axis scores were correlated to site-specific taxon abundances using Spearman's rank correlation.

3.3 Results

3.3.1 Environmental parameters

Pfankuch Index scores (i.e. decreasing channel stability) and NO_3^- concentrations increased significantly with glacier cover (Figure 3.2; Table 3.2). No other environmental parameters showed significant relationships with catchment glacier cover (Figure 3.2). However, water temperature data collected over longer time periods

from nine study sites showed a negative relationship with glacier cover (Appendix 2) and thus co-varied with channel stability. The range and maximum concentrations of DOC (0.3 to 3.8 mg L^{-1}), PO_4^{3-} (0.001 to 0.003 mg L^{-1}), NO_3^- (0.132 to 0.399 mg L^{-1}) and TN (0.066 to 0.311 mg L^{-1}) were low at all sites. There were no significant correlations between diatom taxonomic richness or valve density and these variables.

Figure 3.2 Relationship between catchment glacier cover and physical ((a) watershed area (km^2), (b) site altitude (m above mean sea level), (c) river water temperature (°C), (d) optical turbidity NTU, (e) 1/Pfankuch Index bottom components), chemical ((f) dissolved organic carbon (DOC) (mg L^{-1}), (g) nitrate (NO_3^-) (mg L^{-1}), (h) total nitrogen (TN) (mg L^{-1}), (i) electrical conductivity (µS cm^{-1}), (j) pH) and biological ((k) taxonomic richness, (l) density of diatom valves (valves m^{-2}), (m) Shannon diversity, (n) Pielou's species evenness, (o) taxonomic richness of diatoms classified as threatened, endangered, decreasing or rare on the Red List of Algae for Germany (Lange-Bertalot and Steindorf, 1996)) parameters. Nutrient data were unavailable for sites R1, R2, R3 and R4. Black lines represent statistical model and 95 % confidence intervals (dashed). Model details are provided in Table 3.2.

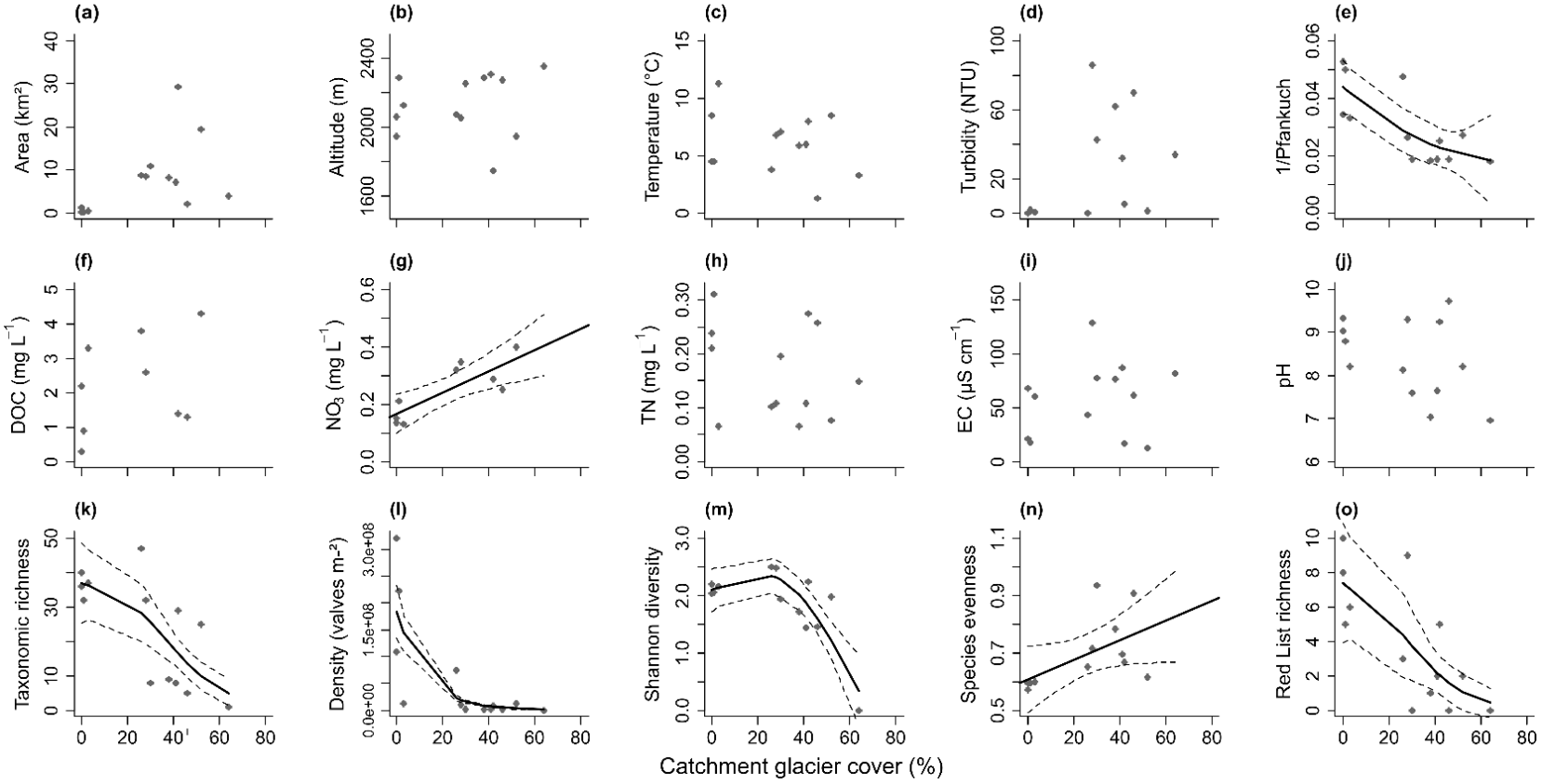

Table 3.2 GLM, GAM and Mantel summary statistics for the effect of glacier cover on physical, chemical and biological parameters.

Dependent variable	Method (Distribution)	χ^2/ *F*	*p*-value	Deviance explained (%)/ R^2
Physical parameters				
Area (km^2)	GLM (Gaussian)	0.33	0.91	50.0
Altitude (m)	GLM (Gaussian)	0.86	0.62	72.2
Water temperature (°C)	GLM (Gaussian)	0.55	0.59	9.9
Turbidity (NTU)	GLM (Gaussian)	0.86	0.45	14.8
1/Pfankuch	GAM (Gaussian)	6.98	< 0.001	58.2
Chemical parameters				
DOC (mg L^{-1})	GLM (Gaussian)	0.97	0.36	12.2
NO_3^- (mg L^{-1})	GLM (Gaussian)	14.45	0.006	67.4
TN (mg L^{-1})	GLM (Gaussian)	0.82	0.39	6.9
PO_4^{3-} (mg L^{-1})	GLM (Gaussian)	0.12	0.73	0.01
EC (mg L^{-1})	GAM (Negative binomial)	6.07	0.05	9.24
pH	GAM (Negative binomial)	0.13	0.94	16.9
Biological parameters				
Taxonomic richness	GAM (Negative binomial)	23.71	< 0.001	43.5
Density (valves m^{-2})	GAM (Negative binomial)	481.50	< 0.001	33.5
Shannon diversity index	GAM (Gaussian)	13.77	< 0.001	73.4
Pielou's evenness	GLM (Gaussian)	4.23	0.066	22.7
Red List richness	GAM (Negative binomial)	12.59	0.002	44.6
Within-site β-diversity				
Sørensen	GAM (Gaussian)	4.23	0.046	45.8
Simpson	GAM (Gaussian)	4.11	0.049	45.1
Nestedness	GLM (Gaussian)	0.56	0.472	4.8
Between-site β-diversity				
Sørensen	Mantel		0.062	0.22
Simpson	Mantel		0.997	-0.37
Nestedness	Mantel		0.009	0.36

3.3.2 Diatom assemblages and taxon biodiversity

Diatom taxonomic richness, overall density and Shannon diversity index increased significantly as glacier cover decreased, with taxonomic richness and Shannon diversity showing pronounced thresholds of change at approximately 28 % catchment glacier cover (Figure 3.2). In total 85 taxa from 29 genera were identified, with taxonomic richness at individual sites ranging from 1 to 47 taxa and being greatest at lower glacier cover (≤ 28 % cover, 32 to 47 taxa). Above 28 % glacier cover, richness did not exceed 29 taxa. Estimated average abundance spanned four orders of magnitude, from 15,111 valves m^{-2} (64 % cover), to 3.20×10^8 valves m^{-2} (0 % cover). The taxonomic richness of Red List taxa increased significantly with reducing glacier cover (Figure 3.2). Pielou's species evenness did not illustrate any significant trend across the gradient (Figure 3.2). Despite the absence of relationships between catchment glacier cover and both total dissimilarity (Sørensen) and turnover (Simpson)

components of between-site β-diversity, nestedness (Nestedness) was reduced significantly by ice loss (Figure 3.3). In contrast, nestedness (Nestedness) was the only component of within-site β-diversity to display no significant correlation with reductions in ice cover. Whilst total dissimilarity (Sørensen) decreased, turnover (Simpson) demonstrated a unimodal response to declining catchment glacier cover (Figure 3.3).

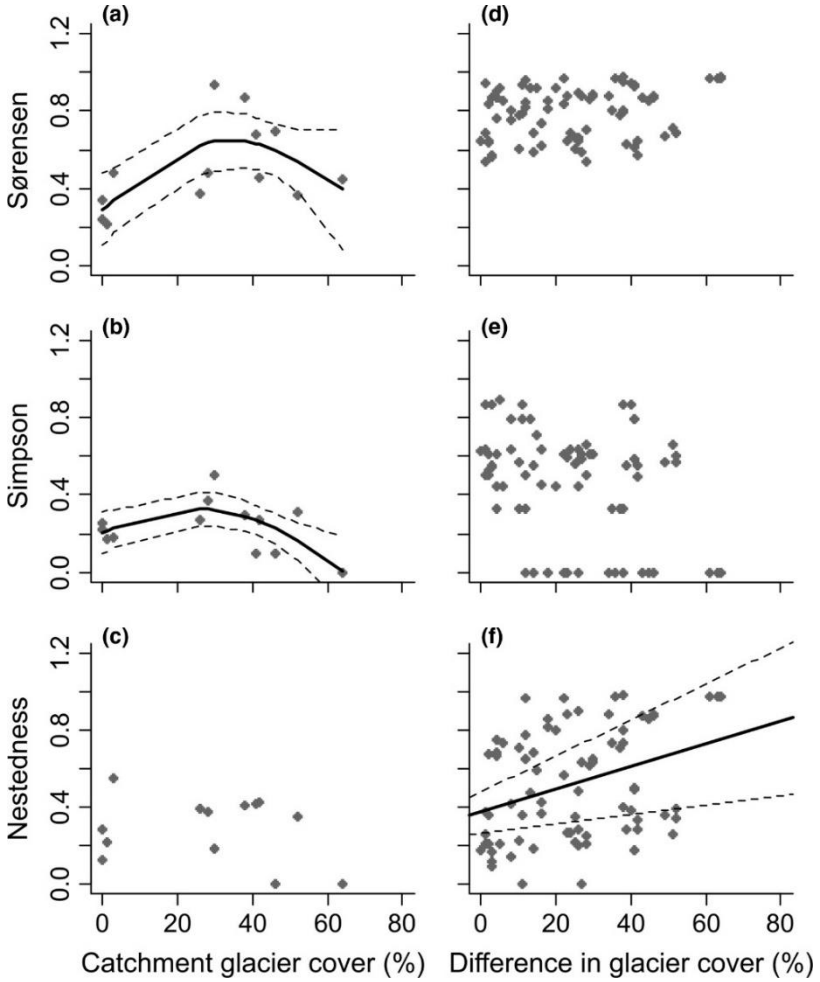

Figure 3.3 Relationships between catchment glacier cover and both within-site β-diversity, (a to c), and between-site β-diversity, (d to f). Components of β-diversity include total dissimilarity (Sørensen), turnover (Simpson) and nestedness (Nestedness). Within-site components are calculated from average Sørensen, Simpson and Nestedness values from dissimilarity matrices computed for the replicate biofilm samples collected at each river site. Between-site components are related to pairwise differences in glacier cover. For (b) and (c) n = 12 as site R1 had a species richness of 1. Black lines represent GAM/GLM lines of best fit and 95 % confidence intervals.

The most abundant diatom species were those attributed to the *A. minutissimum* complex which represented 63.8 % of identified valves and were found at all sites. Other frequent (≥ 10 sites) taxa included *Encyonema ventricosum* (11 sites), *Psammothidium helveticum* and *Encyonema minutum* (10 sites), generalists which were present at ten or more (77 %) sites. Many taxa occurred at just one (29 taxa) or two (10 taxa) sites, with 74 taxa (87 % of taxa) contributing less than 1 % to the estimated total abundance of sampled species. *Caloneis lancettula* and *Eunotia trinacria* were found exclusively at sites ≥ 52 % glacier cover whilst *Chamaepinnularia mediocris*, *Cymbella parva, Gomphonema angustatum, Gomphonema calcareum, Meridion circulare, Reimeria sinuata* f*. antiqua* and *Stauroneis agrestis* were found only within groundwater-fed streams (0 % glacier cover).

Of the 85 taxa identified, nineteen (22 %) were noted on the Red List of Algae for Germany as threatened, endangered, decreasing or rare. *Navicula detenta,* classified as threatened with extinction, was found at only one site. Endangered species included *Achnanthidium caledonicum* (9 sites), *Achnanthidium trinode* (1 site), *Encyonema hebridicum* (1 site), *Encyonema neogracile* (4 sites), *Fragilariforma constricta* (1 site), *Staurosira construens* (1 site), *Rossithidium petersenii* (5 sites) and *Staurosirella lapponica* (2 sites). Red List species were found in greatest abundance (representing 4.3 to 24.3 % of individuals) at river sites ≤ 26 % glacier cover (Figure 3.2), with *A. caledonicum* the most abundant, representing 6.1 % of identified individuals. Sites with more glacier cover had a lower number of these species (Figure 3.2) and of the six taxa found exclusively in river sites with > 28 % glacier cover, only two (*F. constricta, S. construens*) are currently noted on the Red List.

A Shepard Plot (R^2 = 0.99) for the NMDS ordination (stress = 0.023) indicated the accurate preservation of rank orders within the two-dimensional display (Figure 3.4), ensuring that the resulting NMDS configuration represented the original distribution of data within the dissimilarity matrix as closely as possible. The NMDS Axis 1 was significantly ($p < 0.05$) correlated to the density of 23 diatom taxa (Table 3.3). The strongest positive correlations were between Axis 1 and *A. minutissimum* complex species (*A. lineare*, *A. minutissimum, A. caledonicum, A. minutissimum var. cryptophala*). No abundances correlated significantly to NMDS Axis 2. Fitting of significantly correlated environmental parameters illustrated the strong association of glacier cover (R^2 = 0.55, p = 0.013) and 1/Pfankuch Index scores (R^2 = 0.79, p = 0.001)

with Axis 1, whilst pH (R^2 = 0.44, p = 0.039) and NO_3^- concentration (R^2 = 0.39, p = 0.078) were more closely aligned to Axis 2 (Figure 3.4).

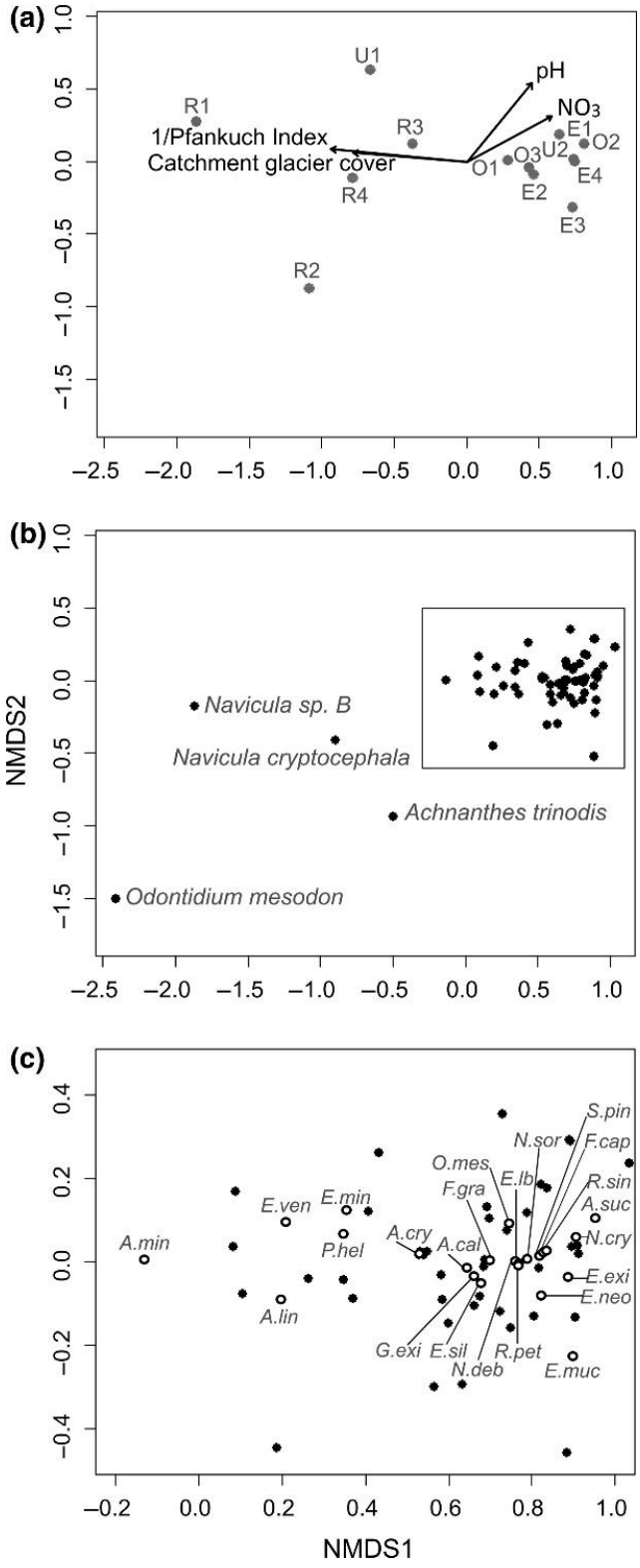

Figure 3.4 *(*a) NMDS ordination plots of river sites and significantly correlated site-specific environmental vectors, (b) NMDS biplot of diatom taxa, (c), enlargement of (b) illustrating the

position of taxa for which there was a significant correlation between estimated absolute abundance and NMDS Axis 1. Abbreviated taxon names are defined in Table 3.3.

Table 3.3 Significant ($p < 0.05$) Spearman's rank correlations (rho) between valve abundance (log_{10} (×+1)) of alpine river diatom taxa and Axis 1 of the NMDS ordination plot (Figure 3.4). R^2 (adj.) values of GLM/GAM relationships between valve abundance (log_{10} (×+1)) and catchment glacier cover, 1/Pfankuch Index scores and NO_3^- (mg L^{-1}) are also displayed. Taxa abbreviations correspond to Figure 3.4c. Relationships with a p-value < 0.001 are marked with a *. All *Achnanthidium* taxa belong to the *Achnanthidium minutissimum* complex.

Taxon	Abbreviation	Axis 1	Glacier cover (%)	1/Pfankuch	NO_3^- (mg L^{-1})
Achnanthidium minutissimum	*A. min*	0.95 *	0.52	0.83 *	0.03
Achnanthidium lineare	*A. lin*	0.94 *	0.63	0.56	0.00
Achnanthidium caledonicum	*A. cal*	0.91 *	0.22	0.72 *	0.00
Achnanthidium minutissimum var. cryptophala	*A. cry*	0.91 *	0.27	0.76 *	0.00
Adlafia suchlandtii	*A. suc*	0.72	0.65	0.42	0.19
Encyonema lange-bertalotii	*E. lb*	0.71	0.54	0.41	0.03
Encyonema minutum	*E. min*	0.90 *	0.26	0.45	0.23
Encyonema neogracile	*E. neo*	0.65	0.30	0.64	0.00
Envyonema silesiacum	*E. sil*	0.87 *	0.32	0.90 *	0.00
Encyonema ventricosm	*E. ven*	0.90 *	0.36	0.46	0.00
Eunotia exigua	*E. exi*	0.54	0.61	0.33	0.00
Eunotia mucophila	*E. muc*	0.59	0.12	0.57	0.00
Fragilaria capucina	*F. cap*	0.63	0.10	0.65	0.00
Fragilaria cf. gracilis	*F. gra*	0.90 *	0.37	0.88 *	0.00
Gomphonema exilissimum	*G. exi*	0.66	0.16	0.43	0.10
Navicula cryptotenella	*N. cry*	0.56	0.42	0.35	0.01
Nitzschia palea var. debilis	*N. deb*	0.88 *	0.82 *	0.79 *	0.11
Nitzschia soratensis	*N. sor*	0.87 *	0.81 *	0.76 *	0.03
Odontidium mesodon	*O. mes*	0.79	0.52	0.39	0.14
Psammothidium helveticum	*P. hel*	0.88 *	0.32	0.72 *	0.00
Reimeria sinuata	*R. sin*	0.88 *	0.32	0.55	0.00
Rossithidium petersenii	*R. pet*	0.77	0.21	0.42	0.06
Staurosirella pinnata	*S. pin*	0.86 *	0.62	0.74 *	0.00

3.4 Discussion

This study provided new insights into the response of alpine river benthic diatom assemblages to decreasing catchment glacier cover. The impact of glacier retreat upon microalgae remains poorly quantified in comparison to other aquatic groups (Rott et al., 2006; Fell et al., 2017) but this study has contributed three original findings. First, alpine river benthic diatom biodiversity and individual taxon densities were influenced significantly by reducing catchment glacier cover. Second, reductions in glacier cover will increase α-diversity but reduce β-diversity, with many taxa potentially becoming

threatened or rare. Third, this research predicts some diatom taxa will be winners (i.e., expanded habitat availability) but others losers in response to glacier retreat, implying a need to reclassify the conservation status of many Austrian alpine river diatom taxa.

3.4.1 Environmental parameters

Pfankuch Index scores and NO_3^- concentrations were the only measured environmental parameters significantly influenced by catchment glacier cover, although longer-term water temperature measurements collected outside of the sampling period suggest thermal drivers are also likely to be important (Appendix 2). This finding is reinforced by long-standing ideas about water temperature and channel stability being key drivers of alpine river macroinvertebrate communities (Milner and Petts, 1994; Milner et al., 2001; Brown et al. 2007b; Cauvy-Fraunié et al., 2015; Lencioni, 2018). The response of alpine benthic diatom assemblages to reducing catchment glacier cover may be driven by subsequent increases in channel geomorphological stability due to lower spatiotemporal discharge variability and riverbed movement (Biggs et al., 1998; Carrivick and Heckmann, 2017). Benthic diatom taxa can be resilient to high flow velocities, particularly those possessing streamlined forms, low motility and strong attachment to benthic substrates (Hieber et al., 2001); morphological traits expressed by *Achnanthidium* spp., *H. arcus* and *Fragilaria* spp. identified at many river sites. However, the shear stress, abrasion and scouring induced by sustained or repeated channel destabilisation resets diatom assemblage succession and restricts taxonomic richness and density (Wellnitz and Rader, 2003; Bona et al., 2012). A reduction in channel reconfiguration events linked to decreasing glacier cover may limit the abundance of generalist pioneer taxa whilst favouring species associated with later stages of succession (Biggs et al.,1998; Kelly et al., 2008). NO_3^- concentrations were significantly elevated at higher glacier cover, reflecting snowpack and subglacial sources and processing of nitrogen compounds (Wynn et al., 2007), but declined with glacier cover. Whilst there was no significant correlation between taxonomic richness or valve density and NO_3^- concentrations, elevated diatom densities at lower glacier cover sites with low NO_3^- concentrations might indicate more efficient uptake of nutrients into biofilms as glaciers are lost.

In addition to glacier runoff, precipitation and snow melt induced peak flows can destabilise river channels. As such, the low outlying taxonomic richness and diatom density values for the Rotmoosache (Figure 3.2k, l; catchment glacier cover of 30, 38, 41 and 64 %) may have been influenced by a high flow event (discharge approximately

three times the month's preflood mean) three days prior to sampling. This event would likely have contributed to sediment mobility and biofilm displacement, putting further constraints on diatom community composition alongside the effects of glacier runoff, prior to the attainment of peak flow. This finding suggested the influence of local weather conditions in combination with catchment-scale deglaciation patterns upon diatom assemblage structure (Hannah et al., 2007).

3.4.2 Diatom assemblages and biodiversity

Benthic diatom richness increased significantly with reducing catchment glacier cover. This finding is supported by previous studies based upon sampling distance from glacier margins in the Canadian Rockies (Gesierich and Rott, 2012) and comparison of alpine rivers fed by different water sources (glacier, snow melt, lake) in the Swiss Alps (Hieber et al., 2001; Robinson and Kawecka, 2005). In this study, high catchment glacier cover significantly constrained absolute abundance with total valve density at the most glacial site (~75 × 10^3 valves m^{-2}) comparable to maximum densities identified adjacent to the Ödenwinkelkees terminus (~81 × 10^3 valves m^{-2}) by Clitherow et al. (2013). Reductions in glacier cover were associated with significantly increased diatom taxonomic richness and density, particularly < 28 % glacier cover. Increases in algal biomass were noted below 11 % glacier cover in the Andes (Cauvy-Fraunié et al., 2016) and Jacobsen et al. (2012) also identified the highest α-diversity for macroinvertebrates to occur at low catchment glacier cover (5 to 30 %). Whilst the rate of increase in diatom taxonomic richness reduced below 3 % glacier cover in this study, the unimodal response observed for macroinvertebrates by Jacobsen et al. (2012) was not identified and complete deglaciation resulted in the highest diatom α-diversity.

Shannon diversity was reduced significantly following a peak at 28 % glacier cover, further indicating this threshold in diatom responses to ice loss. The harsh physicochemical conditions of sites with a high percentage of catchment glacier cover have been identified to reduce the diversity of macroinvertebrates (Brown et al., 2015), bacteria (Freimann et al., 2013), microbes (Wilhelm et al., 2013), nematodes and rotifers (Eisendle-Flöckner et al., 2013) and other diatom assemblages (Thies et al., 2013). It is important to note that the percentage glacier cover of many catchments in the Austrian Alps has already declined below 28 % cover (Koboltschnig and Schöner, 2011) and changes in biodiversity of alpine river diatom assemblages may already have begun.

The unimodal response of within-site β-diversity (Simpson) to diminishing catchment glacier cover demonstrated increased turnover at mid-levels of ice cover, suggesting elevated patchiness of diatom habitat conditions, potentially driven by the greater coexistence of grazing and competing species at these intermediate levels of physicochemical disturbance (Roxburgh et al., 2004; Khamis et al., 2016). Deglaciation and subsequent reductions in within-site β-diversity (total dissimilarity, turnover) may result from stronger biotic pressures upon diatoms (competition from other biofilm components, grazing, parasitism) within groundwater dominated flows (Khamis et al., 2016). This, coupled with reductions in the variability and magnitude of meltwater discharge pulses and more stable river beds at low glacier cover, will reduce the patchy occurrence of diatom taxa within riffle complexes, homogenising river habitats and limiting within-site β-diversity (turnover).

Changes to between-site β-diversity were driven primarily by reductions in nestedness along the gradient of glacier cover, potentially due to the absence of vulnerable cold stenothermic species or presence of groundwater-fed stream specialists assembling in rivers with lower glacier cover (Brown et al., 2007b). As diatom assemblages at sites with high catchment glacier cover appear to be comprised of taxa also found within other sampled river sites, future loss of glacier cover will further reduce β-diversity both within and between sites. This response has also been identified for invertebrates (Jacobsen et al., 2012) and bacterial communities within alpine rivers, as alterations to water sourcing associated with declining glacier cover reduces habitat variability at a landscape-scale (Freimann et al., 2013; Wilhelm et al., 2013). Aquatic groups therefore appear to express uniformity of response to the homogenisation of river habitats induced by glacier retreat, suggesting they are responding in common to physicochemical drivers and/or having strong inter-linkages via food webs.

The rivers sampled in this study were characterised by a small number of highly abundant generalist diatom species found at many sites, and a larger number of specialist species occurring exclusively at a few sites, often in low densities. The most abundant generalist taxa were those representing the *A. minutissimum* complex, which are noted for their cosmopolitan distribution along water temperature, nutrient and pH gradients, within alpine and temperate river systems globally (Potapova and Hamilton, 2007; Kelly et al., 2008). Previous research has documented the high abundance of oligotrophic, cold-adapted *Achnanthidium* spp., *Odontidium mesodon* and *H. arcus* within catchments in the Alps (Gesierich and Rott, 2004),

Himalaya (Cantonati et al., 2001) and Rocky Mountains (Gesierich and Rott, 2012). Of these, *Achnanthidium* spp. (particularly *A. minutissimum*) had a low score on Axis 1 of the NMDS ordination suggesting that these were primary colonisers in situations where channel stability was low. By contrast, species with high scores on Axis 1 (i.e. higher channel stability) tended to display a wider range of growth forms including chain-formers (e.g., *O. mesodon*, *Staurosirella pinnata*) and motile species (*Nitzschia soratensis*) that, taken together, suggest more mature biofilms subject to less disturbance and increased competition (Biggs et al., 1998).

Two species (*C. lancettula, E. trinacria*) were identified exclusively at river sites ≥ 52 % glacier cover. Although these taxa are not documented as cold stenothermic species and display a diversity of habitat preferences in non-alpine catchments, their low motility may drive geographical and genetic isolation within fragmented deglaciating watersheds, despite their tolerance of local habitat conditions (Liu et al., 2013; Dong et al., 2016; Lange-Bertalot et al., 2017). Nineteen taxa were defined on the Red List as threatened, endangered, decreasing or rare (Lange-Bertalot and Steindorf, 1996). *Achnanthidium caledonicum*, listed as endangered, was identified in relatively high abundance at nine sites, suggesting that Austrian alpine rivers may act as a refuge for this species. Previous attention has been drawn to the regional importance of alpine springs as habitats of high freshwater diversity (Cantonati et al., 2012), but the occurrence of *A. caledonicum* at sites influenced by variable catchment glacier cover highlights the requirement to conserve a diversity of alpine rivers to protect rare benthic diatom taxa.

In contrast to threatened taxa, glacier retreat could promote habitat expansion for some species, as reduced meltwater inputs lead to greater groundwater contributions in upstream reaches, opening up possibilities for range expansion of taxa which are specialised to river sites with no glacier cover, following a trend identified for macroinvertebrates (Brown et al., 2007b; Cauvy-Fraunié et al., 2015). For example, seven of the sampled diatom taxa may benefit from deglaciation and have previously been recorded in alpine rivers (e.g., *S. agrestis*), springs (e.g., *M. circulare*) (Falasco and Bona, 2011) and acidic wetland (e.g., *C. mediocris, G. calcareum*) (Buczkó and Wojtal, 2005), disconnected from glacier cover. Deglaciation could be particularly beneficial for populations of *C. mediocris* and *G. calcareum* which are currently noted on the Red List of Algae for Germany as having decreasing populations (Lange-Bertalot and Steindorf, 1996). Whilst maintenance of glacier cover required by some

diatom taxa will not be possible, other threatened taxa could clearly benefit from the expansion of their low glacial habitats. Alpine freshwater conservation strategies therefore need to prevent additional environmental pressures, including those imposed by water abstraction, hydroelectric power facilities, nutrient pollution and tourist infrastructure, which can impact upon both benthic diatoms and the wider aquatic biota in a variety of alpine river types (Khamis et al., 2014a).

Despite broad geographical use of the Red List for identifying the conservation status of river diatoms (Cantonati et al., 2001; Gesierich and Rott, 2004, 2012), application beyond its German reference sites may constrain accurate identification of localised variance in diatom abundances or characterisation of endemic taxa (Falasco and Bona, 2011). Whilst not all sampled species were covered by the list, which has not been revised since 1996, it remains the most complete reference of potentially imperilled diatom taxa (Falasco and Bona, 2011). However, this study suggested a need for reclassification of current Red List conservation status for the six taxa found exclusively ≥ 28 % glacier cover, if they are not identified in other types of river environment. Sustained deglaciation will alter the distribution and persistence of the habitats upon which they depend (Brown et al., 2007a; Fell et al., 2017). Status changes may also be required for the 23 species whose abundance significantly correlated to NMDS Axis 1 (Figure 3.4) and in turn, to the aligned environmental vectors of catchment glacier cover and channel stability.

3.4.3 Wider implications of the diatom assemblage response

Overall this study has demonstrated the sensitivity of alpine benthic diatom biodiversity to reducing catchment glacier cover, a scenario predicted to continue across Austria and the wider European Alps throughout the twenty-first century (Zemp et al., 2006; IPCC, 2013). An important implication of this research is that alteration to diatom assemblage structure could have cascading impacts for higher trophic levels (Woodward, 2009; Clitherow et al., 2013), given their role in providing energy to alpine river food webs (Rott et al., 2006) as principal primary producers and the predominant dietary component of cold-adapted macroinvertebrates (Clitherow et al., 2013). Greater numbers of studies adopting gut contents analysis for alpine macroinvertebrates are needed to determine the extent to which grazing consumers are selective feeders and the potential implications of glacier retreat and environmental warming upon capture mechanisms and feeding behaviours (Gordon et al., 2018).

The ablation rates of individual glaciers are influenced by interacting controls including catchment geomorphology and altitude, basal motion dynamics and local weather conditions, leading to spatiotemporally variable and often non-linear retreat sequences and runoff patterns within glacierised valleys and across alpine regions (Zemp et al., 2006; Huss, 2012; Robson et al., 2016). Whilst a catchment glacier cover chronosequence cannot fully capture this complexity, this research demonstrated that the approach provided a rapid, remote and effective means of quantifying glacier retreat impacts on diatom communities in addition to other biotic components of river ecosystems (Rott et al., 2006; Brown et al., 2007a; Cauvy-Fraunié et al., 2015, 2016; Ren et al., 2017a). Further research is now required in other alpine regions to determine whether the identified response of benthic diatom assemblages to a shrinking cryosphere can be generalised to glacier-fed rivers globally, as evidenced recently for macroinvertebrates (Brown et al., 2018).

Chapter Four: Decreasing glacier cover reveals predictable successional changes in the structure and allometry of river food webs

4.1 Introduction

Many glacierised mountain regions are characterised by rapid and accelerating ice loss (Huss et al., 2017; Beniston et al., 2018). This is altering the flow rate of meltwater inputs to proglacial rivers and subsequently modifying their thermal regime, geomorphic stability and physicochemistry (Milner et al., 2009; Bliss et al., 2014; Huss and Hock, 2018). With many of the world's rivers originating from alpine headwaters, changes to the trophic organisation of food webs will potentially influence aquatic community structure and ecosystem functioning far downstream (Milner et al., 2017). Understanding biotic responses to these changes is critical to inform conservation strategies to limit impacts upon freshwater species and the ecosystem services which they support (Tank et al., 2010; Milner et al., 2017).

Food webs act as the architecture connecting species and underpinning their provision of ecosystem functions (Woodward, 2009). Connectance, trophic and trivariate food web properties describe the structure, trophic interactions and energy transfer efficiencies which influence network sensitivity to natural and anthropogenically driven disturbance gradients (Dunne et al., 2002a; Bersier et al., 2002; Cohen et al., 2009; Woodward et al., 2012). Food web structural and allometric (size-based) change along environmental chronosequences can provide insight into temporal developments in community assembly and natural successional processes (Wardle et al., 1995), but this approach remains rare for freshwater systems (O'Gorman et al., 2012; Layer et al., 2012). Widespread glacier shrinkage initiates primary succession of new aquatic habitats (Milner et al., 2011; Brown and Milner, 2012), providing opportunities to enhance understanding of whole food web assembly. Individual species and community responses to glacier retreat have been studied in some detail (Fell et al., 2017), but the emergent and dynamic properties of ecological networks potentially prevent ecosystem-scale characteristics from being extrapolated from these lower levels of organisation (Woodward, 2009; Woodward et al., 2010a).

Current understanding of individual species feeding linkages in glacierised river systems remains limited because most previous research has constructed food webs

using stable isotope approaches (SIA), which are characterised by coarse taxonomic resolution and lack quantification of food web architecture and size structure (Woodward et al., 2005). However, SIA studies suggested these food webs to be dominated by macroinvertebrate-algal feeding relationships with consumers employing opportunistic, flexible and omnivorous feeding strategies to capitalise upon limited autochthonous resource supply, particularly as glacier-fed rivers above the treeline receive minimal riparian energy subsidy (Zah et al., 2001; Füreder et al., 2003; Fellman et al., 2015; Perić et al., 2015). Direct observation of feeding relationships through gut contents analysis (GCA) can determine interactions between individual species (nodes), which critically influence food web stability, energy flux and response to environmental perturbation (Dunne et al., 2002b; Brown et al., 2011; Lu et al., 2016; Rosi-Marshall et al., 2016). In glacierised alpine catchments, GCA has been used only to determine predation relationships (*Perla grandis,* Diamesinae, Orthocladiinae) (Khamis et al., 2015; Niedrist and Füreder, 2018) and community feeding linkages for one stream with high glacier influence (Clitherow et al., 2013). GCA food webs are required urgently along a gradient from highly-glacial to non-glacial alpine rivers to quantify how whole river ecosystems will respond to future glacier recession.

Food web dynamics studied in other river systems can offer insight into the potential effects of physicochemical and geomorphic alterations imposed by glacier retreat. For example, research spanning geothermal streams in a cold, sub-arctic environment highlighted that increasing water temperature reduced network complexity, stability and connectance, with node biomass alterations dependent upon the thermal tolerance of taxonomic groups (Woodward et al., 2010b; O'Gorman et al., 2012). River channel stability, which increases as glacier influence declines, has been identified to increase predator density, basal and primary consumer biomass and linkage density, with mean chain lengths found to both increase in Arctic rivers (Parker and Huryn, 2006) yet remain invariant in temperate streams (Townsend et al., 1998). In contrast, greater flow intermittency, which is predicted to accompany rapid ice loss in many alpine catchments (Robinson et al., 2016), can temporarily reduce temperate river node abundance, biomass, linkage density (Woodward et al., 2012) and mean chain length (Sabo et al., 2010). It can be expected that river food webs will be influenced concurrently by both the magnitude of reach-scale physicochemical alteration and seasonal variability in discharge volume imposed by glacier retreat. Food webs may undergo overall increases in mean chain length and taxon biomass, as glaciers retreat.

Nine new river food webs derived from GCA along a chronosequence of catchment glacier cover in the central Austrian Alps are presented. While previous research has considered the influence of single components of climate change (e.g., increased water temperature, O'Gorman et al., 2012) upon freshwater webs, this study was designed to capture responses to deglaciation and multiple associated river physicochemical characteristics. This research aimed to test the following hypotheses: (H_1) connectance and trophic food web descriptors, including numbers of nodes, links and chains, will increase with reducing catchment glacier cover, as ice loss increases species abundance and biomass; (H_2) alpine river food webs will be characterised by high directed connectance and short mean food chains lengths, as previously identified for glacier-fed streams, and (H_3) for trivariate networks, mass- (M) abundance (N) regression slopes will remain consistent across food webs, despite reducing catchment glacier cover, as metabolic theory predicts their invariance to environmental disturbance (Brown et al., 2004). Connectance and size structure components were considered together to investigate both food web resolution and quantification (Woodward et al., 2005). This study presented the first description of alpine river food web structure and allometric responses to a quantified gradient representative of glacier retreat and in turn, provided novel evidence of whole aquatic food web assembly along a natural successional gradient.

4.2 Methods and materials

4.2.1 Study area and site selection

Field observations were made at nine river sites across the Hohe Tauern region of the central Austrian Alps, in June and July of 2015 and 2016. This area is characterised by catchments with variable areas of permanent ice cover which share comparable altitude, meteorology and geology (Robson et al., 2016). River sites were positioned across the Eisboden, Obersulzbach and Rotmoos valleys to represent a gradient of 0 to 64 % catchment glacier cover (Appendix 1). To obtain this range of glacier cover, samples were obtained from rivers with a variety of water sources, including channels draining glacier ice, their tributaries, groundwater sourced streams and mixed rivers which were fed by meltwater, aquifer upwelling and spring inputs. Sampling was conducted in riffle complexes as they are a prevalent mesohabitat of glacier-fed mountain rivers and have previously been identified to host greater aquatic invertebrate abundance and richness than pools (Brown and Brussock, 1991).

The catchment glacier cover pertaining to individual river sites was identified remotely using the watershed analysis function of ESRI ArcMap™10.4. To identify river network drainage patterns and automate catchment boundary delineation, flow direction and accumulation models were run upon a filled 10 m ASTER Digital Elevation Model (GitHub, 2016). Boundaries were then checked and refined manually against high-resolution aerial photography. The percentage area of each catchment permanently covered by glacier ice was determined by matching existing maps of glacier outlines (Glaciology Commission, 2015) to sample site watershed boundaries. Initially, ice cover was determined for sites positioned randomly along rivers of each catchment, with those representing the broadest available range of catchment glacier cover selected, provided aerial photography indicated site accessibility. Positioning of sites in river channels at varying distances from individual glacier margins was avoided where possible to limit pseudoreplication.

4.2.2 Field sampling

At each site, macroinvertebrates were sampled with five replicate Surber samples (0.1 m^2, 250 µm mesh net) collected randomly from riffles. Further material was obtained for GCA from bulk samples hand-picked from benthic sediments. To sample biofilms, a standardised area (9 cm^2) of the upper surface of five randomly selected large, fully submerged cobbles were scrubbed with a sterile toothbrush (CEN, 2014). Biofilm samples from site E5 were unavailable due to damage during transport. All biological samples were immediately preserved in 70 % methylated spirits and stored at 4 °C. At each site, water temperature, electrical conductivity and pH were measured with Hanna Instruments (Woonsocket, Rhode Island, USA; HI 9063, HI 9033, HI 98130). Pfankuch Index bottom components (Pfankuch, 1975) were estimated to characterise the stability of channel geomorphology, with reciprocals calculated (1/Pfankuch Index scores) so that lower scores represented less stable stream environments. River water (100 mL) was collected for the ex-situ analysis of optical turbidity and water chemistry. Turbidity was measured using a desktop turbidimeter (HACH 2100A) (Camlab, Cambridge, UK). Nutrient concentrations (phosphate (PO_4^{3-}), nitrate (NO_3^-), total nitrogen (TN)) and dissolved organic carbon (DOC) were detected using an Analytik Jena Multi N/C 2100 elemental thermal oxidation analyser and Two Skalar San ++ Continuous flow auto-analyser.

4.2.3 Laboratory analysis

Surber samples were passed through a standardised 250 µm mesh sieve, to remove inorganic material yet retain small river macroinvertebrates. Sieves were sonicated for 10 min between sites to prevent cross-contamination. All macroinvertebrate individuals were counted and identified to the highest possible resolution following published keys (Appendix 3.1). Identification focused upon invertebrate and periphyton species because they provide the densest linkages in aquatic systems, dominate links in high alpine rivers which typically lack fish populations, and can be quantified microscopically.

Identification of Chironomidae larvae and diatom taxa required digestion procedures to remove organic materials and enable clear observation of head capsule and valve structures. For Chironomidae larvae, individuals from Surber replicates were sorted to genus at x 25 magnification and subsampled according to their proportional contribution to the site community. A minimum of 50 individuals were selected per site unless fewer were present (Brown et al., 2016). Bulk samples were used to increase sample numbers for GCA where available. Individual head capsules were cleared in 10 % potassium hydroxide (KOH) in a water bath (75 °C ± 5 °C) for 15 min and neutralised in 100 % acetic glacial acid for 5 min. Capsules were then dehydrated in 70 % methylated spirit and mounted ventrally in Euparal (Agar Scientific, Stansted, UK) (Brown et al., 2016). For diatom taxa, a homogenised 5 mL biofilm subsample was added to 20 mL of 30 % hydrogen peroxide (H_2O_2) in a water bath (90 °C ± 5 °C) for 3 hours. Remaining H_2O_2 was neutralised using 50 % hydrochloric acid (HCL) and the pellet washed with deionised water by centrifuge at 1200 rpm for 4 min. The centrifuge process was repeated four times (CEN, 2014). Following final aspiration of the supernatant, the pellet was diluted by the addition of 5 mL to 20 mL of deionised water, dependent upon diatom concentration. A 0.5 mL subsample of the resulting suspension was pipetted onto a sterile coverslip, air dried and mounted in Naphrax® (Brunel Microscopes Ltd, Chippenham, UK). A minimum of 500 complete diatom valves were identified where available, to characterise the species composition of individual replicates. To determine diatom density in biofilm samples, the number of valves counted in coverslip transects was used to estimate the total number across the coverslip and multiplied to represent the standardised sample area (Fell et al., 2018). Diatom densities were averaged for each site prior to further analyses. Chironomid larvae head capsules and diatom valves were observed with high-power, oil immersion light microscopy (Leica DM 195 2000, N Plan lens 100x/1.25 oil PH3) (Leica, Milton

Keynes, England) at x 1000 magnification in brightfield view and identified following taxonomic keys (Appendix 3.1).

Non-diatom biofilm components were identified and counted using a Mod-Fuchs Rosenthal Haemocytometer (8.S.748) (depth = 0.2mm) (Hawksley, Lancing, England) (Appendix 3.1). Five 25 µL homogenised subsamples were taken from individual biofilm replicates and all items in the cell counting chamber analysed (625 µL screened per site). The Haemocytometer was swabbed with ethanol between samples to prevent cross-contamination.

To construct a food web for each of the nine sites, feeding relationships were observed directly using GCA of aquatic consumers. Prior to their dissection, the linear body length of individual invertebrate consumers was measured to the nearest 0.01 mm, using a low-powered microscope (Brunel Microscopes Ltd, Wiltshire, UK) and calibrated optical micrometer eye piece at x 25 magnification. Length equated to distance between the head anterior and final abdominal segment posterior (Smock, 1980). Using superfine dissecting forceps, scalpels and pins, the foregut and lining were removed at x 25 magnification. The lining was subsequently discarded and the contents dispersed across a glass slide and secured with Euparal. Gut dissection was not possible for a limited number of very small juvenile Plecoptera, which were mounted whole. Coverslips were scanned at x 200 magnification and organic prey items identified to the lowest practical resolution given the constraints of partial digestion upon classification. GCA items were counted and their length, width and where possible depth measured to the nearest 0.001 mm using a calibrated eye piece graticule at x 1000 magnification. The head capsule width of ingested macroinvertebrate prey was measured, alongside the dimensions of fragmented invertebrate body components. Where ingested head capsules were identified, isolated body fragments were only treated as belonging to additional individuals if their abundance exceeded that attributable to the head capsule species. This approach assumed freshwater invertebrate prey to be consumed whole (Brose et al., 2006). For ingested diatoms, a subsample were measured, with the dimensions of approximately 20 % of each species recorded at each site (or a minimum of 20 measurements per species, unless fewer were available) (CEN, 2015). Inorganic materials (e.g., rock fragments) were noted but not included in food web metric calculations.

GCA may underestimate the abundance of quickly digested materials or those too fragmented for identification. Furthermore, it cannot determine long-term dietary selections or the environmental origin of specific resources (Rosi-Marshall et al., 2016). However, unlike mapping of stable isotopes, direct observation of the gut contents can provide high-resolution taxonomic identification for prey items and describe connections between individual species (Michener and Lajtha, 2007; Rosi-Marshall et al., 2016). It also removes reliance upon naturally variable isotopic signatures which can be affected by fluctuations in flow velocity (Michener and Lajtha, 2007), a daily occurrence in many meltwater-fed alpine rivers (Beniston et al., 2018).

Ash free dry mass (AFDM) was determined to provide a representation of the biomass of amorphous detritus at each river site. Following the sorting and identification of biota, Surber samples were drained of their 70 % methylated spirit preservative and replicate samples combined to represent single river sites. Samples were placed in pre-weighed ceramic dishes, oven dried for approximately 24 h at 105 °C and then stored in a desiccator until repeated measurements identified a constant weight (Steinman and Lamberti, 1996). Samples were ashed for 1 h in a furnace at 550 °C, then cooled and reweighed. Ash free dry mass (mg) was calculated by subtracting this final weight from that of the initial oven dried sample (Steinman and Lamberti, 1996).

4.2.4 Data analysis

Observed feeding linkages for each river site were combined into a food web matrix to show all direct connections between consumers and resources. To ensure links were represented as fully as possible, webs included all consumers for which at least five individuals were available (Ledger et al., 2013; Rosi-Marshall et al., 2016). Terrestrially sourced materials (e.g., pollen) and semi-aquatic taxa were defined as active resources and incorporated into food webs if identified in consumer gut contents. These invertebrate-centric webs focused primarily on the larval phase of insects and engulfing consumers, as prey items were not individually identifiable for taxa with suctorial feeding mechanisms (e.g., Trombidiformes, Tricladida) (Brown et al., 2011). These predators represented a very small number of observations (< 5 % of macroinvertebrates) and so were unlikely to have significantly altered food web interactions. Invertebrate prey found in gut contents but not in the benthos of a specific site (perhaps drifting prey) were excluded as they would have been represented as basal taxa in food webs. As freshwater food webs are strongly size structured and most consumers eat prey of a smaller body size (Brose et al., 2006), ingested Chironomidae

larvae fragments that were difficult to identify (i.e. those where the head capsule was absent) were assigned to taxa that were found in the same replicate Surber as the consumer, but only if individuals of those taxa were smaller than the consumer. If these smaller individuals belonged to two or more species, prey were attributed to a single genus (e.g., *Diamesa*) or family (Chironomidae) node. Rotifers, nematodes, protists and protozoans were incorporated into food webs (Schmid-Araya et al., 2016) via inferred links to amorphous detritus because their extremely small size limited GCA. This enabled their inclusion in connectance food webs without representing them as basal taxa. Food webs were analysed using the *cheddar* package of R 3.2.2 (Hudson et al., 2016) and visualised using FoodWeb3D (Yoon et al., 2004).

Yield effort curves were constructed using the *specaccum* function of the *vegan* package of R (Oksanen et al., 2017), to determine if a sufficient number of macroinvertebrate guts had been analysed to accurately describe the feeding linkages of the food web at each river site. Curves plotted the cumulative number of guts analysed per macroinvertebrate family or species (dependent upon identification resolution) against the cumulative number of identified resources, and randomised the analysis order 1000 times (Appendix 3.2).

Connectance network descriptors were calculated for each of the nine webs following Bersier et al. (2002). Metrics included taxonomic richness (number of nodes, *S*), the number of links between taxa (number of trophic links, *L*), the density of these linkages (linkage density, *L/S*) and the proportion of potential trophic linkages which were realised (directed connectance, L/S^2). The fraction of nodes defined as basal (B), intermediate (I) and top (T) taxa were calculated, alongside the proportion of links connecting these groups. Chain lengths were equivalent to the number of nodes per chain. Feeding relationships were described by the fraction of taxa which consumed resources located on different trophic levels (omnivory), the mean number of prey eaten by each consumer (trophic generality) and the mean number of consumers eating each prey species (trophic vulnerability). The ratio of resource to consumer taxa was also calculated for each site.

Path lengths, defined as the number of trophic links connecting all pairs of nodes, were calculated for each food web. Characteristic path length, the average of all individual path lengths, was then determined to investigate applicability of the two degrees of separation theory (Williams et al., 2002). To explore the extent to which each network

displayed random or scale-free network organisation (Dunne et al., 2002a), mean degree distributions were computed and cumulative degree distributions plotted, with distribution models (power-law, exponential, linear) fitted and R^2 values used to retain the model which best characterised each river site. Global average clustering coefficients were calculated using the *transitivity* function of the *igraph* package of R (Csardi and Nepusz, 2006). Values for each food web were compared to those representing the mean clustering coefficient of 1000 random networks constructed to host identical numbers of nodes and links, using the undirected Erdos-Renyi model.

Biomass (*M*) and abundance (population density; *N*) information were attributed to food web nodes to investigate the influence of glacier retreat on allometric scaling relationships for seven food webs. Sites E5 and U1 were omitted from this analysis because biofilm density data were missing; E5 due to sample damage, and U1 because the species found in consumer guts were absent from the benthos. Counts of all macroinvertebrate and biofilm taxa were scaled to estimate density m^{-2}. To calculate biomass (mg) for Chironomidae larvae and ingested macroinvertebrates, body length was estimated following published regressions with head capsule width (Smock, 1980). Biomass was calculated from body length for all macroinvertebrates using genera, or when available, species-specific regression constants (Smock, 1980; Nolte, 1990) (Appendix 3.3). Dimensions of invertebrates from the Surber samples were used to inform a series of site- and genera-specific length-biomass regressions (Appendix 3.4). These enabled dimensions of body components from macroinvertebrate prey which had become fragmented in the gut, to be used to estimate the biomass of entire individuals, prior to their consumption. Following the European Standard protocol (CEN, 2015), ingested periphyton (e.g., diatoms, desmids, algae, cyanobacteria) were assigned shape categories based upon their length, width and depth measurements, which informed standardised equations used to determine biovolume (Appendix 3.3). Where depth was not visible microscopically, equations provided by the protocol were used to estimate this dimension, and in their absence, depth was assumed to equal width for small freshwater algae (Sun and Lui, 2003; CEN, 2015). Biovolume was converted to biomass using the regression constants of Menden-Deuer and Lessard (2000) (Appendix 3.3).

MN relationships primarily represented macroinvertebrate-periphyton feeding linkages. *M* could not be determined for taxa which lacked published body-size and biomass regressions (e.g., rotifers, nematodes, testate amoeba), whose components in the gut

expressed no relationship to measured taxon body lengths (e.g., claws, spines, tails) or were too damaged to do so (e.g., folded head capsules). *N* could not be calculated for resources which were present in macroinvertebrate guts but absent from Surbers or biofilm scrubs, as m^{-2} abundance (population density) estimates were derived from site-specific samples. Amorphous detritus had no measurable *N*. Calculation of size-based food web descriptors followed Cohen et al. (2009) in the *cheddar* package of R (Hudson et al., 2016). This included determination of the number of food chains per web. The multitrophic statistic community span described the range of *M* and *N* values across whole food webs. Mean count chain length referred to the number of trophic links in a food chain and the mean sum chain length comprised the total length of these links.

Ordinary least squares (OLS) linear regressions were determined for both species-averaged and individual $\log_{10} M$ and $\log_{10} N$ relationships. OLS analysis was performed in base R, with R^2 values used to assess regression significance. Resulting scaling coefficients were compared to those predicted by metabolic theory (individual = -1.00, species-averaged = -0.75) (Brown et al., 2004) and correlated to catchment glacier cover, to determine universality of the *MN* relationships. For *MN* correlations for individual taxa, the biomass of all measured periphyton and macroinvertebrates were placed into size bins of 1 on the $\log_{10}$ scale, with *M* represented as the centre point of every biomass bin and *N* as the number of individual taxa found in each (O'Gorman, 2012). For consumers where biomass was determined for a subsample of the collected population (e.g., Chironomidae), random numbers were drawn from a lognormal distribution with mean and standard deviation values equal to those of the subsample, to estimate biomass for the unmeasured taxa. For resources (e.g., diatoms), the number of measured taxa was determined as a proportion of the total counted per site, and this value used to extrapolate the number of individuals found in each size bin, to represent unmeasured taxa. All invertebrate and periphyton biomass estimates were represented m^{-2}. For Figure 4.3, amorphous detritus biomass was added to periphyton biomass to represent food web basal resource availability.

Relationships between catchment glacier cover and all connectance and trophic food web descriptors were tested using generalised linear models (GLM) and generalised additive models (GAM) in the *mgcv* package of R (Wood, 2011). For GAM, smoothing parameter selection followed Wood (2004). Model fit was assessed using Akaike information criterion, which identified Negative binomial and Gaussian distribution

families as the most parsimonious solutions. The percentage of deviance explained was used to evaluate model performance. GLM and GAM were also used to investigate relationships between physicochemical and nutrient variables and all food web descriptors, alongside correlations between taxonomic richness and abundance (m^{-2}) of macroinvertebrates and diatoms and catchment glacier cover. Analyses were undertaken with and without site O3 due to its position approximately 3.3 km downstream of the Obersulzbachkees proglacial lake. These features have been documented to attenuate the physicochemical conditions imposed by meltwater inputs (Milner and Petts, 1994; Brittain et al., 2001; Milner et al., 2001; Hieber et al., 2001) and in turn, cause catchment glacier cover to be an unreliable predictor of river habitat response. GLM and GAM were also used to test the association between basal, primary consumer, predator and whole web biomass and catchment glacier cover.

4.3 Results

4.3.1 Alpine river biodiversity

A total of 8,437 individual macroinvertebrates were identified across the nine alpine river sites. These included Coleoptera (2), Collembola (54), Diptera (7,407), Ephemeroptera (449), Plecoptera (462), Tricladida (2), Trichoptera (59) and Hydracarina (2) (Appendix 3.5). Mean macroinvertebrate density ranged from 78 to 5114 individuals m^{-2}, with taxonomic richness and density increasing significantly with reducing catchment glacier cover (Table 4.1; Appendix 3.6). Predatory taxa included Simuliidae, Nemouridae spp. and individuals representing the *Baetis alpinus* group. Biofilm samples were dominated by diatom valves (71 taxa), with *Gomphonema*, *Eunotia, Nitzschia* and *Encyonema* the most abundant genera across sites. Although patchily distributed in riffle microhabitats, mean benthic diatom density ranged from 15111 to 3.2×10^8 valves m^{-2} and increased significantly with reducing glacier cover, alongside taxonomic richness (Table 4.1; Appendix 3.6). Biofilm samples also hosted desmids, filamentous green algae, golden algae, fungal spores, plant detritus, testate amoeba and tardigrades (Appendix 3.5).

4.3.2 Food webs

GCA of 737 aquatic macroinvertebrate consumers directly identified 9,027 feeding interactions across the river food webs. Volumetrically, guts were dominated frequently by rock fragments and amorphous detritus, defined as a conglomeration of fine particulate organic matter and partially digested materials (bacteria, microbes, polysaccharides) lacking identifiable cellular structure (Carlough, 1994). Additional gut

contents items included macrobenthos (whole and fragmented macroinvertebrates), meiobenthos (rotifers, nematodes, protists, testate amoeba, ciliates), microbenthos (cyanobacteria, aquatic fungi, filamentous and unicellular green algae, golden algae, microalgae (diatoms, desmids)) and tree, plant and bryophyte material (leaf cells, spores, pollen) (Appendix 3.5). Feeding interactions were dominated by macroinvertebrate-periphyton linkages (Figure 4.1) though yield effort curves suggested that estimates should be considered conservative (Appendix 3.2).

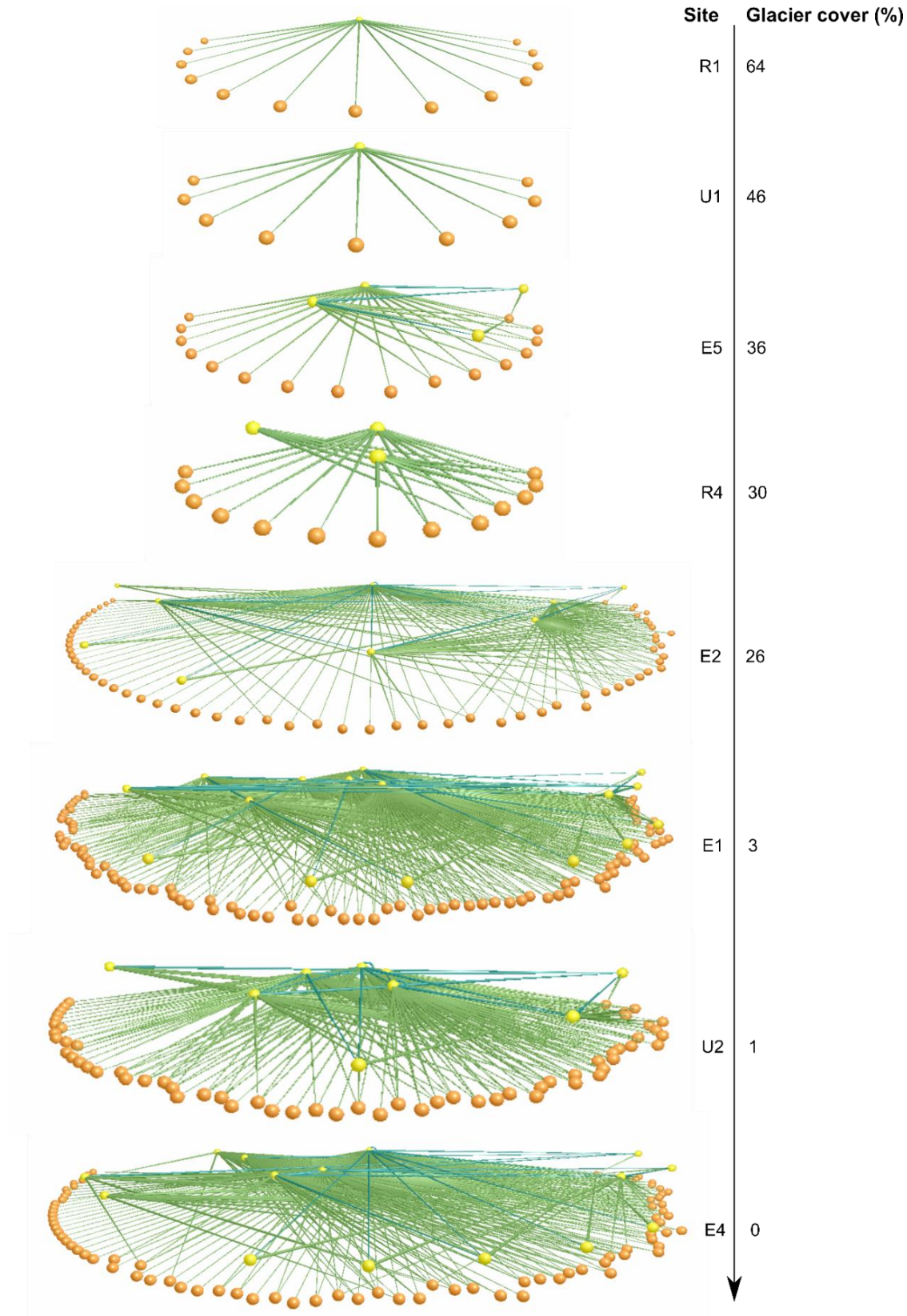

Figure 4.1 Structural alteration of alpine river food webs along a gradient of reducing catchment glacier cover (%). Nodes are defined in Appendix 3.7. Colours differentiate basal nodes (orange circles), consumer nodes (yellow circles), links connecting basal and intermediate nodes (green lines) and linkages between intermediate and top nodes (blue lines).

Catchment glacier cover was associated significantly with fourteen connectance and three trophic descriptors (Appendix 3.8) across the eight alpine river food webs (Figure 4.2, Table 4.1). Reductions in glacier cover significantly increased the number of nodes and both the number and density of linkages which connected them (Figure 4.2a, d, e). The number of food chains also increased, alongside mean and maximum chain lengths (Figure 4.2o, i, j). There were linear increases in the fraction of food web taxa defined as intermediate (non-basal taxa with one or more consumer) and subsequently both increases in the proportion of web links occurring between these intermediate taxa and their basal resources. Subsequently, there were linear reductions in the proportion of links connecting top and basal species (Figure 4.2c, f, g, h). The ratio of resources to consumers showed a unimodal response to reducing catchment glacier cover, with the lowest values identified at approximately 26 % glacier cover (Figure 4.2b). Decline in glacier cover < 26 % was associated with marked increases in the number of nodes (Figure 4.2a), links (Figure 4.2d) and chains (Figure 4.2o).

Reductions in glacier cover were associated with a linear increase in the mean number of consumers ingesting each resource taxa and a linear decrease in the mean number of resource taxa being ingested by each consumer (Figure 4.2m, n). Both mean sum chain lengths and community span were lowest at sites with high glacier cover and increased significantly with ice loss. This increased the total orders of magnitude spanned by taxa biomass and abundance across individual food chains and entire food webs, respectively (Figure 4.2p, q). In contrast, directed connectance and omnivory were not associated with catchment glacier cover (Appendix 3.8). Twelve descriptors for site O3, positioned downstream of a proglacial lake, were higher than expected from the GAM and GLM, with values aligning to river reaches with much lower glacier cover in non-lake-fed catchments (Figure 4.2). Given that this site acted as a major outlier in much of the analyses, its inclusion resulted in fewer significant GAM and GLM relationships and a reduced significance for those which were retained (Appendix 3.9).

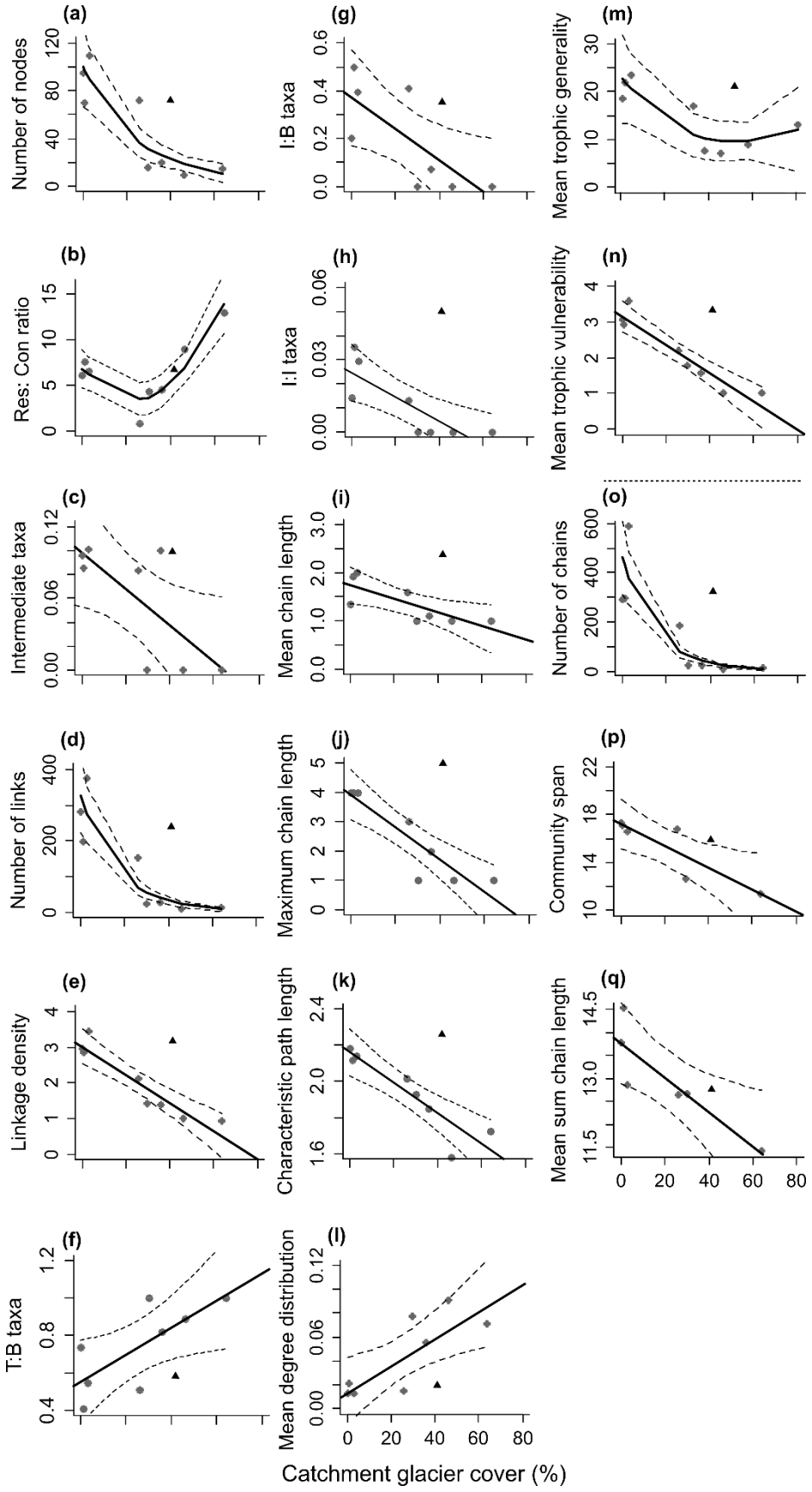

Figure 4.2 Significant GAM/GLM relationships between connectance (a to n) and trophic descriptors (o to q) of alpine river food webs and catchment glacier cover. Res = resource, Con

= consumer. Descriptors are defined in Section 4.2.4. Site O3 (black triangles), which was positioned downstream of a proglacial lake, was not included in the GAM/GLM analysis. Black lines represent lines of best fit (solid) and 95 % confidence intervals (dashed). Model statistics are presented in Table 4.1.

Table 4.1 GAM/GLM statistics for relationships between catchment glacier cover and environmental parameters, biodiversity metrics, connectance and trophic food web descriptors and biomass. Significant correlations between catchment glacier cover and food web metrics are displayed in Figure 4.2, with biomass relationships shown in Figure 4.3. Relationships between catchment glacier cover and biodiversity metrics are illustrated in Appendix 3.6.

Dependent variable	Model (Distribution)	χ^2 / *F*	*p*-value	Deviance explained (%)
Environmental parameters				
Water temperature	GLM (Gaussian)	2.56	0.161	29.9
EC	GLM (Gaussian)	2.20	0.188	26.9
pH	GLM (Gaussian)	0.54	0.490	8.3
1/ Pfankuch Index	GLM (Gaussian)	5.67	0.055	48.6
Turbidity	GAM (Negative binomial)	26.65	< 0.001 ***	74.4
TN	GAM (Negative binomial)	18.35	0.005 **	88.0
TP	GLM (Gaussian)	0.36	0.576	6.7
Biodiversity metrics				
Macroinvertebrate				
Density	GAM (Negative binomial)	129.60	< 0.001 ***	42.0
Taxonomic richness	GAM (Negative binomial)	21.78	< 0.001 ***	90.2
Diatom				
Density	GAM (Negative binomial)	1257	< 0.001 ***	56.2
Taxonomic richness	GAM (Negative binomial)	20.80	< 0.001 ***	80.7
Connectance descriptors				
Node properties				
Number of nodes	GAM (Negative binomial)	46.73	< 0.001 ***	74.9
R: C ratio	GAM (Gaussian)	13.16	0.010 *	84.0
Top taxa	GAM (Gaussian)	1.52	0.306	37.7
Intermediate taxa	GLM (Gaussian)	7.16	0.037 *	54.4
Basal taxa	GAM (Gaussian)	3.46	0.114	58.1
Link properties				
Number of links	GAM (Negative binomial)	120.00	< 0.001 ***	80.7
Linkage density	GLM (Gaussian)	45.10	< 0.001 ***	88.3
Directed connectance	GLM (Gaussian)	5.04	0.066	45.6
T: B taxa	GLM (Gaussian)	7.34	0.035 *	55.0
T: I taxa	GLM (Gaussian)	0.65	0.450	9.8
I: B taxa	GLM (Gaussian)	7.69	0.032 *	56.2
I: I taxa	GLM (Gaussian)	12.34	0.013 *	67.3
Chain properties				
Mean chain length	GLM (Gaussian)	9.37	0.022 *	61.0
Maximum chain length	GLM (Gaussian)	27.96	0.002 **	82.3

Table 4.1 – continued

Dependent variable	Model (Distribution)	χ^2 / *F*	*p*-value	Deviance explained (%)
Characteristic path length	GLM (Gaussian)	28.93	0.002 **	82.8
Mean degree distribution	GLM (Gaussian)	11.62	0.014 *	65.9
Feeding relationship properties				
Omnivory	GLM (Gaussian)	4.34	0.082	42.0
Mean trophic generality	GAM (Negative binomial)	7.69	0.021 *	71.1
Mean trophic vulnerability	GLM (Gaussian)	53.83	< 0.001 ***	90.0
Trophic descriptors				
Number of chains	GAM (Negative binomial)	151.20	< 0.001 ***	79.5
Community span	GLM (Gaussian)	13.93	0.020 *	77.7
Mean sum chain length	GLM (Gaussian)	13.64	0.021 *	77.3
Biomass				
Basal	GAM (Negative binomial)	22.9	< 0.001 ***	63.5
Primary consumer	GAM (Negative binomial)	119.4	< 0.001 ***	33.8
Predator	GAM (Negative binomial)	333.6	< 0.001 ***	63.9
Total	GAM (Negative binomial)	221.2	< 0.001 ***	51.5

Characteristic path length spanned 1.58 to 2.18 across the eight food webs and increased significantly with declining catchment glacier cover (Figure 4.2k). Over 73 % (73.5 to 100 %) of taxa were connected by two or fewer trophic linkages and over 82 % (82.7 to 100 %) by three or fewer links, except for U2 (≤ two links: 54 %; ≤ three links: 66 %). There was a significant linear decrease in the percentage of taxa connected by two or fewer links with reducing glacier cover (R^2 = 0.64) (Appendix 3.10.1). The cumulative degree distributions for each of the eight webs were best characterised by power-law distribution models. Global average clustering coefficients were 4 to 14 times greater for food webs than randomly generated networks with the same number of nodes and links (Appendix 3.10.1).

Declining catchment glacier cover was correlated significantly to reducing turbidity and increasing TN. Connectance and trophic food web descriptors were also associated significantly with physicochemical variables and nutrient concentrations, including optical turbidity (18 descriptors), 1/Pfankuch Index (18 descriptors) and TN (17 descriptors) (Appendix 3.11). While many of these descriptors were those identified as supporting significant relationships with catchment glacier cover, additional correlations include the unimodal reduction in directed connectance with reducing turbidity (GAM: *p*-value = < 0.001; χ^2 = 69.98; deviance explained = 96.6 %) and linear reduction with both increasing channel stability (1/Pfankuch Index) (GLM: *p*-value = 0.024; *F* = 9.02; deviance explained = 60.0 %) and reducing TN (GLM: *p*-value = 0.008; *F* = 15.08; deviance explained = 71.5 %) (Appendix 3.11).

4.3.3 Allometric scaling

Across the food webs *M* spanned 13 orders of magnitude and increased with trophic level. There were significant increases in basal, primary consumer and total biomass with decreasing catchment glacier cover (Figure 4.3; Table 4.1). The biomass of amorphous detritus increased significantly with reducing glacier cover (GAM: *p*-value = < 0.001; χ^2 = 22.53; deviance explained = 62.7 %).

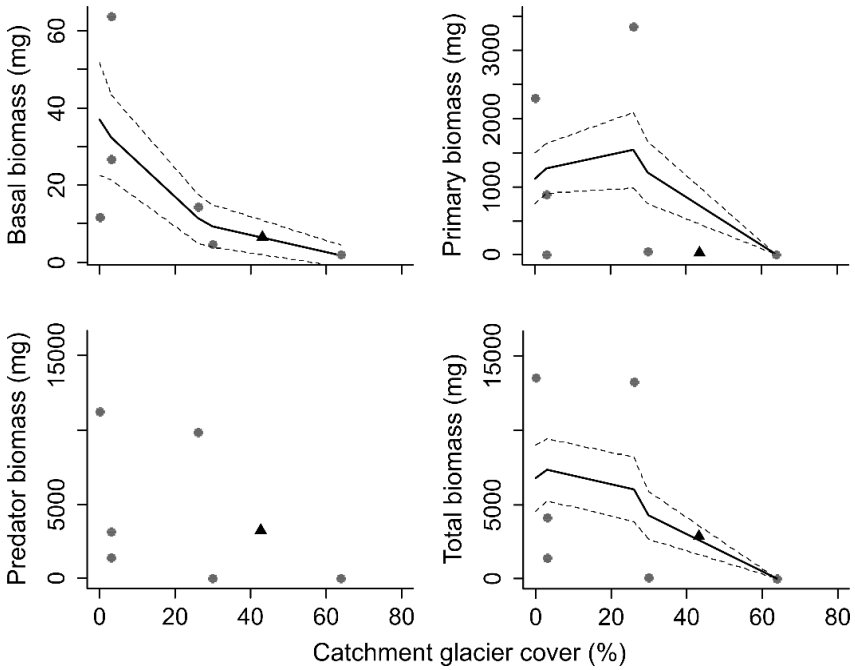

Figure 4.3 Alterations to the total biomass (mg m^{-2}) of basal taxa, primary consumers, predators and all aquatic biota of alpine river food webs along gradients of increasing catchment glacier cover. Black lines represent GAM lines of best fit and 95 % confidence intervals. Summary statistics are presented in Table 4.1. Basal biomass included biomass values for primary producers alongside standing stock of amorphous detritus (AFDM). Predators included taxa with cannibalistic feeding linkages. Biomass information was available for macroinvertebrate and periphyton species but *n* = 6 as diatom biomass estimates were unavailable for sites E5 and U1. Site O3 (black triangles) was influenced by a proglacial lake but not included in these correlations. GAM relationships inclusive of O3 are displayed in Appendix 3.9.2.

All species-averaged (R^2 = 0.64 to 1.00) and individual (R^2 = 0.74 to 1.00) *MN* relationships showed highly significant linear regressions (Figure 4.4, Appendix 3.12). Scaling coefficients for both individual (-0.50 to -0.26) and species-averaged (-0.40 to -0.25) relationships were higher than those predicted by metabolic theory (-1, -3/4) (Brown et al., 2004), with regressions producing shallower slopes between resource and consumer biomass values than expected. Individual slope values declined significantly with reducing catchment glacier cover (Figure 4.4f).

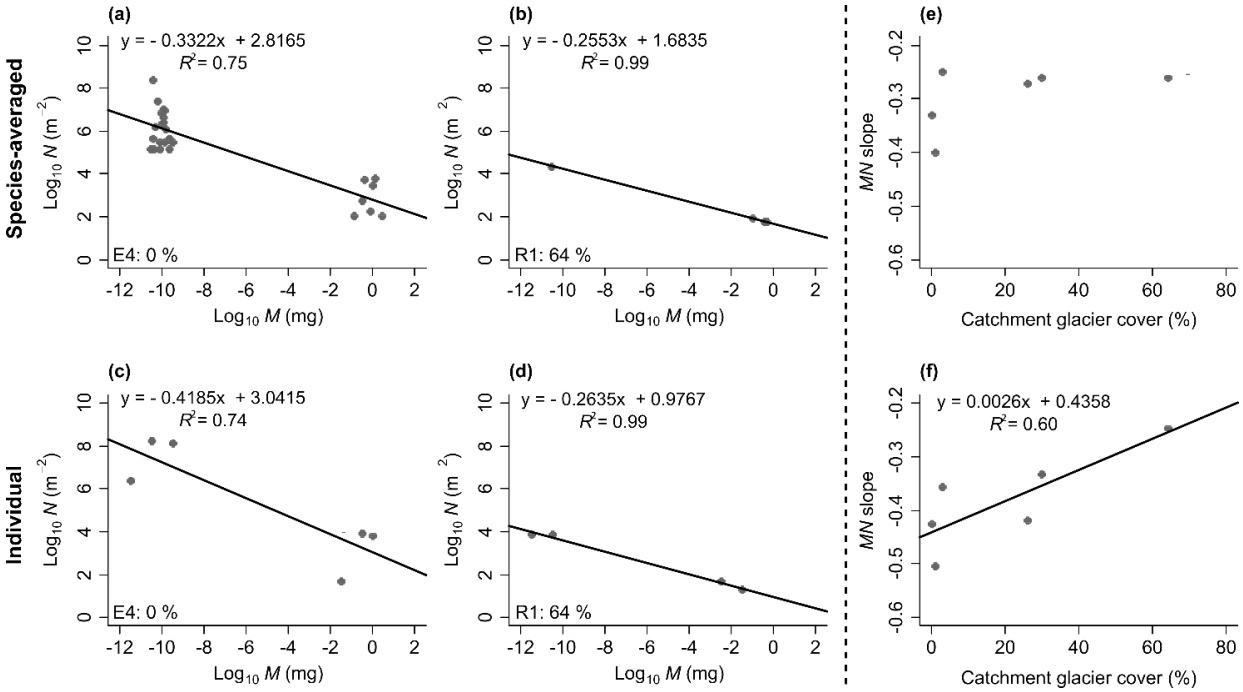

Figure 4.4 Relationships between biomass (*M*) and abundance (*N*) of food web consumers and resources. (a, b) species-averaged *MN* correlation, derived from the mean log_{10} biomass and log_{10} abundance of each consumer and resource species. (c, d) individual *MN* correlation, derived from the log_{10} biomass and log_{10} abundance of all individual macroinvertebrates and periphyton, following their placement into size bins of 1 on the log_{10} scale. For (a to d), examples are displayed for river sites hosting the highest (R1: 64 %) and lowest (E4: 0 %) glacier cover, with information for additional food webs presented in Appendix 3.12. Scaling coefficients are displayed for comparison to those predicted by metabolic theory (species-averaged = -0.75, individual = -1.00) (Brown et al., 2004). (e, f) correlation between the *MN* regression slope value and catchment glacier cover at each river site. Slope values were calculated from site-specific (e) species-averaged and (f) individual *MN* correlations, which are displayed in Appendix 3.12. Here, *n* = 6 as resource abundance estimates were unavailable for E5 and U1. Black lines depict fitted OLS linear regressions.

4.4 Discussion

This study presented nine high-resolution river food webs derived from direct gut contents observation, to generate new understanding of the response of ecological network structure and allometry to reducing catchment glacier cover. Original findings included the significant rewiring of food webs, as demonstrated through changes in connectance and trophic descriptors as glacier cover declined. Many descriptors showed a pronounced threshold of change below approximately 26 % glacier cover. The river networks hosted high clustering coefficients, short mean chain lengths and low directed connectance, potentially underpinning the observed food web restructuring

as glacier cover was lost. The food webs were strongly size structured, with mass and abundance relationships varying systematically along the gradient of glacier cover. Together these findings illustrated the potential for significant successional reorganisation of alpine river food webs imposed by glacier retreat.

4.4.1 Food web structure

Reductions in catchment glacier cover were associated with increased numbers of food web nodes, links and chains, underpinned by observed increases in macroinvertebrate and diatom species richness, abundance and biomass (Figure 4.2; Figure 4.3; Appendix 3.6). This finding enabled acceptance of H_1. The increase in taxonomic biodiversity is supported by previous studies documenting biota responses to attenuation of the harsh physicochemical conditions associated with glacier ice melt inputs (e.g., low water temperature, channel stability) (Brown et al., 2007a; Lencioni et al., 2007; Milner et al., 2009; Brown and Milner, 2012; Niedrist et al., 2018). This study suggested that these responses were enabled by significant increases in the number of feeding linkages (mean trophic generality and vulnerability), linkage density and community span. Each of these descriptors were associated significantly with reducing turbidity and increasing channel stability (Appendix 3.11), physicochemical alterations known to be characteristic of glacier retreat worldwide (Milner and Petts, 1994; Brown et al., 2018). This suggested that food web responses documented here may also be found in other alpine regions.

Food web succession rate along the gradient of reducing catchment glacier cover was modified at a threshold of approximately 26 % glacier cover, below which more rapid increases were identified in node, link and food chain numbers (Figure 4.2). This ‘tipping point’ was characterised by clear changes to the ratio of resource to consumer taxa (Figure 4.2b). Above this threshold the ratio was reduced, as glacier cover declined from 64 to 26 %. This was potentially because some grazing species, including *Rhithrogena semicolorata* and *Heptagenia lateralis*, were found exclusively at river sites > 26 % glacier cover. The absence of predation (excluding cannibalism) at these sites suggested reduced production available to support higher trophic levels, which was corroborated by significant reduction in the biomass of amorphous detritus with increasing glacier cover. Below this threshold the ratio increased, with associated increase in the abundance and biomass of basal taxa (Fell et al., 2018). This could have resulted from biofilm communities benefitting from the warmer water temperatures, less variable flows, reduced turbidity and thus greater light availability

induced by reduced runoff (Hieber et al., 2001; Rott et al., 2006; Wilhelm et al., 2013, Ren et al., 2017b). This may account for increases in the mean number of prey species available to be ingested by each consumer (mean trophic generality) < 26 % glacier cover.

High basal taxa abundance < 26 % glacier cover may be due to reduced algal grazing pressure resulting from a plateau in macroinvertebrate abundance increases (Appendix 3.6). Similar reductions in invertebrate density have been noted below approximately 40 % meltwater contribution in glacierised catchments of the French Pyrenees (Khamis et al., 2016), and the relative abundance of several invertebrate functional groups reached asymptote at 20 to 30 % glacier cover in a global-scale study (Brown et al., 2018). Above 26 % glacier cover, food web structure may be controlled by the physicochemistry and disturbance imposed by ice melt inputs upon unstable proglacial rivers. Below the threshold, this influence appears sufficiently attenuated for a switch to donor-control of network structure led by a proliferation of biofilm. This pattern of community assembly may align to that identified by Brown et al. (2018), who found niche-based species sorting to be replaced by patch dynamics at low glacier cover, with macroinvertebrate dispersal limitation dominating community assembly throughout glacier recession stages, due to the fragmented nature of mountain river networks.

Reducing catchment glacier cover led to the expansion of trophic height, with greater predation leading to an increase in the proportion of consumer nodes defined as intermediate taxa. This reorganisation explains the significant increase in trophic links, linkage density and food chain lengths (number of chains, maximum and mean chain length) with declining glacier cover. Despite this, these eight networks hosted the shortest mean chain lengths documented for river food webs (1.00 to 2.01), leading to partial acceptance of H_2. This characteristic was previously identified by Clitherow et al. (2013) for a glacier-fed stream reach (2.00 to 2.36). Short chain lengths reflect low levels of predation (limited body-size range), a dominance of macroinvertebrate-periphyton linkages and limited omnivory along the glacier cover chronosequence, all potentially driven by the low production of these high-altitude river systems. As snow melt and storm events drive seasonal periods of flood, freezing and dewatering in alpine rivers (Beniston et al., 2018), these short food chains may be maintained by high flow rate variability (Sabo et al., 2010), even in groundwater dominated rivers. Although drainage area, a proxy for ecosystem size, has been identified as a critical influence on

food chain length in networks hosting low productivity (Ward and McCann, 2017), no association was identified with catchment size.

Directed connectance was not associated with catchment glacier cover. Reported values were similar to those documented for a river site (0.05 to 0.19, 2006 to 2011) adjacent to E5 (0.07, 2015) (Clitherow et al., 2013). However, connectance for the eight river food webs (0.03 to 0.11) was within the range or lower than those identified for non-glacierised mountain catchments in Alaska (0.18 to 0.2, Parker and Huryn, 2006) and lowland UK temperate river systems (0.03 to 0.29, Brown et al., 2011), leading to partial rejection of H_2. High connectance has previously been attributed to omnivorous macroinvertebrate feeding in response to limited primary production and riparian energy provision (Zah and Uehlinger, 2001; Zah et al., 2001; Clitherow et al., 2013). However, omnivory was constrained at all eight sites (0.00 to 0.12) due to limited macroinvertebrate predation. Findings suggested preservation of network-level metrics across sites, including directed connectance, despite reduction in node numbers, food web linkages and predatory species at high cover. These metrics altered with web size (richness), while directed connectance remained invariant across networks. This has previously been identified in the response of aquatic food webs to drought disturbance (Ledger et al., 2013), suggesting that these networks may respond comparably to a variety of climate induced environmental stressors. As reduced directed connectance can cause food webs to become less robust to environmental perturbation (Dunne et al., 2002a, b), maintenance of this metric throughout disturbance gradients may indicate their structural resilience to imposed alterations.

Six of the alpine river food webs supported the two degrees of separation theory (Williams et al., 2002) as 81 to 100 % of species pairs shared two or fewer linkages. This was potentially due to the prevalence of generalist feeding strategies, which have been identified to characterise glacier-fed alpine rivers (Zah et al., 2001; Clitherow et al., 2013). The percentage for E5 (82 %) was comparable to an adjacent river site (92 %) sampled by Clitherow et al. (2013). Declining glacier cover led to significant reductions in the proportion of nodes connected by two or fewer links (Appendix 3.10) and subsequently, increases in characteristic path length (Figure 4.2; Table 4.1). This reduction in interconnectedness may have been driven by greater abundance of primary consumers and the introduction of selective predatory taxa at low glacier cover sites. Despite this, the nine food webs hosted short characteristic path lengths, high clustering coefficients and mean degree distributions best described by power-law

relationships. These scale-free or small-world network properties can create food webs which are susceptible to rapid propagation of structural alterations following removal of highly connected species (Williams et al., 2002; Dunne et al., 2002a, b). However, while previous research has predicted imperilment of the *Baetis alpinus* group in deglaciating catchments (Finn et al., 2014), no consumer invertebrates were lost as glacier cover declined, with those adapted to ice melt dominated rivers also present in lower glacier cover streams (e.g., *Diamesa goetghebueri*, *Diamesa cinerella*, *Baetis alpinus* gr.). This suggested that ice loss may not directly drive extirpation at sampled sites, with taxa persisting along the chronosequence or capitalising on other disturbance events to recolonise river sites at lower glacier cover (Milner et al., 2018).

Persistence of taxa as the aquatic community assembled in response to reducing catchment glacier cover aligned to the tolerance mechanisms identified for macroinvertebrates in response to real-time glacier recession (Milner and Robertson, 2010; Brown and Milner, 2012). Consumers at sites with ≥ 36 % glacier cover retained feeding linkages with many prey species (*Diamesa goetghebueri* = 40 % of prey species, *Diamesa cinerella* = 88 %, *Baetis alpinus* gr. = 54 %) despite ice loss. This indicated that reorganisation of river food webs will follow patterns of restructuring rather than catastrophic collapse, as previously predicted for small-world networks experiencing targeted species removal (Solé and Montoya, 2001; Dunne et al., 2002a; Ledger et al. 2013). While rapid structural alteration may prove significant for glacierised regions hosting endemic, cold-stenothermic species (e.g., Pyrenees, Rocky Mountains) (Brown et al., 2007a; Giersch et al., 2016), this study did not find evidence of cascading species loss in river food webs. As illustrated by Montoya and Solé (2002), the small-world properties of these observed food webs may enable them to respond rapidly to short term disturbances and recover quickly from environmental perturbations, dampening the impact of glacier retreat.

Catchment geomorphology strongly modified food web structure through the mechanism of proglacial lake formation. Proglacial lake outlets have previously been identified to host higher water temperatures and channel stability in comparison to glacier-fed streams of similar altitude, increasing macroinvertebrate and algal abundance (Milner and Petts, 1994; Brittain et al., 2001; Milner et al., 2001; Hieber et al., 2001). Findings noted this physicochemical disparity between site O3 below the Obersulzbachkees (42 % glacier cover; mean water temperature: 8.0°C; 1/Pfankuch: 0.025) and site U1, which had comparable catchment glacier cover but no lake inputs

(46 % glacier cover; mean water temperature: 1.3 °C; 1/Pfankuch: 0.019). Site O3 had linkage density, mean trophic vulnerability and numbers of nodes, links and chains that were comparable to river sites with 0 to 3 % glacier cover, despite its catchment retaining 42 % glacier cover at the time of sampling. This site also hosted the longest mean chain lengths, characteristic path lengths and highest omnivory of the nine food webs (Figure 4.2; Appendix 3.9.2). This research provided first observation of geomorphic context impacting whole food web structure, in addition to individual taxonomic groups (Appendix 3.9), with lakes potentially accelerating the transition to donor-controlled assembly even for river food webs at high glacier cover. Further research is required to determine the downstream attenuation of lake influence, and the implications of this discontinuity between runoff production and glacier influence upon cold stenothermic populations in a greater number of alpine drainage networks. This is pertinent given the proliferation of proglacial lake formation in deglaciating watersheds in Austria (Buckel et al., 2018) and other glacierised regions (Carrivick and Heckmann, 2017; Otto, 2019).

4.4.2 Allometric scaling

All nine alpine river food webs were characterised by inverted biomass structures, as total biomass increased with trophic level, and predator biomass exceeded that of basal taxa. This pattern is frequently identified for energy transfer in temperate freshwater ecosystems (Vadeboncoeur and Power, 2017). The inversion was also evident in scaling coefficients for both individual and species-averaged *MN* relationships, which were higher than those predicted by metabolic theory (Brown et al., 2004). As identified by Clitherow et al. (2013), this disparity in alpine river food webs may reflect higher consumer or lower resource abundances in comparison to theoretical autochthonous supported networks, potentially because not all available energy sources were captured in *MN* plots. The contribution of amorphous detritus, which was observed in all consumer gut contents, was not included given the absence of a definable *N*. However, unlike for many temperate river systems (Perkins et al., 2018), energy from riparian detrital inputs in these above treeline river sites has previously been documented as minimal (Zah and Uehlinger, 2001) and thus, may not provide a critical energy source to alpine rivers.

Additional energy inputs may include other observed species lacking an *N* value at each river site, in part because many taxa found in gut contents were absent from the biofilm environment. This may have been because glacier-fed river invertebrates are

characterised by low abundances and patchy spatial distribution, potentially hindering their capture in river samples (Clitherow et al., 2013). The contribution of energy sources not investigated in this study may also explain elevated consumer abundances. These may include small meiofauna species (nematodes, protists, rotifers, protozoa) not retained by the 250 µm Surber mesh (Schmid-Araya et al., 2002) and microbial assemblages (Archaea, bacteria, fungi) in the biofilm community (Ren et al., 2017b). Further research is required to quantify the contribution of these resources to macroinvertebrate diets and to assess the quality of their nutritional provision, which may be temporally dynamic (Finlay et al., 1999; Perkins et al., 2010). Metabarcoding and high-throughput DNA-based sequencing could be included to integrate the contribution of algae, microbes and meiofauna, whose small size limits GCA through direct observation (Sheppard and Harwood, 2005; Creer et al., 2010; Hotaling et al., 2017a; Ren et al., 2017b; Vadeboncoeur and Power, 2017; Banerji et al., 2018).

Consumer biomass may appear greater than that which the observed resource supply could sustain, if food web structure reflected a legacy effect of temporal variability in basal energy supply. Previous research has documented both periphyton (e.g., *Hydrurus foetidus*) blooms and absences in alpine rivers during the spring ice melt period, potentially induced by the impacts of glacier nutrient release and flood events upon benthic microfauna (Uehlinger et al., 2002; Rott et al., 2006; Uehlinger et al., 2010). Within- and between-season fluctuations in watershed resource supply may result in consumers capitalising upon ‘windows of opportunity’ (Uehlinger et al., 2002, p. 20; Gabbud et al., 2019) to increase their biomass, and then persisting during intermittent periods of low energy availability with reduced consumption. Uehlinger et al. (2010) identified similar seasonal patterns of periphyton biomass in glacier-fed and groundwater dominated stream reaches, perhaps underpinning the absence of a significant relationship between species-averaged *MN* scaling coefficients and catchment glacier cover. In contrast, the significant relationship between individual *MN* slope values and catchment glacier cover illustrated greater disparity between observed and predicted biomass structuring at high glacier cover sites. This potentially reflects the more efficient use of available resources by consumer species, which although found throughout the chronosequence of sites, may have adapted to the lower basal biomass availability in these reaches (Woodward et al., 2010b; Vadeboncoeur and Power, 2017; Niedrist and Füreder, 2018).

Comparison of individual abundances between high (64 %) and low (0 %) glacier cover river sites demonstrated that resource *N* increased by approximately four orders of magnitude while consumer *N* by one order. Therefore, as glacier cover declined, the rate of increase in basal taxa abundance was greater than that of consumer taxa. This may suggest that biofilm species were able to exploit the change in river habitat (increased water temperature and channel stability) more rapidly than macroinvertebrates, with these smaller taxa colonising sites more quickly. The lag in consumer abundance increase was also noted as a reduction in the increase of macroinvertebrate abundance < 26 % glacier cover. This was potentially influenced by dispersal limitation constraints, which disproportionately influence larger organisms (Brown et al., 2018). Disparity in the increase of basal taxa relative to macroinvertebrates with declining glacier cover ensured that individual *MN* relationships altered systematically along the chronosequence (Figure 4.4f). This led to rejection of H_3, which in alignment with metabolic theory, predicted this relationship to remain invariant despite environmental perturbation (Brown et al., 2004; Woodward et al., 2012). This response was recently identified for river food webs receiving terrestrial subsidies, which increased the abundance of top predatory fish species relative to basal taxa (Perkins et al., 2018). It has also been observed in streams affected by drought, where reductions in predator pressure were accompanied by a proliferation of basal species (Woodward et al., 2012), similar to the response identified in sampled alpine rivers. In contrast to the latter study of a specific disturbance event, this research provided new evidence of a natural environmental gradient perturbing individual *MN* scaling relationships in river habitats, with increased basal taxa altering both the connectance descriptors of food webs, alongside their size structure. As the body mass and abundance of individual organisms critically influences their metabolic rate, the changes to network size structure driven by reducing glacier cover can be expected to alter the processing rates of biogeochemical cycles in alpine river ecosystems (Yvon-Durocher and Allen, 2012).

4.4.3 Wider implications of river food web responses to glacier retreat

Declining catchment glacier cover significantly reorganised the structure and allometric scaling of nine river food webs in the central Austrian Alps. A chronosequence approach enabled observation of developments in river food web community assembly along the catchment glacier cover gradient. Food web succession was modified at approximately 26 % glacier cover, with an increase in basal taxa abundance and biomass below this ‘tipping point’. This was potentially sustained by attenuation of the

harsh physicochemical conditions associated with ice melt inputs and suggested dominance of donor-controlled assembly of river food webs. Glacier retreat is often associated with prolific proglacial lake formation in mountainous regions (Carrivick and Heckmann, 2017; Buckel et al., 2018; Otto, 2019) and as these features established environmental conditions more characteristic of rivers sites at low glacier cover, they appear to accelerate this development of food webs. Low directed connectance, scale-free organisation and the shortest reported river food chain lengths may explain the ability of these food webs to restructure rapidly (Montoya and Solé, 2002). However, tolerance supported assembly appears to have limited the extirpation of taxa during this structural reorganisation, potentially as cold-adapted species were able to efficiently assimilate available biofilm resources. This has implications for aquatic conservation management strategy, but research is required to determine the pervasiveness of this resilience in other glacierised regions. With the European Alps predicted to lose up to 89 % of their glacier volume by 2100 (EEA, 2016), significant rewiring of alpine river food webs will be widespread, altering the abundance, density and biomass of aquatic species. This may influence the primary production, ecosystem metabolism and nutrient cycling processes which these communities sustain (Tank et al., 2010; Ulseth et al., 2018).

Chapter Five: Glacier loss accelerates fungal decomposition of river organic matter

5.1 Introduction

The retreat of mountain glaciers worldwide is accelerating at an unprecedented rate, with climate change predicted to drive continued ice loss throughout the twenty-first century (Zemp et al., 2015; Huss and Hock, 2018). Sustained reduction in ice melt contributions to proglacial river systems is rapidly altering their geomorphological, hydrological and ecological characteristics, with implications for freshwater ecosystem service provision downstream (Bliss et al., 2014; Milner et al., 2017). Despite proliferation of research considering the impact of such modifications upon aquatic ecological community structure (Brown et al., 2007a; Milner et al., 2009; Gesierich and Rott, 2012; Jacobsen et al., 2012; Wilhelm et al., 2013; Ren et al., 2017b), far less is understood of how functional processes will be influenced by glacier retreat, and the role of microbial biodiversity in driving these ecosystem functions, such as carbon cycling (Singer et al., 2012; Freimann et al., 2013; Wilhelm et al., 2013).

Organic matter (OM) decomposition is a critical process in aquatic ecosystems as it strongly regulates energy availability to benthic food webs (Cummins, 1974; Tank et al., 2010). Gradual degradation, mineralisation and catabolism of organic material through physical fragmentation and saprotroph community processing is also responsible for substantial release of carbon in gaseous (CO_2, CH_4), dissolved and particulate forms (Battin et al., 2008; Aufdenkampe et al., 2011; Striegl et al., 2012; Singer et al., 2012; Raymond et al., 2013). Reorganisation of microbial community structure has been identified to determine OM decomposition rates in terrestrial environments (Glassman et al., 2018). While there have been recent global-scale investigations of aquatic OM processing (Follstad Shah et al., 2017; Tiegs et al., 2019), linkages between measured decomposition rates and specific microbial taxa, saprotrophic groups and their associated genes, remain to be studied.

In many high-altitude mountain rivers, sources of terrestrial OM are limited to riparian grasses, shrubs and wind-blown material. Downstream, inputs typically increase with distance from glacier margins and the emergence of sub-alpine forest at lower-altitude (Zah and Uehlinger, 2001; Yue et al., 2016). Breakdown of this terrestrial allochthonous OM, alongside autochthonous sources (e.g., macrophytes, algae) and material

released from melting glacier ice, critically augments energy derived from primary production, which may be constrained by the low water temperatures and high turbidity of glacier-fed rivers (Tank et al., 2010; Milner et al., 2017). Previous studies of OM decay in glacierised catchments highlight the importance of physical fragmentation as a mechanism of decomposition in proglacial rivers (Robinson et al., 2000; Robinson and Jolidon, 2005). Glacier runoff reduces channel stability and increases suspended sediment concentration and discharge variability (Milner et al., 2017), potentially limiting the retention time of OM and increasing abrasion and autolysis rates (Ferreira et al., 2006). Sustained glacier retreat may however increase the OM inputs available for breakdown in mountain rivers, as ice loss leads to greater geomorphic stability and increased habitat availability for herbaceous riparian plants, whose leaf litter may enter streams (McKernan et al., 2018).

Biological decomposition of OM in glacier-fed rivers is driven primarily by cold-stenothermic fungal hyphomycetes, including *Lemonniera aquatica* and *Tricladium curvisporum*, which tolerate water temperatures approaching freezing (Gessner et al., 1998; Robinson et al., 2000; Suter et al., 2011). Successional development of microbial communities upon organic materials in proglacial rivers leads to subsequent colonisation by bacterial families hosting saprophytic taxa, including Rhodobacteraceae and Comamonadaceae (Bayer et al., 2006; Wilhelm et al., 2013). Next-generation sequencing (NGS) of microbial communities in proglacial habitats (ice, snow, streams, lakes, glacier forefields) has indicated high levels of bacterial and fungal biodiversity in glacier-fed rivers (Wilhelm et al., 2013; Freimann et al., 2013; Ren et al., 2017b; Hotaling et al., 2017a). Biomass and material processing rates are constrained though by the low water temperature and high turbidity imposed by meltwater inputs (Gessner et al., 1998; Robinson et al., 2000; Robinson and Jolidon, 2005). However, few studies consider the functional effects of microbial community responses to declining glacier cover. Use of different field and laboratory protocols among publications currently prevents the investigation of geographic patterns in the role of biofilm taxa in OM decomposition. Understanding of how microbial communities drive ecosystem functioning is needed urgently as glacier retreat may accelerate riverine OM processing as warmer water temperatures and more stable channel substrates increase favourability of conditions for aquatic microbial activity (Wilhelm et al. 2013; Freimann et al., 2013). Increased understanding of carbon processing in glacier-fed river systems is required to improve current knowledge of the contribution of freshwaters to the global carbon cycle (Battin et al., 2008; Singer et al., 2012; Raymond et al., 2013).

This study investigated how changing catchment glacier cover across six countries on four continents affected river ecosystem decomposition of cellulose. Cellulose is the world's most abundant organic molecule and a major component of detrital inputs to river systems (Bayer et al., 2006; Tiegs et al., 2007; Tiegs et al., 2019). Decomposition rates, aquatic microbial community abundance, and copy numbers of a functional gene (cellobiohydrolase I) which critically underpins the hydrolysis of crystalline cellulose (Bayer et al., 2006), were assessed using standardised methods to determine if there were globally coherent patterns in the linkages between microbial biodiversity and decomposition. It was hypothesised that: (H_1) the abundance of river fungi and bacteria would increase with reducing glacier cover and associated increases in water temperature, channel stability and reductions in turbidity; (H_2) cellulose decomposition rates across the six glacierised regions would be associated positively with increased copy numbers of the fungal gene cellobiohydrolase I (*cbhI*) and in turn, (H_3) cellulose decomposition rates would increase with reducing catchment glacier cover. A multi-region approach enabled new global-scale understanding of the processes controlling OM decomposition in glacier-fed mountain rivers, as previous studies of leaf litter breakdown and associated microbial communities have been undertaken only in a single catchment of the Swiss Alps (Gessner et al., 1998; Robinson et al., 1998; Robinson and Gessner, 2000; Robinson et al., 2000; Robinson and Jolidon, 2005).

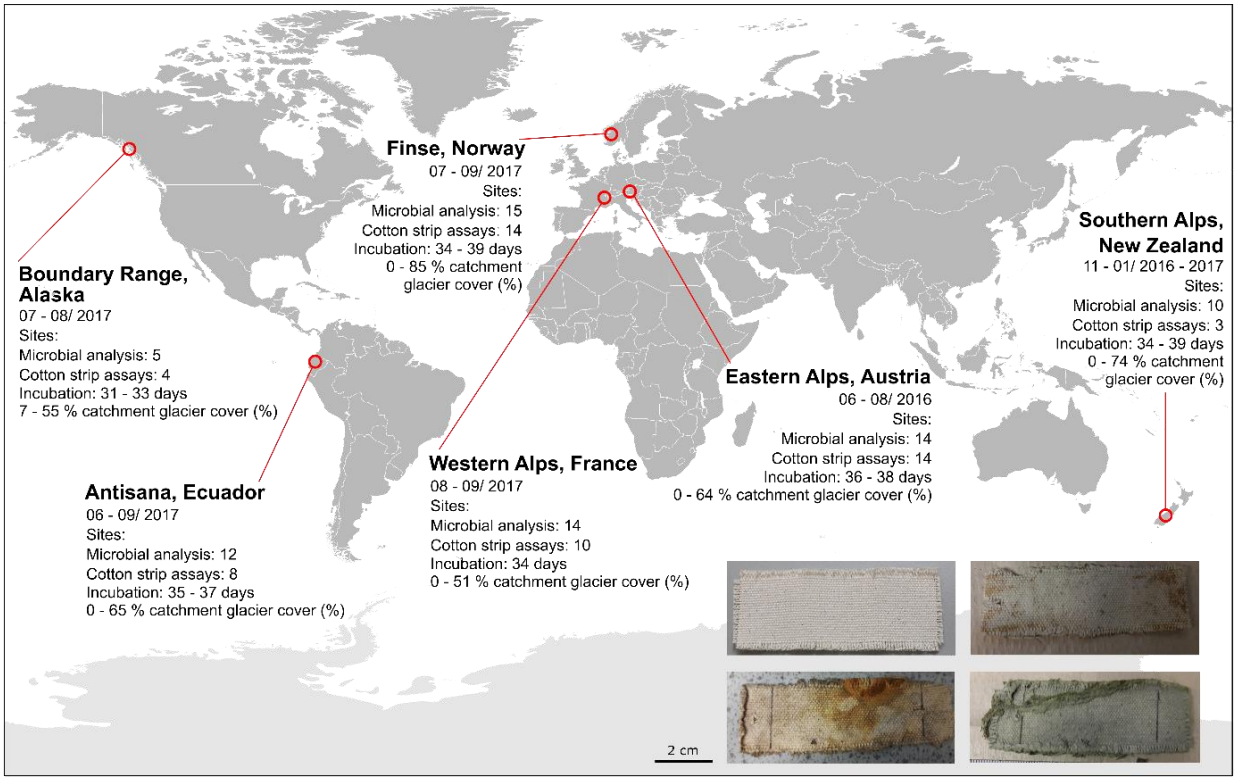

Figure 5.1 Global distribution of glacierised mountain study regions. Observations were made at 74 river sites. Cotton strip assays were successfully incubated at 53 sites and microbial analysis performed for 70 sites. Images display examples of cotton strips before (top left) and after river incubation. Basemap adapted from GitHub (2019).

5.2 Methods and materials

5.2.1 Study areas

Standardised cotton strip assays were incubated in riffles of glacier-fed rivers, their tributaries and groundwater sourced streams of catchments across mountainous regions of Alaska, Austria, Ecuador, France, New Zealand and Norway (Figure 5.1). Study sites were located on four continents, from -44° to 60° latitude, and in both hemispheres. A total of 74 river sites were selected, each with minimal anthropogenic influence and spanning an overall gradient of 0 to 85 % catchment glacier cover. The percentage of each river catchment permanently covered by ice was calculated by delineating watershed areas for individual river sites (filled 5 m to 30 m ASTER Digital Elevation Models) using manually refined watershed analysis functions of ArcMap™ 10.4 (hydrology tools) and calculating the regional ice area (GLIMS, 2018) within these boundaries. The experiments were performed during boreal and austral summer months (2016 and 2017) to capture the highest possible decomposition rates. Further sampling site information is available in Appendix 1.

5.2.2 Field sampling

5.2.2.1 Environmental parameters

At each river site, electrical conductivity (EC) and pH were measured with Hanna Instruments (HI9033, HI98130, Woonsocket, Rhode Island, USA). A YSI Pro Plus water quality meter (Xylem, Yellow Springs, Ohio, USA) was used for rivers in Alaska and a HQ40D portable multi meter (HACH, Düsseldorf, Germany) for sites in Ecuador and France. Hourly water temperatures were recorded throughout the cotton strip incubation periods using iButton Fobs (DS1990A-F5, Foshan, China) (France, Ecuador) or TinyTag Plus 2 data loggers (Gemini, Chichester, UK) (all other sites). Pfankuch Index bottom components (Pfankuch, 1975) were estimated for all sites except those in Alaska, with reciprocal values (1/Pfankuch Index) calculated to enable higher scores to represent greater river channel stability. Water samples (100 mL) were collected for ex-situ optical turbidity and nutrient concentration analysis. A desktop turbidimeter (HACH 2100A) (Camlab, Cambridge, UK) was used for turbidity assessment and total nitrogen (TN) and total phosphate (TP) concentrations were identified using a Two Skalar San ++ Continuous flow auto-analyser. Dissolved organic carbon (DOC) and dissolved carbon (DC) were detected using an Analytik Jena Multi N/C 2100 elemental thermal oxidation analyser. All measurements and samples were collected at the time of cotton strip incubation, but nutrient information was unavailable for some sites (Appendix 1).

5.2.2.2 Decomposition assay

Following the CELLulose Decomposition EXperiment (CELLDEX) protocol of Tiegs et al. (2015a), rectangular cotton strips (8 cm x 2.5 cm) were created from > 95 % cellulose artist's fabric (Fredrix Artist Canvas, Georgia, USA (unprimed 12-oz heavy-weight cotton fabric, style #548)) (Tiegs et al., 2013). Strips comprised exactly 27 threads, with 3 mm of fray along each edge. Cotton strips measure the capacity of river ecosystems to process cellulose (Imberger et al., 2010). While they may have a different nutrient content and physical structure to riparian and autochthonous inputs entering mountain rivers, the natural prevalence of cellulose in terrestrial and aquatic materials and the standardised form of the strips enabled between-site comparison of a decomposition process which may hold greater ecological relevance than leaf pack assays, given the minimal litter contribution to high-altitude rivers (Zah and Uehlinger, 2001; Bayer et al., 2006; Tiegs et al., 2013; Tiegs et al., 2019). Cotton strips were stored in a sterile environment and transported flat to minimise damage and fraying. Control strips were created and transported identically but were returned without river

incubation. The number of control strips was approximately 15 % of the deployed strips in each region. In total, 450 cotton strips and controls were made, stored and analysed.

At each site, four cotton strips were cable tied to nylon cord (1 m long, 3 mm wide) which was staked to the river bed in riffles at individual sites (Tiegs, 2015a). Rocks were placed upstream of each strip upon the cord, to keep them flat upon benthic sediments and aligned to the current. Points of similar water depth and turbulence were selected to ensure strips were influenced by comparable environmental conditions (Tiegs et al., 2013). A temperature logger recording hourly measurements was placed in a white plastic tube to shield it from solar radiation and abrasion and cable tied to one of the stakes at each site. For sites with high catchment glacier cover and highly unstable river beds, additional cotton strips (up to 6) were incubated and secured with steel rebar (300 mm long, 10 mm wide), to ensure some would remain in-situ for the experiment duration.

Cotton strip assays were incubated for 37 days, or as close to this duration as field logistics and weather conditions permitted (min. 31 to max. 39 days). This period was designed to maximise the potential of achieving 50 % tensile strength loss, the point of decay at which cotton strips are believed to be colonised by the microbial community, but not shredding invertebrates (Tiegs et al., 2013). Cotton strips were excluded from analysis if found above the water level upon collection, or where hourly temperature measurements indicated intermittent exposure, as this prevented representation of exclusively aquatic decomposition processes. Strips were cut from their cable binders, gently cleared of debris, and a 2 cm subsample of one cotton strip from each river site was detached using sterilised scissors and preserved in 1 mL of RNA*later*™ Stabilization Solution (ThermoFisher Scientific, Massachusetts, USA) (Tiegs, 2015c). These subsamples were stored at 4 °C for transport and then -80 °C in the laboratory prior to molecular analysis. All remaining strips were submerged in 100 % ethanol for 30 s on site, to halt microbial activity (Tiegs, 2015b).

5.2.3 Laboratory analysis

5.2.3.1 Tensile strength determination

All cotton strips, minus the subsamples, were oven dried (40 °C, 26 hrs) and stored within a desiccator prior to tensile strength determination. An advanced video extensometer (2663-821) (SN:5076) (Instron, High Wycombe, UK) was used to determine the maximum tensile strength of all incubated and control strips, extending

at a consistent rate of 2 cm min^{-1}, with 1 cm portions of each strip end secured within the grips (Tiegs, 2015b). To calibrate the instrument, cotton strips constructed using the CELLDEX protocol but not transported or incubated, were tested until their break points aligned to a consistent range and the machine jaws were sufficiently adjusted to minimise slippage. The sample order was randomised, with control strips processed throughout the sample run to identify instrument drift. Room pressure and temperature were kept constant across sample runs, and multiple sites processed together to minimise variability of conditions between testing. Strips which broke along the point of contact with the machine jaws were excluded from analysis (*n* = 4, 0.9 %), as were those whose maximum tensile strength remained higher than the mean control strip value (*n* = 22, 5.0 %). For these strips, biological variation lay within the range of technical variation and the two could not be separated.

5.2.3.2 Molecular methods

DNA was extracted from a standardised 1.5 cm^2 section of the 2 cm^2 preserved cotton strip subsamples. Extraction followed the Cetyl Trimethylammonium Bromide protocol (Griffiths et al., 2000) and DNA was eluted into 50 µL of polymerase chain reaction (PCR) grade water (Invitrogen, Waltham, Massachusetts, USA). This approach was selected to enable rapid extraction and purification of DNA. The abundance of DNA in individual samples was quantified using the Quant-iT PicoGreen dsDNA assay kit (Invitrogen), to enable normalisation of all samples to 1 ng $µL^{-1}$.

Polymerase Chain Reaction (PCR) was performed to fragment DNA strands, isolate specific target regions and create multiple copies of these regions for sequencing (Illumina, 2013). Primer sets were annealed to the bacterial 16S rRNA gene, the fungal internal transcribed spacer region (ITS) and the fungal cellobiohydrolase I (*cbhI*) gene within DNA extracted from each cotton strip subsample. These regions were targeted to represent the bacteria and fungi present at each river site, as they are widely used for molecular analysis and are both stable and pervasive within their respective microbial communities (Herlemann et al., 2011; Toju et al., 2012). First stage PCR reactions were performed in a 25 µL reaction volume with 3 µL of DNA template, 12.5 µL appTAQ RedMix (2X) polymerase (Appleton Woods Ltd, Birmingham, UK), 1 µL of 4 µmol of each primer and 6 µL of PCR grade water. All PCR reactions also contained 1.5 µL of 1 % bovine serum albumin (BSA) to remove inhibitors (e.g., humic acids) and increase the yield of PCR amplification (Kreader, 1995). To target the bacterial 16S rRNA gene, the primer sets Bakt_341F (5'-CCTACGGNGGCWGCAG -3') and

Bakt_805R (5'-GACTACHVGGGTATCTAATCC-3') were used (Herlemann et al., 2011) and for fungi, the ITS2 region was amplified using the ITS3_KYO2 primer (5'-GATGAAGAACGYAGYRAA-3') (Toju et al., 2012) and ITS4 primer (5'-TCCTCCGCTT ATTGATATGC-3') (Gardes and Bruns, 1993). The fungal *cbhI* gene was targeted using the primer sets fungcbhIF (5'-CCAA[C,T]TGCTA[C,T]ACI[A,G]G[C,T]AA-3') and fungcbhIR (5'-GC[C,T]TCCCAIAT[A,G]TCCATC-3') (Edwards et al., 2008). All primer sets contained Illumina overhang adapters to ensure compatibility with the sequencing platform following PCR. PCR reactions were run on a 96 Well Thermo Cycler (Applied Biosystems, Warrington, UK) with the following PCR programmes used for the bacterial 16S rRNA gene (95 °C for 3 min; 95 °C for 0.25 min; 57 °C for 15 s and 72 °C for 30 s for 30 cycles; 72 °C for 7 min) and the fungal ITS2 region (95 °C for 3 min; 95 °C for 15 s; 51 °C for 15 s and 72 °C for 30 s for 35 cycles; 72 °C for 7 min). PCR amplicon libraries for each target region were then prepared separately for Illumina next-generation sequencing (NGS) using an Illumina Nextera™ XT Library Prep Kit (Illumina, Cambridge, UK) and associated protocol (Illumina, 2013).

NGS was performed on an Illumina MiSeq platform (Illumina, 2013), to determine the sequence of nucleotide base pairs present within each PCR amplicon (Illumina, 2013). Prior to loading onto the flow cell, quantification of each pooled amplicon library and the final pool containing multiple libraries, was determined using a NEBNEXT® Library Quant Kit for Illumina®. Sequencing of multiple amplicon libraries was achieved via multiplexing on the same run using an Illumina MiSeq reagent kit v3 (600 cycles) generating 300 bp paired end reads (Illumina, 2013). Samples for which Agarose gel electrophoresis indicated an absence of PCR amplicon were excluded from sequencing analysis (excluded bacteria: 32 samples; fungi: 46 samples) after confirmation of absence via quantitative Polymerase Chain Reaction (qPCR) targeting of the same regions. Despite optimisation of PCR annealing temperature, BSA addition, volume of DNA template and cycle number for each primer set, amplification of the *cbhI* gene was too low to support molecular sequencing at all river sites.

qPCR was performed to determine the copy number (abundance) of specific DNA target regions present on each cotton strip subsample. As qPCR detects the abundance of DNA during the exponential phase of each PCR cycle, it provides a more accurate estimation in comparison to end point PCR (McKew and Smith, 2017). In turn, it was able to identify copy numbers for each of the target regions, including the *cbhI* gene, which had low PCR amplification. qPCR conditions were identical to PCR but

primer sets did not contain Illumina overhang adapters. qPCR DNA standards were created from end point PCR amplification where the template DNA was 1 µL of DNA extract from all samples that had been pooled together. qPCR was performed separately for each target region, with each plate including a serial dilution of the purified standards ranging from 10^1 to 10^9, non-template (negative) controls and each sample, which were all included in triplicate. The assays were run on a CFX real-time system (Bio-Rad, Hercules, California, USA) and their conditions, reagents and the determination of copy numbers for each sample for each target region, followed McKew and Smith (2017). Resulting amplicons of the target regions were purified using a QIAquick PCR purification kit (Qiagen, Hilden, Germany) (McKew and Smith, 2017) and quantified using the Quant-iT PicoGreen dsDNA assay kit (Invitrogen). The copy numbers for each target region were then calculated cm^{-2}.

5.2.4 Data analysis

5.2.4.1 Tensile strength loss determination

Maximum tensile strength was calculated as a percentage of initial strength lost for each strip incubation period (Tiegs et al., 2013).

$$\textit{Tensile strength loss} = \left((1-\left(\frac{TSImax}{TSCmean}\right)\right) \times 100\right) / \textit{ incubation period (DD)}$$

Adapted from Tiegs et al. (2013, p.134)

This equation uses the maximum tensile strength of each river incubated strip (TSImax) and the mean tensile strength of all control strips (TSCmean), unincubated but transported to specific regions. Temperature-adjusted degree-days (DD) were calculated by summing the mean temperatures recorded for each 24-hour period during the cotton strip incubation. This enabled temperature normalised comparison of tensile strength loss across regions, as mean river water temperature can vary dramatically on diurnal and seasonal timescales in glacierised catchments (Dickson et al., 2012). Percentage tensile strength loss was averaged across all replicate strips to provide a mean value per river site. Non-temperature-adjusted cellulose decomposition rates were determined by representing the incubation period in days, in place of degree-days. These values were compared to those reported for rivers in eleven other biomes (Tiegs et al., 2019). An Arrhenius plot was constructed to correlate these daily decomposition values to inverted relative mean water temperature following Tiegs et al.

(2019), to determine the influence of river temperature upon decomposition rates (Appendix 4.1).

5.2.4.2 Bioinformatic analysis

Paired-read amplicon libraries obtained from the Illumina sequencer were subjected to quality control, including sequencing trimming, error correction and the removal of poor-quality sequences and chimeric PCR artefacts, following Dumbrell et al. (2017). Classifications were then assigned to each sequence, to taxonomically classify the Operational Taxonomic Units (OTUs) determined from the amplicon libraries (Dumbrell et al., 2017). Data tables were produced detailing the abundance of OTU reads per sample site and the taxonomic classification of each OTU. For fungi (ITS), trophic mode and a confidence ranking describing this assignment were identified for each OTU utilising the FUNGuild database (Nguyen et al., 2016). Additional tables were constructed to host associated environmental information.

5.2.4.3 Ecoinformatic analysis

Negative controls were removed from OTU tables following confirmation that contamination was negligible (bacteria: 6 to 12 reads; fungi: 1 to 8 reads). Three sites containing very low numbers of sequences (1, 41 and 84 reads) were also removed from the fungal (ITS) OTU tables and all samples rarefied to the smallest library size. Rarefaction was selected in preference to alternative procedures of normalisation as an effective method to standardise differential library sizes for microbial data (Weiss et al., 2017). Therefore, OTU abundance referred to the abundance of reads/sequences recorded for each OTU, relative to the minimum library size. Subsets of the fungal (ITS) OTU table were created to represent only OTUs with saprotrophic trophic modes. Further subsets were created for members of the phylum Ascomycota, order Saccharomycetales and genus *Tetracladium*, as they have previously been identified to encompass saprotrophic aquatic hyphomycetes adapted to glacier-fed freshwater environments (Wang et al., 2015; Zang et al., 2016).

5.2.4.4 Statistical analysis

Generalised linear models (GLM) and generalised additive models (GAM) were used to test linear and non-linear relationships between catchment glacier cover (fixed effect) and the following response variables: percentage tensile strength loss, the qPCR determined abundance of bacterial (16S), fungal (ITS) and *cbhI* gene amplicon copy numbers, the abundance of fungal OTUs classified as Ascomycota,

Saccharomycetales, *Tetracladium* or saprotrophic, physicochemical variables (mean river water temperature, 1/Pfankuch Index, EC, pH, optical turbidity) and nutrient concentrations (TN, TP, DOC, DC) across the six study regions. GAMs were also constructed to test the effect of fungal (ITS) and *cbhI* copy number on tensile strength loss. Models were computed in the *mgcv* package of R v. 3.3.2 (Wood, 2011), with best fit evaluated using Akaike information criterion (AIC) values and performance assessed through the percentage of deviance explained. For GAM, smoothing parameter selection followed (Wood, 2004), with Gaussian and Negative binomial distributions identified. The *mgcv* package was also used to construct generalised linear mixed models (GLMM) and generalised additive mixed models (GAMM) to incorporate the effect of absolute latitude (random effect). Some mixed models did not include data collected in Alaska, France and New Zealand due to low (n = < 5) sample numbers. The influence of latitude was considered to be statistically significant if mixed models produced lower AIC values relative to fixed effect only models. The *manyglm* function of the *mvabund* package of R (Wang et al., 2018) was used to fit GLMs (Poisson) to individual OTU responses to catchment glacier cover and tensile strength loss, with relationship significance determined from Wald statistics. The taxonomically classified OTUs which correlated significantly to these parameters were further investigated using the UNITE Community Database (Nilsson et al., 2018). Statistical analysis was performed with and without river sites influenced by proglacial lake inputs, as noted from aerial photography, as the presence of upstream lakes has been found to accelerate leaf litter decomposition rates in glacier-fed rivers (Robinson et al., 1998; Robinson and Gessner, 2000).

5.3 Results

5.3.1 Environmental parameters

For the six glacierised regions combined, there were significant correlations between catchment glacier cover and mean river water temperature, and tensile strength loss and pH, TP and DC (Table 5.1). Fungal (ITS) copy number was related significantly to pH and dissolved carbon concentrations (DC, DOC), while significant relationships between bacterial (16S) copy number and environmental parameters remained absent across sampled river sites. The abundance of saprotrophic fungal OTUs was associated significantly with mean river water temperature, 1/Pfankuch Index, TN, TP, DC and DOC concentrations, and *cbhI* gene copy numbers with mean river water temperature, pH, turbidity and DC (Table 5.1). There were also significant relationships between the abundance of Ascomycota OTUs and mean river water temperature,

turbidity, 1/Pfankuch and DOC and between genus *Tetracladium* and TN and TP concentrations. The order Saccharomycetales was not related significantly to any environmental parameters (Table 5.1).

5.3.2 Microbial community and cellulose decomposition

Reductions in catchment glacier cover were associated with a globally consistent pattern of increased fungal (ITS) copy number (Figure 5.2a), with non-linear increases in the abundance of OTUs for fungal subgroups, including the phylum Ascomycota (Figure 5.2c), genus *Tetracladium* (Figure 5.2d) and taxa classified as hosting saprotrophic trophic modes (Figure 5.2e) (FUNGuild database, Nguyen et al., 2016). Bacterial (16S) copy number remained consistent across the glacier cover gradient (Figure 5.2b). At a taxon-scale, the abundance of four bacterial (16S) and eighteen fungal (ITS) OTUs were related significantly to catchment glacier cover, with four bacterial (16S) and one fungal (ITS) OTUs correlated significantly to tensile strength loss (Appendix 4.2). As 252 bacterial (16S) and 283 fungal (ITS) OTUs were found exclusively > 52 % glacier cover, approximately 7 % of the bacterial (16S) and 27 % of the fungal (ITS) community were restricted to high glacier cover river sites.

The functional *cbhI* gene copy number increased significantly with glacier loss across all regions (Figure 5.2f), showing a marked increase below approximately 40 % glacier cover. Both *cbhI* gene and fungal (ITS) copy numbers were associated with greater tensile strength loss (Figure 5.2g, h). There was no significant correlation between catchment glacier cover and cotton strip tensile strength loss across all regions (Figure 5.3a). However, there was a significant linear decrease in tensile strength loss with reductions in catchment glacier cover for river sites which supported microbial amplification (bacteria (16S), fungi (ITS)) but not *cbhI* gene copy numbers (Figure 5.3b). River sites where the *cbhI* gene was found on cotton strip assays were identified across the gradient of catchment glacier cover, as were those lacking microbial amplification (Figure 5.3b).

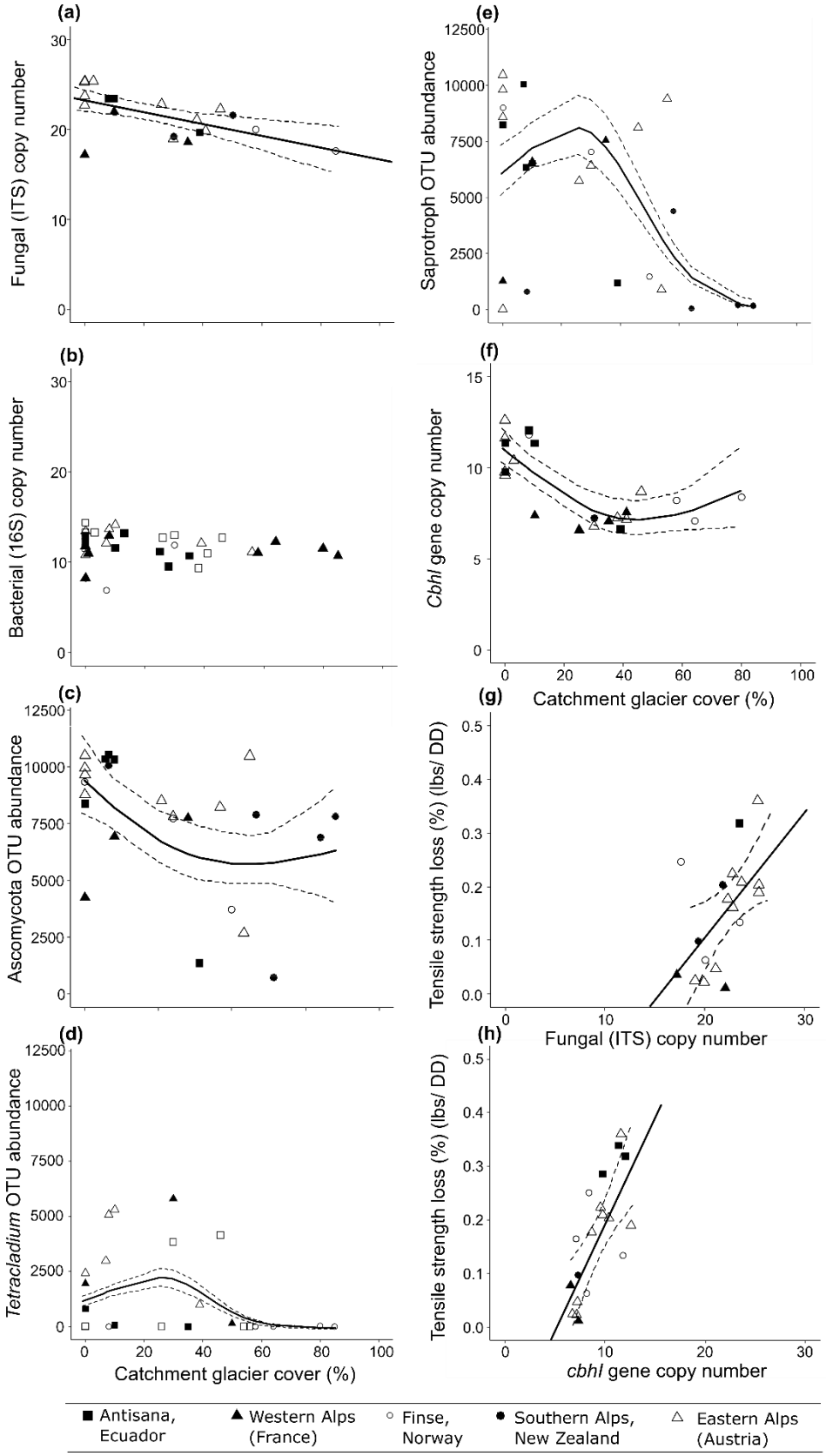

Figure 5.2 Globally synchronous GLM/GAM relationships between catchment glacier cover, tensile strength loss of river incubated cotton strips and abundance of their cotton assay microbial communities. (a) Increasing fungal (ITS) copy numbers with declining catchment

glacier cover, (b) bacterial (16S) copy numbers with decreasing glacier cover, (c) non-linear increase of Ascomycota OTU abundance with reducing glacier cover, (d) unimodal response of *Tetracladium* OTU abundance with glacier ice loss, (e) increasing saprotrophic fungal OTU abundance with declining in glacier cover, (f) increasing *cbhI* amplicon copy numbers with ice loss, (g) linear increase in tensile strength loss with increasing fungal (ITS) copy numbers and (h) increasing tensile strength loss with increasing *cbhI* gene copy numbers. There were no microbial amplicons identified at river sites in the Alaska Boundary Range. Copy number = ln copy number cm^{-2}. DD = degree-days (Section 5.2.4.1). Sample numbers vary as bacterial (16S), fungal (ITS) and *cbhI* copy numbers were not present at all river sites.

Table 5.1 GLM/GAM model summary statistics for relationships between catchment glacier cover (%), tensile strength loss (%) (lbs/ degree-day), microbial qPCR copy numbers (ln copy number cm^{-2}) (bacteria = 16S, fungi = ITS, *cbhI* gene), fungal OTU abundance (Ascomycota, *Tetracladium*, saprotrophs) and environmental parameters (Temp = water temperature (°C)) for six glacierised regions. Relationships are displayed in Figure 5.2 and Appendix 4.5.

***Independentl* dependent variables**	**Model**	**χ^2/ *F***	***p*-value**	**Deviance explained (%)**
Catchment glacier cover (%) (%glac)				
%glac vs ITS	GLM (Gaussian)	11.47	0.003 **	37.6
%glac vs 16S	GLM (Gaussian)	0.75	0.394	2.2
%glac vs Ascomycota	GAM (Negative binomial)	14.99	< 0.001 ***	13.5
%glac vs *Tetracladium*	GAM (Negative binomial)	386.10	< 0.001 ***	23.1
%glac vs saprotroph	GAM (Negative binomial)	305.70	< 0.001 ***	28.9
%glac vs *cbhI* gene	GAM (Gaussian)	18.88	< 0.001 ***	65.4
%glac vs temp	GLM (Gaussian)	40.03	< 0.001 ***	45.5
Tensile strength loss (%) (lbs/DD)				
cbhI vs TS loss	GLM (Gaussian)	20.25	< 0.001 ***	65.4
ITS vs TS loss	GLM (Gaussian)	7.66	0.014 *	32.4
pH vs TS loss	GLM (Gaussian)	10.07	0.003 **	17.3
TP vs TS loss	GLM (Gaussian)	4.13	0.048 *	17.4
DC vs TS loss	GLM (Gaussian)	4.42	0.049 *	16.2
Environmental parameters				
Temp vs Ascomycota	GLM (Gaussian)	4.89	0.039 *	20.5
Temp vs *cbhI* gene	GLM (Gaussian)	5.04	0.038 *	22.9
Temp vs saprotroph	GAM (Negative binomial)	170.70	< 0.001 ***	20.4
pH vs *cbhI* gene	GLM (Gaussian)	5.66	0.027 *	21.2
pH vs ITS	GLM (Gaussian)	7.21	0.015 *	27.5
Turbidity vs Ascomycota	GAM (Negative binomial)	11.47	0.003 **	10.1
Turbidity vs *cbhI*	GAM (Gaussian)	5.78	0.011 *	37.9
1/Pfankuch vs Ascomycota	GAM (Negative binomial)	12.07	0.002 **	10.3
1/Pfankuch vs saprotroph	GAM (Negative binomial)	39.48	< 0.001 ***	6.1
DC vs *cbhI*	GLM (Gaussian)	8.79	0.014 *	46.8
DC vs ITS	GLM (Gaussian)	8.09	0.015 *	40.3
DC vs saprotroph	GAM (Negative binomial)	52.63	< 0.001 ***	21.5
DOC vs Ascomycota	GAM (Negative binomial)	7.21	0.027 *	37.1
DOC vs ITS	GLM (Gaussian)	8.15	0.015 *	40.5
DOC vs saprotroph	GAM (Negative binomial)	38.31	< 0.001 ***	13.1
TP vs saprotroph	GAM (Negative binomial)	20.81	< 0.001 **	4.6
TP vs *Tetracladium*	GLM (Gaussian)	5.05	0.036 *	20.2
TN vs saprotroph	GAM (Negative binomial)	37.65	< 0.001 ***	6.4
TN vs *Tetracladium*	GLM (Gaussian)	4.43	0.048*	17.4

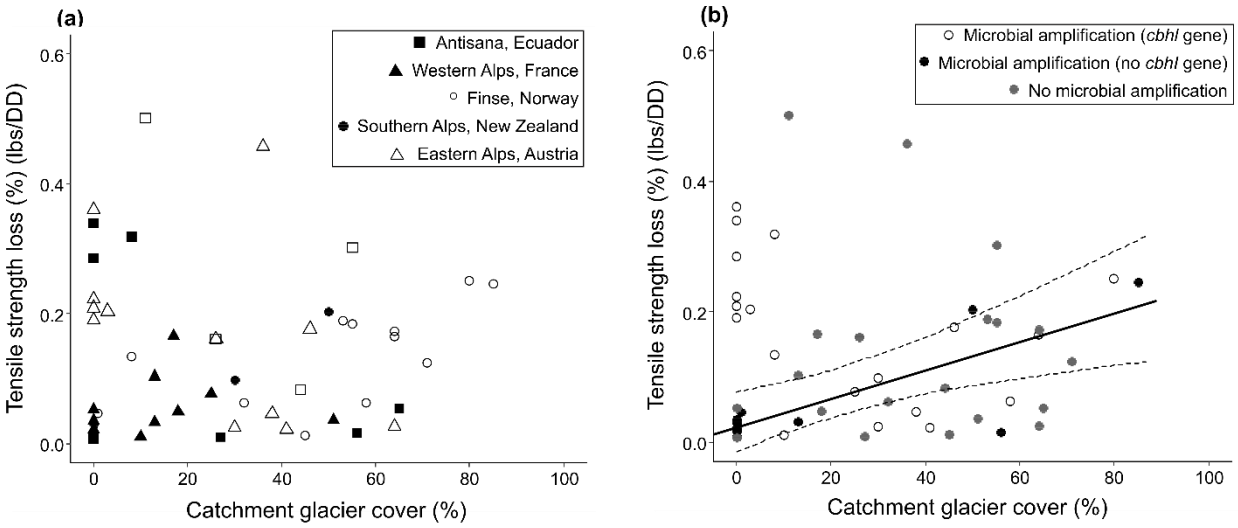

Figure 5.3 Relationships between tensile strength loss and reducing catchment glacier cover for (a) all sampled river sites and (b) sites hosting qPCR amplification (copy numbers). Sites are separated to highlight those which supported all microbial amplicons (16S, ITS, *cbhI*), presence of 16S and ITS amplicons but not the *cbhI* gene, and an absence of all copy numbers. The significant linear relationship between glacier cover and sites with only 16S and ITS amplification (no *cbhI* gene) is illustrated (GLM (Gaussian): $F = 12.57$, p-value = 0.006 **, deviance explained = 58.3 %).

The significance of relationships displayed in Figure 5.2 were not altered by removal of river sites influenced by proglacial lake inputs (Appendix 4.3), or inclusion of absolute latitude as a random effect. GLMM and GAMM consistently produced higher AIC values than comparative fixed effect models (Appendix 4.4). An Arrhenius plot illustrated that there was no significant relationship between mean river water temperature and daily cellulose decomposition rates (Appendix 4.1). Non-temperature-adjusted cellulose decomposition rates were within the range of those documented for rivers in a diversity of tropical and temperate biomes, yet also hosted the lowest values reported (Figure 5.4).

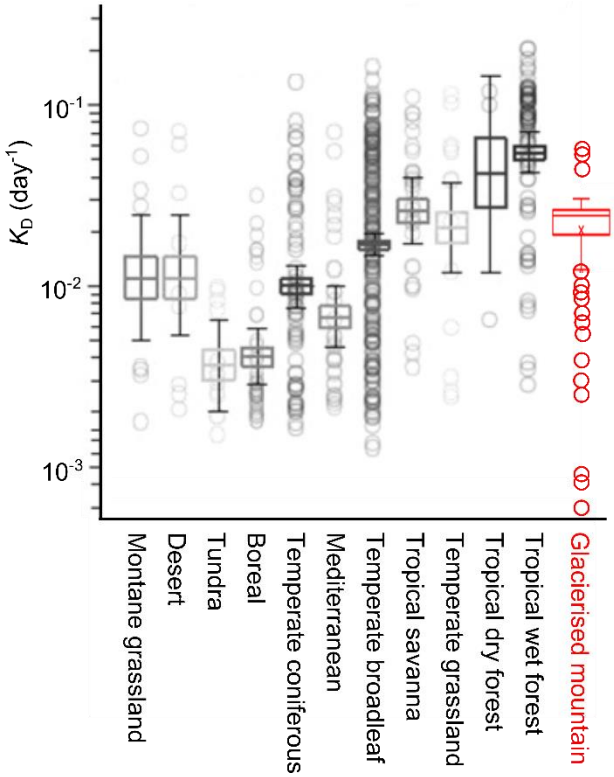

Figure 5.4 Comparison of $\log_{10}$ daily cellulose decomposition rates (k_D) in glacierised mountain rivers (red) and rivers representing eleven other biomes (grey). The k_D values represent the potential capacity of each river ecosystem to decompose cellulose, when unadjusted for water temperature. Adapted from Tiegs et al. (2019).

5.4 Discussion

The loss of glacier ice is a pattern characteristic of most mountain regions worldwide (Huss and Hock, 2018). This study identified that glacier retreat is driving globally coherent increases in the copy number of river fungi (ITS) and their *cbhI* gene, which are associated significantly with the accelerated decomposition of cellulose in deglaciating regions. In turn, this study provided new understanding of the linkages between microbial biodiversity and ecosystem functioning in mountain rivers. Findings suggested that such cryospheric changes can be expected to drive large-scale alterations in river carbon cycling, by enhancing the conditions for aquatic fungal decomposition of particulate carbon.

5.4.1 Environmental parameters

The warming of river waters associated with decreasing catchment glacier cover and ice melt contributions is well documented (Milner and Petts, 1994; Milner et al., 2001). Increasing water temperature was correlated significantly to enhanced abundance of fungal OTUs (Ascomycota, saprotrophs) and their *cbhI* gene copy numbers, a

response which may underpin the sensitivity of ecosystem metabolism to water temperature (Follstad Shah et al., 2017). Ulseth et al. (2018) noted that reduced snow melt inputs increased river ecosystem respiration, resulting in accelerated carbon processing rates and supporting the findings of this study. Fungal abundance (ITS copy numbers, Ascomycota and saprotroph OTU abundance) was correlated negatively with DOC, potentially as greater numbers of taxa were available to catabolise OM. In addition, at low glacier cover river sites where fungal abundance was greatest, their community respiration may have been proceeding faster in the comparatively warmer waters, processing carbon at an accelerated rate. Alongside water temperature, global patterns of increased Ascomycota OTU abundance were also correlated significantly with increased channel stability and reduced turbidity, contributing to the acceptance of H_1. These parameters have previously been identified to enhance microbial abundance in glacier-fed rivers (Robinson et al., 1998; Wilhelm et al., 2013; Eisendle-Flöckner et al., 2013). As supported by previous research, increase in nutrient concentrations (TP, TN) correlated to both a proliferation of saprotrophic fungal abundance (saprotroph and *Tetracladium* OTU abundance) and accelerated decomposition rates (tensile strength loss, TP) (Robinson and Gessner, 2000; Yue et al., 2016). Cotton strip assays provided a locally unlimited carbon source throughout their incubation period in the studied mountain rivers, where particulate OM supply is naturally low and patchily distributed across sediment microhabitats (Singer et al., 2012). As such, this study was able to investigate the effects of catchment glacier cover and its associated physicochemical variables upon cellulose decomposition rates while constraining the potentially confounding influence of resource supply.

5.4.2 Microbial community and cellulose decomposition

There was no correlation between bacterial (16S) copy number and both declining glacier cover and the environmental parameters underpinning glacier influence. This was potentially due to the short incubation period of cotton strip assays, as aquatic fungi often dominate the initial microbial colonisation of complex materials, and this conditioning may be a prerequisite for increased bacterial abundance (Bayer et al., 2006). Benthic sediments and biofilms have previously been documented to host higher bacterial cell abundances in groundwater dominated streams than glacier-fed channels (Battin et al., 2004; Freimann et al., 2013). In turn, longer cotton assay incubation times may be required to further investigate the contribution of bacteria to OM processing in glacierised catchments, which may currently be underestimated (Glassman et al., 2018). Taxa of the order Cytophagales and genus *Flavobacterium*

may drive bacterial cellulose decomposition in deglaciating catchments, as increases in their OTU abundance were significantly associated with increased tensile strength loss across the six sampling regions (Appendix 4.2). Nevertheless, the incubation of cotton strips provided a valuable mechanism for investigating the effect of fungal colonisation on decomposition rates in glacier-fed rivers.

Multi-region increases in fungal copy number despite the absence of a bacterial response enabled only partial acceptance of H_1. Peaks in the abundance of *Tetracladium* and saprotrophic fungal OTUs at approximately 30 % glacier cover align with the intermediate disturbance theory (Townsend et al., 1997). This could be attributable to reductions in both the harsh abiotic environmental conditions sustained at high glacier cover river sites and the intensive competition imposed at low cover sites, as previously identified for the abundance (Khamis et al., 2016) and richness (Jacobsen et al., 2012; Cauvy-Fraunié et al., 2014) of glacier-fed river invertebrates. Despite global increases in overall fungal (ITS) copy number with glacier decline, the abundance of taxa previously identified to inhabit glacier-fed streams and ice environments, including Helotiales and Ascomycota species (Czeczuga and Orlowska, 1999; Wang et al., 2015; Zhang et al., 2016), may be reduced by reductions in glacier cover, unless the increase in water temperature induced by ice loss does not exceed the tolerances of these specialists. The OTU abundance of psychrophilic species was noted to both increase (*Lemonniera centrosphaera, Tetracladium marchalianum*) and decrease (*Tetracladium* spp., Leotiomycetes, Ascomycota) with reducing glacier cover (Appendix 4.2) and further research is required to detail the occurrence of such taxa in river habitats, such as sediments.

While amplification of the *cbhI* gene at river sites cannot confirm its expression, the significant association between copy number and tensile strength loss suggested that across the six glacierised regions, increases in this functional gene were associated with increased cellulose decomposition, leading to acceptance of H_2. Greater significance and model fit (Table 5.1) for the relationship between tensile strength loss and *cbhI* gene copy number in comparison to fungal (ITS) copy number suggested that microbial traits were a stronger predictor of ecosystem function than taxonomy (Green et al., 2008). Amplification of the *cbhI* gene across the gradient from 0 to 80 % catchment glacier cover in multiple mountain regions illustrated the pervasiveness of fungal catabolism of OM. These findings are supported by previous work on alpine rivers in the Val Roseg catchment, Switzerland, which used leaf pack assays (Gessner

et al., 1998; Robinson et al., 1998). Here, a reduction in fungal biomass at proglacial sites was observed but there was a cold-adapted, saprotrophic fungal community present, despite harsh physicochemical conditions (Gessner et al., 1998; Robinson et al., 1998). This research unpicks the genetic basis of the observed decomposition function for the first time, and shows it to be globally coherent. Increase in *cbhI* gene amplicon copy number accelerated below approximately 40 % glacier cover, despite concurrent reductions in the abundance of saprotroph OTUs, which may reflect limitations in understanding of trophic mode for many fungal taxa (Nguyen et al., 2016). However, significant associations between tensile strength loss and catchment glacier cover for river sites hosting microbial (16S, ITS) but not *cbhI* amplification suggested that additional cellulolytic enzymes may be contributing to cotton strip hydrolysis alongside cellobiohydrolase I (Figure 5.3b).

The fungal communities of glacier-fed rivers have previously been found to drive OM processing rates comparable to temperate river systems (Gessner et al., 1998). This was supported by this study, as although decay of cotton strips cannot be directly compared to that of leaf packs, the daily cellulose decomposition rates identified across all sampled rivers (log_{10} *mean*: -1.70, log_{10} *range*: -1.25 to -3.22) illustrated that while three assays hosted the lowest tensile strength loss reported for rivers of any biome, values for many glacierised mountain rivers were in alignment with cotton strips incubated in rivers of temperate grassland and tropical savanna (Tiegs et al., 2019). Tensile strength loss may have been reduced for three glacier-fed rivers due to low cotton strip colonisation rates, with amplification of fungi (ITS) and the *cbhI* gene observed only at 34 % of river sites. Colonised strips supported low fungal (ITS) OTU numbers, with a total of 1056 OTUs identified, and the mean number per region ranging from 60 (Southern Alps, New Zealand) to 129 (Eastern Alps, Austria). This was reduced even in comparison to glacier-fed rivers in Svalbard (162 OTUs), but microbes were obtained from water samples rather than incubated cotton assays (Zhang et al., 2016). Tensile strength loss rates may have been comparable to rivers in other biomes as cold freshwaters have previously been identified to host leaf pack decay rates similar to streams with greater water temperatures and nutrient concentrations (Cristiano et al., 2019). This suggested that other environmental drivers and/or biological interactions might influence OM processing rates (Cristiano et al., 2019), concurrently to temperature sensitive fungal catabolism. These processes may have contributed to absence of a significant relationship between non-degree-day adjusted cellulose decomposition rates and river water temperature across sampled river sites.

Furthermore, although low sample numbers in some regions may have prevented observation of significant trends, cold adaptation in decomposer communities may explain why no latitude effect was evident, despite previous studies showing strong effects on river fungi communities (Seena et al., 2019).

Tensile strength loss was observed at river sites for which microbial amplification was absent (20 river sites), suggesting that processes other than microbial decomposition could be important contributors. Physical abrasion at some sites was likely to have been enhanced where strips became dislodged from their initial position in contact with the river bed, exposing them to turbulence in the water column, repeated collisions with the bed and reducing contact (thus colonisation potential) with benthic biofilms. Additionally, this study did not exclude invertebrates from the cotton strips. However, aquatic shredders preferentially select preconditioned substrates for their increased palatability and incubation periods have previously been identified as insufficient for the established microbial community to create this environment (Tiegs et al., 2007). Some Chironomidae were found upon cotton strips but they are likely to have used them as refuge sites or for grazing of colonised fungi and bacteria, rather than as direct food sources, as identified for leaf pack assays deployed in alpine streams (Gessner et al., 1998). Archaea may also decompose OM in rivers but their role is currently poorly understood (Manerkar et al., 2008).

Absence of a significant relationship between tensile strength loss and catchment glacier cover led to rejection of H_3. This lack of correlation may be underpinned by the simultaneous operation of biological (*cbhI* gene) and non-biological (no microbial amplification) mechanisms of cellulose decomposition throughout the gradient of glacier cover. Previous global assessments of river leaf litter decomposition have encountered difficulty in linking decay rates to components of climate change (water temperature increases) due to complex, interacting decay mechanisms (Boyero et al., 2011). By focusing analysis of decomposition rates upon cotton strip assays, which were known to be colonised by fungi (Tiegs et al., 2013), it was possible to identify the biological basis of decomposition. However, physical and biological processes will have interacted at some sites, with the presence of *cbhI* gene amplicons not predicating absence of physical degradation and absence of microbial amplification not excluding the contribution of additional biological drivers (e.g., Archaea, alternative cellulase enzymes, microbes currently unclassified in the FUNGuild database (Nguyen et al., 2016), microbes not yet recognised as saprotrophic). Future use of cotton strip assays

should consider ways to minimise the contribution of physical breakdown processes (e.g., protection within mesh) with greater certainty.

5.4.3 Evaluating the suitability of cotton strip assays for mountain river systems

Glacier-fed rivers are characterised by high flow variability, supporting both flood events and intermittent flows, alongside high turbidity, sediment mobility, suspended sediment concentrations and low mean water temperatures (Milner et al., 2017) which may have physically degraded cotton strips and limited their microbial colonisation. The approximate 37 day incubation period may have been insufficient for cotton strips to reach 50 % tensile strength loss, particularly at the coldest river sites, limiting sensitivity of the decomposition measurements using an extensometer. Despite steps to promote cotton strip and data logger retention (Section 5.2.2.2), exposure of strips during this incubation period to harsh physicochemical conditions and flow variability prevented the recovery of a further 97 cotton strips (18 additional river sites) originally deployed across three of the regions, resulting in a retrieval rate of approximately 72 %. However, alternative aquatic decomposition assays (e.g., leaf packs, tea bags) would have been exposed equally to these conditions and the comparatively streamlined shape of cotton strips may have minimised their detachment. Doubling the number of replicate strips recommended by the CELLDEX protocol (Tiegs, 2015a) and sampling multiple river sites representative of singular catchment glacier cover percentages may improve the suitability of cellulose assays for measuring aquatic decomposition in glacier-fed rivers. Cotton strips hold high biological relevance in these allochthonous energy limited systems and facilitated successful microbial profiling. However, any extension of the incubation period must be weighed against increased risk of non-retrieval.

5.4.4 Wider implications and further research

This research was the first to investigate cellulose decomposition rates in glacierised mountain rivers, and to assess their response to global reductions in catchment glacier cover. Extension of the CELLDEX protocol into glacier-fed streams delivered a standardised, ecologically relevant decomposition assay suitable for microbial profiling, provided that increased cotton strip numbers, site replicates and stabilising equipment were used. Aquatic cellulose decomposition appeared to be influenced by copy number of the cellobiohydrolase I gene, and as declining catchment glacier cover drove global increases in the copy number of both fungal taxa and subsequently *cbhI* gene amplicons, glacier retreat may accelerate OM decomposition rates in glacierised

catchments. At a multi-regional scale, catchment glacier cover and cellulose decomposition were not correlated significantly, potentially because physical fragmentation decay mechanisms were difficult to control across the gradient of glacier cover. Cotton assays contribute to the standardised investigation of organic carbon processing rates in rivers (Tiegs et al., 2019) which is of critical importance given the role of freshwater decomposition in the global carbon cycle (Battin et al., 2008; Raymond et al., 2013). Previous studies documented that glacier retreat will increase dissolved organic carbon availability to downstream habitats and CO_2 to the atmosphere through modification of biofilm community structure and metabolism (Battin et al., 2004; Singer et al., 2012; Ulseth et al., 2018). This study advances understanding of this role of fungal taxa by quantifying a functional mechanism (*cbhI* driven decomposition of cellulose) which will accelerate this ecosystem response with sustained ice loss. Further research should consider the implications of this altered carbon cycling for the trophic energy transfer of benthic food webs (Tank et al., 2010), in the context of changing OM provision in mountain catchments, as herbaceous riparian vegetation communities colonise and expand with glacier retreat (McKernan et al., 2018).

Chapter Six: Alpine river ecosystem response to glacier retreat: current scientific understanding and proposed future research directions

6.1 Introduction

This chapter synthesises the key findings of this thesis in the context of current scientific understanding regarding the response of alpine river ecosystems to glacier retreat. The original contributions of each analytical data chapter are reviewed to address the four objectives underpinning this research. Information is then collated from across these chapters and recently published literature to refine the conceptual models presented in Chapter Two and, in turn, describe the application of thesis findings to alpine river research and conservation strategy. Limitations of the research approach and individual chapters are discussed and future study recommendations proposed. This discussion concludes by summarising the principal contributions of this thesis to the understanding of alpine river ecosystem response to glacier retreat.

6.2 Objective 1: Analytical research synopsis

Chapter Two developed a novel conceptual understanding of the multitrophic responses of alpine river communities to reducing catchment glacier cover (Objective 1). The literature synthesis underpinning development of this model highlighted three critical research gaps. First, there was requirement to extend focus beyond river macroinvertebrates, to ensure the responses of additional taxonomic groups (e.g., microbes, diatoms, protists, vertebrates) were described in detail. Previous research suggested that some groups were highly sensitive to reductions in catchment glacier cover (Rott et al., 2006; Gesierich and Rott, 2012; Eisendle-Flöckner et al., 2013); supported endemic species vulnerable to the associated physicochemical alterations (Falasco and Bona, 2011; Biffi et al., 2016) and yet made important contributions to ecosystem functioning in glacierised catchments (Gessner et al., 1998; Rott et al., 2006; Ulseth et al., 2018; Tiegs et al., 2019). In turn, Chapter Three quantified the implications of declining glacier cover for benthic diatom assemblages, the principal primary producers in alpine river systems (Objective 2). Second, the simultaneous and interacting responses of aquatic biota needed to be considered collectively, as taxonomic groups are not impacted by glacier retreat in isolation (Woodward et al., 2010b). Furthermore, species responses are often dissimilar to those of higher levels of

biological organisation (Appendix 5.1). Chapter Four therefore described the influence of reducing glacier cover on alpine river food web structure and allometry, to capture network-scale responses (Objective 3). Third, previous studies highlighted the importance of considering the relationship between biodiversity and ecosystem functioning (Cardinale et al., 2000; Besemer, 2015), as aquatic community structure and processing may respond differently to the natural environmental perturbations imposed by glacier retreat. Much less is known of how freshwater ecosystem function rates will be influenced by glacier retreat. Consequently, Chapter Five investigated links between microbial community abundance and cellulose decomposition rates across six glacierised regions (Objective 4).

The three analytical data chapters were intrinsically linked. The influence of declining catchment glacier cover on food web structure modifies trophic interactions between consumer and resource communities, altering benthic diatom and microbial assemblages. For aquatic fungi, increased abundance was associated with increased cellulose decomposition rates. Furthermore, organic matter decay, alongside primary production, drives and mediates energy supply to alpine river food webs. Increasing abundance of basal taxa appeared to induce successional rewiring of these freshwater networks. Bottom-up processes predominantly influenced river food web assembly, altering their structure, allometry and trophic interactions with reductions in glacier cover.

6.2.1 Objective 2: Response of benthic diatom biodiversity to declining catchment glacier cover

Chapter Three quantified the response of alpine benthic diatom biodiversity to a gradient of declining catchment glacier cover in the European Alps (Objective 2). Through collection, identification and numeration of diatom valves from rivers of the Eisboden, Obersulzbach and Rotmoos valleys in the central Austrian Alps, this study determined assemblage- and taxon-scale biodiversity responses to declining glacier cover and the environmental parameters underpinning this gradient. The impact of glacier recession upon biofilm taxa remains less studied in comparison to other aquatic biodiversity (Battin et al. 2016; Fell et al., 2017), but this research identified that their responses aligned closely to those of additional taxonomic groups, including macroinvertebrates. For example, reductions in catchment glacier cover were associated with significant increases in taxonomic richness, valve density and Shannon diversity but unimodal declines in within-site turnover (total dissimilarity) and linear

decreases in between-site nestedness. This pattern of increased α-diversity but reduced β-diversity was previously identified with glacier recession for macroinvertebrates (Brown et al., 2007b; Jacobsen et al., 2012) and bacterial communities (Wilhelm et al., 2013). This thesis confirmed increases in taxonomic richness with ice loss for these taxonomic groups, alongside benthic diatoms (Appendix 5.2). This illustrated uniformity of response to reducing ice melt inputs and the accompanying homogenisation of river habitats (Khamis et al., 2016). In addition, alterations to diatom assemblage composition as glacier cover declined were strongly associated with increasing channel stability, similar to macroinvertebrate communities in glacier-fed rivers (Milner and Petts, 1994; Milner et al., 2001). Although resilient to high flows, bed mobility can damage and detach biofilm architecture, limiting succession of communities in response to both meltwater pulses and precipitation driven flood events, as identified in the Rotmoos catchment (Hieber et al., 2001; Wellnitz and Rader, 2003; Bona et al., 2012; Fell et al., 2018). This research provided further evidence that aquatic taxa are responding in similar ways to reducing glacier cover, potentially due to the comparable biotic implications of physicochemical drivers or through strong food web linkages.

At a species-scale, benthic diatoms illustrated a spectrum of responses to declining glacier cover, with taxa facing habitat loss or expansion based upon their positioning along the chronosequence. For example, *Caloneis lancettula* and *Eunotia trinacria* were identified exclusively at river sites ≥ 52 % glacier cover, where their low motility may drive genetic isolation given the fragmented nature of deglaciating headwaters (Dong et al., 2016; Lange-Bertalot et al., 2017). While six taxa found only in rivers ≥ 28 % glacier cover may also become threatened by continued ice loss, seven species confined to river sites without glacier cover could experience an upstream proliferation of their habitat conditions with reducing ice melt inputs (Table 6.1), as previously documented for alpine river macroinvertebrates (Lencioni, 2018). Diatom taxa associated with low or no glacier cover hosted greater valve densities and a broader range of growth forms (chain-forming, high motility), suggesting more mature, stable biofilms in comparison to high glacier cover sites. This potentially supported greater rates of primary production and aligned to the proliferation of basal taxa and production driven food web assembly identified < 26 % glacier cover in Chapter Four. As alpine river food webs are primarily supported by this autochthonous energy supply with limited riparian subsidy (Zah and Uehlinger, 2001), the identified alterations to river diatom biodiversity in response to reducing catchment glacier cover could influence the

reorganisation of whole aquatic networks and provide new insight into the understanding of resource-base dynamics in deglaciating catchments.

Table 6.1 River macroinvertebrates, diatoms and microbes which may benefit or be imperilled by sustained reductions in catchment glacier cover. Potential 'winners' were taxa identified exclusively at river sites with 0 % catchment glacier cover and potential 'losers' those only at river sites > 28 % glacier cover. Sites above this threshold are threatened by continued deglaciation, with many catchments in the Austrian Alps already supporting glacier ice below this percentage of cover (Koboltschnig and Schöner, 2011). This information can act as an initial guide to taxa responses but further study is required to determine their adaption capacity or presence in alternative habitats.

Taxa	'Winners'	'Losers'	Source
Macroinvertebrates	Nemouridae *Protonemura* Nemouridae *Nemoura*	*Diamesa insignipes* *Heptagenia lateralis* Heptageniidae sp. A *Rhithrogena semicolorata*	Chapter Four
Benthic diatoms	*Chamaepinnularia mediocris* *Cymbella parva* *Gomphonema angustatum* *Gomphonema calcareum* *Meridion circulare* *Reimeria sinuata f. antiqua* *Stauroneis agrestis*	*Caloneis lancettula* *Diatoma vulgaris* *Eunotia trinacria* *Fragilaria constricta* *Navicula* sp. B *Staurosira construens*	Chapter Three
Microbes	97 fungal (ITS) OTUs: e.g., *Meliniomyces* spp. *Cistella* spp. *Pleosporales* spp.	557 fungal (ITS) OTUs: e.g. *Tetracladium* spp. *Cistella* spp. *Itersonilia perplexans*	Chapter Five
	435 bacterial (16S) OTUs: e.g. *Mucilaginibacter* spp. *Fibrobacter* spp. *Luteolibacter* spp.	459 bacterial (16S) OTUs: e.g., Cellvibrio spp. *Methylococcus* spp. *Flavobacterium* spp.	

6.2.2 Objective 3: Response of river food webs to declining catchment glacier cover

Chapter Four investigated alterations to the structure and allometry of alpine river food webs along a chronosequence of declining catchment glacier cover in the central Austrian Alps (Objective 3). Nine new river food webs were constructed from gut contents analysis and described using connectance and trophic descriptors. This study was the first to document the rewiring of river food webs along the natural successional gradient imposed by glacier retreat. Reducing catchment glacier cover increased node number, mean chain length and community span, with the rate of increase accelerated below a threshold of approximately 26 % glacier cover. This 'tipping point' was underpinned by a proliferation of basal taxa abundance and biomass, potentially due to

the attenuation of meltwater influence (Hieber et al., 2001; Rott et al., 2006; Battin et al., 2016). Above 26 % glacier cover, food web assembly may have been controlled by the disturbance regime imposed by ice melt, but below this threshold, these inputs appear sufficiently reduced to enable donor-controlled mechanisms to dominate. Proglacial lake inputs were found to accelerate the succession of a river food web beyond this threshold, despite the site watershed hosting 42 % glacier cover. Lakes have previously been noted to increase mean water temperature and channel stability, aligning macroinvertebrate (Milner and Petts, 1994; Brittain et al., 2001; Milner et al., 2001) and algal (Hieber et al., 2001) community composition to those associated with non-glacial river reaches. For the first time, geomorphic context was also identified to modify food web descriptors, such as linkage density and mean trophic vulnerability, to be comparable to those for low cover river sites. Despite low directed connectance, small-world topology and the shortest reported river food chain lengths, structural reorganisation of food webs along the glacier cover gradient did not result in the extirpation of pioneer species such as *Diamesa cinerella, Diamesa goetghebueri* and members of the *Baetis alpinus* group (found ≥ 36 % catchment glacier cover). Colonising species were also found at low glacier cover river sites and retained many of their feeding linkages, suggesting that the tolerance assembly mechanisms previously documented for river invertebrates (Milner and Robertson, 2010; Brown and Milner, 2012) might function across whole food webs.

Food web metrics did not align to the predictions of metabolic theory, with scaling coefficients representing individual and species-averaged mass-abundance regressions higher (shallower slopes) than expected (Brown et al., 2004), despite minimal terrestrial subsidy to these above treeline reaches (Perkins et al., 2018). Such disparity may be explained by food webs not capturing the full mass and abundance contribution of all basal resources (e.g., microbes, amorphous detritus), or the inverted biomass pyramids which characterise these and many other freshwater ecosystems (Vadeboncoeur and Power, 2017). In addition, macroinvertebrate consumers may have capitalised upon seasonal and within-catchment periphyton availability driven by the response of biofilm architecture to meltwater or storm induced flood pulses (as identified in Chapter Three) (Uehlinger et al., 2002; Gabbud et al., 2019). As individual mass-abundance slope values increased significantly with increasing glacier cover, consumers found at high cover river sites may have possessed greater energy transfer efficiencies in adaption to the lower water temperatures and reduced channel stability. The rate of increase in macroinvertebrate abundance failed to keep pace with that of

basal taxa as glacier cover declined, potentially due to dispersal constraints imposed by the fragmented configuration of mountain river networks, which disproportionately impact larger species (Brown et al., 2018). These findings provided a first description of the significant reorganisation of river connectance food webs in response to a shrinking cryosphere.

6.2.3 Objective 4: Response of microbial communities, functional genes and ecosystem functioning to declining catchment glacier cover

Chapter Five quantified the relationship between river microbial abundance and cellulose decomposition rates in mountainous regions of six countries (Objective 4). Through tensile strength determination and molecular sequencing (qPCR, Illumina sequencing) of standardised cotton strip assays, this research documented the potential microbial catabolism driving organic matter decomposition in glacierised catchments and for the first time, the role of the functional gene (*cbhI*) underpinning this ecosystem process. While the structural complexity and nutritional composition of cotton strips may have varied from that of riparian shrubs and grasses entering mountain rivers, their constituent cellulose is the most abundant organic polymer in leaf litter substrates and in turn, its decomposition dominates the release of carbon from freshwaters (Bayer et al., 2006; Tiegs et al., 2019). This study investigated the relationship between biodiversity and ecosystem functioning, as increases in the abundance of fungal taxa were correlated significantly with proliferation of *cbhI* copy number and in turn, accelerated tensile strength loss. Chapter Five also noted the possible contribution of additional cellulolytic enzymes to cotton strip hydrolysis, but further research is required to identify and quantify the associated gene amplicons. Global increases in the OTU abundance of fungal (ITS) taxa (Ascomycota, *Tetracladium*, saprotrophs) with reducing glacier cover were not matched by those of bacteria (16S), potentially as cotton strip incubation periods were insufficient to capture the successional transition from initial fungal colonisation of aquatic substrates to later bacterial cellulolytic activity (Bayer et al., 2006). Noted increases in fungal (ITS) copy number may have masked reduction of cold-stenothermic saprotrophs including *Tetracladium marchalianum* and *Tetracladium psychrophilum*, which have previously been identified in glacial habitats (Wang et al., 2015; Zang et al., 2016), if the increases in river water temperature driven by reducing catchment glacier cover exceeded their tolerances (Table 6.1).

Absence of a significant relationship between declining catchment glacier cover and cellulose decomposition rates across the six glacierised regions was potentially due to the influence of physical degradation processes, which are difficult to standardise in natural river experiments. Despite this, sustained glacial ice loss can be expected to accelerate organic matter decomposition rates in mountain catchments through increased fungal catabolism. This will potentially increase the release of CO_2 and CH_4, alongside dissolved and particulate organic carbon, to the atmosphere and sediments of downstream river, estuary and marine habitats (Battin et al., 2008; Striegl et al., 2012; Singer et al., 2012; Ulseth et al., 2018). While the importance of freshwater ecosystems in the global carbon cycle is widely recognised (Battin et al., 2008) and the role of glacier-fed rivers remains comparatively less described (Singer et al., 2012), this study highlighted an important functional mechanism which may underpin the accelerating rate of carbon emissions from aquatic cellulose decay. This research determined cotton strip assays to be a suitable method for investigating cellulose decomposition in glacierised river catchments, provided the CELLDEX protocol for their deployment (Tiegs et al., 2015) was adjusted to include increased assays, site replicates and greater efforts to fix equipment in highly unstable channels. The standardised composition, ecological relevance and successful microbial profiling of cotton strips enabled this study to provide novel insight into the ecosystem functioning of glacierised mountain rivers.

6.3 Application of key findings to research and conservation practice

As development of the conceptual models presented in Chapter Two informed focus of the analytical data chapters, they were tested and refined with respect to findings obtained from glacierised mountain rivers, particularly of the Austrian Alps (Objective 1). Local geographic validation of model predictions was used to test the generality of literature-derived principals in sampled catchments and their scope extended through consideration of recently published research. This enabled discussion of the contribution of thesis findings to current glacier-fed river ecosystem research and alpine freshwater conservation strategy.

6.3.1. Application of key findings to research

6.3.1.1 Multitrophic responses to reducing catchment glacier cover

Analytical Chapters Three, Four and Five were used to refine the conceptual models presented in Chapter Two. Data predominantly collected from rivers in the Eisboden, Obersulzbach and Rotmoos valleys of the Austrian Alps, alongside microbial

information from six glacierised regions, were used to provide initial validation of the literature-derived models of Figure 2.4, Figure 2.5 and Figure 2.6. While published research has recently considered the distribution of macroinvertebrates (Gabbud et al., 2019) and diatoms (Rotta et al., 2018) in deglaciating rivers, further ground truthing of these models is required in additional alpine regions, to broaden their geographical representation.

The observed macroinvertebrate community provided validation of Figure 2.4, with the first occurrence of species conforming to widely accepted assembly patterns noted for alpine rivers of the Northern Hemisphere (Milner et al., 2001; Milner, 2016). Figure 6.1 adapted Figure 2.4 to consider these occurrences in response to catchment glacier cover rather than water temperature, to capture the additional physicochemical alterations across this chronosequence (e.g., increased electrical conductivity, reduced turbidity and suspended sediment concentrations) (Figure 6.1). Both models captured Chironomidae sub-families Diamesinae and Orthocladiinae pioneering high glacier cover sites, with Simuliidae, Limnephilidae, Nemouridae and Leuctridae colonising successively with ice loss (Figure 6.1a; Milner et al., 2001). However, rivers sampled for this thesis hosted a greater diversity of macroinvertebrates at high glacier cover, with species representing Nemouridae, Heptageniidae, Hydrachnoidea and the *Baetis alpinus* group present alongside the first appearance of *Diamesa* (Figure 6.1a). Nemouridae have previously been observed to migrate from non-glacial tributaries to sites of high catchment glacier cover, preventing the expected dominance of *Diamesa* spp. (Lencioni, 2018). These taxa may have represented local variability in this globally generalised summer assembly pattern, with differences in macroinvertebrate communities recently identified at a reach- and catchment-scale (Gabbud et al., 2019). Alternatively, alterations may have resulted from a lack of sampling sites representative of > 64 % catchment glacier cover, ensuring that communities defined as high glacier cover in this study aligned more closely to those representing mid-levels of cover in the original model (Figure 2.4; Figure 6.1a).

Many macroinvertebrates occurred at both high glacier cover and river sites throughout the gradient of catchment glacier cover, maintaining many of their feeding linkages as glacier ice was lost. This suggested that river invertebrate assembly was driven by tolerance mechanisms, as previously observed during real-time glacier retreat at Wolf Point Creek in Glacier Bay, Alaska (Milner and Robertson, 2010; Milner and Brown, 2012), although observations were based upon space-for-time chronosequences of

river sites. While this pattern was noted for many diatom and microbial taxa, tolerance mechanisms may not extend across these taxonomic groups as *Caloneis lancettula* and *Eunotia trinacria* alongside approximately 7 % of bacterial (16S) and 27 % of fungal (ITS) OTUs, were identified at river sites > 52 % glacier cover only.

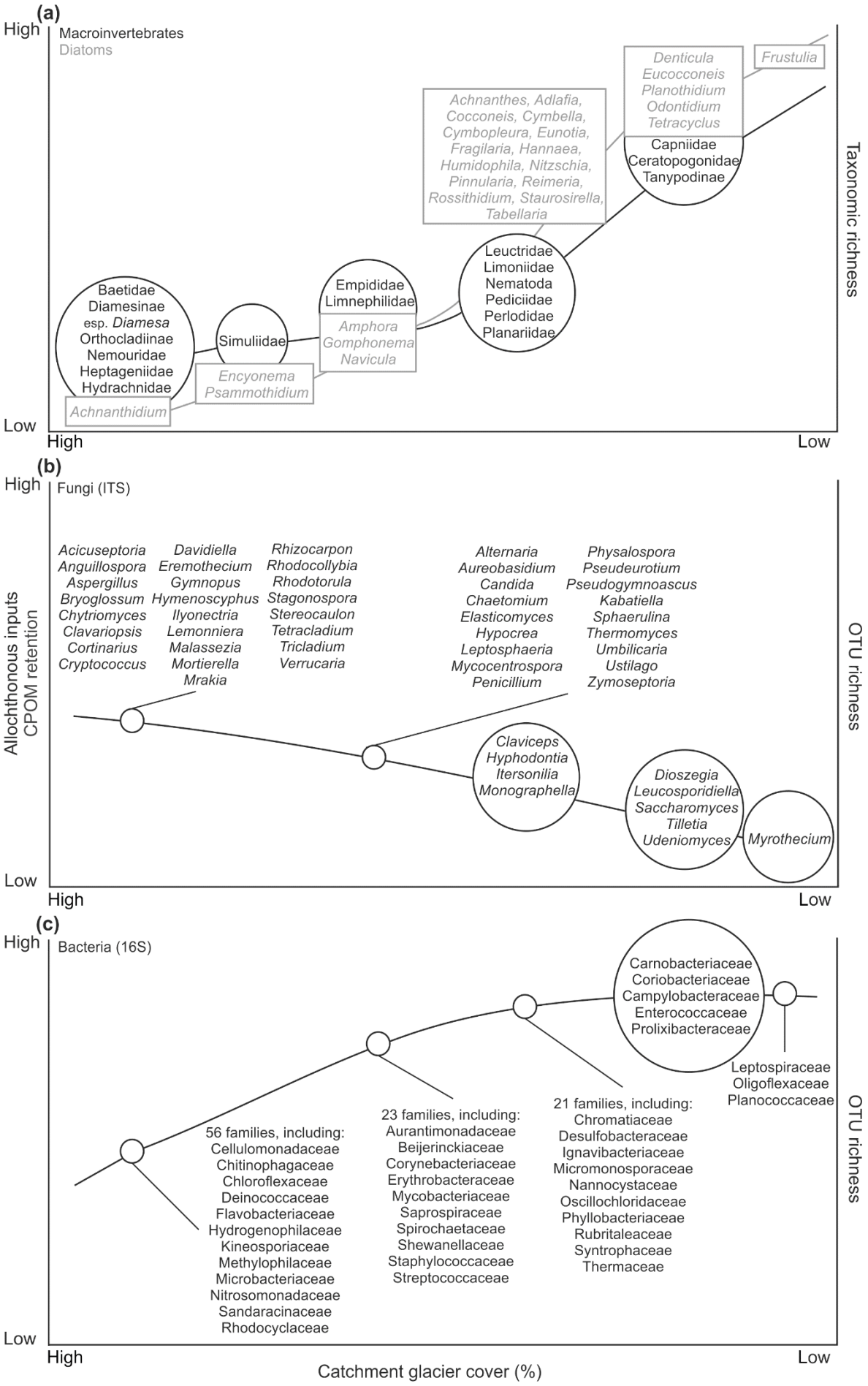
(a)
High
Macroinvertebrates
Diatoms
Low
High
Low
Taxonomic richness
Baetidae
Diamesinae
esp. Diamesa
Orthocladiinae
Nemouridae
Heptageniidae
Hydrachnidae
Achnanthidium
Simuliidae
Encyonema
Psammothidium
Empididae
Limnephilidae
Amphora
Gomphonema
Navicula
Leuctridae
Limoniidae
Nematoda
Pediciidae
Perlodidae
Planariidae
Achnanthes, Adlafia,
Cocconeis, Cymbella,
Cymbopleura, Eunotia,
Fragilaria, Hannaea,
Humidophila, Nitzschia,
Pinnularia, Reimeria,
Rossithidium, Staurosirella,
Tabellaria
Denticula
Eucocconeis
Planothidium
Odontidium
Tetracyclus
Frustulia
Capniidae
Ceratopogonidae
Tanypodinae
(b)
High
Fungi (ITS)
Low
High
Low
Allochthonous inputs
CPOM retention
OTU richness
Acicuseptoria
Anguillospora
Aspergillus
Bryoglossum
Chytriomyces
Clavariopsis
Cortinarius
Cryptococcus
Davidiella
Eremothecium
Gymnopus
Hymenoscyphus
Ilyonectria
Lemonniera
Malassezia
Mortierella
Mrakia
Rhizocarpon
Rhodocollybia
Rhodotorula
Stagonospora
Stereocaulon
Tetracladium
Tricladium
Verrucaria
Alternaria
Aureobasidium
Candida
Chaetomium
Elasticomyces
Hypocrea
Leptosphaeria
Mycocentrospora
Penicillium
Physalospora
Pseudeurotium
Pseudogymnoascus
Kabatiella
Sphaerulina
Thermomyces
Umbilicaria
Ustilago
Zymoseptoria
Claviceps
Hyphodontia
Itersonilia
Monographella
Dioszegia
Leucosporidiella
Saccharomyces
Tilletia
Udeniomyces
Myrothecium
(c)
High
Bacteria (16S)
Low
High
Low
OTU richness
Carnobacteriaceae
Coriobacteriaceae
Campylobacteraceae
Enterococcaceae
Prolixibacteraceae
Leptospiraceae
Oligoflexaceae
Planococcaceae
56 families, including:
Cellulomonadaceae
Chitinophagaceae
Chloroflexaceae
Deinococcaceae
Flavobacteriaceae
Hydrogenophilaceae
Kineosporiaceae
Methylophilaceae
Microbacteriaceae
Nitrosomonadaceae
Sandaracinaceae
Rhodocyclaceae
23 families, including:
Aurantimonadaceae
Beijerinckiaceae
Corynebacteriaceae
Erythrobacteraceae
Mycobacteriaceae
Saprospiraceae
Spirochaetaceae
Shewanellaceae
Staphylococcaceae
Streptococcaceae
21 families, including:
Chromatiaceae
Desulfobacteraceae
Ignavibacteriaceae
Micromonosporaceae
Nannocystaceae
Oscillochloridaceae
Phyllobacteriaceae
Rubritaleaceae
Syntrophaceae
Thermaceae
Catchment glacier cover (%)

◄ **Figure 6.1** First occurrence and richness of river (a) macroinvertebrates (black circles), benthic diatoms (grey squares), (b) fungal (ITS) OTUs and (c) bacterial (16S) OTUs along a gradient of reducing catchment glacier cover. This model revises and extends Figure 2.4 with data obtained from rivers in (a) the Austrian Alps and (b, c) five additional glacierised regions (Appendix 1). Relationships between richness and catchment glacier cover are displayed in more detail in Appendix 5.2.

Field data enabled the first occurrence of benthic diatom taxa along the gradient of reducing glacier cover to be described in greater detail than previously determined through literature synthesis (Figure 2.5; Figure 6.1a). Figure 2.5 noted that species representing *Achnanthes*, *Odontidium* and *Fragilaria* dominated glacier-fed streams across Europe, North America and the Himalaya (Cantonati et al., 2001; Gesierich and Rott, 2012) but while present in sampled rivers, these taxa occurred at mid and low-levels of glacier cover. As evidenced in Figure 6.1a and Figure 6.2c, high glacier cover sites were predominantly colonised not by cold water specialists as expected (e.g., *Hannaea arcus*) (Antoniades and Douglas, 2002), but by generalist taxa, tolerant of a broad range of temperature, pH and nutrient conditions in and beyond alpine watersheds (e.g., *Achnanthidium minutissimum*) (Potapova and Hamilton, 2007). This, together with the occurrence of some high glacier cover diatom taxa in river sites lacking ice melt inputs, suggested that cold-adapted species colonising highly glacial sites were not stenothermic, and tolerated the physicochemical and flow regime conditions imposed by both meltwaters and groundwater flows. The assumption of a transition in first occurrence taxa from specialists to generalists with reducing catchment glacier cover (Figure 2.5) appears in part reversed, with broader physicochemical tolerance facilitating assembly in these dynamic, high glacier cover sites.

As for macroinvertebrates, none of the diatom species identified at river sites hosting 0 to 64 % catchment glacier cover have previously been documented as cold-stenothermic taxa. This was despite the occurrence of such species in other alpine catchments (Brown et al., 2009b; Falasco and Bona, 2011; Muhlfeld, 2011; Cantonati et al., 2012; Jacobsen et al., 2012). This suggested that these cold water specialists required greater ice cover than was represented by the sampled rivers, potentially resulting in their extirpation from study catchments during earlier stages of glacier retreat. Furthermore, Rotta et al. (2018) illustrated that deglaciation can continue to threaten diatom taxa even at stages of low or no glacier cover, as ice loss will increase the proportional contribution of water sourced from permafrost thaw in many alpine

headwater catchments. This has been reported to significantly reduce diatom species richness and diversity (Rotta et al., 2018) and in turn, Figure 6.1a may not be applicable to such watersheds.

Assembly of fungal (ITS) and bacterial (16S) OTUs in glacier-fed streams may align to the patterns of succession identified for river macroinvertebrates and diatoms (Figure 6.1). Successional development of community structure has previously been identified for fungal assemblages along a chronosequence of deglaciation in glacier forefield soils (Tian et al., 2017). This study identified sequential first occurrence of fungi (ITS) genera and bacteria (16S) families along the glacier cover gradient (Figure 6.1b, c) with many OTUs (bacteria = 7%; fungi = 27 %) found exclusively > 52 % cover. Given the presence of taxa lacking cosmopolitan distribution, this pattern supported the 'moderate to pronounced endemicity model of microbial biogeography' previously reported for aquatic hyphomycetes along a global latitudinal gradient (Seena et al., 2019, p. 313). As microbial populations hosted a greater proportion of taxa identified only in high glacier cover sites, they may be more vulnerable than macroinvertebrates to species loss with sustained glacier retreat, if not identified in alternative river habitats. This potential specialisation of taxa in highly glacial environments may also explain the greater fungal OTU richness at high glacier cover (Figure 6.1b). Recent DNA sequencing of microbial communities is furthering the understanding of cold-adapted taxa responses to climate change (Margesin and Collins, 2019). Glacierised mountain river species are influenced by glacier retreat both through alteration of channel physicochemistry and discharge patterns (Wilhelm et al., 2013; Freimann et al., 2013), and because loss of glacial habitats (e.g., cryoconite holes, supraglacial ponds and streams, moulins, subglacial meltwaters, permafrost) will alter the fungal and bacterial species pools which contribute to proglacial meltwater environments (Hotaling et al., 2017a).

Further research is required to verify the predicted first occurrence of certain alpine river biofilm species (non-diatom algae, protists, microfauna) (Figure 2.5) with reducing catchment glacier cover, as benthos samples were limited by Surber mesh size (250 µm vs. ~ 10 µm) and potentially sub-optimal preservation of small, soft-bodied organisms (70 % methylated spirit vs. formalin). Some microfauna were determined from macroinvertebrate diets, but these may not be representative of river species composition due to selective feeding or predation avoidance behaviours, including use of reach-scale refugia (Gordon et al., 2018; Mathers et al., 2019). Furthermore, reliance

on morphological identification limited inclusion of small, complex biofilm forms (Manoylov, 2014). Despite this, sampled algae aligned to Figure 2.5, with cold-adapted specialists (e.g., *Hydrurus foetidus*) occurring at high glacier cover sites (Figure 6.2d). Gut contents analysis identified the first occurrence of testate amoeba species along a contemporary glacier cover gradient, with absence at high cover sites (Figure 6.2d). These protozoa may contribute significantly to food web structure as they are often the principal grazers of microbial species in freshwaters (Weitere et al., 2018). Gut contents analysis also highlighted the input of plant materials to river invertebrate diets. While allochthonous resources are reportedly minimal for alpine streams above the treeline (Zah and Uehlinger, 2001), terrestrially derived pollen was evident at many high cover river sites and has previously been noted as an important source of carbon in temperate freshwater food webs (Masclaux et al., 2013). These wind-blown inputs may be underestimated in glacier-fed rivers, particularly as pollen grains are known to be deposited upon, and later released during the melting of, glacier ice (Festi et al., 2017). While pollen may be resistant to breakdown in the guts of macroinvertebrates, it potentially provides an in-stream nutrient source for heterotrophic bacteria (Masclaux et al., 2013). Further study is paramount to providing additional reference sites to validate the vertebrate component of Figure 2.5, as sampled rivers in the central Austrian Alps are not known to support fish or mammal populations.

Invertebrates
(predators/ cannibals)

Invertebrates
(herbivores)

Diatoms

Biofilm (non-diatoms)

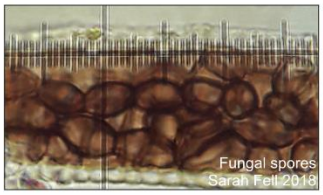

(a)

Baetidae *Baetis alpinus* gr. **Diamesinae** (*Diamesa goetghebueri, D. insignipes*) **Hydrachnidae** *sp.* **Nemouridae** *Amphinemura* **Orthocladiinae** *Brillia bifida*

Heptageniidae (*Ecdyonurus venosus*)

D. bertrami *D. cinerella* **Simuliidae**

Coleoptera

Empididae *Clinocerinae* **Limnephilidae** juv. Orthocladiinae (*Orthocladius frigidus, O. rivicola, Parorthocladius nudipennis*)

Chironomidae (*Cricotopus vierriensis*) **Leuctridae** *Leuctra* Limnephilidae (*Acrophylax zerberus, Consorophylax* sp.) **Limoniidae** (*Cheilotrichia, Rhypholophus*) **Nematoda** **Pediciidae** *Dicranota* **Perlodidae** juv. **Planariidae**

Capniidae *Capnia* juv. Chironomidae (*Chaetocladius piger* gr., *Microspectra atrofasciata*) Perlodidae (*Diura bicaudata, Isoperla*) Leuctridae (*Leuctra sinuata*) Nemouridae (*Nemurella pictetii, Protonemura austrica*) **Tanypodinae**

Ceratopogonidae

(b)

Heptageniidae (*Rhithrogena semicolorata, Heptagenia lateralis*, sp.)

Chironomidae spp.

Plecoptera juv.

(c)

Achnanthidium *minutissimum* complex

Encyonema (*E. minutum, E. latens, E. ventricosum*) ***Psammothidium*** *helveticum*

Amphora *pediculus* ***Gomphonema*** *gracile* ***Navicula*** *cryptocephala*

Achnanthidium trinode ***Adlafia*** *minuscula* ***Cocconeis*** *euglypta* ***Cymbella*** sp. ***Cymbopleura*** *amphicephala* *Encyonema* spp. ***Eunotia*** spp. ***Fragilaria*** spp. *Gomphonema* (*G. exilissimum, G. parvulum complex*) ***Hannaea*** *arcus* ***Humidophila*** *perpusilla* *Navicula* spp. ***Nitzschia*** spp. ***Pinnularia*** spp. ***Reimeria*** *sinuata* ***Rossithidium*** *petersenii* ***Staurosirella*** *pinnata* ***Tabellaria*** *flocculosa*

Denticula *tenuis* ***Eucocconeis*** *laevis* *Gomphonema* spp. ***Planothidium*** *frequentissimum* ***Odontidium*** *mesodon* ***Tetracyclus*** *rupestris*

Adlafia suchlandtii *Navicula detenta*

Frustulia *rhomboides* *Staurosirella lapponica*

(d)

Algae (non-diatom)
Bacteria
Fungi
Testate amoebae
Tardigrada

Chrysophyceae sp. Filamentous algal spp. Fungal hyphae **Hydruraceae** (*Hydrurus foetidus*) Microalgae sp.

Chlorellaceae (*Chlorella* spp.) **Cyanophyta** (*Homeothrix* spp.)

Centropyxidae (*Centropyxis pontigulasiformis*) **Cyanophyta** (filamentous) **Hyalospheniidae** (*Nebela* sp.)

Cladophoraceae (*Cladophora glomerata*) Cyanophyta (*Spirulina* sp.) **Desmidiaceae** (*Cosmarium* spp.) **Zygnemataceae** (*Spirogyra*)

Centropyxidae (*Centropyxis aerophila*) **Hyalospheniidae** (*Hyalosphenia subflava*) **Paraquadrulidae** (*Paraquadrula irregularis*)

Arcellidae (*Arcella* spp.) Hyalospheniidae (*Quadruella cf. longicollis*) **Tardigrada**

Individual biomass

High — Medium — Low

Catchment Glacier Cover

◄ **Figure 6.2** First occurrence of macrofauna, meiofauna and microfauna and their individual biomass along a gradient of reducing catchment glacier cover for river sites in the central Austrian Alps. Taxonomic information revises the model of Chapter Two (Figure 2.5). While species-level information is provided where possible, the first occurrence of each family/order is marked in bold text to facilitate comparison with previously presented models. Taxa identified at site O3, influenced by proglacial lake inputs, are not included. Grey open circles represent the mean individual biomass of each species present at river sites. For diatoms, biomass values are averaged across sites. Macroinvertebrate and diatom data were derived from Surber and rock scrub samples, but other biotic groups were identified from macroinvertebrate gut contents analysis, given the poor preservation of non-diatom biofilm taxa. Diatoms are displayed separately to other biofilm species given the greater taxonomic resolution available for this group. Taxa are representative of summer river communities and vertebrate populations were absent from study streams. Biomass information was unavailable for non-diatom algae, bacteria, fungi and microfauna communities.

Figure 2.5 predicted increases in individual biomass with reducing catchment glacier cover, across multitrophic taxonomic groups. For invertebrates, the rate of increase was predicted to slow at low glacier cover, due to the anticipated constraints on energy availability and biomass imposed by greater predation and competition at higher population densities (Flory and Milner, 1999; Jacobsen et al., 2012). However, observations illustrated accelerated increases in individual biomass for predatory macroinvertebrates, which consistently had the highest individual biomass at each sampled site (Figure 6.2a). Deceleration in the rate of increased macroinvertebrate abundance < 26 % glacier cover (Appendix 3.6), despite sustained increases in individual biomass (Figure 6.2a), suggested that this proliferation may have been supported by greater resource assimilation efficiency, rather than availability. This has previously been noted for cold-adapted *Diamesa* spp. at high glacier cover river sites (Niedrist and Füreder, 2018) but research is yet to determine the prevalence of such adaptions in groundwater dominated alpine reaches.

Field observations noted that taxa with exclusively herbivorous feeding behaviour were not found > 30 % glacier cover (Figure 6.2b), a trend unidentified by literature-derived Figure 2.5. This was potentially due to diatoms, a key component of cold-adapted invertebrate diets (Niedrist and Füreder, 2017), being found in insufficient density above this percentage of catchment glacier cover (Figure 3.2). Some taxa (e.g., *Achnanthes* sp., *Fragilaria* spp.) expressed strong benthic attachment forms which increase their resistance to grazing (Hieber et al., 2001; Gesierich and Rott, 2012).

Availability of diatoms and other biofilm resources may have been reduced further across the glacier cover gradient outside of spatially and temporally dynamic algal blooms (Uehlinger et al., 2002; Gabbud et al., 2019). This could explain why individual biomass was decoupled from glacier cover for herbivorous invertebrates, but not that of predatory species with greater dietary flexibility (Figure 6.2a, b). Many of the aquatic invertebrates predicted to be herbivorous (Figure 2.5) were predatory in sampled rivers due to cannibalism between 30 and 64 % catchment glacier cover (Figure 4.1). This, alongside previous documentation of this behaviour (Clitherow et al., 2013), provided evidence to support the importance of biotic interactions in shaping community assembly even in physicochemically harsh environments, with this role of stochastic interactions suggested in recent publications (Brown et al., 2018; Lencioni, 2018).

Increases in individual vertebrate biomass predicted in Figure 2.5 aligned to the trend observed for diatoms and predatory macroinvertebrates (Figure 6.2a, c). However, further research is required in additional catchments to determine if the proliferation of basal resources and larger-bodied invertebrates at low glacier cover could provide sufficient energy transfer and assimilation in higher trophic levels, to support continued increases in vertebrate body mass. Alternatively, predicted increases in predator biomass and density could be facilitated by riparian subsidy (Larsen et al., 2016; Perkins et al., 2018). Rivers in catchments where the legacy effect of valley climate, aspect and geomorphology enables the development and preservation of glaciers at low-altitude or near the permanent treeline, as in regions of Alaska and New Zealand, will have greater provision of organic matter than high-altitude streams with comparable catchment glacier cover. Greater riparian vegetation inputs may lead to stronger top-down control of food web assembly as predators thrive upon subsidies, while reduced terrestrial contributions could enable bottom-up control of assembly driven by the basal taxa proliferation identified in Chapter Four. In turn, the varying composition, stability and successional stage of vegetation communities in the riparian zones of glacier-fed rivers (Zah and Uehlinger, 2001; Klaar et al., 2015; McKernan et al., 2018) may prevent globally synchronous individual biomass and food web responses to reducing catchment glacier cover. This suggests an additional mechanism, alongside proglacial lake formation, through which geomorphic context can influence valley-scale ecological responses to glacier retreat.

6.3.1.2 Food web responses to reducing catchment glacier cover

Data presented in Chapter Four were used to test the predictions of Figure 2.6 regarding alterations to food web structure and connectance descriptors along a gradient of reducing catchment glacier cover. The model suggested that as river reaches previously influenced by ice melt inputs became dominated by groundwater flows, their food webs would align to the structural characteristics of networks at low glacier cover river sites (Figure 2.6; Lavandier and Décamps, 1983). The collated data provided first evidence of this transition, with ice loss increasing node and link numbers and mean chain lengths (Figure 6.3), alongside linkage and predator densities. As predicted (Zah et al., 2001; Füreder et al., 2003; Clitherow et al., 2013; Neidrist and Füreder, 2017), feeding relationships were predominantly between macroinvertebrates and both benthic diatoms and amorphous detritus. However, species richness, linkage density and the prevalence of detritivore feeding were underestimated (Figure 6.3). While few individuals fed exclusively upon detritus, this resource was identified in all macroinvertebrate gut contents. Figure 2.6 captured the dramatic increase in taxa densities with reducing glacier cover but the significant reduction in directed connectance was not observed. This was potentially due to the dominance of macroinvertebrate-periphyton links, limited occurrence of omnivory, few predators and subsequently, small body-size spectra at sampled river sites (Chapter Four). The model was amended (Figure 6.3) to represent this alteration but is only applicable for alpine river systems lacking proglacial lake influence, as these features were found to accelerate this transition, disconnecting catchment glacier cover from the predicted influence of ice melt inputs.

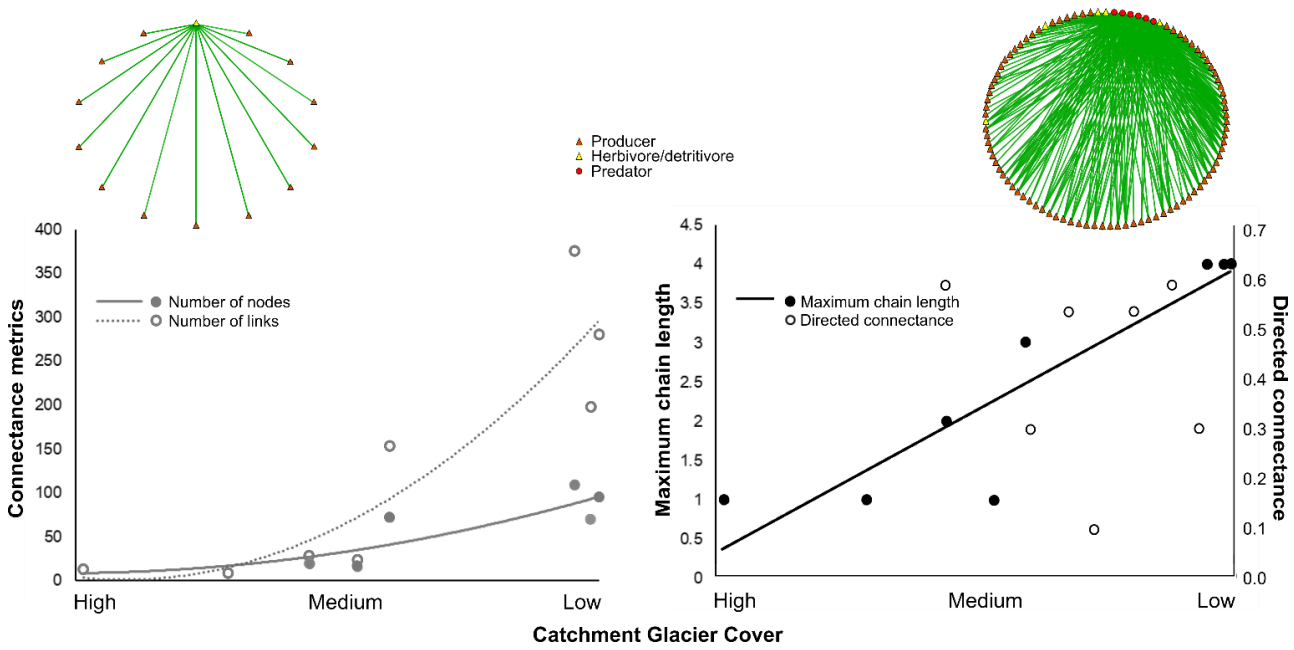

Figure 6.3 Alteration to the connectance descriptors of alpine river food webs along a gradient of reducing catchment glacier cover. This figure revises Figure 2.6 following amendments informed by field observations in rivers of the Austrian Alps.

Figure 2.6 predicted a unimodal increase in food web node and link numbers with reducing catchment glacier cover. This was informed by Jacobsen et al. (2012) who identified this trend for river invertebrate taxonomic richness in alpine rivers globally. Here, α-diversity was greatest at intermediate levels of glacier cover but relatively reduced by harsh physicochemical conditions at highly glacial sites and increased competition pressures in reaches with greater groundwater influence (Jacobsen et al., 2012). However, these observed connectance descriptors increased at an accelerated rate across the chronosequence of reducing catchment glacier cover (Figure 6.3). This trend aligned to the sustained increases in macroinvertebrate and diatom richness across sampled river sites (Appendix 3.6; Figure 3.2). The disparity may have been driven by variable competition and predation pressures across and within watersheds (Gabbud et al., 2019).

Although not represented in Figure 2.6, the number of nodes and links in alpine river food webs increased more rapidly below approximately 26 % catchment glacier cover (Figure 6.3). This aligned to accelerated increase in other food web descriptors, including community span, alongside greater abundance and biomass of basal taxa. Increases in diatom valve density were also noted below approximately 28 % glacier cover in Chapter Three (Figure 3.2), and Cauvy-Fraunié et al. (2016) highlighted increased herbivore and algal community biomass < 11 % glacier cover in an

experimentally manipulated Ecuadorian alpine river. Biotic proliferation was potentially driven by the attenuation of ice melt inputs (Hieber et al., 2001; Rott et al., 2006; Battin et al., 2016) and reduced algal grazing pressure. Plateaus in the increasing abundance of macroinvertebrates have been documented < 26 % glacier cover in the Austrian Alps (Fell et al., 2018) and 40 % meltwater contribution in the French Pyrenees (Khamis et al., 2016). Using Threshold Indicator Analysis, Milner et al. (2017) also identified significant changes to the community composition of glacier-fed rivers in the Italian Alps at approximately 30 % catchment glacier cover. In turn, the observed alterations to food web descriptors, and potential shift from disturbance regime to donor-controlled assembly processes, may occur across a range of 11 to 30 % catchment glacier cover. The 'tipping point' may be dependent upon local catchment influences on alpine biofilm communities, including organic matter supply and flow rate variability (Battin et al. 2016). Therefore, rapid and significant reorganisation of river food webs may already characterise watersheds that have deglaciated beyond this threshold, which are prevalent in Austria (Koboltschnig and Schöner, 2011) and the wider European Alps (Brown et al., 2018).

Connectance descriptors identified that while some observed food webs were characterised by an extreme structure, many aligned to the spectrum of network metrics represented by 241 river landscapes, sampling periods and disturbance regimes (Figure 6.4; Appendix 5.3). Collation of data from 37 published studies highlighted that while some alpine river sites had the lowest directed connectance (0, 3 and 26 % catchment glacier cover) and mean chain lengths (30, 46 and 64 % catchment glacier cover) reported, others supported similar values to those recorded for rivers draining forests and grasslands (Figure 6.4b, c). Two of the three lowest linkage density values were found at high catchment glacier cover (≥ 46 % glacier cover) (Figure 6.4d). The low link numbers and species richness of sampled rivers aligned to those of connectance food webs describing other rivers fed by ice and snow melt (Lavandier and Décamps, 1983; Clitherow et al., 2013; Parker and Huryn, 2013), but three networks representing intermittent streams produced the lowest documented values (López-Rodríguez et al., 2012) (Figure 6.4a). Sampled river sites formed two groups, representing high and low link number and species richness values (Figure 6.4a), with the threshold for their separation at 26 % catchment glacier cover. Accelerated increase in node and link numbers below this 'tipping point' resulted in significant structural reorganisation of alpine river food webs (Figure 4.1). Rivers predominantly fed by glacier meltwaters host some of the harshest physicochemical

conditions imposed upon freshwater communities (Milner et al., 2017), and this study suggested that subsequently their food webs adopt an intensified form of the structures identified in other biomes (Figure 6.4). However, attenuation of ice melt inputs and transition along a harsh-benign gradient (Khamis et al., 2016) rapidly enabled connectance network descriptors to resemble temperate and even tropical river systems (Figure 6.4).

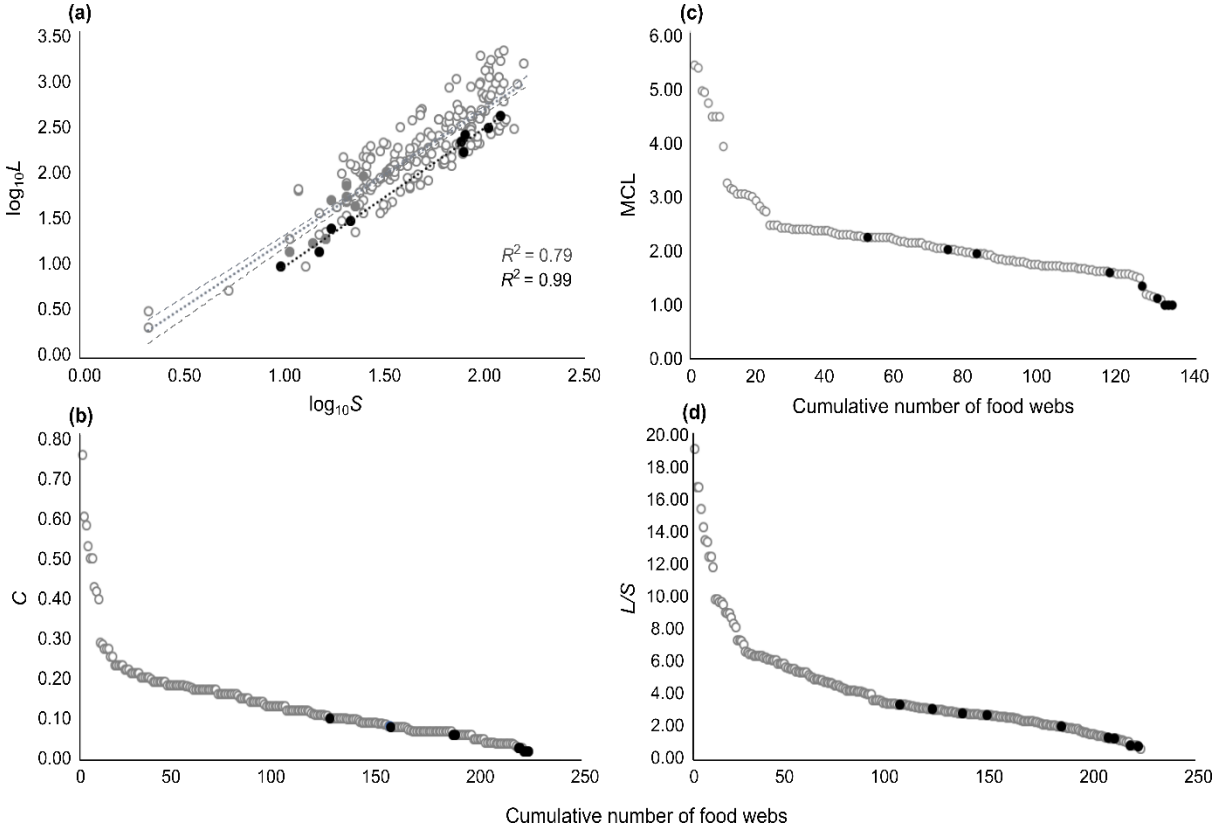

Figure 6.4 Metrics for the nine alpine river networks presented in Chapter Four (black circles) compared to 241 river food webs derived from 37 published studies (grey open circles). Studies were identified using the Web of Science (15 March 2019) with a combination of search terms (river, food web, connectance). River connectance food webs were collated to represent a diversity of environments, altitudes, latitudes, years, seasons and disturbance regimes but may not be exhaustive. (a) Relationship between $\log_{10}$ species richness (S) and $\log_{10}$ link number (L) for constructed and published food webs, with literature pertaining to other rivers fed by ice and snow melt highlighted (grey circles) and 95 % confidence intervals shown, (b) directed connectance (C) (L/S^2) values for constructed and published food webs, (c) mean shortest chain lengths (MCL) for constructed and published food webs, (d) linkage density (L/S) for constructed and published food webs. Literature references are provided in Appendix 5.3.

6.3.1.3 Microbial community structure and ecosystem functioning response to reducing catchment glacier cover

Chapter Five identified deglaciating catchments to support both the lowest daily cellulose decomposition rates reported for river cotton strip assays and a range of values which aligned to those documented for streams in temperate and tropical biomes (Figure 6.4). This research suggested that as for connectance food web descriptors, mountain rivers represented the threshold of this ecosystem function, but also its scope, with glacier-fed streams hosting ecosystem structure (Figure 6.4) and functioning (Figure 5.4) comparable to other river systems. When unadjusted for water temperature, glacierised mountain rivers hosted mean tensile strength loss rates higher than identified for other cold environments, including boreal forest and tundra (Figure 6.4; Tiegs et al., 2019). Some cold streams have previously been reported to decay leaf litter packs at rates which appear unrelated to mean water temperature and nutrient concentration (Cristiano et al., 2019), suggesting that further research is required to identify organic material decay processes independent of physicochemical parameters. Glacier-fed rivers may therefore host carbon release rates comparable to lower altitude freshwater ecosystems and, as reducing glacier cover was associated with accelerated fungal catabolism of organic matter, this contribution can be expected to increase with sustained glacier retreat. Climate change and ice loss may further increase carbon emissions from alpine rivers as increased river bank stability, spring air temperatures and length of the summer growing period, favour greater colonisation and succession of herbaceous riparian vegetation communities, potentially increasing supply of organic materials to streams for processing (Klaar et al., 2015; McKernan et al., 2018; Rogora et al., 2018).

Recent research has explored the relationships between biofilm biodiversity and ecosystem functioning in river networks, with studies identifying microbial community structure and processing to respond both synchronously and disparately to environmental perturbations (Besemer, 2015). This study did not identify the complex mechanisms which mediate these linkages, including niche partitioning and functional redundancy (Besemer, 2015), but noted a positive biodiversity-ecosystem functioning association between fungal (ITS) copy number and accelerated cellulose decomposition rates, in deglaciating catchments. This study furthered understanding of this association in glacierised mountain regions as the *cbhI* functional gene appeared to provide a mechanistic link between diversity and productivity in these river systems. However, gene amplification could not be directly linked to specific fungal (ITS) taxa

and biodiversity-ecosystem functioning relationships have previously been identified to alter with environmental disturbance events (Cardinale et al. 2000). Further research is required to determine the distribution of other functional genes in glacier-fed river biofilm communities and to consider how the seasonal physicochemical, hydrological and geomorphic alterations imposed by glacier retreat influence their expression (Ren et al. 2017a). As cotton strip assays captured both microbial structure and processing responses to reducing catchment glacier cover, this study lends further support (Tiegs et al., 2019) to their use in the bioassessment of mountain river integrity (Gessner and Chauvet, 2002).

6.3.2 Application of key findings to conservation practice

Identification of nineteen diatom taxa noted as threatened, endangered, decreasing or rare on the Red List of Algae for Germany (Lange-Bertalot and Steindorf, 1996) justifies expansion of conservation focus beyond previously recommended alpine spring habitats (Cantonati et al., 2012) to include rivers influenced by variable catchment glacier cover. For example, Austrian alpine rivers may act as a refuge for *Achnanthidium caledonicum,* as this endangered species was identified across eight sites, representing 0 to 52 % glacier cover. This research suggested that revision of the Red List may be required to reassess both the status of taxa which could benefit from deglaciation, two of which are currently noted to have decreasing populations (*Chamaepinnularia mediocris, Gomphonema calcareum*), and taxa found exclusively ≥ 28 % glacier cover, which may lose their habitat with sustained ice loss (Table 6.1). The 23 taxa whose abundance correlated significantly to NMDS Axis 1 (Figure 3.4) and the aligned vectors of channel stability and glacier cover may also require future conservation status, given their sensitivity to glacier influence. Further study is required to confirm the presence of these taxa in alternative river habitats (Section 6.4.2). This research requirement extends beyond diatoms to cold-adapted species in additional taxonomic groups (e.g., *Tetracladium psychrophilum*, *T. marchalianum*, *Baetis alpinus* gr., Iberian desman, Eurasian shrew, Pyrenean brook newt) (Table 6.1). As for diatom taxa, many macroinvertebrate species were identified throughout the gradient of reducing catchment glacier cover and appear cold-adapted rather than cold-stenothermic. In turn, high glacier cover consumers may also benefit from future deglaciation as their abundance and taxonomic richness increased with ice loss (Figure 4.1). However, the widely documented threat that glacier retreat imposes upon certain endemic river invertebrates (Brown et al., 2009b; Muhlfeld et al., 2011; Finn et al., 2014; Giersch et al., 2016), means that further study is required to determine the

presence of rare taxa in the Austrian river sites. For example, cold water specialist species including *Eukiefferiella cyanea*, *Leuctra rauscheri* and *Protonemura nimborum* have previously been identified in the Austrian Alps but were not sampled during this study (Füreder et al., 2007).

Current alpine freshwater conservation management is constrained by limited information regarding the distribution, abundance and adaptive capacity of river macroinvertebrates (Giersch et al., 2016; Lencioni, 2018), meiobenthic taxa and microbes. Furthermore, the sustained ice cover required by certain aquatic species cannot be achieved. However, this research could be applied to conservation strategies by i) highlighting the potential benefits of deglaciation for species of multiple taxonomic groups adapted to expanding low and no glacier cover river habitats (Table 6.1); ii) identifying tolerance in cold-adapted, non-endemic river invertebrate populations which may prevent their extirpation following ice loss and iii) directing conservation efforts ≥ 26 % glacier cover. Above this threshold, additional environmental stressors including nutrient pollution, water abstraction and flow rate alterations resulting from agriculture, tourism and hydroelectric energy production (Khamis et al., 2014a), could be targeted to alleviate pressure upon taxa already facing habitat loss. This information could also be shared with organisations and projects involved in developing local aquatic conservation management strategies, including the Hohe Tauern National Park, the WWF European Alpine Program (Save the Alpine Rivers!) and the European Union Strategic Planning for Alpine River Ecosystems project.

Collaborative management efforts could drive measures such as the translocation of rare or endemic river taxa from current locations of comparatively high population density, to glacierised catchments predicted to retain ≥ 26 % glacier cover for several decades. Hotaling et al. (2017b) suggested that the insulating capacity of debris cover upon some rock glaciers may reduce their melt rates, making their proglacial streams suitable sites for the preservation of cold stenothermic populations. Establishment or expansion of communities in these habitats may provide high-altitude species with the greatest chance of longer-term survival, although potential success rates remain uncertain (Khamis et al., 2014a; Giersch et al., 2016), particularly for less conspicuous taxa which are difficult to identify without genetic analysis. As suggested for the possible relocation of Pyrenean brook newts (*Calotriton asper*), molecular techniques must be employed to ensure the movement of genetically diverse populations

(Valbuena-Ureña et al., 2018). Recent studies have called for alpine river management to replace the focus on threatened species to consider instead the importance of increased habitat connectivity within and between alpine watersheds (Khamis et al., 2014a). In turn, conservation of the biodiversity of mountain rivers must be considered as an intrinsic component of broader strategies to protect the wider alpine environment.

6.4 Research limitations and future research directions

6.4.1 Research approach

A chronosequence approach was adopted to sample catchments with varying proportions of permanent ice cover in preference to the long-term monitoring of rivers influenced by real-time glacier recession, which was not achievable within the project timeframe (Thompson et al., 2012). Although pseudoreplication of site selection was avoided where possible, it was necessary in certain valleys to repeatedly sample single glacier-fed river channels at variable distances from the ice margins, to obtain sites representative of an extensive gradient of catchment glacier cover. While care was taken to use the most recent available ice extent information (GLIMS, 2018), the accuracy of glacier cover representation may have been constrained by the occurrence of glacier retreat since its production (2000 to 2016). This was particularly evident for Rob Roy glacier in the Southern Alps of New Zealand, as the ice outlines were last updated in 1978 (GLIMS, 2018). However, only three microbial samples and two cotton strip assays were successfully retrieved from this catchment. Furthermore, as detailed in Chapter Three, measurement of catchment glacier cover cannot quantify ice melt production, runoff rates, discharge volumes or variability in these processes, which are modified by multiple parameters including valley geomorphology, local and regional climate patterns, ice thickness, basal motion dynamics, surface debris cover and proglacial lakes (Zemp et al., 2006; Huss, 2012; Robson et al., 2016; Carrivick and Heckmann, 2017). However, this proxy for glacier retreat was found to correlate significantly to an alternative measure of glacier influence (multivariate glaciality index) (Appendix 5.4) and was calculated remotely prior to fieldwork, with limited resource requirements in comparison to in-situ methods (e.g., water chemistry or wavelet analysis) (Brown et al., 2009a; Cauvy-Fraunié et al., 2014). Gradients of catchment glacier cover continue to be a widely adopted approach for investigating the response of aquatic ecosystems to deglaciation and have previously been identified to capture the biotic responses documented for real-time glacier recession (Jacobsen et al., 2012; Giersch et al., 2016; Ren et al., 2017b; Brown et al., 2018; Lencioni, 2018; Niedrist and Füreder, 2018). Future collation of chronosequence information and its extension into

less studied mountainous regions (e.g., the Andes, China, Russia, Figure 2.2) is critical to determine if the global synchronicity identified for river invertebrate responses to glacier retreat (biodiversity, functional traits, assembly processes) (Jacobsen et al., 2012; Brown et al., 2018) occur in other taxonomic groups and in turn, inform the generality of ecological theory across alpine rivers.

Field observations (physicochemical parameters, Surber samples, biofilm scrubs) were primarily conducted from single in-situ spot measurements. This approach was necessary given fieldwork time constraints but may have failed to capture the continuous variability of many parameters which are influenced by diurnal and seasonal cycles in discharge and flow rate in glacier-fed river systems (Milner et al., 2001; Bliss et al., 2014; Huss and Hock, 2018). Longer-term deployment of temperature loggers (Chapter Five) suggested periods of stream intermittency across three of the mountainous regions, with dewatering predicted to become more frequent in many alpine catchments experiencing continued deglaciating (Robinson et al., 2016). Use of fixed flow gauge information also identified precipitation driven flood events which potentially contributed to the destabilisation of biofilm architecture (Chapter Three). In turn, this higher resolution environmental information was critical to understanding the biotic responses noted during spot sampling and future research should aim to establish longer-term monitoring of these physicochemical and hydraulic parameters.

Field measurements were collected during boreal and austral summer months, to maximise river site accessibility and comparison to previously published research. Thesis findings cannot be extrapolated beyond summer river communities, yet they remain intrinsically connected to biotic processes occurring at less studied time periods. These include the ‘windows of opportunity’ for consumer feeding during spring ice melt induced nutrient release and algal blooms (Uehlinger et al., 2002, p. 20; Uehlinger et al., 2010; Fellman et al., 2015) and the persistence of aquatic communities beneath winter snow cover, which remain poorly described (Brown et al., 2015). Future research requires extended sampling to capture the influence of these events upon aquatic biodiversity as these summer observations reflect one component of annual community dynamics (Brown et al., 2015). This research focus is urgent as climate change is predicted to drive earlier and prolonged melt seasons and extended ice-free periods in many alpine catchments, potentially decoupling seasonal patterns of resource availability and demand (Durant et al., 2007; Huss et al., 2017).

6.4.2 Researching alpine river benthic diatom communities

The Red List of Algae for Germany remains the most complete reference of imperilled diatom species, but it lacks Austria specific reference sites, does not cite all identified taxa and was last updated in 1996 (Falasco and Bona, 2011), potentially leading to inaccurate representation of diatom vulnerability in sampled river sites (Fell et al., 2018). Therefore, both classification of Austrian freshwater diatoms and reclassification of those which may benefit or perish following glacier retreat, requires extensive sampling of assemblage composition over a greater number of alpine catchments. Field observations must determine if the taxa found exclusively at certain percentages of catchment glacier cover in Chapter Two are also identified in alternative reach habitats across the Austrian Alps.

Further research could expand the taxonomic focus of Chapter Two to consider functional trait responses of benthic diatoms to reducing catchment glacier cover. This may develop understanding of their morphological, behavioural and life history adaptions to the environmental conditions imposed by glacier retreat. For freshwater diatoms, Passy (2007) and later Rimet and Bouchez (2012), defined ecological guilds to group functionally comparable taxa. The occurrence of these classifications could be correlated to both glacier cover and its associated physicochemical parameters (river water temperature, electrical conductivity, pH, turbidity, channel stability) as ecological guilds are currently described for approximately 63 % of the diatom species identified across the Austrian Alps sites (Rimet and Bouchez, 2012). Given the extensive, standardised sampling of benthic diatoms for the bioassessment of water quality under the Water Framework Directive (CEN, 2014), data sets may be available to determine these relationships along additional chronosequences of glacier cover in the European Alps. However, watersheds < 10 km^2 are not monitored under the framework, potentially limiting the provision of information for many headwater streams and tributaries (BMNT, 2019). This autecological study could also be expanded to consider the implications of deglaciation upon the wider periphyton community (filamentous and unicellular algae, cyanobacteria), with traits potentially identified through use of Reynolds Functional Groups (Kruk et al., 2017). The response of benthic diatom assemblages to glacier retreat may be influenced significantly by biotic interactions within biofilm communities and this has implications for future energy supply to alpine river food webs (Chapter Four).

6.4.3 Researching alpine river food webs

Microbial assemblages were not comprehensively captured in alpine river food web construction (Chapter Four), despite previous literature documenting the importance of their contribution to benthic biomass and energy supply (Hotaling et al., 2017a; Ren et al., 2017a; Vadeboncoeur and Power, 2017). However, as investigation of cotton strip microbial communities fostered partnership with the Molecular Ecology Group of the University of Essex (Chapter Five), further collaboration could facilitate DNA-based next-generation sequencing of the microbial community integral to alpine river food webs. Molecular analysis has previously been employed to determine the sensitivity of aquatic microbenthic (Archaea, bacteria, fungi) diversity and functioning to the physicochemical alterations induced by glacier retreat (Battin et al., 2004; Wilhelm et al., 2013; Hotaling et al., 2017a; Ren et al., 2017a; Ren et al., 2017b). However, studies are yet to integrate biofilm microbial linkages into holistic descriptions of trophic networks (Weitere et al., 2018) for alpine rivers. DNA barcoding analysis may also enable inclusion of additional taxa poorly represented in gut contents derived food webs due to their small body size (Sheppard and Harwood, 2005). A proliferation of metabarcoding and high-throughput sequencing studies have increased understanding of meiofauna (protists, rotifers, protozoa) biodiversity in freshwaters (Boscaro et al., 2017; Debroas et al., 2017; Banerji et al., 2018; Boenigk et al., 2018) and could be used to investigate their predation behaviours in alpine rivers, provided finer Surber mesh and a more suitable sample preservative (e.g., formalin) were used. Combined gut contents and stable isotope analysis has highlighted the requirement for greater meiofaunal taxonomic resolution in river food webs as amalgamating multiple species as singular nodes can alter link numbers, linkage density and consumer-resource ratios significantly (Schmid-Araya et al., 2016). This focus is particularly important for protists given that variation in their abundance suggests a stronger association with deglaciation than for other biofilm taxa (Eisendle-Flöckner et al., 2013).

Future research could extend the use of molecular analysis to characterise the genetic composition of gut contents derived from all sampled consumers and in turn, describe in greater detail the trophic linkages across alpine river food webs (Sheppard and Harwood, 2005; Carreon-Martinez and Heath, 2010). This could reduce the error associated with taxonomic identification of partially digested organic material and determine links to prey not visible microscopically (Sheppard and Harwood, 2005). As yield-effort curves suggested insufficient characterisation of some consumer diets through gut contents analysis despite bulk sampling efforts, these molecular studies

could be conducted upon composite alpine river food webs (Clitherow et al., 2013). Multiple Surber samples could be combined to augment the number of individuals representing each species, providing samples were collected at the same time.

To add further ecological value to the nine alpine river food webs constructed in Chapter Four, trophic linkages between consumer and resource pairs could be weighted through quantification of biomass flow. Literature-derived ratios of biomass and secondary production could be used to model food web specific secondary production estimates using the biomass values calculated from body length and periphyton shape for each node (Chapter Four). This trophic basis of production method could be applied to determine bottom-up biomass flux across links directly observed in the connectance food webs (Ledger et al., 2013). This approach would inform calculations of quantitative descriptors which could be determined for food webs along the chronosequence of glacier cover. Allometric diet breadth modelling, supported by the species-averaged biomass and abundance data already collected, could then be used to predict the impact of alterations to energy flow across whole trophic networks in response to glacier retreat (O'Gorman et al., 2018). Furthermore, analysis of the functional traits supported by macroinvertebrates found across the gradient of catchment glacier cover may further understanding of the mechanisms underpinning their resource assimilation behaviours under different environmental conditions. Niedrist and Füreder (2017) stressed the importance of these invertebrate trophic relationships to further understand the response of alpine river ecosystem structure to continued ice loss.

6.4.4 Researching glacierised mountain river organic matter decomposition

A key limitation of Chapter Five was that the contributions of microbial catabolism and assumed physical abrasion to cellulose decomposition rates could not be separated or independently quantified, constraining a mechanistic understanding of river decay processes. While leaf pack studies have decoupled shredding invertebrate activity from the impacts of flow velocity using artificial channels (Ferreira et al., 2006), or macroinvertebrate decomposition from microbial autolysis through exclusion cages (Langhans et al., 2008), separation of mechanical and microbe influences remains limited. However, future studies could position cotton assays in mesh bags to reduce the influence of in-stream physical degradation processes. While macroinvertebrates were believed to be unable to colonise the cotton strips during the experimental incubation period (Tiegs et al., 2013; Tiegs et al., 2019), use of a mesh covering could

also exclude their shredding activity with greater certainty. As flow patterns and local sediment retention may be altered within these bags (Ferreira et al., 2006), further research is required to determine a design which effectively constrains abrasion processes. Additional natural experiments could be used to investigate alternative functional processes, including benthic respiration rates, to more comprehensively characterise ecosystem functioning in glacier-fed rivers.

Future molecular analysis of cotton strip microbial assemblages could include extraction of RNA alongside DNA. This would quantify copy numbers of the *cbhI* gene which have been transcribed in the analysed cells, indicating activity in addition to presence of this gene in the fungal community (Griffiths et al., 2000). While RNA remains a less stable extraction component (Griffiths et al., 2000), this analysis could advance mechanistic understanding of aquatic organic matter decomposition and potentially identify stages in the chronosequence of declining catchment glacier cover experiencing heightened cellulose degradation activity, with implications for energy availability to benthic food webs. As Chapter Five indicated contribution of additional cellulases to cotton strip hydrolysis (Figure 5.3), functional genes of other cellobiohydrolases, endoglucanases and ß-glucosidases could be sequenced as their combined action is required to fully decompose cellulose and release CH_4 and CO_2 to the atmosphere (Bayer et al., 2006). As bacterial taxa can host some of these genes alongside fungi (Bayer et al., 2006), this additional sequencing, together with longer incubation of cotton strip assays, could further understanding of the microbial community succession underpinning this component of the global carbon cycle.

Future research considering mountain river decomposition rates and associated microbial community structure could focus on greater integration of the findings of Chapter Five into global-scale ecosystem functioning projects. The standardised CELLDEX protocol has been used in an as yet unpublished multi-regional Arctic study (Ring of Fire Project, Imperial College London) and collaboration with the associated research group could facilitate data comparison, to determine further geographical variability in this ecosystem process. Suggested refinement of the cotton strip assay to increase its suitability for use in glacier-fed rivers (Chapter Five) could also inform deployment in additional mountain catchments. Placement of cotton strips in reaches adjacent to the permanent snow line would enable investigation of cellulose degradation at the alpine-Arctic region boundary. Ecotones can increase the abundance and diversity of specific aquatic taxa (Heegaard et al., 2006) and

subsequently may host significant and disproportionate ecosystem functioning rates in comparison to alpine or Arctic river reaches. As climate change and glacier retreat is predicted to alter the altitudinal range of inter-annual snow cover across mountain watersheds (Huss et al., 2017; Rogora et al., 2018), the influence of these transition zones upon aquatic systems may change in deglaciating catchments.

6.5 Thesis conclusions

This thesis has illustrated that sustained reductions in catchment glacier cover will align meltwater dominated river communities to those sourced predominantly by groundwaters. This is with regard to the biodiversity of individual taxonomic groups (benthic diatoms), the structure of aquatic food webs (connectance, trophic descriptors) and the rate of their ecosystem functions (organic matter decomposition). This transition, although accelerated below a threshold of approximately 26 % catchment glacier cover, did not occur for sampled rivers as a catastrophic collapse of trophic interactions and species loss. Instead, it proceeded through predictable successional changes to the first occurrence and assembly of river taxa along the chronosequence of declining glacier cover. Alterations to food web structure below this threshold were driven by increased benthic taxa biomass, indicating bottom-up control of assembly processes with the attenuation of ice melt inputs. Findings suggested that the influences of water temperature and channel stability upon community composition were accompanied by biotic processes (e.g., cannibalism, predation, herbivory, detritivory, potential assimilation efficiency adaptions) throughout the gradient of glacier cover. Alterations to the physicochemistry and biotic environment of alpine freshwaters may prevent them from sustaining the niche conditions required by certain taxa, potentially impairing the conservation status not only of macroinvertebrates, but cold water specialists from a broad range of taxonomic groups (microbes, algae, protists, vertebrates). However, other species dependent on low glacier cover rivers could thrive during upstream habitat expansion.

The harsh physicochemical and discharge regimes of rivers in glacierised mountain catchments ensured that they represented an extreme in the ecosystem structure and functioning rates documented for river systems. However, deglaciation rapidly aligned these properties to those of rivers in temperate and tropical biomes, within alpine catchments. In turn, this thesis identified glacier-fed rivers to both support (e.g., increased α-diversity with reducing physicochemical harshness) and prevent (e.g., pioneer taxa as generalists not specialists) generalisation of ecological theory derived

from lower altitude running waters. It has contributed to biodiversity-ecosystem functioning theory, as glacier retreat drove global increases in fungal taxa and their functional gene (*cbhI*) which accelerated cellulose decomposition rates and in turn, the potential contribution of mountain rivers to the global carbon cycle. However, the response of multitrophic alpine river communities to glacier loss may be mediated by geomorphic context, including the proliferation of proglacial lake formation, permafrost thaw, riparian vegetation succession and length of the summer growth season, which could influence water sourcing and organic matter subsidy to glacier-fed rivers.

Exponential human population growth, coupled with its sustained reliance upon a hydrocarbon dominated energy supply, is predicted to increase carbon emissions and drive global warming 2 °C beyond pre-industrial temperatures (IPCC, 2013; Shannon et al., 2019). This anthropogenically forced climate change will continue to accelerate the thinning and retreat of mountain glaciers worldwide (Huss et al., 2017; Beniston et al., 2018). Between 2011 and 2100, loss of global glacier volume could exceed 64 %, with thesis study regions of Alaska, central Europe, Scandinavia and New Zealand predicted to lose over 75 % of their ice volume (Shannon et al., 2019). Through investigation at varying geographical (single- and multi-region) and biological (genes, populations, food webs, functional processes) scales, this thesis demonstrates that such reductions in catchment glacier cover will drive major alterations to the biodiversity, food web structure and ecosystem functioning of alpine river systems.

References

Antoniades, D. and Douglas, M. S. 2002. Characterization of high Arctic stream diatom assemblages from Cornwallis Island, Nunavut, Canada. *Canadian Journal of Botany.* **80**(1), pp. 50-58.

Arntzen, J. W., Denoël, M., Juzmin, S., Ishchenko, V., Beja, P., Andreone, F., Jehle, R., Nyström, P., Miaud, C. and Anthony, B. 2009. *Ichthyosaura alpestris. International Union for Conservation of Nature (IUCN) Red List of Threatened Species*. [Online]. [Accessed 10 January 2016]. Available from: www.iucnredlist.org/details/59472/0

Aufdenkampe, A. K., Mayorga, E., Raymond, P. A., Melack, J. M., Doney, S. C., Alin, S. R., Aalto, R. E. and Yoo, K. 2011. Riverine coupling of biogeochemical cycles between lands, oceans, and atmosphere. *Frontiers in Ecology and the Environment*. **9**(1), pp. 53-60.

Banerji, A., Bagley, M., Elk, M., Pilgrim, E., Martinson, J. and Domingo, J. S. 2018. Spatial and temporal dynamics of a freshwater eukaryotic plankton community revealed via 18S rRNA gene metabarcoding. *Hydrobiologia*. **818**(1), pp. 71–86.

Baselga, A., Orme, D., Villeger, S., De Bortoli, J. and Leprieur, F. 2017. *betapart: Partitioning Beta Diversity into Turnover and Nestedness Components. R package version 1.4-1*. [Online]. [Accessed 27 December 2018]. Available from: https://CRAN.R-project.org/package=betapart

Battarbee, R. W. and Kneen, M. J. 1982. The use of electronically counted microspheres in absolute diatom analysis. *Limnology and Oceanography*. **27**(1), pp. 184–188.

Battin, T.J., Wille, A., Sattler, B. and Psenner, R. 2001. Phylogenetic and functional heterogeneity of sediment biofilms along environmental gradients in a glacial stream. *Applied and Environmental Microbiology.* **67**(2), pp. 799–807.

Battin, T. J., Wille, A., Psenner, R. and Richter, A. 2004. Large-scale environmental controls on microbial biofilms in high-alpine streams. *Biogeosciences*. **1**(2), pp. 159–171.

Battin, T. J., Kaplan, L. A., Findlay, S., Hopkinson, C. S., Marti, E., Packman, A. I., Newbold, J. D. and Sabater, F. 2008. Biophysical controls on organic carbon fluxes in fluvial networks. *Nature Geoscience*. **1**, pp. 95–100.

Battin, T. J., Besemer, K., Bengtsson, M. M., Romani, A. M. and Packmann, A. I. 2016. The ecology and biogeochemistry of stream biofilms. *Nature Reviews Microbiology*. **14**, pp. 251–263.

Bayer, E. A., Shoham, Y. and Lamed, R. 2006. Cellulose-decomposing bacteria and their enzyme systems. *Prokaryotes*, **2**, pp. 578–617.

Beniston, M., Farinotti, D., Stoffel, M., Andreassen, L. M., Coppola, E., Eckert, N., Rantini, A., Giacona, F., Hauck, C., Huss, M., Huwald, H., Lehning, M., López-Moreno, J. I., Magnusson, J., Marty, C., Morán-Tejéda, E., Morin, S., Naaim, M., Provenzale, A., Rabatel, A., Six, D., Stötter, J., Strasser, U., Terzago, S. and Vincent, C. 2018. The

European mountain cryosphere: a review of its current state, trends, and future challenges. *Cryosphere*. **12**(2), pp. 759–794.

Bersier, L.F., Banašek-Richter, C. and Cattin, M.F. 2002. Quantitative descriptors of food-web matrices. *Ecological Society of America*. **83**(9), pp. 2394–2407.

Besemer, K. 2015. Biodiversity, community structure and function of biofilms in stream ecosystems. *Research in Microbiology.* **166**(10), pp. 774-781.

Biffi, M., Charbonnel, A., Buisson, L., Blanc, F., Némoz, M. and Laffaille, P. 2016. Spatial differences across the French Pyrenees in the use of local habitat by the endangered semi-aquatic Pyrenean desman (*Galemys pyrenaicus*). *Aquatic Conservation: Marine and Freshwater Ecosystems.* **26**(4), pp. 761–774.

Biggs, B. J. F., Stevenson, R. J. and Lowe, R. L. 1998. A habitat matrix conceptual model for stream periphyton. *Archiv Fur Hydrobiologie*. **143**(1), pp. 21–56.

Blenkinsopp, S. A. and Lock, M. A. 1994. The impact of storm-flow on river biofilm architecture. *Journal of Phycology*. **30**(5), pp. 807–818.

Bliss, A., Hock, R. and Radić, V. 2014. Global response of glacier runoff to twenty-first century climate change. *Journal of Geophysical Research: Earth Surface*. **119**(4), pp. 717-730.

Boenigk, J., Wodniok, S., Bock, C., Beisser, D., Hempel. C., Grossmann, L., Lange, A. and Jensen, M. 2018. Geographic distance and mountain ranges structure freshwater protist communities on a European scale. *Metabarcoding and Metagenomics.* **2**(2), e21519.

Bona, F., La Morgia, V. and Falasco, E. 2012. Predicting river diatom removal after shear stress induced by ice melting. *River Research and Applications*. **28**(8), pp. 1289–1298.

Boscaro, V., Rossi, A., Vannini, C., Verni, F., Fokin, S. I. and Petroni, G. 2017. Strengths and biases of high-throughput sequencing data in the characterization of freshwater ciliate microbiomes. *Environmental Microbiology*. **73**(4), pp. 865–875.

Boyero, L., Pearosn, R. G., Gessner, M. O., Barmuta, L. A., Ferreira, V., Garça, M. A. S., Dudgeon, D., Boulton, A. J., Callisto, M., Chauvet, E., Helson, J. E., Bruder, A., Albariño, R. J., Yule, C. M., Arunachalam, M., Davies, J. N., Figueroa, R., Flecker, A. S., Ramírez, A., Death, R. G., Iwata, T., Mathooko, J. M., Mathuriau, C., Gonçalves Jr., J. F., Moretti, M. S., Jinggut, T., Lamothe, S., M'Erimba, C., Ratnarajah, L., Schimdler, M. H., Castela, J., Buria, L. M., Cornejo, A., Villanueva, V. D. and West, D. C. 2011. A global experiment suggests climate warming will not accelerate litter decomposition in streams but might reduce carbon sequestration. *Ecology Letters*. **14**(3), pp. 289–94.

Brittain, J. E., Saltveit, S. J., Castella, E., Bogen, J., Bønsnes, T. E., Blakar, I., Bremnes, T., Haug, I. and Velle, G. 2001. The macroinvertebrate communities of two contrasting Norwegian glacial rivers in relation to environmental variables. *Freshwater Biology*. **46**(12), pp. 1723–1736.

Brose, U., Jonsson, T., Berlow, E. L., Warren, P., Banasek-Richter, C., Bersier, L. F., Blanchard, J. L., Brey, T., Carpenter, S. R., Blandenier, M. F. C., Cushing, L., Dawah, H. A., Dell, T., Edwards, F., Harper-Smith, S., Jacob, U., Ledger, M. E., Martinez, N. D.,

Memmott, J., Mintenbeck, K., Pinnegar, J. K., Rall, B. C., Rayner, T. S., Rueman, D. C., Ruess, L., Ulrich, W., Williams, R. J., Woodward, G. and Cohen, J. E. 2006. Consumer-resource body-size relationships in natural food webs. *Ecology*. **87**(10), pp. 2411–2417.

Brown, A. V. and Brussock, P. P. 1991. Comparison of benthic invertebrates between riffles and pools. *Hydrobiologia.* **220**(2), pp. 99-108.

Brown, J. H., Gillooly, J. F., Allen, A. P., Savage, V. M. and West, G. B. 2004. Toward a metabolic theory of ecology. *Ecological Society of America*. **85**(7), pp. 1771–1789.

Brown, L. E., Hannah, D. M. and Milner, A. M. 2003. Alpine stream habitat classification: An alternative approach incorporating the role of dynamic water source contributions. *Arctic, Antarctic, and Alpine Research*. **35**(3), pp. 313–322.

Brown, L. E., Hannah, D. M. and Milner, A. M. 2007a. Vulnerability of alpine stream biodiversity to shrinking glaciers and snowpacks. *Global Change Biology*. **13**(5), pp. 958–966.

Brown, L. E., Milner, A. M. and Hannah, D. M. 2007b. Groundwater influence on alpine stream ecosystems. *Freshwater Biology*. **52**(5), pp. 878–890.

Brown, L. E., Hannah, D. M. and Milner, A. M. 2009a. ARISE: a classification tool for Alpine RIver and Stream Ecosystems. *Freshwater Biology*. **54**(6), pp. 1357–1369.

Brown, L. E., Cereghino, R. and Compin, A. 2009b. Endemic freshwater invertebrates from southern France: Diversity, distribution and conservation implications. *Biological Conservation*. **142**(11), pp. 2613–2619.

Brown, L. E., Edwards, F. K., Milner, A. M., Woodward, G. and Ledger, M. E. 2011. Food web complexity and allometric scaling relationships in stream mesocosms: implications for experimentation. *Journal of Animal Ecology*. **80**(4), pp. 884–895.

Brown, L. E. and Milner, A. M. 2012. Rapid loss of glacial ice reveals stream community assembly processes. *Global Change Biology*. **18**(7), pp. 2195–2201.

Brown, L. E., Dickson, N. E., Carrivick, J. L. and Füreder, L. 2015. Alpine river ecosystem response to glacial and anthropogenic flow pulses. *Freshwater Science*. **34**(4), pp. 1201–1205.

Brown, L. E., Ramchunder, S. J., Beadle, J. M. and Holden, J. 2016. Macroinvertebrate community assembly in pools created during peatland restoration. *Science of the Total Environment*. **569–570**, pp. 361–372.

Brown, L. E., Khamis, K., Wilkes, M., Blaen, P., Brittain, J. E., Carrivick, J. L., Fell, S. C., Friberg, N., Füreder, L., Gíslason, G. M., Hainie, S., Hannah, D. M., James, W. H. M., Lencioni, V., Ólafsson, J. S., Robinson, C. T., Saltveit, S. J., Thompson, C. and Milner, A. M. 2018. Functional diversity and community assembly of river invertebrates show globally consistent responses to decreasing glacier cover. *Nature Ecology & Evolution*. **2**, pp. 325–333.

Buckel, J., Otto, J. C., Prasicek, G. and Keuschnig, M. 2018. Glacial lakes in Austria - Distribution and formation since the Little Ice Age. *Global and Planetary Change*. **164**, pp. 39–51.

Buczkó, K. and Wojtal, A. Z. 2005. Moss inhabiting siliceous algae from Hungarian peat bogs. *Studia Botanica Hungarica*. **36**, pp. 21–42.

Bundesministerium Nachhaltigkeit und Tourismus (BMNT). 2019. *The Water Information System Austria* [Online]. [Accessed 27 March 2019]. Available from: http://www.bmnt.gv .at/ wasser/wisa/fachinformation/ngp/ngp-2015/karten/OW/ow-typologie.html

Cadbury, S. L., Milner, A. M. and Hannah, D. M. 2011. Hydroecology of a New Zealand glacier-fed river: linking longitudinal zonation of physical habitat and macroinvertebrate communities. *Ecohydrology*. **4**(4), pp. 520–531.

Cantonati, M., Corradini, G., Jüttner, I. and Cox, E. J. 2001. Diatom assemblages in high mountain streams of the Alps and the Himalaya. *Nova Hedwigia*. **12**, pp. 37–61.

Cantonati, M., Füreder, L., Gerecke, R., Jüttner, I. and Cox, E. J. 2012. Crenic habitats, hotspots for freshwater biodiversity conservation: toward an understanding of their ecology. *Freshwater Science*. **31**(2), pp. 463–480.

Cardinale, B. J., Nelson. K. and Palmer, M. A. 2000. Linking species diversity to the functioning of ecosystems: on the importance of environmental context. *Oikos*. **91**(1), pp. 175–183.

Carlough, L. A. 1994. Origins, structure and trophic significance of amorphous seston in a blackwater river. *Freshwater Biology.* **31**(2), pp. 227-237.

Carreon-Martinez, L. and Heath, D. D. 2010. Revolution in food web analysis and trophic ecology: diet analysis by DNA and stable isotope analysis. *Molecular Ecology*. **19**(1), pp. 25–27.

Carrivick, J. L. and Heckmann, T. 2017. Short-term geomorphological evolution of proglacial systems. *Geomorphology*. **287**, pp. 3–28.

Castella, E., Adalsteinsson, H., Brittain, J. E., Gíslason, G. M., Lehmann, A., Lencioni, V., Lods-Crozet, B., Maiolini, B., Milner, A. M., Ólafsson, J. S., Saltveit, S. J. and Snook, D. L. 2001. Macrobenthic invertebrate richness and composition along a latitudinal gradient of European glacier-fed streams. *Freshwater Biology*. **46**(12), pp. 1811–1831.

Cauvy-Fraunié, S., Condom, T., Rabatel, A., Villacis, M., Jacobsen, D. and Dangles, O. 2013. Technical note: Glacial influence in tropical mountain hydrosystems evidenced by the diurnal cycle in water levels. *Hydrology and Earth System Sciences*. **17**(12), pp. 4803–4816.

Cauvy-Fraunié, S., Espinosa, R., Andino, P., Dangles, O. and Jacobsen, D. 2014. Relationships between stream macroinvertebrate communities and new flood-based indices of glacial influence. *Freshwater Biology*. **59**(9), pp. 1916–1925.

Cauvy-Fraunié, S., Espinosa, R., Andino, P., Jacobsen, D. and Dangles, O. 2015. Invertebrate metacommunity structure and dynamics in an Andean glacial stream network facing climate change. *PLoS ONE*. **10**(8).

Cauvy-Fraunié, S., Andino, P., Espinosa, R., Calvez, R., Jacobsen, D. and Dangles, O. 2016. Ecological responses to experimental glacier-runoff reduction in alpine rivers. *Nature Communications*. **7**(12025).

Centre for Biodiversity Genomics. 2010. *Rhyacophila [image]. Barcode of Life Data Systems*. [Online]. [Accessed 14 February 2017]. Available from: www.boldsystems.org/index.php /Taxbrowser_Taxonpage?taxon=rhyacophilidae&searchTax=

Centre for Biodiversity Genomics. 2011. *Leptophlebiidae [image]. Barcode of Life Data Systems*. [Online]. [Accessed 14 February 2017]. Available from: www.boldsystems.org /index.php/Taxbrowser_Taxonpage?taxon=leptophleniidae&searchTax=

Centre for Biodiversity Genomics. 2013. *Hydropsychidae [image]. Barcode of Life Data Systems*. [Online]. [Accessed 22 February 2017]. Available from: www.boldsystems.org/index.php/Taxbrowser_Taxonpage?taxid=1469

Clitherow, L. R., Carrivick, J. L. and Brown, L. E. 2013. Food web structure in a harsh glacier-fed river. *PLoS ONE*. **8**(4).

Cohen, J. E., Schittler, D. N., Raffaelli, D. G. and Reuman, D. C. 2009. Food webs are more than the sum of their tritrophic parts. *Proceedings of the National Academy of Sciences of the United States of America*. **106**(22), pp. 335–340.

Comas, M. and Ribas, A. 2015. Why are the prevalence and diversity of helminths in the endemic Pyrenean brook newt *Calotriton asper* (Amphibia, Salamandridae) so low? *Journal of Helminthology*. **89**(2), pp. 175–181.

Comité Européen de Normalisation (CEN). 2014. *Water Quality - Guidance Standard for the Routine Sampling and Preparation of Benthic Diatoms from Rivers and Lakes. EN 13946*. Geneva: Comité Européen de Normalisation.

Comité European de Normalisation (CEN). 2015. *Water Quality - Guidance on the Estimation of Phytoplankton Biovolume, EN 16695: 2015*. Geneva: Comité European de Normalisation.

Creer, S., Fonseca, V. G., Porazinska, D. L., Giblin-Davis, R. M., Sung, W., Power, D. M., Packer, M., Carvalho, G. R., Blaxter, M. L., Lambshead, P. J. and Thomas, W. K. 2010. Ultrasequencing of the meiofaunal biosphere: practice, pitfalls and promises. *Molecular Ecology*. **19**(1), pp. 4–20.

Cristiano, G., Cicolani, B., Miccoli, F. P. and Di Sabatino, A. 2019. A modification of the leaf-bags method to assess spring ecosystem functioning: benthic invertebrates and leaf-litter breakdown in Vera Spring (Central Italy). *PeerJ,* **7**:e6250.

Csardi, G. and Nepusz, T. 2006. *The igraph Software Package for Complex Network Research*. [Online]. [Accessed 18 March 2019]. Available from: http://pdfs.semanticsholar.org/1d27 /44b 835196577f5f2610698a8ddd177ced4f5c.pdf

Culverhouse, P. F., Macleod, N., Williams, R., Benfield, M. C., Lopes, R. M. and Picheral, M. 2014. An empirical assessment of the consistency of taxonomic identifications. *Marine Biology Research*. **10**(1), pp. 73-84.

Cummins, K. W. 1974. Structure and function of stream ecosystems. *BioScience*. **24**(11), pp. 631–641.

Czeczuga, B. and Orlowska, M. 1999. Hyphomycetes in the ice of water reservoirs. *Roczniki*

Akademii Medycznej w Bialymstoku. **44**, pp. 64-75.

Debroas, D., Domaizon, I., Humbert, J. F., Jardiller, L., Lepère, C., Oudart, A. and Taib, N. 2017. Overview of freshwater microbial eukaryotes diversity: a first analysis of publicly available metabarcoding data. *FEMS Microbiology Ecology*. **93**(4).

Dekar, M. P., Magoulick, D. D. and Huxel, G. R. 2009. Shifts in the trophic base of intermittent stream food webs. *Hydrobiologia*. **635**(1), pp. 263–277.

Deuterostrom. 2011. *Euglena sp. [image]. Wikimedia Commons*. [Online]. [Accessed: 14 February 2017]. Available from: https://commons.wikimedia.org/wiki/File:Euglena_sp. jpg

Dickson, N. E., Carrivick, J. L. and Brown, L. E. 2012. Flow regulation alters alpine river thermal regimes. *Journal of Hydrology*. **464-465**, pp. 505-516.

Dong, X., Li, B., He, F., Gu, Y., Sun, M., Zhang, H., Tan, L., Xiao, W., Liu, S. and Cai, Q. 2016. Flow directionality, mountain barriers and functional traits determine diatom metacommunity structuring of high mountain streams. *Scientific Reports*. **6**(24711).

Dorava, J. M. and Milner, A. M. 2000. Role of lake regulation on glacier-fed rivers in enhancing salmon productivity: the Cook Inlet watershed, south-central Alaska, USA. *Hydrological Processes*. **14**(16-17), pp. 3149–3159.

Dumbrell, A. J., Ferguson, R. M. W. and Clark, D. R. 2017. Microbial community analysis by single-amplicon high-throughput next generation sequencing: Data analysis - from raw output to ecology. In: McGenity, T. J., Timmis, K. N. and Nogales, B. (eds.). *Hydrocarbon and Lipid Microbiology Protocols*. Hiedlberg, Germany: Springer, pp.155-206.

Dunne, J. A., Williams, R. J. and Martinez, N. D. 2002a. Food-web structure and network theory: The role of connectance and size. *Proceedings of the National Academy of Sciences of the United States of America*. **99**(20), pp. 12917–12922.

Dunne, J. A., Williams, R. J. and Martinez, N. D. 2002b. Network structure and biodiversity loss in food webs: robustness increases with connectance. *Ecology Letters*. **5**(4), pp. 558–567.

Durant, J. M., Hjermann, D. O., Ottersen, G. and Stenseth, N. C. 2007. Climate and the match or mismatch between predator requirements and resource availability. *Climate Research*. **33**(3), pp. 271–283.

Edwards, I. P., Upchurch, R. A. and Zak, D. R. 2008. Isolation of fungal cellobiohydrolase I genes from sporocarps and forest soils by PCR. *Applied and Environmental Microbiology.* **74**(11), pp. 3481-3489.

Eisendle-Flöckner, U., Jersabek, C. D., Kirchmair, M., Hashold, K. and Traunspurger, W. 2013. Community patterns of the small riverine benthos within and between two contrasting glacier catchments. *Ecology and Evolution*. **3**(9), pp. 2832–2844.

European Environment Agency (EEA). 2016. *Glaciers* [online]. [Accessed 6 December 2018]. Available from: http://www.eea.europa.eu/data-and-maps/indicators/ glaciers-

2/assessment

Falasco, E. and Bona, F. 2011. Diatom community biodiversity in an alpine protected area: a study in the maritime Alps natural park. *Journal of Limnology*. **70**(2), pp. 157–167.

Fell, S. C., Carrivick, J. L. and Brown, L. E. 2017. The multitrophic effects of climate change and glacier retreat in mountain rivers. *BioScience*. **67**(10), pp. 897–911.

Fell, S. C., Carrivick, J. C., Kelly, M., Füreder, L. and Brown, L. E. 2018. Declining glacier cover threatens the biodiversity of alpine river diatom assemblages. *Global Change Biology*. **24**(12), pp. 5828-5840.

Fellman, J. B., Hood, E., Raymond, P. A., Hudson, J., Bozeman, M. and Arimitsu, M. 2015. Evidence for the assimilation of ancient glacier organic carbon in a proglacial stream food web. *Limnology and Oceanography*. **60**(4), pp. 1118–1128.

Ferreira, V., Graça, M., De Lima, J. L. M. P. and Gomes, R. 2006. Role of physical fragmentation and invertebrate activity in the breakdown rate of leaves. *Archiv fur Hydrobiologie*. **165**(4), pp. 493–513.

Festi, D., Carturan, L., Kofler, W., Fontana, G. D., De Blasi, F., Cazorzi, F., Bucher, E., Mair, V., Gabrielli, P. and Oeggl, K. D. 2017. Linking pollen deposition and snow accumulation on the Alto dell'Ortles glacier (South Tyrol, Italy) for sub-seasonal dating of a firm temperate core. *The Cryosphere*. **11**(2), pp. 937-948.

Finlay, J. C., Power, M. E. and Cabana, G. 1999. Effects of water velocity on algal carbon isotope ratios: implications for river food web studies. *Limnology and Oceanography*. **44**(5), pp. 1198–1203.

Finn, D. S., Khamis, K. and Milner, A. M. 2013. Loss of small glaciers will diminish beta diversity in Pyrenean streams at two levels of biological organisation. *Global Ecology and Biogeography*. **22**(1), pp. 40–51.

Fleming, S. W. 2005. Comparative analysis of glacial and nival streamflow regimes with implications for lotic habitat quantity and fish species richness. *River Research and Applications*. **21**(4), pp. 363–379.

Flory, E. A. and Milner, A. M. 1999. The role of competition in invertebrate community development in a recently formed stream in Glacier Bay National Park, Alaska. *Aquatic Ecology*. **33**(175).

Follstad Shah, J. J., Kominoski, J. S., Ardón, M., Dodds, W. K., Gessner, M. O., Griffiths, N. A., Hawkins, C. P., Johnson, S. L., Lecerf, A. LeRoy, C. J., Manning, D. W. P., Rosemond, A. D., Sinsabaugh, R. L., Swan, C. M., Webster, J. R. and Zeglin, L. H. 2017. Global synthesis of the temperature sensitivity of leaf litter breakdown in streams and rivers. *Global Change Biology*. **23**(8), pp. 3064–3075.

Freimann, R., Bürgmann, H., Findlay, S. E. and Robinson, C. T. 2013. Bacterial structures and ecosystem functions in glaciated floodplains: contemporary states and potential future shifts. *ISME Journal*. **7**(12), pp. 2361–2373.

Friberg, N., Dybkjær, J. B., Ólafsson, J. S., Gíslason, G. M., Larsen, S. E. and Lauridsen, T. L. 2009. Relationship between structure and function in streams contrasting in temperature. *Freshwater Biology*. **54**(10), pp. 2051–2068.

Füreder, L., Welter, C. and Jackson, J.K. 2003. Dietary and stable isotope ($\delta^{13}C$, $\delta^{15}N$) analysis in alpine stream insects. *Hydrobiology*. **88**(3-4), pp. 314–331.

Füreder, L. 2007. Life at the edge. Habitat condition and bottom fauna of alpine running waters. *International Review of Hydrobiology*. **92**(4-5), pp. 491-513.

Gabbud, C., Robinson, C. T. and Lane, S. N. 2019. Sub-basin and temporal variability of macroinvertebrate assemblages in Alpine streams: when and where to sample? *Hydrobiologia.* **830**(1), pp. 179-200.

Gardes, M. and Bruns, T. D. 1993. ITS primers with enhanced specificity for basidiomycetes - application to the identification of mycorrhizae and rusts. *Molecular Ecology*. **2**(2), pp. 113-118.

Gesierich, D. and Rott, E. 2004. Benthic algae and mosses from aquatic habitats in the catchment of a glacial stream (Rotmoos. Ötztal, Austria). *Berichte Des Naturwissenschaftlichen-Medizinischen Verein Innsbruck.* **91**, pp. 7–42.

Gesierich, D. and Rott, E. 2012. Is diatom richness responding to catchment glaciation? A case study from Canadian headwater streams. *Journal of Limnology*. **71**(1), pp. 72–83.

Gessner, M. O., Robinson, C. T. and Ward, J. V. 1998. Leaf breakdown in streams of an Alpine glacial floodplain: Dynamics of fungi and nutrients. *Journal of the North American Benthological Society*. **17**(4), pp. 403–419.

Gessner, M. O. and Chauvet, E. 2002. A case for using litter breakdown to assess functional stream integrity. *Ecological Applications.* **12**(2), pp. 498-510.

Gessner, M.O. and Robinson, C.T. 2003. Aquatic hyphomycetes in alpine streams. In: Ward, J. V. and Uehlinger, U. (eds.). *Ecology of a Glacial Flood Plain*. Dordrecht: Kluwer Academic Publishers, pp. 123-137.

Giersch, J., Hotaling, S., Kovach, R. P., Jones, L. A. and Muhlfeld, C. C. 2016. Climate-induced glacier and snow loss imperils alpine stream insects. *Global Change Biology*. **23**(7), pp. 2577–2589.

Gíslason, G. M., Adxalsteinsson, H., Hansen, I., Ólafsson, J. S., Svavarsdóttir, K. 2001. Longitudinal changes in macroinvertebrate assemblages along a glacial river system in central Iceland. *Freshwater Biology*. **46**(12), pp. 1713–1751.

GitHub. 2016. *GitHub.* [Online]. [Accessed 28 December 2018]. Available from: https://github.com/openterrain/openterrain/wiki/Terrain-Data

GitHub. 2019. *Natural Earth Vector: 50m_cultural/ne_50m_admin_0_countries.shp.* [Online]. [Accessed 6 February 2010]. Available from: https://github.com/nvkelso/natural-earthvector/blob/master/50m_cultural/ne_50m_admin_0_countries.shp.

Glaciology Commission. 2015. *Austrian Glacier Inventory*. [Online]. [Accessed: 28 December 2018]. Available from: https://www.glaziologie.at/gletscherinventar.html

Glassman, S. I., Weihe, C., Li, J., Albright, M. B. N., Looby, C. I., Martiny, A. C., Treseder, K. K., Allison, S. D. and Martiny, J. B. H. 2018. Decomposition responses to climate depend on microbial community composition. *Proceedings of the National Academy of Sciences*. **115**(47), pp. 11994–11999.

Gleason, H. A. 1926. The individualistic concept of the plant association. *Bulletin of the Torrey Botanical Club*. **53**(1), pp. 7–26.

Global Land Ice Measurements from Space (GLIMS). 2018. *GLIMS Glacier Viewer.* [Online]. [Accessed 01 March 2019]. Available from: http://www.glims.org/maps/glims

Gobiet, A., Kotlarski, S., Beniston, M., Heinrich, G., Rajczak, J. and Stoffel, M. 2014. 21st century climate change in the European Alps-A review. *Science of the Total Environment*. **493**, pp. 1138–1151.

Gordon, T. A. C., Neto-Cerejeira, J., Furey, P. C. and O'Gorman, E. J. 2018. Changes in feeding selectivity of freshwater invertebrates across a natural thermal gradient. *Current Zoology*. **64**(2), pp. 231–242.

Green, J. L., Bohannan, B. J. M. and Whitaker, R. J. 2008. Microbial biogeography: From taxonomy to traits. *Science*. **320**, pp. 1039-1042.

Griffiths, R. I., Whiteley, A. S., O'Donnell, A. G. and Bailey, M. J. 2000. Rapid method for coextraction of DNA and RNA from natural environments for analysis of ribosomal DNA- and rRNA-based microbial community composition. *Applied and Environmental Microbiology*. **66**(12), pp. 5488–5491.

Guiry, M. D. 2018. *Algaebase*. [Online]. [Accessed 28 December 2018]. Available from: https://www.algaebase.org/

Hakenkamp, C. C. and Morin, A. 2000. The importance of meiofauna to lotic ecosystem functioning. *Freshwater Biology*. **44**(1), pp. 165–175.

Hannah, D. M., Brown, L. E., Milner, A. M., Gurnell, A. M., McGregor, G. R., Petts, G. E., Smith, B. P. G. and Snook, D. L. 2007. Integrating climate-hydrology-ecology for alpine river systems. *Aquatic Conservation: Marine and Freshwater Ecosystems*. **17**(6), pp. 636–656.

Hari, R. E., Livingstone, D. M., Siber, R., Burkhardt-Holm, P. and Güttinger, H. 2005. Consequences of climatic change for water temperature and brown trout populations in Alpine rivers and streams. *Global Change Biology*. **12**(1), pp. 10–26.

Heegaard, E., Lotter, A. F. and Birks, H. J. B. 2006. Aquatic biota and the detection of climate change: are there consistent aquatic ecotones? *Journal of Paleolimnology*. **35**(3), pp. 507–518.

Herlemann, D. P. R., Labrenz, M., Jürgens, K., Bertilsson, S., Waniek, J. J. and Andersson, A. F. 2011. Transitions in bacterial communities along the 2000 km salinity gradient of the Baltic Sea. *Microbial Population and Community Ecology*. **10**(5), pp. 1571–1579.

Hieber, M., Robinson, C. T., Rushforth, S. R. and Uehlinger, U. 2001. Algal communities associated with different alpine stream types. *Arctic, Antarctic, and Alpine Research*.

33(4), pp. 447–456.

Hotaling, S., Hood, E. and Hamilton, T. 2017. Microbial ecology of mountain glacier ecosystems: biodiversity, ecological connections and implications of a warming climate. *Environmental Microbiology*. **19**(8), pp. 2935–2948.

Hotaling, S., Finn, D. S., Giersch, J. J., Weisrock, D. W. and Jacobsen, D. 2017b. Climate change and alpine stream biology: progress, challenges and opportunities for the future. *Biological Reviews.* **92**(4), pp. 2024-2045.

Hudson, L. N., Reuman, D. and Emerson, R. 2016. *cheddar: Analysis and Visualisation of Ecological Communities. R Package Version 0.1 - 631.* [Online]. [Accessed 12 November 2018]. Available from: https://cran.r-project.org/package=cheddar

Huss, M., Farinotti, D., Bauder, A. and Funk, M. 2008. Modelling runoff from highly glacierized alpine drainage basins in a changing climate. *Hydrological Processes*. **22**(19), pp. 3888–3902.

Huss, M. 2012. Extrapolating glacier mass balance to the mountain-range scale: the European Alps 1900-2100. *Cryosphere*. **6**(4), pp. 713–727.

Huss, M., Bookhagen, B., Huggel, C., Jacobsen, D., Bradley, R. S., Clague, J. J., Vuille, M., Buytaert, W., Cayan, D. R., Greenwood, G., Mark, B. G., Milner, A. M., Weingartner, R. and Winder, M. 2017. Toward mountains without permanent snow and ice. *Earth's Future*. **5**(5), pp. 418–435.

Huss, M. and Hock, R. 2018. Global-scale hydrological response to future glacier mass loss. *Nature Climate Change.* **8**, pp. 135-140.

Hutterer, R., Meinig, H., Bertoloni, S., Krytufek, B., Sheftel, B., Stubbe, M., Samiya, R., Ariunbold, J., Buuveibaatar, V., Dorjderem, S., Monkhzul, T., Otgonbaater, M. and Tsogbadrakh, M. 2016. *Neomys fodiens. International Union for Conservation of Nature (IUCN) Red List of Threatened Species*. [Online]. [Accessed 30 December 2016]. Available from: www.iucnredlist.org/details/29658/0

Ilg, C. and Castella, E. 2006. Patterns of macroinvertebrate traits along three glacial stream continuums. *Freshwater Biology*. **51**(5), pp. 840–853.

Illumina. 2013. *16S Metagenomic Sequencing Library Preparation*. [Online]. [Accessed 11 July 2018]. Available from: http://www.illumina./com/context/dam/illuminasupport/documents/documentation/chemistry_documentation/16s/16s-metagenomic-library-prep-guide-15044223-b.pdf

Imberger, S. J., Thompson, R. M. and Grace, M. R. 2010. Searching for effective indicators of ecosystem function in urban streams: assessing cellulose decomposition potential. *Freshwater Biology.* **55**, pp. 2089-2106.

Intergovernmental Panel on Climate Change (IPCC). 2013. *Climate Change 2013: The Physical Science Basis. Contribution of Working Group I to the Fifth Assessment Report of the Intergovernmental Panel on Climate Change*. Stocker, T. F., Qin, D., Plattner, G. K.,

Tignor, M., Allen, S. K., Boschung, A. J., Nauels, A., Xia, Y., Bex, V. and Midgley, P. M. (eds.). Cambridge: Cambridge University Press.

Jacobsen, D. and Dangles, O. 2012. Environmental harshness and global richness patterns in glacier-fed streams. *Global Ecology and Biogeography*. **21**(6), pp. 647-656.

Jacobsen, D., Milner, A. M., Brown, L. E. and Dangles, O. 2012. Biodiversity under threat in glacier-fed river systems. *Nature Climate Change*. **2**(5), pp. 361–364.

Jacobsen, D., Cauvy-Fraunié, S., Andino, P., Espinosa, R., Cueva, D. and Dangles, O. 2014. Runoff and the longitudinal distribution of macroinvertebrates in a glacier-fed stream: implications for the effects of global warming. *Freshwater Biology*. **59**(10), pp. 2038–2050.

Jansson, P., Hock, R. and Schneider, T. 2003. The concept of glacier storage: a review. *Journal of Hydrology*. **282**(1), pp. 116–129.

Jüttner, I., Williams, D. M., Levkov, Z., Falasco, E., Battegazzore, M., Cantonati, M., Van de Vijver, B., Angele, C. and Ector, L. 2015. Reinvestigation of the type material *Odontidium hyemale* (Roth) Kützing and related species, with descriptions of four new species in the genus *Odontidium* (Fragilariaceae, Bacillariophyta). *Phytotaxa*. **234**(1), pp. 1–36.

Jüttner, I., Williams, D. M., Gurung, S., Van de Vijver, B., Levkov, Z., Sharma, C. M., Sharma, S. and Cox, E. J. 2017. The genus *Odontidium* (Bacillariophyta) in the Himalaya - a preliminary account of some taxa and their distribution. *Phytotaxa*. **332**(1), pp. 1–21.

Kawecka, B., Kownacka, M. and Kownacki, A. 1971. General characteristics of the biocoenosis in the streams of the Polish High Tatras. *Acta Hydrobiologica Sinica*. **13**, pp. 465–476.

Kelly, M. 2000. Identification of common benthic diatoms in rivers. *Field Studies*, **9**, pp. 583–700.

Kelly, M. G., Juggins, S., Gutherie, R., Pritchard, S., Jamieson, J., Rippey, B., Hirst, H. and Yallop, M. 2008. Assessment of ecological status in U.K. rivers using diatoms. *Freshwater Biology*. **53**(2), pp. 403–422.

Khamis, K., Hannah, D. M., Clarvis, H., Brown, L. E. and Milner, A. M. 2014a. Alpine aquatic ecosystem conservation policy in a changing climate. *Environmental Science and Policy*. **43**, pp. 39–55.

Khamis, K., Hannah, D. M., Brown, L. E., Tiberti, R. and Milner, A. M. 2014b. The use of invertebrates as indicators of environmental change in alpine rivers and lakes. *Science of the Total Environment*. **493**, pp. 1242–1254.

Khamis, K., Brown, L. E., Hannah, D. and Milner, A. 2015. Experimental evidence that predator range expansion modifies alpine stream community structure. *Freshwater Science*. **34**(1), pp. 66–80.

Khamis, K., Brown, L. E., Hannah, D. and Milner, A. 2016. Glacier–groundwater stress gradients control alpine river biodiversity. *Ecohydrology*. **9**(7), pp. 1263–1275.

Klaar, M. J., Kidd, C., Malone, E., Bartlett, R., Pinay, G., Chapin, F. S. and Milner, A. M. 2015. Vegetation succession in deglaciated landscapes: implications for sediment and landscape stability. *Earth Surface Processes and Landforms*. **40**(8), pp. 1088-100.

Koboltschnig, G. R. and Schöner, W. 2011. The relevance of glacier melt in the water cycle of the Alps: the example of Austria. *Hydrology and Earth System Sciences.* **15**(6), pp. 2039–2048.

Krammer, K. and Lange-Bertalot, H. 2004. Bacillariophyceae: 4. Teil: Achnanthaceae, Kritische Ergänzungen zu Achnanthes s.l., Navicula s.str (2/4). In: Ettl, H., Gärtner, G., Heynig, H., Mollenhauer, D. (eds.). *Süβwasserflora von Mitteleuropa.* München: Elsevier.

Krammer, K. and Lange-Bertalot, H. 2007a. Bacillariophyceae: 1. Teil: Naviculaceae (2/1). In: H. Ettl, J. Gerloff, H. Heynig, D. Mollenhauer (eds.). *Süβwasserflora von Mitteleuropa*. München: Elsevier.

Krammer, K. and Lange-Bertalot, H. 2007b. Bacillariophyceae: 2. Teil: Bacillariaceae, Epithemiaceae, Surirellaceae (2/2). In: H. Ettl, J. Gerloff, H. Heynig, D. Mollenhauer (eds.). *Süβwasserflora von Mitteleuropa*. München: Elsevier.

Krammer, K. and Lange-Bertalot, H. 2008. Bacillariophyceae: 3. Teil: Centrales, Fragilariaceae, Eunotiaceae (2/3). In: H. Ettl, J. Gerloff, D. Mollenhauer (eds.). *Süβwasserflora von Mitteleuropa*. Heidelberg: Springer.

Kreader, C. A. 1995. Relief of amplification inhibition in PCR with bovine serum albumin or T4 gene 32 protein. *Applied and Environmental Microbiology*. **62**(3), pp. 1102–1106.

Kruk, C., Devercelli, M., Huszar, V. L. M., Hernández, E., Beamud, G., Diaz, M., Silva, L. H. S. and Segura, A. M. 2017. Classification of Reynolds phytoplankton functional groups using individual traits and machine learning techniques. *Freshwater Biology*. **62**(10), pp. 1681–1692.

Kuzmin, S., Papenfuss, T., Sparreboom, M., Ugurtas, I. H., Anderson, S., Beebee, T., Denoël, M., Andreone, F., Anthony, B., Schmidt, B., Ogrodowczyk, A., Ogielska, M., Bosch, K., Tarkhnishvili, D. and Ischenko, V. 2009. *Salamandra. International Union for Conservation of Nature (IUCN) Red List of Threatened Species*. [Online]. [Accessed 10 January 2016]. Available from: www.iucnredlist.org/details/59467/0

Lange-Bertalot, H. and Steindorf, A. 1996. Rote liste der limnischen kieselalgen (Bacillariophyceae) Deutschlands. *Schriftenreihe Fur Vegetationskunde*. **28**, pp. 633–677.

Lange-Bertalot, H., Hofmann, G., Werum, M. and Cantonati, M. 2017. *Freshwater Benthic Diatoms of Central Europe: Over 800 Common Species Used in Ecological Assessment. English Edition with Updated Taxonomy and Added Species*. Oberreifenberg: Koeltz Botanical Books.

Langhans, S. D., Tiegs, S., Gessner, M. O., Tockner, K. 2008. Leaf-decomposition heterogeneity across a riverine floodplain mosaic. *Aquatic Sciences*. **70**(3), pp. 337–346.

Larsen, S., Muehlbauer, J. D. and Marti, E. 2016. Resource subsidies between stream and terrestrial ecosystems under global change. *Global Change Biology*. **22**(7), pp. 2489–2504.

Lavandier, P. and Décamps, H. 1983. Un torrent d'altitude dans les Pyrénées: L'Estaragne. In: Lamotte, M. and Bourlière, F. (eds.). *Ecosystèmes Limniques*. Paris: Masson, pp. 81–111.

Layer, K., Riede, J. O., Hildrew, A. G. and Woodward, G. 2012. Food web structure and stability across a wide pH gradient. *Advances in Ecological Research.* **42**, pp. 265-299.

Ledger, M. E., Brown, L. E., Edwards, F. K., Milner, A. M. and Woodward, G. 2013. Drought alters the structure and functioning of complex food webs. *Nature Climate Change*. **3**(3), pp. 223–227.

Lencioni, V., Rossaro, B. and Maiolini, B. 2007. Alpine chironomid distribution: a mere question of altitude? In: Andersen, T. (ed.). *Contributions to the Systematics and Ecology of Aqutic Diptera - A Tribute to Ole A Sæther*. Columbus: The Caddis Press, pp. 165–180.

Lencioni, V. 2018. Glacial influence and stream macroinvertebrate biodiversity under climate change: Lessons from the Southern Alps. *Science of the Total Environment*. **622–633**, pp. 563–575.

Liu, J., Soininen, J., Han, B. P. and Declerck, S. A. J. 2013. Effects of connectivity, dispersal directionality and functional traits on the metacommunity structure of river benthic diatoms. *Journal of Biogeography*. **40**(12), pp. 2238–2248.

Lobo, E. A., Heinrich, C. G., Schuch, M., Wetzel, C. E. and Ector, L. 2016. Diatoms as bioindicators in rivers. In: Necchi, O. (ed.). *River Algae*. Cham: Springer. pp. 245-271.

López-Rodríguez, M. J., Peralta-Maraver, I., Geatani, B., Sainz-Cantero, C. E., Fochetti, R. and Tierno de Figueroa, J. M. 2012. Diversity patterns and food web structure in a Mediterranean intermittent stream. *International Review of Hydrobiology.* **97**(6), pp. 485-496.

Lu, X., Gray, C., Brown, L. E., Ledger, M. E., Milner, A. M., Mondragon, R. J., Woodward, G. and Ma, A. 2016. Drought rewires the cores of food webs. *Nature Climate Change*. **6**(9), pp. 875–878.

Ludwig, G. and Schnittler, M. 1996. *Rote Liste der Pflanzen Deutschlands*. [Online]. [Accessed 26 January 2017]. Available from: www.bfn.de/fileadmin/MDB/documents/RoteListePflanzen.pdf

Ludwig, G., Sinsch, U. and Pelster, B. 2015. Behavioural adaptations of *Rana temporaria* to cold climates. *Journal of Thermal Biology*. **49–50**, pp. 82–90.

Maiolini, B. and Lencioni, V. 2001. Longitudinal distribution of macroinvertebrate assemblages in a glacially influenced stream system in the Italian Alps. *Freshwater Biology.* **46**(12), pp. 1625-1639.

Malard, F., Uehlinger, U., Zah, R. and Tockner, K. 2006. Flood-pulse and riverscape dynamics in a braided glacial river. *Ecology*. **87**(3), pp. 704–716.

Manerkar, M. A., Seena, S. and Bärlocher, F. 2008. Q-RT-PCR for assessing archaea, bacteria, and fungi during leaf decomposition in a stream. *Microbial Ecology*. **56**(3), pp. 467–473.

Manoylov, K. M. 2014. Taxonomic identification of algae (morphological and molecular): Species concepts, methodologies and their implications for ecological bioassessment. *Phycological Society of America*. **50**(3), pp. 409–424.

Margesin, R. and Collins, T. 2019. Microbial ecology of the cryosphere (glacial and permafrost habitats): current knowledge. *Applied Microbiology and Biotechnology.* In press.

Masclaux, H., Perga, M. E., Kagami, M., Desvilettes, C., Bourider, G. and Bec, A. 2013. How pollen organic matter enters freshwater food webs. *Limnology and Oceanography*. **58**(4), pp. 1185–1195.

Mathers, K. L., Rice, S. P. and Wood, P. J. 2019. Predator, prey, and substrate interactions: the role of faunal activity and substrate characteristics. *Ecosphere*. **10**(1), e02545.

McKernan, C., Cooper, D. J. and Schweiger, E. W. 2018. Glacial loss and its effect on riparian vegetation of alpine streams. *Freshwater Biology*. **63**(6), pp. 518–529.

McKew, B. A. and Smith, C. J. 2017. Real-time PCR approaches for analysis of hydrocarbon-degrading bacterial communities. In: McGenity, T. J., Timmis, K. N. and Nogales, B. (eds.). *Hydrocarbon and Lipid Microbiology Protocols*. Hiedlberg, Germany: Spinger, pp. 45-64.

Menden-Deuer, S. and Lessard, E. J. 2000. Carbon to volume relationships for dinoflagellates, diatoms, and other protest plankton. *Limnology and Oceanography*. **45**(3), pp. 569–579.

Michener, R. and Lajtha, K. 2007. *Stable Isotopes in Ecology and Environmental Science*. 2nd Edition. Oxford, England: Blackwell Publishing Ltd.

Milner, A. M. and Petts, G. E. 1994. Glacial rivers: physical habitat and ecology. *Freshwater Biology*. **32**(2), pp. 295–307.

Milner, A. M., Brittain, J. E., Castella, E. and Petts, G. E. 2001. Trends of macroinvertebrate community structure in glacier-fed rivers in relation to environmental conditions: a synthesis. *Freshwater Biology*. **46**(12), pp. 1833–1847.

Milner, A. M., Brown, L. E. and Hannah, D. M. 2009. Hydroecological response of river systems to shrinking glaciers. *Hydrological Processes*. **23**(1), pp. 62–77.

Milner, A. M. and Robertson, A. L. 2010. Colonization and succession of stream communities in Glacier Bay, Alaska; What has it contributed to general successional theory? *River Research and Applications.* **26**(1), pp. 26-35.

Milner, A. M., Robertson, A. L., Brown, L. E., Sønderland, S.H., McDermott, M. and Veal, A. J. 2011. Evolution of a stream ecosystem in recently deglaciated terrain. *Ecology*. **92**(10), pp. 1924–1935.

Milner, A. M. 2016. The Milner and Petts (1994) conceptual model of community structure within glacier-fed rivers: 20 years on. In: Gilvear, D. J., Greenwood, M.T., Thoms, M. C. and Wood, P.J. (eds.). *River Science: Research and Management for the 21st Century*. Hoboken: Wiley. pp. 156–170.

Milner, A. M., Khamis, K., Battin, T J., Brittain, J. E., Barrand, N. E., Füreder, L., Cauvy-Fraunié, S., Gíslason, G. M., Jacobsen, D., Hannah, D. M., Hodson, A. J., Hood, E., Lencioni, V., Ólafsson, J. S., Robinson, C. T., Tranter, M. and Brown, L. E. 2017. Glacier shrinkage driving global changes in downstream systems. *Proceedings of the National Academy of Sciences*. **114**(37), pp. 9770–9778.

Milner, A. M., Picken, J. L., Klaar, M. J., Robertson, A. L., Clitherow, L. R., Eagle, L. and Brown, L. E. 2018. River ecosystem resilience to extreme flood events. *Ecology and Evolution.* **9**(16), pp. 835-8363.

Montoya, J. M. and Solé, R. V. 2002. Small world patterns in food webs. *Journal of Theoretical Biology.* **214**(3), pp. 405-412.

Morris, E. K., Caruso, T., Buscot, F., Fischer, M., Hancock, C., Maier, T. S., Meiners, T., Müller, C., Obermaier, E., Prati, D., Socher, S. A., Sonnemann, I., Wäschke, N., Wubet, T., Wurst, T., Wurst, S. and Rillig, M. C. 2014. Choosing and using diversity indices: insights for ecological applications from the German Biodiversity Exploratories. *Ecology and Evolution*. **4**(18), pp. 3514–3524.

Muhlfeld, C. C., Giersch, J. J., Hauer, F. R., Pederson, G. T., Luikart, G., Peterson, D. P., Downs, C. C. and Fagre, D. B. 2011. Climate change links fate of glaciers and an endemic alpine invertebrate. *Climatic Change*. **106**(2), pp. 337–345.

Nautiyal, P., Mishra, A. S. and Verma, J. 2015. The health of benthic diatom assemblages in lower stretch of a lesser Himalayan glacier-fed river, Mandakini. *Journal of Earth System Science*. **124**(2), pp. 383–394.

Nguyen, N. H., Song, Z., Bates, S. T., Branco, S., Tedersoo, L., Menke, J., Schilling, J. S. and Kennedy, P. G. 2016. FUNGuild: An open annotation tool for parsing fungal community datasets by ecological guild. *Fungal Ecology*, **20**, pp. 241–248.

Niedrist, G. H. and Füreder, L. 2017. Trophic ecology of alpine stream invertebrates: current status and future research needs. *Freshwater Science*. **36**(3), pp. 466–478.

Niedrist, G. H. and Füreder, L. 2018. When the going gets tough, the tough get going: The enigma of survival strategies in harsh glacial stream environments. *Freshwater Biology*. **63**(10), pp. 1260–1272.

Niedrist, G. H., Cantonati, M. and Füreder, L. 2018. Environmental harshness mediates the quality of periphyton and chironomid body mass in alpine streams. *Freshwater Science*. **37**(3), pp. 519–533.

Nilsson, R. H., Larsson, K. H., Taylor, A. F. S., Bengtsson-Palme, J., Jeppesen, T. S., Schigel, D., Kennedy, P., Picard, K., Glöckner, F. O., Tedersoo, L., Saar, I., Kõljaig, U. and Abarenkov, K. 2018. *UNITE Community: Communication and Identification of DNA Based Fungal Species*. [Online]. [Accessed 26 January 2019]. Available from: https://unite.ut.ee/search.php#fndtn-panel1

Nolte, U. 1990. Chironomid biomass determination from larval shape. *Freshwater Biology*. **24**(3), pp. 443–451.

O'Gorman, E. J., Pichler, D. E., Adams, G., Benstead, J. P., Cohen, H., Craig, N., Cross, W. F., Demars, B. O. L., Friberg, N., Gíslason, G. M., Gudmundsdóttir, R., Hawczak, A., Hood, J. M., Hudson, L. N., Johansson, L., Johansson, M. P., Junker, J. R., Laurila, A., Manson, J. R., Mavromati, E., Nelson, D., Ólafsson, J. S., Perkins, D. M., Petchey, O. L., Plebani, M., Reuman, D. C., Rall. B. C., Stewart, R., Thompson, M. S. A. and Woodward, G. 2012. Impacts of warming on the structure and functioning of aquatic communities: Individual- to ecosystem-level responses. *Advances in Ecological Research*. **47**, pp. 81–176.

O'Gorman, E., J., Petchey, O. L., Faulkner, K., Gallo, B., Gordon, T. A. C., Neto-Cerejeiral, J., Pichler, D. E., Thompson, M. S. and Woodward, G. 2018. *Simplified Food Webs in Warmer Environments Following the Loss of Consumer Species*. Unpublished.

Oksanen, J., Guillaume Blanchet, F., Friendly, M., Kindt, R., Legendre, P., McGlinn, D., Minchin, P. R., O'Hara, R. B., Simpson, G. L., Solymos, P., Stevens, M. H. H., Szoecs, E. and Wagner, H. 2017. *vegan: Community Ecology Package. R Package Version. 2.4*-3. [Online]. [Accessed 28 December 2018]. Available from: https://CRAN.R-Project.org/package=vegan

Oksanen, J. 2019. *Vegan: ecological diversity* [Online]. [Accessed 12 June 2018]. Available from: http://cran.r-project.org/web/packages/vegan/vignettes/diversity-vegan.pdf

Otto, J-C. 2019. Proglacial lakes in high mountain environments. In: Heckmann, T. and Morche, D. (eds.). *Geomorphology of Proglacial Systems: Landform and Sediment Dynamics in Recently Deglaciated Alpine Landscapes*. Cham, Switzerland: Springer Nature Switzerland. pp. 231-247.

Parker, S. M. and Huryn, A. D. 2006. Food web structure and function in two Arctic streams with contrasting disturbance regimes. *Freshwater Biology*. **51**(7), pp. 1249–1263.

Parker, S. M. and Huryn, A. D. 2013. Disturbance and productivity as codeterminants of stream food web complexity in the Arctic. *Limnology and Oceanography*. **58**(6), pp. 2158-2170.

Passy, S. I. 2007. Diatom ecological guilds display distinct and predictable behavior along nutrient and disturbance gradients in running waters. *Aquatic Botany*. **86**(2), pp. 171–178.

Pepin, N., Bradley, R. S., Diaz, H. F., Baraer, M., Caceres, E. B., Frosythe, N., Fowler, H., Greenwood, G., Hashmi, M. Z., Liu, X. D., Miller, J. R., Ning, L., Ohmura, A., Palazzi, E., Rangwala, I., Schöner, W., Severskiy, I., Shahgedanova, M., Wang, M. B., Williamson, S. N. and Yag, D. Q. 2015. Elevation-dependent warming in mountain regions of the world. *Nature Climate Change*. **5**(5), pp. 424–430.

Perić, M. S., Schubert, C. J. and Robinson, C. T. 2015. Do alpine stream insects change their feedings habits in response to environmental change? In *PACE15: Symposium on Plant and Animal Conservation Ecology*. Dübendorf, Switzerland: Eawag.

Perkins, D. M., Reiss, J., Yvon-Durocher, G. and Woodward, G. 2010. Global change and food webs in running waters. *Hydrobiologia.* **657**(1), pp. 181-198.

Perkins, D. M., Durance, I., Edwards, F. K., Grey, J., Hildrew, A. G., Jackson, M., Jones, J. I., Lauridsen, R. B., Layer-Dobra, K., Thompson, M. S. A. and Woodward, G. 2018. Bending the rules: exploitation of allochthonous resources by a top-predator modifies size-abundance scaling in stream food webs. *Ecology Letters*. **21**(12), pp. 1771-1780.

Peter, H. and Sommaruga, R. 2016. Shifts in diversity and function of lake bacterial communities upon glacier retreat. *ISME Journal*. **10**(7), pp. 1545–1554.

Pfankuch, D. J. 1975. *Stream Reach Inventory and Channel Stability Evaluation.* Northern Region, Montana: US Department Forest Service.

Pickett, S. T. A. 1989. Space-for-time substitution as an alternative to long-term studies. In: Likens, G. E. (ed.). *Long-Term Studies in Ecology*. New York: Springer, pp. 110–135.

Ponomarev, D., Van Kolfschoten, T., Van Der Plicht, J. and Kosintsev, P. 2015. Lateglacial desman discovered in Sed'yu-1 (Komi Republic, Russia), a site in the far northeast of Europe. *Quaternary International*. **378**, pp. 88–98.

Potapova, M. and Hamilton, P. B. 2007. Morphological and ecological variation within the *Achnanthidium minutissimum* (Bacillariophyceae) species complex. *Journal of Phycology*. **43**(3), pp. 561–575.

Queiroz, I., Bertrand, A. and Khakhin, G. V. 1996. Status and conservation of Desmaninae in Europe. In: *Nature and Environment nº 76*. Strasbourg: Council of Europe.

Raymond, P., Hartmann, J., Lauerwald, R., Sobek, S., McDonald, C., Hoover, M., Butman, D., Striegl, R., Mayorga, E., Humborg, C., Kortelainen, P., Dürr, H., Meybeck, M., Ciais, P and Guth, P. 2013. Global carbon dioxide emissions from inland waters. *Nature*. **503**(7476), pp. 355-359.

Ren, Z., Gao, H., Elser, J. J. and Zhao, Q. 2017a. Microbial functional genes elucidate environmental drivers of biofilm metabolism in glacier-fed streams. *Scientific Reports*. **7**(12668).

Ren, Z., Gao, H. and Elser, J. J. 2017b. Longitudinal variation of microbial communities in benthic biofilms and association with hydrological and physicochemical conditions in glacier-fed streams. *Freshwater Science*. **36**(3), pp. 479–49.

Rimet, F. and Bouchez, A. 2012. Life-forms, cell-sizes and ecological guilds of diatoms in European rivers. *Knowledge and Management of Aquatic Ecosystems*. **406**(1), pp. 1-14.

Robertson, A. L., Brown, L. E., Klaar, M. J. and Milner, A. M. 2015. Stream ecosystem responses to an extreme rainfall event across multiple catchments in southeast Alaska. *Freshwater Biology*. **60**(12), pp. 2523–2534.

Robinson, C. T., Gessner, M. O. and Ward, J. 1998. Leaf breakdown and associated macroinvertebrates in alpine glacial streams. *Freshwater Biology*. **40**(2), pp. 215–228.

Robinson, C. T. and Gessner, M. O. 2000. Nutrient addition accelerates leaf breakdown in an alpine springbrook. *Oecologia*. **122**(2), pp. 258–263.

Robinson, C. T., Gessner, M. O., Callies, K. A., Jolidon, C. and Ward, J. V. 2000. Larch needle

breakdown in contrasting streams of an alpine glacial floodplain. *Journal of the North American Benthological Society*. **19**(2), pp. 250–262.

Robinson, C. T. and Jolidon, C. 2005. Leaf breakdown and the ecosystem functioning of alpine streams. *Journal of the North American Benthological Society*. **24**(3), pp. 495-508.

Robinson, C. and Kawecka, B. 2005. Benthic diatoms of an alpine stream/lake network in Switzerland. *Aquatic Sciences*. **67**(4), pp. 492–506.

Robinson, C. T., Tonolla, D., Imhof, B., Vukelic, R. and Uehlinger, U. 2016. Flow intermittency, physico-chemistry and function of headwater streams in an Alpine glacial catchment. *Aquatic Sciences*. **78**(2), pp. 327-341.

Robson, B. A., Hölbling, D., Nuth, C., Strozzi, T. and Dahl, S. O. 2016. Decadal scale changes in glacier area in the Hohe Tauern National Park (Austria) determined by object-based image analysis. *Remote Sensing*. **8**(67), pp. 1-23.

Rogora, M., Frate, L., Carranza, M. L., Freppaz, M., Stanisci, A., Bertani, R., Brambilla, A., Canullo, R., Carbognani, M., Cerrato, C., Chelli, S., Cremonese, E., Cutini, M., Di Musciano, M., Erschbamer, B., Godone, D., Locchi, M., Isabellon, M., Magnani, A., Mazzola, I., Morra de Cella, U., Pauli, H., Petey, M., Petriccione, B., Porro, F., Psenner, R., Rossetti, G., Scotti, A., Sommaruga, R., Tappeiner, U., Theurillat, J. P., Tomaselli, M., Viglietti, D., Viterbi, R., Vittoz, P., Winkler, M. and Matteucci, G. 2018. Assessment of climate change effects on mountain ecosystems through a cross-site analysis in the Alps and Apennines. *Science of The Total Environment.* **624**, pp. 1429-1442.

Rosi-Marshall, E. J., Wellard Kelly, H. A., Hall. R. O. and Vallis, K. A. 2016. Methods for quantifying aquatic macroinvertebrate diets. *Freshwater Science*. **35**(1), pp. 229–236.

Rott, E., Cantonati, M., Füreder, L. and Pfister, P. 2006. Benthic algae in high altitude streams of the Alps - a neglected component of the aquatic biota. *Hydrobiologia*. **562**(1), pp. 195–216.

Rotta, F., Cerasino, L., Occhipinti-Ambrogi, A., Rogora, M., Seppi, R. and Tolotti, M. 2018. Diatom diversity in headwaters influenced by permafrost thawing: First evidence from the Central Italian Alps. *Advances in Oceanography and Limnography.* **9**(2), pp.79-96.

Roxburgh, S. H., Shea, K. and Wilson, B. 2004. The intermediate disturbance hypothesis: patch dynamics and mechanisms of species coexistence. *Ecology.* **85**(2), pp. 359-371.

Sabo, J. L., Finlay, J. C., Kennedy, T. and Post, D. M. 2010. The role of discharge variation in scaling of drainage area and food chain length in rivers. *Science.* **330**(6006), pp. 965-967.

Schmid-Araya, J. M. and Schmid, P. E. 2000. Trophic relationships: integrating meiofauna into a realistic benthic food web. *Freshwater Biology*. **44**(1), pp. 149–163.

Schmid-Araya, J. M., Hildrew, A. G., Roberston, A., Schmid, P. E. and Winterbottom, J. 2002. The importance of meiofauna in food webs: evidence from an acid stream. *Ecology*. **83**(5), pp. 1271–1285.

Schmid-Araya, J. M., Schmid, P. E., Tod, S. P. and Esteban, G. F. 2016. Trophic positioning of

meiofauna revealed by stable isotopes and food web analysis. *Ecology.* **97**(11), pp. 3099-3109.

Scott, K. R., Morgan, R. M., Jones, V. J. and Cameron, N. G. 2014. The transferability of diatoms to clothing and the methods appropriate for their collection and analysis in forensic geoscience. *Forensic Science International*. **241**, pp. 127–137.

Seena, S., Bärlocher, F., Sobral, O., Gessner, M. O., Dudgeon, D., McKie, B. C., Chauvet, E., Boyero, L., Ferreira, V., Frainer, A., Bruder, A., Matthaei, C. D., Fenoglio, S., Sridhar, K. R., Albariño, R. J., Douglas, M. M., Encalada, A. C., Garcia, E., Ghate, S. D., Giling, D. P., Gonçalves, V., Iwata, T., Landeira-Dabarca, A., McMaster, D., Medeiros, A. O., Naggea, J., Pozo, J., Raposeiro, P. M., Swan, C. M., Tenkiano, N. S. D., Yule, C. and Graça, M. A. S. 2019. Biodiversity of leaf litter fungi in streams along a latitudinal gradient. *Science of The Total Environment*. **661**, pp. 306-315.

Shannan, S., Smith, R., Wiltshire, A., Payne, T., Huss, M., Betts, R., Caesar, J., Koutroulis, A., Jones, D. and Harrison, S. 2019. Global glacier volume projections under high-end climate change scenarios. *The Cryosphere*. **13**(325-350).

Sheppard, S. K. and Harwood, J. D. 2005. Advances in molecular ecology: tracking trophic links through predator-prey food-webs. *Functional Ecology*. **19**(5), pp. 751–762.

Singer, G. A., Fasching, C., Wilhelm, L., Niggemann, J., Steier, P., Dittmar, T. and Battin, T. J. 2012. Biogeochemically diverse organic matter in Alpine glaciers and its downstream fate. *Nature Geoscience.* **5**, pp. 710-714.

Sinnatamby, R. N., Babaluk, J. A., Power, G., Reist, J. D. and Power, M. 2012. Summer habitat use and feeding of juvenile Arctic charr, *Salvelinus alpinus*, in the Canadian High Arctic. *Ecology of Freshwater Fish*. **21**(2), pp. 309–322.

Smock, L. A. 1980. Relationships between body size and biomass of aquatic insects. *Freshwater Biology*. **10**(4), pp. 375–383.

Solé, R. V. and Montoya, J. M. 2001. Complexity and fragility in ecological networks. *Proceedings of the Royal Society B*. **268**(1480), pp. 2039–2045.

Spaulding, S. 2018. *Diatoms of the United States*. [Online]. [Accessed 28 December 2018]. Available from: https://westerndiatoms.colorado.edu/

Staatliche Naturwissenschaftliche Sammlungen Bayerns (SNSB). 2010. *Perla grandis [image]. Barcode of Life Data Systems*. [Online]. [Accessed 14 February 2017]. Available from: www.boldsystems.org/index.php/Taxbrowser_Taxonpage?taxid=186556

Steinman, A. D. and Lamberti, G. A. 1996. Biomass and pigments of benthic algae. In: Hauer, F. R. and Lamberti, G. A. (eds.). *Methods in Stream Ecology*. San Diego: Academic Press.

Striegl, R. G., Dornblaser, M. M., McDonald, C. P., Rover, J. R and Sets, E. G. 2012. Carbon dioxide and methane emissions from the Yukon River system. *Global Biogeochemical Cycles.* **26**(4).

Sun, J. and Lui, S. 2003. Geometric models for calculating cell biovolume and surface area for

phytoplankton. *Journal of Plankton Research*. **25**(11), pp. 1331–1346.

Suter, S. G., Rees, G. N., Watson, G. O., Suter, P. J. and Silvester, E. 2011. Decomposition of native leaf litter by aquatic hyphomycetes in an alpine stream. *Marine and Freshwater Research*. **62**(7), pp. 841–849.

Tank, J. L., Rosi-Marshall, E. J., Griffiths, N. A., Entrekin, S. A. and Stephen, M. L. 2010. A review of allochthonous organic matter dynamics and metabolism in streams. *Journal of the North American Benthological Society*. **29**(1), pp. 118–146.

Thies, H., Nickus, U., Tolotti, M., Tessadri, R. and Krainer, K. 2013. Evidence of rock glacier melt impacts on water chemistry and diatoms in high mountain streams. *Cold Regions Science and Technology*. **96**, pp. 77–85.

Thompson, R. M., Dunne, J. A. and Woodward, G. 2012. Freshwater food webs: towards a more fundamental understanding of biodiversity and community dynamics. *Freshwater Biology*. **57**(7), pp. 1329–1341.

Thompson, C., David, E., Freestone, M. and Robinson, C. T. 2013. Ecological patterns along two alpine glacial streams in the Fitzpatrick Wilderness, Wind River Range, USA. *Western North American Naturalist*. **73**(2), pp. 137–147.

Thorp, J. H. and Rogers, C. 2011. *Field Guide to Freshwater Invertebrates of North America*. China: Elsevier.

Tian, J., Qiao, Y., Wu, B., Chen, H., Li, W., Jiang, N., Zhang, X. and Liu, X. 2017. Ecological succession pattern of fungal community in soil along a retreating glacier. *Frontiers in Microbiology*. **8**(1028).

Tiegs, S. D., Langhans, S. D., Tockner, K. and Gessner, M. O. 2007. Cotton strips as a leaf surrogate to measure decomposition in river floodplain habitats. *Journal of the North American Benthological Society*. **26**(1), pp. 70–77.

Tiegs, S. D., Clapcott, J. E., Griffiths, N. A. and Boulton, A. J. 2013. A standardized cotton-strip assay for measuring organic-matter decomposition in streams. *Ecological Indicators*. **32**, pp. 131–139.

Tiegs, S. D. 2015a. *CELLDEX Protocol Part 1*. [Online]. [Accessed 11 July 2018]. Available from: https://www.researchgate.net/publication/281243407_CELLDEX_Protocol_Part_1

Tiegs, S. D. 2015b. *CELLDEX Protocol Part 2*. [Online]. [Accessed 11 July 2018]. Available from: https://www.researchgate.net/publication/283645782_CELLDEX_Protocol_Part_2

Tiegs, S. D. 2015c. *Protocol for microbial DNA/RNA sampling - CELLDEX Protocol*. [Online]. [Accessed 11 July 2018]. Available from: http://www.researchgate.net/publications/281 1245895 _Protocol_for_microbial_DNARNA_sampling_-_CELLDEX_Project

Tiegs, S. D., Costello, D. M., Isken, M. W., Woodward, G., McIntyre, P. B., Gessner, M. O., Chauvet, E., Griffiths, N. A., Flecker, A. S., Acuña, V., Albariño, A., Allen, D. C., Alonso, C., Andino, P., Arango, C., Aroviita, J., Barbosa, M. V. M., Barmuta, L. A., Baxter, C.,

Bell, T. D. C., Bellinger, B., Boyero, L., Brown, L. E., Bruder, A., Bruesewitz, D. A., Burdon, F. J., Callisto, M., Canhoto, C., Capps, K. A., Castillo, M. M., Clapcott, J., Colas, F., Colón-Gaud, C., Cornut, J., Crespo-Pérez, V., Cross, W. F., Culp, J. M., Danger, M., Dangles, O., De Eyto, E., Derry, A. M., Díaz Villanueva, V., Douglas, M. M., Elosegi, A., Encalada, A. C., Entrekin, S., Espinosa, R., Ethaiya, D., Ferreira, V., Ferriol, C., Flanagan, K. M., Fleituch, T., Follstad Shah, J. J., Frainer, A., Friberg, N., Frost, P. C., Garcia, E. A., García Lago, L., García Soto, P. E., Ghate, S., Giling, D. P., Gilmer, A., Gonçalves Jr, J., F., Gonzales, R. K., Graça, M. A. S., Grace, M., Grossart, H-P., Guérold, F., Gulis V., Hepp, L. U., Higgins, S., Hishi, T., Huddart, J., Hudson, J., Imberger, S., Iñiguez-Armijos, C., Iwata, T., Janetski, D. J., Jennings, E., Kirkwood, A. E., Koning, A. A., Kosten, S., Kuehn, K. A., Laudon, H., Leavitt, P. R., Lemes da Silva, A. L., Leroux, S. J., LeRoy, C. J., Lisi, P. J., MacKenzie, R., Marcarelli, A. M., Masese, F. O., McKie, B. G., Medeiros, A. O., Meissner, K., Miliša, M., Mishra, S., Miyake, Y., Moerke, A., Mombrikotb, S., Mooney, R., Moulton, T., Muotka, T., Negishi, J. N., Neres-Lima, V., Nieminen, M. L., Nimptsch, J., Ondruch, J., Paavola, R., Pardo, I., Patrick, C. J., Peeters, E. T. H. M., Pozo, J., Pringle, C., Prussian, A., Quenta, E., Quesada, A., Reid, B., Richardson, J. S., Rigosi, A., Rincón, J., Risnoveanu, G., Robinson, C. T., Rodríguez-Gallego, L., Royer, T. V., Rusak, J. A., Santamans, A. C., Selmeczy, G. B., Simiyu, G., Skuja, A., Smykla, J., Sponseller, R., Stoler, A., Swan, C. M., Szlag, D., Teixeira-de Mello, F., Tonkin, J. D., Uusheimo, S., Veach, A. M., Vilbaste, S., Vought, L. B. M., Wang, C-P., Webster, J. R., Wilson, P. B., Woelfl, S., Xenopoulos, M. A., Yates, A. G., Yoshimura, C., Yule, C. M., Zhang, Y. X. and Zwart, J. A. 2019. Global patterns and drivers of ecosystem functioning in rivers and riparian zones. *Science Advances*. **5**(1).

Toju, H., Tanabe, A. S., Yamamoto, S. and Sato, H. 2012. High-coverage ITS primers for the DNA-based identification of Ascomycetes and Basidiomycetes in environmental samples. *PLoS ONE*, **7**(7).

Townsend, C. R., Scarsbrook, M. R. and Dolédec, S. 1997. The intermediate disturbance hypothesis, refugia, and biodiversity in streams. *Limnology and Oceanography*. **42**(5), pp. 938–949.

Townsend, C. R., Thompson, R. M., McIntosh, A. R., Kilroy, C., Edwards, E. and Scarsbrook, M.R. 1998. Disturbance, resource supply and food-web architecture in streams. *Ecology Letters.* **1**(3), pp. 200-209.

Uehlinger, U., Malard, F. and Ward, J. W. 2002. Ecological windows in glacial stream ecosystems. *EAWAG News*. **54e**(16–17), pp. 21–21.

Uehlinger, U., Robinson, C. T., Hieber, M., Zah, R. 2010. The physico-chemical habitat template for periphyton in alpine glacial streams under a changing climate. *Hydrobiologia*. **657**(1), pp. 107–121.

Ulseth, A. J., Bertuzzo, E., Singer, G. A., Schelker, J. and Battin, T. J. 2018. Climate-induced

changes in spring snowmelt impact ecosystem metabolism and carbon fluxes in an alpine stream network. *Ecosystems*. **21**(2), pp. 373–390.

Vadeboncoeur, Y. and Power, M. E. 2017. Attached algae: The cryptic base of inverted trophic pyramids in freshwaters. *Annual Review of Ecology, Evolution and Systematics*. **48**, pp. 255–279.

Valbuena-Ureña, E., Oromi, N., Soler-Membrives, A., Carranza, S., Amat, F., Camarasa, S., Denoël, M., Guillaume, O., Sanuy, D., Loyau, A., Schmeller, D. S. and Steinfartz, S. 2018. Jailed in the mountains: genetic diversity and structure of an endemic newt species across the Pyrenees. *PLoS ONE.* **13**(8).

Wang, M., Jiang, X., Wu, W., Hao, Y., Su, Y., Cai, L., Xiang, M. and Liu, X. 2015. Psychrophilic fungi from the world's roof. *Persoonia.* **34**, pp. 100-112.

Wang, X., Zheng, B., Liu, L. and Li, L. 2014. Use of diatoms in river health assessment. *Annual Research & Review in Biology*. **4**(24), pp. 4054–4074.

Wang, Y., Maumann, U., Wright, S. and Warton, D. 2018. *mvabund: Statistical Methods for Analysing Multivariate Abundance Data.* [Online]. [Accessed 2 November 2018]. Available from: https://cran.r-project.org/package=mvabund

Ward, C. L. and McCann, K. S. 2017. A mechanistic theory for aquatic food chain length. *Nature Communications.* **8**(2028).

Wardle, D. A., Yeates, G. W., Watson, R. N. and Nicholson, K. S. 1995. Development of the decomposer food-web, trophic relationships, and ecosystem properties during a three-year primary sucession in sawdust. *Oikos.* **73**(2), pp. 155-166.

Weiss, S., Xu, Z. Z., Peddada, S., Amir, A., Bittinger, K., Gonzalez, A., Lozupone, C., Zaneveld, J. R., Váquez-Baeza, Y., Birmingham, A., Hyde, E. R. and Knight, R. 2017. Normalization and microbial differential abundance strategies depend upon data characteristics. *Microbiome.* **5**(1).

Weitere, M., Erken, M., Majdi, N., Arndt, H., Norf, H., Reinshagen, M., Traunspurger, W., Walterscheid, A. and Way, J. K. 2018. The food web perspective on aquatic biofilms. *Ecological Monographs*. **88**(4), pp. 545-559.

Wellnitz, T. and Rader, R. B. R. 2003. Mechanisms influencing community composition and succession in mountain stream periphyton: interactions between scouring history, grazing, and irradiance. *Journal of the North American Benthological Society*. **22**(4), pp. 528–541.

Wilhelm, L., Singer, G., Fasching, C., Battin, T. J. and Besemer, K. 2013. Microbial biodiversity in glacier-fed streams. *ISME Journal*. **7**(8), pp. 1651–1660.

Williams, R. J., Berlow, E. L., Dunne, J. A., Barabási, A. L. and Martinez, N. D. 2002. Two degrees of separation in complex food webs. *Proceedings of the National Academy of Sciences of the United States of America*. **99**(20), pp. 12913–12916.

Witkowski, A., Kotusz, J., Popiolek, M. and Kusznierz, J. 2008. Summer dynamics of density and biomass of the Arctic charr, *Salvelinus alpinus*, in a polar stream (SW Spitsbergen). *Polish Polar Research*. **29**, pp. 237–243.

Wood, S. N. 2004. Stable and efficient multiple smoothing parameter estimation for generalized additive models. *Journal of the American Statistical Association*. **99**(467), pp. 673–686.

Wood, S. N. 2011. Fast stable restricted maximum likelihood and marginal likelihood estimation of semiparametric generalized linear models. *Journal of the Royal Statistical Society: Series B (Statistical Methodology)*. **73**(1), pp. 3–36.

Woodward, G., Speirs, D. C. and Hildrew, A. G. 2005. Quantification and resolution of a complex, size-structured food web. *Advances in Ecological Research*. **36**, pp. 85–131.

Woodward, G. 2009. Biodiversity, ecosystem functioning and food webs in fresh waters: assembling the jigsaw puzzle. *Freshwater Biology*. **54**(10), pp. 2171–2187.

Woodward, G., Perkins, D. M. and Brown, L. E. 2010a. Climate change and freshwater ecosystems: impacts across multiple levels of organization. *Philosophical Transactions of the Royal Society B*. **365**(1549), pp. 2093–2106.

Woodward, G., Benstead, J. P., Beveridge, O. S., Blanchard, J., Brey, T., Brown, L. E., Cross, W. F., Friberg, N., Ings, T. C., Jacob, U., Jennings, S., Ledger, M. E., Milner, A. M., Montoya, J. M., O'Gorman, E., Olesen, J. M., Petchey, O. L., Pichler, D. E., Reuman, D. C., Thompson, M. S. A., Van Veen, F. J. F. and Yvon-Durocher, G. 2010b. Ecological networks in a changing climate. *Advances in Ecological Research*. **42**, pp. 71–138.

Woodward, G., Brown, L. E., Edwards, F. K., Hudson, L. N., Milner, A. M., Reuman, D. C. and Ledger, M. E. 2012. Climate change impacts in multispecies systems: drought alters food web size structure in a field experiment. *Philosophical Transactions of the Royal Society B*. **367**(1605), pp. 2990–2997.

World Wilde Fund for Nature (WWF). 2018. *Living Planet Report - 2018: Aiming Higher*. Grooten, M. and Almond, R. E. A (eds.). Gland: WWF.

Wrona, F. J., Prowse, T. D., Reist, J. D., Hobbie, J. E., Lévesque, L. M. and Vincent, W. F. 2006. Climate change effects on aquatic biota, ecosystem structure and function. *Ambio*. **35**(7), pp. 359–369.

Wynn, P. M., Hodson, A. J., Heaton, T. H. E. and Chenery, S. R. 2007. Nitrate production beneath a High Arctic glacier, Svalbard. *Chemical Geology*. **244**(1–2), pp. 88–102.

Yoon, I., Williams, R., Levine, E., Yoon, S., Dunne, J. and Martinez, N. 2004. Webs on the web (WOW): 3D visualisation of ecological networks on the WWW for collaborative research and education. In: *Proceedings of the IS&T/SPIE Symposium on Electronic Imaging. Visualisation and Data Analysis*. **5295**, pp. 124–132.

Yue, K., Wu, F., Yang, W., Zhang, C., Peng, U., Tan, B., Xu, Z. and Huang, C. 2016. Cellulose dynamics during foliar litter decomposition in an alpine forest meta-ecosystem. *Forests.* **7**(8), pp. 176-188.

Yvon-Durocher, G. and Allen, A. P. 2012. Linking community size structure and ecosystem functioning using metabolic theory. *Philiosophical Transactions of the Royal Society B.* **367**(1605), pp. 2998-3007.

Zah, R., Burgherr, P., Bernasconi, S. M. and Uehlinger, U. 2001. Stable isotope analysis of macroinvertebrates and their food sources in a glacier stream. *Freshwater Biology*. **46**(7), pp. 871–882.

Zah, R. and Uehlinger, U. 2001. Particulate organic matter inputs to a glacial stream ecosystem in the Swiss Alps. *Freshwater Biology*. **46**(12), pp. 1597–1608.

Zang, T., Wang, N. F., Zhang, Y. Q. Liu, H. Y. and Yu, L. Y. 2016. Diversity and distribution of aquatic fungal communities in the Ny-Ålesund region, Svalbard (High Arctic). *Microbial Ecology.* **71**(3), pp. 543-554.

Zemp, M., Haeberli, W., Hoelzle, M. and Paul, F. 2006. Alpine glaciers to disappear within decades? *Geophysical Research Letters*. **33**(13), pp. 1–4.

Zemp, M., Frey, H., Gärtner-Roer, I., Nussbaumer, S. U., Hoelzle, M., Paul, F., Haeberli, W., Denzinger, F., Ahlstrøm, A. P., Anderson, B., Bajracharya, S., Baroni, C., Braun, L. N., Cáceres, B. E., Caassa, G., Cobos, G., Dávila, L. R., Delgado Granados, H., Demuth, M. N., Espizua, L., Fischer, A., Fujita, K., Gadek, B., Ghazanfar, A., Hagen, J. O., Holmlund, P., Karimi, N., Li, Z., Pelto, M., Pitte, P., Popovnin, V. V., Portocarrero, C. A., Prinz, R., Sangewar, C. V., Severskiy, I., Sigurdsson, O., Soruco, A., Usubaliev, R. and Vincent, C. 2015. Historically unprecedented global glacier decline in the early 21st century. *Journal of Glaciology*. **61**(228), pp. 745–762.

Appendices

Appendix 1: Study site information

Table A1.1 Study site descriptions. Numbers indicate field research teams: [1] = Sarah Fell, Lee Brown, Jonathan Carrivick [2] = Sarah Fell, Jonathan Carrivick, [3] = Eran Hood, [4] = Sophie Cauvy-Fraunié, [5] = Sophie Cauvy-Fraunié, Verónica Crespo-Pérez. Letters and symbols denote sampling strategy: B = Biological sampling (Surber sampling and biofilm rock scrubs), D = Decomposition sampling (cotton strip assays and microbial sampling), - = microbial samples not collected, * = tensile strength information not available.

Alpine region	Valley/ area	Date	Sampling	Chapter	Site code	Aspect	Site coordinates	Altitude (m)	Glacier cover (%)
Eastern Alps, Austria[1]	Eisboden	Jun/ Jul 2015 (B)	B, D	3, 4, 5	E1	N	47.12436, 12.63836	2129	3
			B,	3, 4	E2		47.13125, 12.63408	2074	26
			B, D	3, 5	E3		47.13416, 12.63749	2052	28
		Jun-Jul/ Jul-Aug 2016 (D)	B, D	3, 4, 5	E4		47.13477, 12.63710	2056	0
			B, D	3, 4, 5	E5		47.12213, 12.63853	2154	36
			D	5	E6		47.13359, 12.63351	2084	0
			D	5	E7		47.13269, 12.63310	2074	0
			D	5	E8		47.12702, 12.61150	2053	54
			B, D	3, 4, 5	U1		47.14075, 12.65157	2275	46
			B	3, 4	U2		47.13979, 12.65328	2286	1
	Obersulzbach	As above	B	3	O1	NW	47.13371, 12.28085	1948	52
			B, D	3, 5	O2		47.13371, 12.28345	1942	0
			B	3, 4	O3		47.14214, 12.27648	1746	42
			D	5	O4		47.12963, 12.28068	1971	56
	Rotmoos	Jun (B)/ Jul-Aug 2016 (D)	B, D	3, 4, 5	R1	N	46.83104, 11.04022	2351	64
			B, D	3, 5	R2		46.83633, 11.03612	2305	41
			B, D	3, 5	R3		46.83981, 11.03206	2286	38
			B, D	3, 4, 5	R4		46.84623, 11.01827	2253	30
Southern Alps, New Zealand[2]	Franz Josef	Nov-Dec 2016/ Jan 2017	D*	5	NZ1	N	-43.44090, 170.17216	244	74
			D*-	5	NZ2		-43.43055, 170.16893	223	0
			D*	5	NZ3		-43.43052, 170.16948	215	69
			D*-	5	NZ4		-43.80187, 170.11348	627	43
	Fox	As above	D*-	5	NZ5	W	-43.49925, 170.05319	251	60
			D*	5	NZ6		-43.49513, 170.04167	216	58
			D	5	NZ7		-43.47817, 170.00835	178	50
	Birch Hill	As above	D*	5	NZ8	E	-43.79560, 170.07564	999	23
			D*	5	NZ9		-43.79737, 170.08762	814	9
			D*	5	NZ10		-43.80122, 170.11798	614	7
	Rob Roy	As above	D*-	5	NZ11	S	-44.47506, 168.72736	758	48
			D	5	NZ12		-44.47523, 168.72809	769	0
			D*	5	NZ13		-44.48070, 168.72632	709	38
			D	5	NZ14		-44.50284, 168.72032	401	30
Southern Norway[3]	Finse/ Hardangervidda Plateau	Jul/ Aug-Sep 2017	D	5	NR1	S	60.58883, 7.44862	1224	32
			D	5	NR2		60.58931, 7.44816	1212	45
			D	5	NR3		60.57460, 7.47961	1310	85
			D	5	NR4		60.57524, 7.48529	1310	71
			D	5	NR5		60.57416, 7.49382	1290	1
			D	5	NR6		60.56763, 7.50173	1367	8
			D	5	NR7		60.57802, 7.50746	1369	80
			D	5	NR8		60.58072, 7.51330	1228	58
			D	5	NR9		60.58464, 7.51981	1229	64
			D	5	NR10		60.58464, 7.51981	1217	55
			D	5	NR11		60.58880, 7.44874	1219	53
			D	5	NR12		60.59002, 7.55209	1209	0
			D	5	NR13		60.59410, 7.53861	1209	0
			D	5	NR14		60.59410, 7.53861	1392	64
			D*	5	NR15		60.57603, 7.47641	1309	73

Table A1.1 – continued

Alpine region	Valley/ area	Date	Sampling	Chapter	Site code	Aspect	Site coordinates	Altitude (m)	Glacier cover (%)
Alaska[4]	Boundary Range	Jul-Aug 2017	D	5	AK1	SW	58.364416, -134.478486	23	26
			D*	5	AK2	SSW	58.528439, -134.805948	7	40
			D	5	AK3	S	58.404140, -134.581596	17	55
			D	5	AK4	W	58.652052, -134.914173	14	11
			D	5	AK5	SSW	58.528330, -134.805990	7	44
Eastern Alps, France[5]	Vanoise (Chavière)	Aug-Sep 2017	D	5	FR1	NNE	45.296718, 6.645947	2504	51
			D	5	FR2		45.297519, 6.650509	2445	0
			D*	5	FR3		45.283214, 6.668080	2413	28
			D	5	FR4		45.287004, 6.669283	2327	18
			D*	5	FR5		45.287728, 6.669109	2326	0
			D	5	FR6		45.296980, 6.672500	2255	0
			D	5	FR7		45.305088, 6.669824	2079	10
			D	5	FR8		45.312892, 6.681206	1981	13
			D*	5	FR9		45.325402, 6.692855	1895	41
			D*	5	FR10		45.339042, 6.694818	1766	13
	Vanoise (Les Allues)	As above	D	5	FR11	N	45.328562, 6.625382	2222	25
			D*	5	FR12		45.329039, 6.625382	2233	35
			D-	5	FR13		45.346282, 6.620300	2030	17
			D	5	FR14		45.346917, 6.616693	2016	0
			D	5	FR15		45.361990, 6.585158	1714	13
Ecuador[6]	Antisana	Jun-Oct 2017	D	5	EC1	W	-0.46987, -78.1829	4366	0
			D	5	EC2		-0.49556, -78.1961	4208	27
			D*	5	EC3		-0.49458, -78.2013	4179	11
			D*	5	EC4		-0.49458, -78.1996	4193	17
			D	5	EC5		-0.50470, -78.2162	4086	0
			D*	5	EC6		-0.50550, -78.2162	4083	7
			D	5	EC7		-0.51282, -78.2158	4037	0
			D*	5	EC8		-0.51306, -78.2156	4039	10
			D	5	EC9		-0.51374, -78.2174	4034	8
			D	5	EC10		-0.47776, -78.17014	4512	65
			D	5	EC11		-0.49240, -78.17238	4474	56
			D	5	EC12		-0.46530, -78.16520	4493	39

Table A1.2 Environmental parameters for sampled rivers. For sites hosting cotton strip assays, observations were made at the time of their incubation. Water chemistry analysis was performed in 2015 (Eisboden and Obersulzbach sites), 2016 (Rotmoos sites and TN for all Austrian Alps sites) and 2017 (all remaining sites).

Site Code	Temp. (°C)	EC ($\mu S\ cm^{-1}$)	pH	Turbidity (NTU)	1/ Pfankuch	DOC ($mg\ L^{-1}$)	DC ($mg\ L^{-1}$)	PO_4 ($mg\ L^{-1}$)	NO_3 ($mg\ L^{-1}$)	TN ($mg\ L^{-1}$)	TP ($mg\ L^{-1}$)
E1	11.35	60	8.22	0.41	0.033	3.3	2.6	0.001	0.132	0.066	-0.002
E2	4.00	43.5	8.13	0	0.048	3.8		0.002	0.321	0.102	
E3	6.55	129	9.30	86	0.026	2.6	9.3	0.001	0.348	0.108	-0.001
E4	4.60	68.3	9.03	0	0.034	2.2	1.1	0.003	0.152	0.211	0.001
E5	2.35	107	9.38	157	0.018	8.1	4.8	0.001	0.158	0.262	
E6	5.90	2.76	4.00	0	0.033		1.3				-0.002
E7	8.70	69.80	6.28	2.84	0.034		9.0				-0.001
E8	2.65	1.86	4.50	3.52	0.019						
O1	8.50	12	8.20	1.29	0.027	4.3	2.5	0.001	0.399	0.077	
O2	8.50	20.5	9.33	0	0.053	0.3	5.2	0.001	0.136	0.238	0.001
O3	8.00	17	9.26	4.97	0.025	1.4	2.9	0.001	0.287	0.275	
O4	4.45	16.2	9.04	17.06	0.024	0.5	3.5	0.001	0.312	0.217	
R1	3.30	81.9	6.96	34.14	0.018		10.4			0.148	0.001
R2	5.95	87.7	7.65	31.88	0.016		13.7			0.109	-0.001
R3	5.85	77	7.04	62	0.018		12.0			0.066	-0.001
R4	7.10	78	7.59	42.60	0.019		8.7			0.196	0.001
U1	1.30	61.1	9.73	70	0.019	1.3	5.9	0.001	0.250	0.258	0.000
U2	4.50	17.2	8.80	1.66	0.050	0.9		0.000	0.209	0.311	
NZ1	2.65	74.6	7.79	118	0.018					0.008	0.000
NZ2	10.05	7.9	7.58	0.31	0.024					0.148	0.001
NZ3	3.25	69.5	7.89	108	0.018					0.109	-0.001
NZ4	7.00	82.7	7.49	26.69	0.018					0.066	-0.001
NZ5	2.60	106.3	7.42	168	0.023					0.196	0.001
NZ6	2.65	118.4	7.55	169	0.023					0.066	-0.002
NZ7	5.05	137	7.53	287	0.024					0.211	0.001
NZ8	4.40	33.4	6.80	0	0.022					0.102	-0.001
NZ9	6.55	36.6	7.02	0.08	0.022					0.258	0.000
NZ10	8.90	39.9	7.72	0.31	0.022					0.043	-0.002
NZ11	5.85	34.4	7.51	23.38	0.020					0.239	-0.001
NZ12	13.15	43	7.41	0.47	0.029					0.305	-0.001

Table A1.2 – continued

Site Code	Temp. (°C)	EC (µS cm^{-1})	pH	Turbidity (NTU)	1/ Pfankuch	DOC (mg L^{-1})	DC (mg L^{-1})	PO_4 (mg L^{-1})	NO_3 (mg L^{-1})	TN (mg L^{-1})	TP (mg L^{-1})
NZ13	6.80	25.7	6.90	16.75	0.019					0.217	-0.002
NZ14	8.50	34.3	6.79	3.13	0.029					0.238	0.001
NR1	8.65	18	7.23	3.17	0.025			0.004	0.092	0.09	0.022
NR2	8.45	11.9	7.01	1.87	0.029			0.003	0.077	0.11	0.019
NR3	1.20	8.3	6.98	42.94	0.020			0.003	0.091	0.11	0.019
NR4	2.50	19.1	7.04	10.07	0.022			0.003	0.076	0.25	0.018
NR5	8.30	19.6	7.02	32.41	0.050			0.007	0.117	0.18	0.020
NR6	8.90	8.8	6.65	0.41	0.059			0.006	0.103	0.22	0.026
NR7	1.40	6.4	6.64	48.27	0.021			0.003	0.077	0.18	0.021
NR8	3.05	11.9	6.71	136	0.022			0.004	0.123	0.18	0.020
NR9	3.40	10.7	6.84	62	0.028			0.004	0.099	0.67	0.021
NR10	1.00	11.2	6.85	62	0.333			0.004	0.111	0.21	0.005
NR11	3.00	10.4	6.93	33.39	0.029			0.003	0.078	0.25	0.005
NR12	7.60	27.9	7.11	2.04	0.053			0.002	0.071	0.01	0.004
NR13	9.25	12	6.76	1.11	0.053			0.002	0.335	0.07	0.005
NR14	2.70	14.5	7.29	19.54	0.026			0.002	0.029	0.35	0.003
NR15	4.80	28.6	7.23	46.15	0.019			0.019	0.326	0.15	0.004
AK1	5.78	23.8	6.50	44.33							
AK2	2.57	19.1	6.30	114.33							
AK3	3.45	20.1	6.50	85.47							
AK4	8.35	19.5	6.20	13.67							
AK5	3.43	12.4	6.30	41.97							
FR1	11.90	87.7	7.94	160	0.021	0.7	13.3			0.373	0.044
FR2	15.00	116.2	7.86	19	0.022	1.7	13.1			0.405	0.039
FR3	8.00	59.2	7.96	700	0.040	3.1	15.9			0.359	0.037
FR4	10.28	153	7.69	17	0.022	0.3	15.2			0.225	0.035
FR5	12.90	77.6	7.94	15	0.032	0.5	14.2			0.364	0.049
FR6	13.61	109.5	7.88	11	0.037	3.9	13.6			0.255	0.052
FR7	9.80	635	7.67	150	0.032	2.2	7.6			0.311	0.056
FR8	13.10	98.2	8.11	25	0.029	0.7	5.3			0.302	0.052

Table A1.2 – continued

Site Code	Temp. (°C)	EC (µS cm^{-1})	pH	Turbidity (NTU)	1/ Pfankuch	DOC (mg L^{-1})	DC (mg L^{-1})	PO_4 (mg L^{-1})	NO_3 (mg L^{-1})	TN (mg L^{-1})	TP (mg L^{-1})
FR10	11.09	232	7.75	190	0.021	2.1	11.5			0.250	0.057
FR11	6.14	839	7.17	2	0.026	5.5	16.7			0.325	0.060
FR12	3.50	229	7.58	2000	0.053	1.9	17.6			0.317	0.051
FR13	5.25	331	7.53	1600	0.017	2.7	15.2			0.334	0.079
FR14	8.00	1711	7.19	0.05	0.019	2.9	16.6			0.446	0.063
FR15	7.70	403	7.61	1100	0.048	2.4	19.1			0.221	0.060
EC1	14.60	20.7	7.56	4.01	0.243					0.34	0.032
EC2	12.60	26.2	7.96	145	0.043					0.88	0.025
EC3	10.10	44.5	7.75	161	0.043					0.56	0.032
EC4	8.20	25.3	7.52	220	0.036					0.85	0.045
EC5	9.70	200.9	6.75	0.50	0.023					0.69	0.042
EC6	9.70	91.7	7.15	47	0.038					0.66	0.241
EC7	7.30	133.2	7.29	0.70	0.034					0.83	
EC8	10.50	107.7	7.70	3.58	0.037					0.53	0.232
EC9	9.70	107.6	7.52	7.21	0.031					0.66	0.175
EC10	10.30	15.9	7.32	148	0.029						0.203
EC11	10.70	10.2	7.14	359	0.025						
EC12	12.90	20.9	7.31	73.7	0.013						

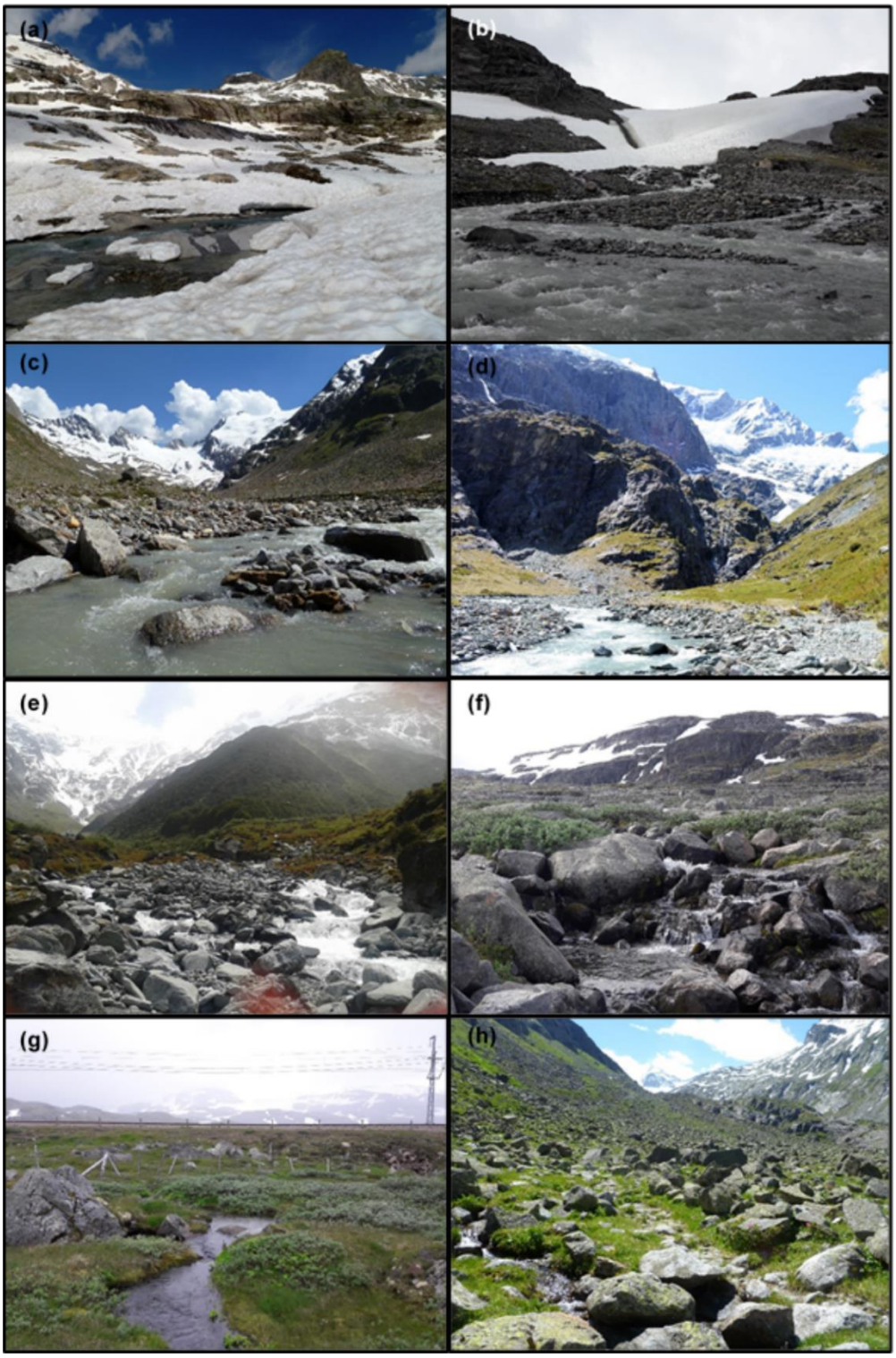

Figure A1.1 River sites along a gradient of catchment glacier cover. Images exemplify the different river habitats sampled. These included rivers with high (a, b) (a = E8, 54 % glacier cover; b = NR3, 85 % glacier cover), medium (c, d) (c = R3, 38 % glacier cover; d = NZ11, 48 % glacier cover), low (e, f) (e = NZ9, 9 % glacier cover, NR5, 1 % glacier cover) and zero (g, h) (g = NR13, h = O2, both 0 % glacier cover) catchment glacier cover. Site codes are defined in Table A1.1.

Appendix 2: Supporting information for Chapter Three

River water temperature data were collected from spot measurements using Hanna Instrument HI9063 (Woonsocket, Rhode Island, USA). In turn, the readings may have been influenced by the time of sampling, particularly given the spatiotemporal variability of water temperature in glacier-fed streams. In attempt to obtain more representative temperature data, TinyTag Plus 2 temperature loggers (Chichester, UK) were successfully incubated in nine rivers in the Austrian Alps (Chapter Five). They remained in-situ for approximately 38 days, logging at 1 h resolution. This higher frequency data identified a significant negative relationship between mean river water temperature and catchment glacier cover.

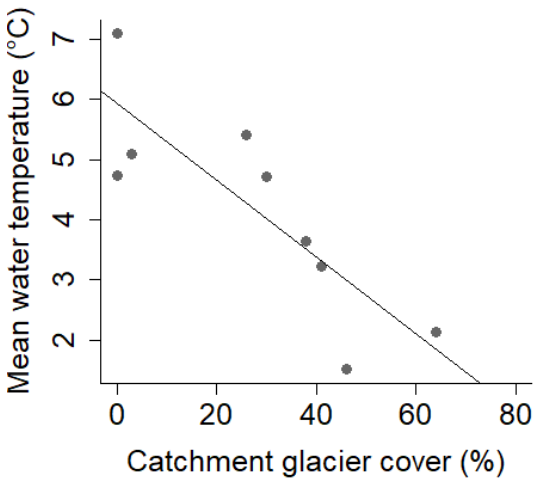

Figure A2.1 Mean daily water temperature as a function of catchment glacier cover for nine river sites in the central Austrian Alps.

Appendix 3: Supporting information for Chapter Four

Appendix 3.1: Taxonomic identification references

Reference materials used to identify food web consumers and their resources.

Macrobenthos

Initial classification to order/family followed Dobson et al. (2012) with higher resolution identification obtained from genus/species specific keys.

Dobson, M., Pawley, S., Fletcher, M. and Powell, A. 2012. *Guide to Freshwater Invertebrates.* Cumbria, UK: Freshwater Biological Association.

Diptera

Brooks, S.J., Langdon, P.G. and Hieri, O. 2007. *The Identification and Use of Palaearctic Chironomidae Larvae in Palaeoecology. QRA Technical Guide No. 10.* London, UK: Quaternary Research Association.

Dobson, M. 2013. Family-level keys to freshwater fly (Diptera) larvae: a brief review and a key to European families avoiding use of mouthpart characters. *Freshwater Reviews.* **6**, pp. 1-32.

Jedlička, L., Kúdela, M. and Stloukalová, V. 2004. Key to the identification of blackfly pupae (Diptera: Simuliidae) of Central Europe. *Biologia – Section Zoology.* **59**(15), pp. 157–178.

Rossaro, B. and Lencioni, V. 2015a. A key to larvae of *Diamesa* Meigen, 1835 (Diptera, Chironomidae), well known as adult males and pupae from Alps (Europe). *Journal of Entomological and Acarological Research.* **47**(5516), pp. 123-138.

Rossaro, B. and Lencioni, V. 2015b. A key to larvae of species belonging to the genus *Diamesa* from Alps and Apennines (Italy). *European Journal of Environmental Sciences*. **5**(1), pp. 62–79.

Schmid, P.E. 1993. *A Key to the Larval Chironomidae and their Instars from Austrian Danube Region Streams and Rivers, with Particular Reference to a Numerical Taxonomic Approach. Part I: Diamesinae, Prodiamesinae and Orthocladiinae*. Wien, Austria: Federal Institute for Water Quality.

Sinclair, B. J. 2008. *The Systematics of New World Clinocera Meigen (Diptera: Empididae: Clinocerinae).* Ottawa, Canada: NRC Research Press.

Sundermann, A., Lohse, S., Beck, L. A. and Haase, P. 2007. Key to the larval stages of aquatic true flies (Diptera), based on the operational taxa list for running waters in Germany. *International Journal of Limnology.* **43**(1), pp. 61-74.

Ephemeroptera

Bauernfeind, E. and Soldán, T. 2012. *The Mayflies of Europe (Ephemeroptera).* Ollerup, Denmark: Apollo Books.

Elliott, J. M., Humpesch, U. H. and Macan, T. T. 1988. *Key to the Larvae of the British Ephemeroptera: with Ecological Notes.* Cumbria, UK: Freshwater Biological Association.

Plecoptera

Zwick, P. 2004. Key to the West Palaearctic genera of stoneflies (Plecoptera) in the larval stage. *Limnologica.* **34**, pp. 315-348.

Trichoptera

Waringer, J and Graf, W. 1997. *Atlas der Österreichischen Köcherfliegenlarven unter Einschluß der Angrezenden Gebiete.* Wien, Austria: Facultas-Universitätsverlag.

Waringer, J. and Wolfram, G. 2013. Key and bibliography of the genera of European Trichoptera larvae. *Zootaxa.* **3640**(2): 101-151.

Meiobenthos

Overview sources covering identification of meiobenthos included:

Crutcher, R. 2018. *MicrolabNW Photomicrograph Gallery*. [Online]. [Accessed 24 September 2018]. Available from: http://www.microlabgallery.com

Plewka, M. 2018. *Pling: Life in Water.* [Online]. [Accessed 24 September 2018]. Available from: http://www.plingfactory.de/Science/GruKlaOeko/Teichleben/e-TL3.html

Rotifers

Pontin, R. 1978. *A Key to the Freshwater Planktonic and Semi-Planktonic Rotifera of the British Isles*. Cumbria, UK: Freshwater Biological Association.

Testate amoeba

Charman, D. J., Hendon, D. and Woodland, W. A. 2000. *The Identification of Testate Amoeba (Protozoa: Rhizopoda) in Peats. Technical Guide no. 9*. London, UK: Quaternary Research Association.

Siemensma, F. J. 2018. *Microworld: World of Amoeboid Organisms*. [Online]. [Accessed 24 September 2018]. Available from: https://www.arcella.nl

Microbenthos

Overview sources listed for meiobenthos were also used in the identification of microbenthos.

Desmids

Bayer, M. and Mann, D. 2018. *DIADIST: Diatom and Desmid Identification by Shape and Texture (Royal Botanic Garden Edinburgh)*. [Online]. [Accessed 24 September 2018]. Available from: http://rbg-web2.rbge.org.uk/DIADIST/index.htm?ww_intro.htm&main

Diatoms

Kelly, M. 2000. Identification of common benthic diatoms in rivers. *Field Studies*, **9**, pp. 583-700.

Krammer, K. and Lange-Bertalot, H. 2004. Bacillariophyceae: 4. Teil: Achnanthaceae, Kritische Ergänzungen zu Achnanthes s.l., Navicula s.str (2/4). In: Ettl, H., Gärtner, G., Heynig, H., Mollenhauer, D. (eds.). *Süβwasserflora von Mitteleuropa.* München: Elsevier.

Krammer, K. and Lange-Bertalot, H. 2007a. Bacillariophyceae: 1. Teil: Naviculaceae (2/1). In: H. Ettl, J. Gerloff, H. Heynig, D. Mollenhauer (eds.). *Süβwasserflora von Mitteleuropa*. München: Elsevier.

Krammer, K. and Lange-Bertalot, H. 2007b. Bacillariophyceae: 2. Teil: Bacillariaceae, Epithemiaceae, Surirellaceae (2/2). In: H. Ettl, J. Gerloff, H. Heynig, D. Mollenhauer (eds.). *Süβwasserflora von Mitteleuropa*. München: Elsevier.

Krammer, K. and Lange-Bertalot, H. 2008. Bacillariophyceae: 3. Teil: Centrales, Fragilariaceae, Eunotiaceae (2/3). In: H. Ettl, J. Gerloff, D. Mollenhauer (eds.). *Süβwasserflora von Mitteleuropa*. Heidelberg: Springer.

Lange-Bertalot, H. and Steindorf, A. 1996. Rote liste der limnischen kieselalgen (Bacillariophyceae) Deutschlands. *Schriftenreihe Fur Vegetationskunde*. **28**, pp. 633–677.

Lange-Bertalot, H., Hofmann, G., Werum, M. and Cantonati, M. 2017. *Freshwater Benthic Diatoms of Central Europe: Over 800 Common Species used in Ecological Assessment. English Edition with Updated Taxonomy and Added Species*. Oberreifenberg: Koeltz Botanical Books.

Spaulding, S. 2018. *Diatoms of the United States.* [Online]. [Accesssed 24 September 2018]. Available from: http://westerndiatoms.colorado.edu/

Fungi

Ingold, C. T. 1975. *Guide to Aquatic Hyphomycetes*. Cumbria, UK: Freshwater Biological Association.

Shearer, C. A. and Raja, H. A. 2010. *Freshwater Ascomycetes Database*. [Online]. [Accessed 24 September 2018]. Available from: http://fungi.life.illinois.edu/

Green algae

Gesierich, D and Rott, E. 2004. Benthic algae and mosses from aquatic habitats in the catchment of a glacial stream (Rotmoos, Ötztal, Austria). *Berichte des Naturwissenschaftlichen-Medizinischen Verein Innsbruck.* **91**(7), pp. 7-42.

Tree, plant and bryophyte material

Boris, N. R., Kürschner, W. M. and Krystyn, L. 2009. A detailed palynological study of the Triassic – Jurassic transition in key sections of the Eiberg Basin (Northern Calcareous Alps, Austria). *Review of Palaeobotany and Palynology.* **156**(3-4), pp. 376-400.

Demske, D., Tarasov, P. E. and Nakagawa, T. 2013. Atlas of pollen, spores and further non-pollen palynomorphs recorded in the glacial-interglacial late Quaternary sediments of Lake Suigetsu, central Japan. *Quaternary International.* **290-291**, pp. 165-238.

Rosi-Marshall, E. J., Wellard Kelly, H. A., Hall Jr., R. O. and Vallis, K. A. 2016. Methods for quantifying aquatic macroinvertebrate diets. *Freshwater Science*. **35**(1), pp. 229 – 236.

Schumilovskikh, L. S., Schlütz, F., Achterberg, I., Bauerochse, A. and Leuschne, H. H. 2015. Non-pollen palynomorphs from Mid-Holocene peat of the raised bog Borsteler Moor (Lower Saxony, Germany). *Studia Quaternaria.* **32**(1), pp. 5-18.

Personal communication

Identification advice was kindly provided by Steve Brooks (Chironomidae), Francois Edwards (macroinvertebrates) and Martyn Kelly (diatoms).

Appendix 3.2: Yield effort curves

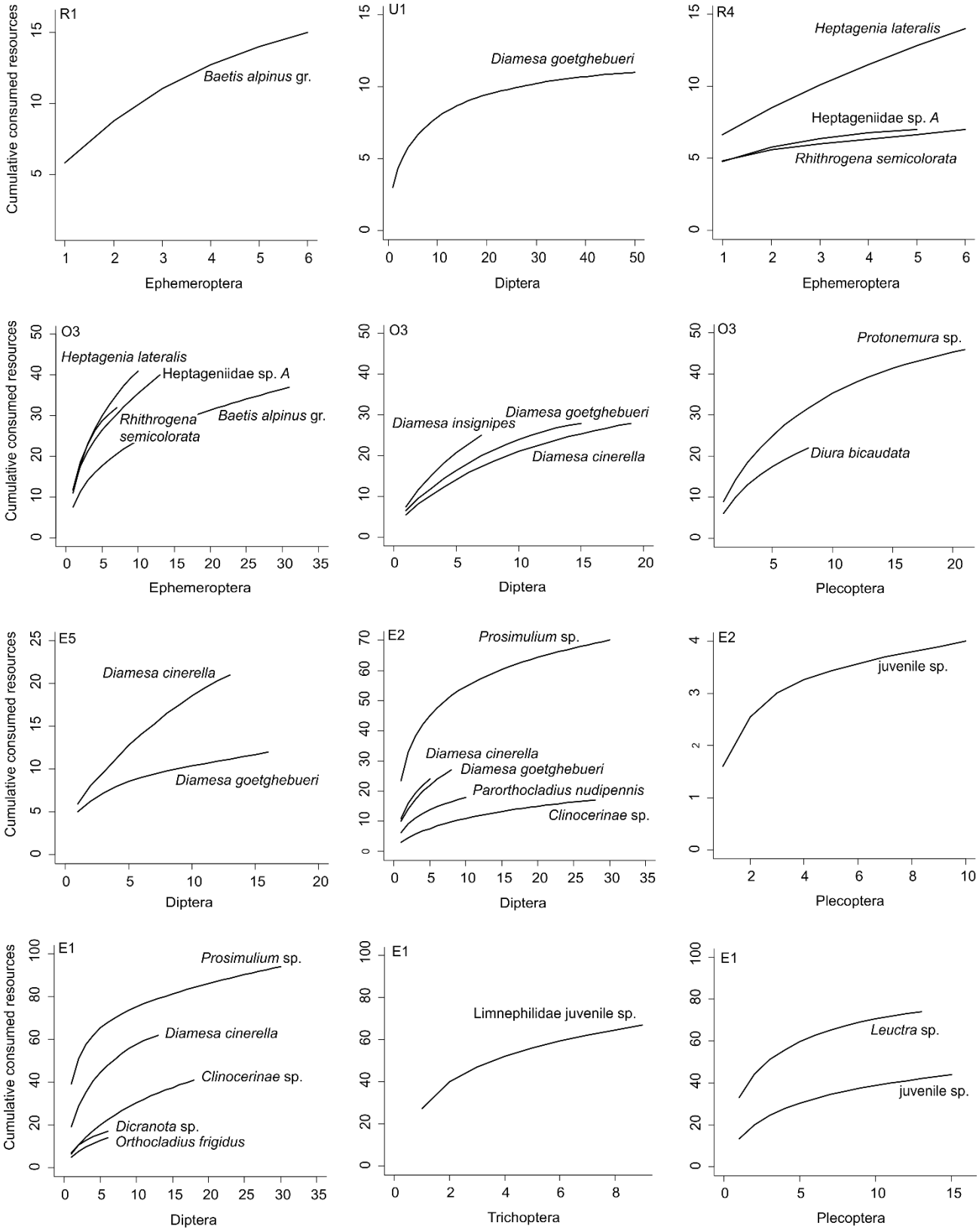

Figure A3.2 - continued

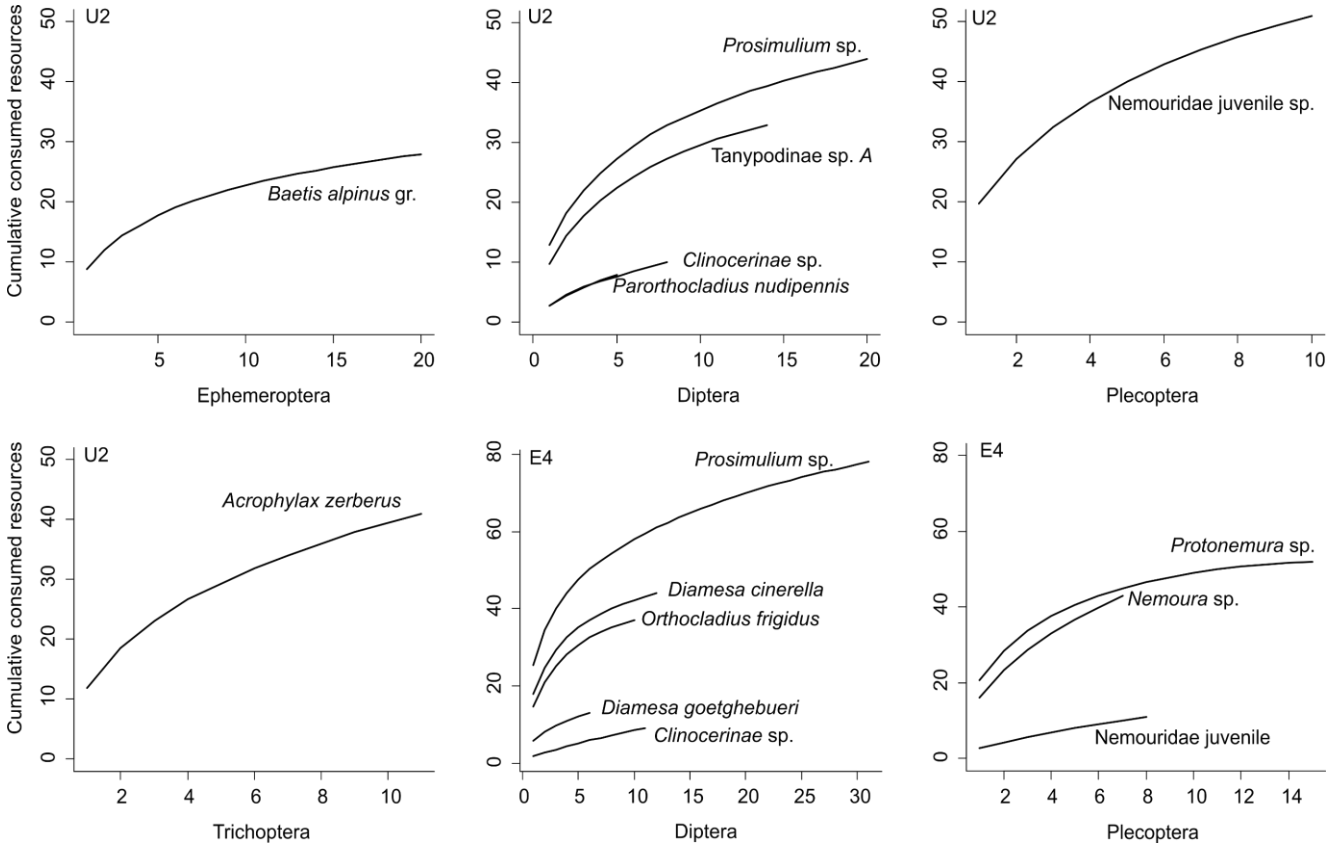

Figure A3.2 Species accumulation curves for all consumers represented by ≥ 5 individual gut contents at each of the nine alpine river sites. Some curves suggested that additional gut contents may have enhanced the characterisation of feeding linkages (Banašek-Richter et al., 2004). Sample size in some instances reflected the low abundance of macroinvertebrates in ice melt dominated river reaches. However, sample numbers were maximised by the analysis of bulk sampled individuals, removal of rare taxa (< 5 individuals) and gut contents analysis of a minimum of 20 individuals per species, where present. All available and suitable individuals were included in the analysis procedures for each river site.

Appendix 3.3: Estimations of biomass for aquatic macroinvertebrates and periphyton

Published predictive equations were used to estimate body length (mm) and biomass (mg) of both consumer and ingested macroinvertebrates across the nine food webs. For Chironomidae larvae, body length (*L*, mm) was estimated from head capsule width (*HCW*, mm) using:

$$L = -3.62 + 29.73\,HCW \quad (1)$$ (Smock, 1980, Table 5)

For all other macroinvertebrates, body length was measured to 0.01 mm using a calibrated optical micrometer eye piece at x 25 magnification. Linear body length equated to the distance between the head anterior and final abdominal segment posterior (Smock, 1980). Biomass (*W*, mg) was then determined for all consumer and ingested macroinvertebrates from body length (*L*, mm), with family, genera or species-specific regression constants (*a*, *b*).

$$\ln W = \ln a + b^{*} \ln L \quad (2)$$ (Smock, 1980, p.376)

Table A3.3.1 Taxa specific regression constants for Equation (2).

Taxa	ln *a*	ln *b*	Reference
Diptera	-5.221	2.43	Smock, 1980, Table 3
Chironomidae/ Orthocladiinae	-5.279	2.32	Smock, 1980, Table 2
Diamesa	-6.231	2.602	Nolte, 1990, Table 1
Micropsectra atrofasciata	-7.321	2.588	Nolte, 1990, Table 1
Orthocladius spp.	-6.228	2.264	Nolte, 1990, Table 1
Tanypodinae	-5.573	2.41	Smock, 1980, Table 2
Simuliidae	-5.339	2.55	Smock, 1980, Table 2
Ephemeroptera	-5.021	2.88	Smock, 1980, Table 3
Baetis spp.	-5.714	3.20	Smock, 1980, Table 2
Plecoptera	-6.075	3.39	Smock, 1980, Table 3
Trichoptera	-6.266	3.12	Smock, 1980, Table 3

Ingested periphyton (e.g., diatoms, desmids, algal cells, cyanobacteria) were assigned shape categories based upon their genus or species (CEN, 2015). A calibrated optical micrometer was used to measure their length (*h*), width (*w*) and depth (*d*) to the nearest 0.001 mm at x 1000 magnification, to inform standardised equations and correction factors to calculate cell biovolume (*V*, μm^3) (CEN, 2015). Predictive equations were used to estimate depth when this dimension was not visible microscopically (CEN, 2015). In their absence (*Achnanthes, Cymbopleura, Diatoma,*

Eucocconeis, Gomphonema, Meridion, Planothidium, Psammothidium, Reimeria, Stauroneis), depth was assumed to equal width for small freshwater algae (Sun and Lui, 2003).

Cylinder	$V = 1/4\ \pi\ d^2\ h$	
Cuboid	$V = d\ w\ h$	
Elliptic cylinder	$V = 1/4\ \pi\ d\ w\ h$	
Ellipsoid	$V = 1/6\ \pi\ d\ w\ h$	
Lanceolate cylinder	$V = 2/\pi\ d\ w\ h$	
Pyramid	$V = 1/3\ d\ w\ h$	
Rhomboid prism	$V = 1/2\ d\ w\ h$	
Sphere	$V = 1/6\ \pi\ d^3$	
Spheroid	$V = 1/6\ \pi\ w^2\ h$	
Tetrahedron	$V = 1/12\ \sqrt{3}\ w^2\ h$	(adapted from CEN, 2015, Annex A)

Shape categories and correction factors included:

Cylinder: *Cladophora glomerata,* filamentous algal spp., cyanobacteria, *Homeothrix, Spirulina*

Cuboid: *Pinnularia* spp. (correction factor: * 0.9), *Tabellaria flocculosa*

Elliptic cylinder: *Achnanthes* spp., *Achnanthidium minutissimum*, *Amphora pediculus* (correction factor: * 0.65), *Cymbella* spp., *Cymbopleura amphicephala* (correction factor: * 0.9), *Diatoma* spp., *Encyonema* spp. (correction factors: *neogracile*, *latens* type, *lange-bertalotii* = * 0.65, *minutum*, *silesacum*, *ventricosum* = * 0.8), *Eucocconeis laevis*, *Eunotia* spp. (correction factor: *1.03), *Fragilaria* spp., *Hannaea arcus* (correction factor: * 1.03), *Humidophila perpusilla*, *Navicula* spp., *Odontidium mesodon*, *Planothidium frequentissimum*, *Psammothidium helveticum*, *Reimeria sinuata*, *Stauroneis agrestis* (correction factor: * 0.9), *Staurosirella* spp.

Ellipsoid: Desmid *cosmarium* (half-cell basis).

Lanceolate cylinder: *Cymbella parva* (correction factor: * 0.8), *Adlafia minuscula*, *Nitzschia dissipata*, *N. fonticola* (correction factor: *1.15).

Pyramid*: Gomphoneis* spp. (correction factor: *0.9), *Gomphonema* spp. (correction factor: *0.9), *Meridion circulare* (correction factor: * 0.9).

Rhomboid prism: *Nitzschia palea* var. *debilis*, *N. gracilis*, *N. soratensis, N.* spp*.* (correction factors: *1.15)

Sphere: Individual algal cells

Spheroid: *Chlorella*

Tetrahedron: Desmid *staurodesmus*

Biovolume (V, μm^3) was converted to cell carbon content (C, pg C) using the regression constants (a, b) of Menden-Deuer and Lessard (2000), in their non-$\log_{10}$ transformed form.

(3) $C = a\ V^{b}$ (adapted from CEN, 2015, Table C.1)

Table A3.3.2 Regression constants for Equation (3), adapted from Menden-Deuer and Lessard (2000, Table 4).

Taxa	*a*	*b*
Diatoms	0.288	0.811
Diatoms > 3000 μm^3	0.117	0.881
Protist plankton	0.216	0.939
Protist plankton < 3000 μm^3	0.261	0.860

The carbon values (C, pg C) were then divided by 1,000,000,000 for conversion to biomass (W, mg). This approach may underestimate diatom biomass given that only carbon content is considered. However, representation of periphyton biomass as carbon biomass is widely adopted given the complexities of more accurate measurements (CEN, 2015).

Appendix 3.4: Study-specific macroinvertebrate body-size relationships

Regressions were determined between macroinvertebrate body length and dimensions of their individual body parts, for taxa identified in the Surber samples. If no relationship was evident at a specific site (*n*), measurements from across the nine sampling sites were collated (*n* = 9). Regression equations were then used to estimate the body length of macroinvertebrate prey from the size of individual body parts found fragmented in the gut contents of consumers. In turn, further regressions published in the literature were used to estimate their biomass (Appendix 3.3). Relationships were determined at the taxonomic resolution available for identified ingested body parts and for which a regression was evident. If head capsules were identified in the gut contents, their width was used to estimate body length and biomass (Appendix 3.3), with fragmented body parts assumed to have been originally attached to that individual. Regressions were only used to calculate the body length of individuals if body part abundance suggested presence of further prey (e.g., one Chironomid larvae head capsule but more than two mandibles present).

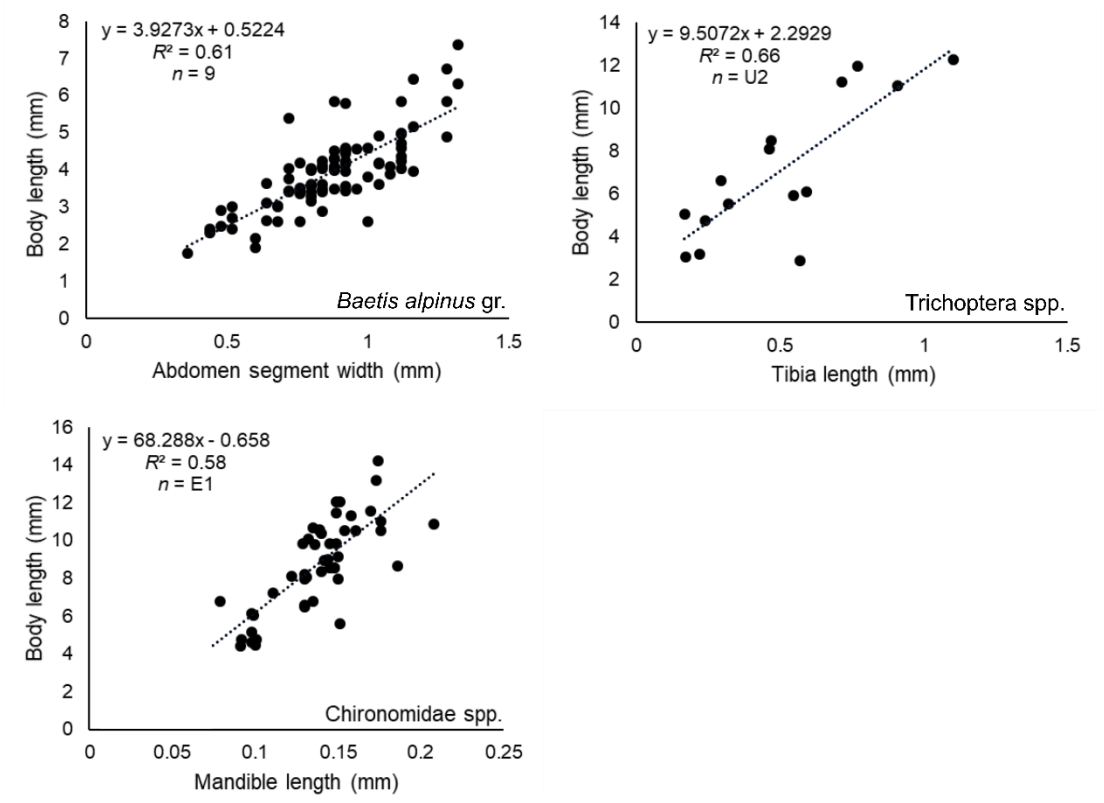

Figure A3.4 Significant study-specific relationships between aquatic macroinvertebrate body length and body part dimensions. Abdomen segment width refers to the widest abdominal segment available for measurement.

No regressions could be identified between body length and mentum width (Chironomidae, Simuliidae), first abdominal segment width (Plecoptera) and leg segment lengths (Baetidae, Plecoptera), at any or all sites. Insufficient availability of preserved antennae (Baetidae, Plecoptera, Tanypodinae) and tails (Baetidae) in the Surber samples prevented regression with these items identified in the gut. It was also not possible to identify correlation between body length and the length or width of macroinvertebrate claws, spines, gills and hairs. All measurements were made using a calibrated eye piece graticule at x 25 to x 1000 magnification.

Table A3.5 Taxa sampled from rivers in the Austrian Alps. Brackets in the class and family columns note sub-class and sub-family classifications. Node = the species included in the nine alpine river food webs and corresponds to Figure A3.7. While identification of diatom taxa within the biofilm samples noted individuals comprising the *Achnanthidium minutissimum* species complex, this level of separation was not possible for partially digested valves, which were classified together as *Achnanthidium minutissimum*.

Phylum	Class	Order	Family	Genus	Species	Classification	Node
Amoebozoa	Myxomycetes				(capillitium)		91
Amoebozoa	Tubulinea	Arcellinida	Arcellidae	*Arcella*	spp.		14
Amoebozoa	Tubulinea	Arcellinida	Centropyxidae	*Centropyxis*	*aerophila*	Deflandre 1929	9
Amoebozoa	Tubulinea	Arcellinida	Centropyxidae	*Centropyxis*	*pontigulasiformis*	Beyens, Chardez & De Bock, 1986	145
Amoebozoa	Tubulinea	Arcellinida	Hyalospheniidae	*Hyalosphenia*	*subflava*	Cash & Hopkinson 1909	121
Amoebozoa	Tubulinea	Arcellinida	Lesquereusiidae	*Quadrulella*	*cf. longicollis*		
Amoebozoa	Tubulinea	Arcellinida	Paraquadrulidae	*Paraquadrula*	*irregularis type*	Wallich, 1863	103
Amoebozoa	Tubulinea	Arcellinida	Nebelidae	*Nebela*	sp.		136
Arthropoda	Arachnida (Acari)	Trombidiformes	Hydrachnoidea		sp. A		
Arthropoda	Arachnida (Acari)	Trombidiformes	Hydrachnoidea		sp. B		
Arthropoda	Entognatha (Collembola)						
Arthropoda	Insecta	Coleoptera			sp. A		
Arthropoda	Insecta	Coleoptera			sp. B		
Arthropoda	Insecta	Diptera	Blephariceridae				
Arthropoda	Insecta	Diptera	Ceratopogonidae				
Arthropoda	Insecta	Diptera	Chironomidae		sp.		8
Arthropoda	Insecta	Diptera	Chironomidae (Chironominae)	*Micropsectra*	*atrofasciata*	Kieffer 1911	
Arthropoda	Insecta	Diptera	Chironomidae (Diamesinae)	*Diamesa*	spp.		123
Arthropoda	Insecta	Diptera	Chironomidae (Diamesinae)	*Diamesa*	*bertrami*	Edwards 1935	
Arthropoda	Insecta	Diptera	Chironomidae (Diamesinae)	*Diamesa*	*cinerella*	(Meigen) Gisti 1835	2
Arthropoda	Insecta	Diptera	Chironomidae (Diamesinae)	*Diamesa*	*goetghebueri*	Pagast 1947	3
Arthropoda	Insecta	Diptera	Chironomidae (Diamesinae)	*Diamesa*	*insignipes*	(Kieffer) Kieffer & Thienemann 1908	146
Arthropoda	Insecta	Diptera	Chironomidae (Orthocladiinae)		spp.		15
Arthropoda	Insecta	Diptera	Chironomidae (Orthocladiinae)	*Brilla*	*bifida*	Kieffer 1909	
Arthropoda	Insecta	Diptera	Chironomidae (Orthocladiinae)	*Chaetocladius*	*piger gr.*	Goetghebuer 1913	
Arthropoda	Insecta	Diptera	Chironomidae (Orthocladiinae)	*Cricotopus*	*vierriensis*	Goetghebuer 1935	
Arthropoda	Insecta	Diptera	Chironomidae (Orthocladiinae)	*Orthocladius*	*rivicola*	Kieffer 1911	
Arthropoda	Insecta	Diptera	Chironomidae (Orthocladiinae)	*Orthocladius*	*frigidus*	Zetterstedt 1838	1
Arthropoda	Insecta	Diptera	Chironomidae (Orthocladiinae)	*Parorthocladius*	*nudipennis*	Kieffer 1908	101
Arthropoda	Insecta	Diptera	Chironomidae (Orthocladiinae)	*Parorthocladius*	sp.		
Arthropoda	Insecta	Diptera	Chironomidae (Tanyipodinae)		sp. A		102
Arthropoda	Insecta	Diptera	Chironomidae (Tanyipodinae)		sp. B		
Arthropoda	Insecta	Diptera	Chironomidae (Tanyipodinae)	*Tanytarsini*	sp.		
Arthropoda	Insecta	Diptera	Empididae	*Clinocerinae*			11

Table A3.5 - continued

Phylum	Class	Order	Family	Genus	Species	Classification	Node
Arthropoda	Insecta	Diptera	Limoniidae	*Cheilotrichia*			
Arthropoda	Insecta	Diptera	Limoniidae	*Rhypholophus*			
Arthropoda	Insecta	Diptera	Pediciidae	*Dicranota*			122
Arthropoda	Insecta	Diptera	Psychodidae				
Arthropoda	Insecta	Diptera	Simuliidae	*Prosimulium*			5
Arthropoda	Insecta	Diptera	Thaumaleidae	*Thaumalea*			
Arthropoda	Insecta	Ephemeroptera	Baetidae	*Baetis*	*alpinus gr.*		103
Arthropoda	Insecta	Ephemeroptera	Heptageniidae		sp. A		141
Arthropoda	Insecta	Ephemeroptera	Heptageniidae	*Ecdyonurus*	*venous*	Fabricius 1775	
Arthropoda	Insecta	Ephemeroptera	Heptageniidae	*Heptagenia*			
Arthropoda	Insecta	Ephemeroptera	Heptageniidae	*Heptagenia*	*lateralis*	Curtis 1834	143
Arthropoda	Insecta	Ephemeroptera	Heptageniidae	*Rhithrogena*	*semicolorata*	Curtis 1834	142
Arthropoda	Insecta	Plecoptera	Capniidae	*Capnia*	juvenile		
Arthropoda	Insecta	Plecoptera	Chloroperlida	*Chloroperla*			
Arthropoda	Insecta	Plecoptera	Leuctridae		sp. A		
Arthropoda	Insecta	Plecoptera	Leuctridae		sp. B		
Arthropoda	Insecta	Plecoptera	Leuctridae		sp. C		
Arthropoda	Insecta	Plecoptera	Leuctridae		juvenile		
Arthropoda	Insecta	Plecoptera	Leuctridae	*Lecutra*	sp.		116
Arthropoda	Insecta	Plecoptera	Leuctridae	*Lecutra*	*leuctra*		
Arthropoda	Insecta	Plecoptera	Leuctridae	*Lecutra*	*sinuata*		
Arthropoda	Insecta	Plecoptera	Nemouridae		juvenile		7
Arthropoda	Insecta	Plecoptera	Nemouridae	*Amphinemura*			
Arthropoda	Insecta	Plecoptera	Nemouridae	*Nemoura*			6
Arthropoda	Insecta	Plecoptera	Nemouridae	*Nemurella*	*pictetii*	Klapálek 1900	
Arthropoda	Insecta	Plecoptera	Nemouridae	*Protonemura*			4
Arthropoda	Insecta	Plecoptera	Nemouridae	*Protonemura*	*austriaca*	Theischinger 1976	
Arthropoda	Insecta	Plecoptera	Nemouridae	*Protonemura*	*meyeri*	Pictet 1841	
Arthropoda	Insecta	Plecoptera			sp.		
Arthropoda	Insecta	Plecoptera			juvenile		118
Arthropoda	Insecta	Plecoptera	Perlodidae		sp.		
Arthropoda	Insecta	Plecoptera	Perlodidae		juvenile		
Arthropoda	Insecta	Plecoptera	Perlodidae	*Diura*	*bicaudata*	Linnaeus 1758	147
Arthropoda	Insecta	Plecoptera	Perlodidae	*Isoperla*			

Table A3.5 - continued

Phylum	Class	Order	Family	Genus	Species	Classification	Node
Arthropoda	Insecta	Trichoptera	Limnephilidae		sp. A		
Arthropoda	Insecta	Trichoptera	Limnephilidae		sp. B		
Arthropoda	Insecta	Trichoptera	Limnephilidae		sp. C		
Arthropoda	Insecta	Trichoptera	Limnephilidae		juvenile		117
Arthropoda	Insecta	Trichoptera	Limnephilidae	*Acrophylax*	*zerberus*	Brauer 1867	104
Arthropoda	Insecta	Trichoptera	Limnephilidae	*Consorophylax*			
Ascomycota	Sordariomycetes	Pyrenomycetes	Annulatascaceae	*Ascitendus*	*austriacus*	(Réblová, Winka & Jaklitsch) Campbell & Shearer	
Bacillariophyta	Bacillariophyceae	Achnanthales	Achnanthaceae	*Achnanthes*	sp. A		83
Bacillariophyta	Bacillariophyceae	Achnanthales	Achnanthaceae	*Achnanthes*	sp. B		128
Bacillariophyta	Bacillariophyceae	Bacillariales	Bacillariaceae	*Denticula*	*tenuis*	Kützing 1844	134
Bacillariophyta	Bacillariophyceae	Bacillariales	Bacillariaceae	*Nitzschia*	sp. A		84
Bacillariophyta	Bacillariophyceae	Bacillariales	Bacillariaceae	*Nitzschia*	*dissipata*	(Kützing) Grunow 1860	94
Bacillariophyta	Bacillariophyceae	Bacillariales	Bacillariaceae	*Nitzschia*	*elegantula*	(Grunow) van Heurck 1881	
Bacillariophyta	Bacillariophyceae	Bacillariales	Bacillariaceae	*Nitzschia*	*fonticola*	(Grunow) van Heurck 1881	63
Bacillariophyta	Bacillariophyceae	Bacillariales	Bacillariaceae	*Nitzschia*	*gracilis*	Hantzsch 1860	
Bacillariophyta	Bacillariophyceae	Bacillariales	Bacillariaceae	*Nitzschia*	*inconspicua*	Grunow 1862	
Bacillariophyta	Bacillariophyceae	Bacillariales	Bacillariaceae	*Nitzschia*	*palea var. debilis*	(Kützing) Grunow 1880	93
Bacillariophyta	Bacillariophyceae	Bacillariales	Bacillariaceae	*Nitzschia*	*soratensis*	Morales & Vis 2007	99
Bacillariophyta	Bacillariophyceae	Cocconeidales	Achnanthidiaceae	*Achnanthidium*	*caledonicum*	(Lange-Bertalot) Lange-Bertalot 1999	
Bacillariophyta	Bacillariophyceae	Cocconeidales	Achnanthidiaceae	*Achnanthidium*	*lineare*	Smith 1855	
Bacillariophyta	Bacillariophyceae	Cocconeidales	Achnanthidiaceae	*Achnanthidium*	*linearis f. curta*	Smith ex Boyer 1916	
Bacillariophyta	Bacillariophyceae	Cocconeidales	Achnanthidiaceae	*Achnanthidium*	*microcephalum*	Kützing 1844	
Bacillariophyta	Bacillariophyceae	Cocconeidales	Achnanthidiaceae	*Achnanthidium*	*minutissimum*	(Kützing) Czarnecki 1994	33
Bacillariophyta	Bacillariophyceae	Cocconeidales	Achnanthidiaceae	*Achnanthidium*	*minutissimum var. cryptophala*	Grunow 1880	
Bacillariophyta	Bacillariophyceae	Cocconeidales	Achnanthidiaceae	*Achnanthidium*	*trinode*	(Arnott ex Ralfs) Pritchard 1861	
Bacillariophyta	Bacillariophyceae	Cocconeidales	Achnanthidiaceae	*Eucocconeis*	*cf. laevis*		138
Bacillariophyta	Bacillariophyceae	Cocconeidales	Achnanthidiaceae	*Eucocconeis*	*laevis*	(Østrup) Lange-Bertalot 1999	52
Bacillariophyta	Bacillariophyceae	Cocconeidales	Achnanthidiaceae	*Planothidium*	*frequentissimum*	Lange-Bertalot 1999	45
Bacillariophyta	Bacillariophyceae	Cocconeidales	Achnanthidiaceae	*Psammothidium*	*helveticum*	(Hustedt) Bukhtiyarova & Round 1996	32
Bacillariophyta	Bacillariophyceae	Cocconeidales	Achnanthidiaceae	*Rossithidium*	*petersenii*	(Hustedt) Round & Bukhtiyarova 1996	
Bacillariophyta	Bacillariophyceae	Cocconeidales	Cocconeidaceae	*Cocconeis*	*euglypta*	Ehrenberg 1854	
Bacillariophyta	Bacillariophyceae	Cymbellales	Anomoeoneidaceae	*Adlafia*	*minuscula*	(Grunow) Lange-Bertalot 1999	46
Bacillariophyta	Bacillariophyceae	Cymbellales	Anomoeoneidaceae	*Adlafia*	*suchlandtii*	(Hustedt) Lange-Bertalot 1998	

Table A3.5 - continued

Phylum	Class	Order	Family	Genus	Species	Classification	Node
Bacillariophyta	Bacillariophyceae	Cymbellales	Cymbellaceae	*Cymbella*	sp. A		88
Bacillariophyta	Bacillariophyceae	Cymbellales	Cymbellaceae	*Cymbella*	sp. B		127
Bacillariophyta	Bacillariophyceae	Cymbellales	Cymbellaceae	*Cymbella*	*excisa*	Kützing 1844	
Bacillariophyta	Bacillariophyceae	Cymbellales	Cymbellaceae	*Cymbella*	*helvetica*	Kützing 1844	
Bacillariophyta	Bacillariophyceae	Cymbellales	Cymbellaceae	*Cymbella*	*parva*	(Smith) Kirchner in Cohn 1878	96
Bacillariophyta	Bacillariophyceae	Cymbellales	Cymbellaceae	*Cymbopleura*	*amphicephala*	(Naegeli) Krammer 2003	59
Bacillariophyta	Bacillariophyceae	Cymbellales	Gomphonemataceae	*Encyonema*	sp.		92
Bacillariophyta	Bacillariophyceae	Cymbellales	Gomphonemataceae	*Encyonema*	*hebridicum*	Grunow ex Cleve 1891	
Bacillariophyta	Bacillariophyceae	Cymbellales	Gomphonemataceae	*Encyonema*	*lange-bertalotii*	Krammer 1997	65
Bacillariophyta	Bacillariophyceae	Cymbellales	Gomphonemataceae	*Encyonema*	*latens*	(Krasske) Mann 1990	48
Bacillariophyta	Bacillariophyceae	Cymbellales	Gomphonemataceae	*Encyonema*	*minutum*	(Hilse) Mann 1990	36
Bacillariophyta	Bacillariophyceae	Cymbellales	Gomphonemataceae	*Encyonema*	*neogracile*	Krammer 1997	29
Bacillariophyta	Bacillariophyceae	Cymbellales	Gomphonemataceae	*Encyonema*	*reichardtii*	(Krammer) Mann 1990	
Bacillariophyta	Bacillariophyceae	Cymbellales	Gomphonemataceae	*Encyonema*	*silesiacum*	(Bleisch) Mann 1990	58
Bacillariophyta	Bacillariophyceae	Cymbellales	Gomphonemataceae	*Encyonema*	*ventricosum*	Grunow 1875	109
Bacillariophyta	Bacillariophyceae	Cymbellales	Gomphonemataceae	*Gomphoneis*	*quadripunctata*	(Østrup) Dawson ex Ross & Sims 1978	150
Bacillariophyta	Bacillariophyceae	Cymbellales	Gomphonemataceae	*Gomphonema*	sp. A		56
Bacillariophyta	Bacillariophyceae	Cymbellales	Gomphonemataceae	*Gomphonema*	sp. A type		87
Bacillariophyta	Bacillariophyceae	Cymbellales	Gomphonemataceae	*Gomphonema*	sp. B		60
Bacillariophyta	Bacillariophyceae	Cymbellales	Gomphonemataceae	*Gomphonema*	sp. C		105
Bacillariophyta	Bacillariophyceae	Cymbellales	Gomphonemataceae	*Gomphonema*	sp. D		114
Bacillariophyta	Bacillariophyceae	Cymbellales	Gomphonemataceae	*Gomphonema*	*angustatum*	(Kützing) Rabenhorst 1864	
Bacillariophyta	Bacillariophyceae	Cymbellales	Gomphonemataceae	*Gomphonema*	*aquemineralis*	Lange-Bertalot & Reichardt	40
Bacillariophyta	Bacillariophyceae	Cymbellales	Gomphonemataceae	*Gomphonema*	*calcareum*	Cleve 1868	47
Bacillariophyta	Bacillariophyceae	Cymbellales	Gomphonemataceae	*Gomphonema*	*exilissimum*	(Grunow) Lange-Beratlot & Reichardt 1996	43
Bacillariophyta	Bacillariophyceae	Cymbellales	Gomphonemataceae	*Gomphonema*	*gracile*	Ehrenberg 1838	67
Bacillariophyta	Bacillariophyceae	Cymbellales	Gomphonemataceae	*Gomphonema*	*lagenula*	(Kützing) 1844	
Bacillariophyta	Bacillariophyceae	Cymbellales	Gomphonemataceae	*Gomphonema*	*micropus*	Kützing 1844	49
Bacillariophyta	Bacillariophyceae	Cymbellales	Gomphonemataceae	*Gomphonema*	*olivaceum type*	(Hornemann) Brébisson 1838	149
Bacillariophyta	Bacillariophyceae	Cymbellales	Gomphonemataceae	*Gomphonema*	*parvulum*	(Kützing) Kützing 1849	55
Bacillariophyta	Bacillariophyceae	Cymbellales	Gomphonemataceae	*Gomphonema*	*(parvulum species complex) A*		42
Bacillariophyta	Bacillariophyceae	Cymbellales	Gomphonemataceae	*Gomphonema*	*(parvulum species complex) B*		41
Bacillariophyta	Bacillariophyceae	Cymbellales	Gomphonemataceae	*Gomphonema*	*(parvulum species complex) C*		137
Bacillariophyta	Bacillariophyceae	Cymbellales	Gomphonemataceae	*Gomphonema*	*(parvulum species complex) D*		132

Table A3.5 - continued

Phylum	Class	Order	Family	Genus	Species	Classification	Node
Bacillariophyta	Bacillariophyceae	Cymbellales	Gomphonemataceae	*Gomphonema*	*parvulum var. parvulum*	Grunow 1880	
Bacillariophyta	Bacillariophyceae	Cymbellales	Gomphonemataceae	*Reimeria*	*sinuata*	(Gregory) Kociolek & Stoermer 1987	34
Bacillariophyta	Bacillariophyceae	Cymbellales	Gomphonemataceae	*Reimeria*	*sinuata f. antiqua*	(Grunow) Kociolek & Stoermer 1987	
Bacillariophyta	Bacillariophyceae	Eunotiales	Eunotiaceae	*Eunotia*	sp. A		86
Bacillariophyta	Bacillariophyceae	Eunotiales	Eunotiaceae	*Eunotia*	sp. B		107
Bacillariophyta	Bacillariophyceae	Eunotiales	Eunotiaceae	*Eunotia*	*bilunaris*	(Ehrenberg) Mills 1934	106
Bacillariophyta	Bacillariophyceae	Eunotiales	Eunotiaceae	*Eunotia*	*boreoalpina*	Lange-Bertalot & Nörpel-Schempp 1998	
Bacillariophyta	Bacillariophyceae	Eunotiales	Eunotiaceae	*Eunotia*	*diodon*	Ehrenberg 1837	
Bacillariophyta	Bacillariophyceae	Eunotiales	Eunotiaceae	*Eunotia*	*exigua*	(Brébisson ex Kützing) Rabenhorst 1864	108
Bacillariophyta	Bacillariophyceae	Eunotiales	Eunotiaceae	*Eunotia*	*incisa*	Smith ex Gregory 1854	64
Bacillariophyta	Bacillariophyceae	Eunotiales	Eunotiaceae	*Eunotia*	*mucophila*	(Lange-Bertalot et al.) Lange-Bertalot 2007	
Bacillariophyta	Bacillariophyceae	Eunotiales	Eunotiaceae	*Eunotia*	*subarcuatoides*	Alles, Norpel, Lange-Bertalot 1991	
Bacillariophyta	Bacillariophyceae	Eunotiales	Eunotiaceae	*Eunotia*	*trinacria*	Krasske 1929	
Bacillariophyta	Bacillariophyceae	Fragilariales	Fragilariaceae	*Fragilaria*	sp. A		37
Bacillariophyta	Bacillariophyceae	Fragilariales	Fragilariaceae	*Fragilaria*	sp. B		81
Bacillariophyta	Bacillariophyceae	Fragilariales	Fragilariaceae	*Fragilaria*	sp. B type		90
Bacillariophyta	Bacillariophyceae	Fragilariales	Fragilariaceae	*Fragilaria*	sp. C		
Bacillariophyta	Bacillariophyceae	Fragilariales	Fragilariaceae	*Fragilaria*	*capucina*	Desmazières 1830	140
Bacillariophyta	Bacillariophyceae	Fragilariales	Fragilariaceae	*Fragilaria*	*constricta*	Ehrenberg 1843	
Bacillariophyta	Bacillariophyceae	Fragilariales	Fragilariaceae	*Fragilaria*	*construens*	(Ehrenberg) Grunow 1862	
Bacillariophyta	Bacillariophyceae	Fragilariales	Fragilariaceae	*Fragilaria*	*cf. gracilis*	(Østrup) Huestedt 1950	35
Bacillariophyta	Bacillariophyceae	Fragilariales	Fragilariaceae	*Fragilaria*	*gracilis*	Østrup 1910	54
Bacillariophyta	Bacillariophyceae	Fragilariales	Fragilariaceae	*Fragilaria*	*radians*	(Kützing) Williams & Round 1987	
Bacillariophyta	Bacillariophyceae	Fragilariales	Fragilariaceae	*Odontidium*	*hyemale*	(Roth) Kützing 1844	44
Bacillariophyta	Bacillariophyceae	Fragilariales	Fragilariaceae	*Odontidium*	*mesodon*	(Ehernberg) Kützing 1844	31
Bacillariophyta	Bacillariophyceae	Fragilariales	Staurosiraceae	*Staurosirella*	sp.		51
Bacillariophyta	Bacillariophyceae	Fragilariales	Staurosiraceae	*Staurosirella*	*lapponica*	(Grunow) Williams & Round 1987	
Bacillariophyta	Bacillariophyceae	Fragilariales	Staurosiraceae	*Staurosirella*	*pinnata*	(Ehrenberg) Williams & Round 1988	30
Bacillariophyta	Bacillariophyceae	Licmophorales	Ulnariaceae	*Hannaea*	*arcus*	(Ehrenberg) Patrick 1961	39
Bacillariophyta	Bacillariophyceae	Naviculales	Amphipleuraceae	*Frustulia*	*rhomboides*	(Ehrenberg) De Toni 1891	
Bacillariophyta	Bacillariophyceae	Naviculales	Diadesmidaceae	*Humidophila*	*perpusilla*	(Grunow) Lowe et al. 2014	53
Bacillariophyta	Bacillariophyceae	Naviculales	Naviculaceae	*Caloneis*	*bacillum*	Cleve 1894	
Bacillariophyta	Bacillariophyceae	Naviculales	Naviculaceae	*Navicula*	sp. A		57
Bacillariophyta	Bacillariophyceae	Naviculales	Naviculaceae	*Navicula*	sp. B		50

Table A3.5 - continued

Phylum	Class	Order	Family	Genus	Species	Classification	Node
Bacillariophyta	Bacillariophyceae	Naviculales	Naviculaceae	*Navicula*	sp.C		68
Bacillariophyta	Bacillariophyceae	Naviculales	Naviculaceae	*Navicula*	sp. D		126
Bacillariophyta	Bacillariophyceae	Naviculales	Naviculaceae	*Navicula*	sp. E		115
Bacillariophyta	Bacillariophyceae	Naviculales	Naviculaceae	*Navicula*	*cryptocephala*	Kützing 1844	
Bacillariophyta	Bacillariophyceae	Naviculales	Naviculaceae	*Navicula*	*cryptotenella*	Lange-Bertalot 1985	
Bacillariophyta	Bacillariophyceae	Naviculales	Naviculaceae	*Navicula*	*detenta*	Hustedt 1943	
Bacillariophyta	Bacillariophyceae	Naviculales	Naviculaceae	*Navicula*	*radiosa*	Kützing 1844	
Bacillariophyta	Bacillariophyceae	Naviculales	Naviculales incertae sedis	*Chamaepinnularia*	*mediocris*	(Krasske) Lange-Bertalot, Metzeltin 1996	
Bacillariophyta	Bacillariophyceae	Naviculales	Pinnulariaceae	*Pinnularia*	sp. A		61
Bacillariophyta	Bacillariophyceae	Naviculales	Pinnulariaceae	*Pinnularia*	sp. B		62
Bacillariophyta	Bacillariophyceae	Naviculales	Pinnulariaceae	*Pinnularia*	sp. C		
Bacillariophyta	Bacillariophyceae	Naviculales	Pinnulariaceae	*Pinnularia*	sp. D		129
Bacillariophyta	Bacillariophyceae	Naviculales	Pinnulariaceae	*Pinnularia*	sp. E		133
Bacillariophyta	Bacillariophyceae	Naviculales	Stauroneidaceae	*Stauroneis*	*agrestis*	Petersen 1915	89
Bacillariophyta	Bacillariophyceae	Tabellariales	Tabellariaceae	*Diatoma*	sp. A		100
Bacillariophyta	Bacillariophyceae	Tabellariales	Tabellariaceae	*Diatoma*	sp. B		85
Bacillariophyta	Bacillariophyceae	Tabellariales	Tabellariaceae	*Diatoma*	*vulgaris*	Bory 1824	
Bacillariophyta	Bacillariophyceae	Tabellariales	Tabellariaceae	*Meridion*	*circulare*	(Greville) Agardh 1831	38
Bacillariophyta	Bacillariophyceae	Tabellariales	Tabellariaceae	*Tabellaria*	*flocculosa*	(Roth) Kützing 1844	125
Bacillariophyta	Bacillariophyceae	Tabellariales	Tabellariaceae	*Tetracyclus*	*rupestris*	(Braun ex Rabenhorst) Grunow 1885	
Bacillariophyta	Bacillariophyceae	Thalassiophysales	Catenulaceae	*Amphora*	*pediculus*	(Kützing) Grunow ex Schmidt 1875	66
Charophyta	Trebouxiophyceae	Chlorellales	Chlorellaceae	*Chlorella*			124
Chlorophyta	Ulvophyceae	Cladophorales	Cladophoraceae	*Cladophora*			
Chlorophyta	Ulvophyceae	Cladophorales	Cladophoraceae	*Cladophora*	*glomerata*	(Linnaeus) Kützing 1843	28
Charophyta	Zygnematophyceae	Desmidiales	Desmidiaceae	*Cosmarium*	spp.		69
Charophyta	Zygnematophyceae	Desmidiales	Desmidiaceae	*Staurodesmus*	spp.		110
Charophyta	Zygnematophyceae	Zygnematales	Zygnemataceae	*Spirogyra*			24
Ciliophora					sp.		148
Coniferophyta	Pinopsida	Pinales	Cupressaceae	*Juniperus*	(pollen)		130
Coniferophyta	Pinopsida	Pinales	Pinaceae	*Abies*	(pollen)		77
Coniferophyta	Pinopsida	Pinales	Pinaceae	*Pinus*	(pollen)		
Cyanobacteria					sp. A (filamentous)		80
Cyanobacteria					sp. B		139
Cyanobacteria	Cyanophyceae	Oscillatoriales	Homoeotrichaceae	*Homoeothrix*			

Table A3.5 - continued

Phylum	Class	Order	Family	Genus	Species	Classification	Node
Cyanobacteria	Cyanophyceae	Spirulinales	Spirulinaceae	*Spirulina*			25
Dinoflagellata					sp. A (cyst)		
Dinoflagellata					sp. B (cyst)		119
Dinoflagellata					sp. C (cyst)		120
Dinoflagellata					sp. D (cyst)		12
Nematoda					sp.		10
Ochrophyta	Chrysophyceae				sp. A		27
Ochrophyta	Chrysophyceae	Hydrurales	Hydruraceae	*Hydrurus*	*foetidus*	(Villars) Trevisan 1848	23
Platyhelminthes	Rhabditophora	Tricladida	Planariidae		sp.		
Rotifera	Monogononta	Plioma	Bachionidae	*Keratella*	*hiemalis*	Carlin 1943	13
Tardigrada					sp.		
Tracheophyta	Magnoliopsida	Ericales	Ericaceae	*Calluna*	(pollen)		112
Tracheophyta	Magnoliopsida	Fagales	Fagaceae	*Quercus*	(pollen)		79
Tracheophyta	Magnoliopsida	Malpighiales	Salicaceae	*Salix*	(pollen)		78
Unidentified materials							
Amorhpous detritus							16
Aquatic fungi type 1							72
Black carbon							
Bryophyte leaf cells							17
Filamentous algal spp.							26
Foraminiferal test lining							
Fungal ascospore type 3							135
Fungal ascospore type 4							98
Fungal spore A							73
Fungal spore B							74
Fungal spore C							75
Fungal spore D							76
Fungal spore E							95
Fungal hyphae type 1							70
Fungal hyphae type 2							97
Fungal hyphae type 3							151
Grass pollen							111
Green brown algal cells							144
Leaf detritus							20
Microalgae sp. A							21
Microalgae sp. B							22
Moss spore type 1							18
Moss spore type 2							19
Rock fragments							
Unidentified diatom spp.							
Unidentified pollen sp. A							113
Unidentified pollen sp. B							131

Appendix 3.6: Richness and abundance of river macroinvertebrates and diatom valves

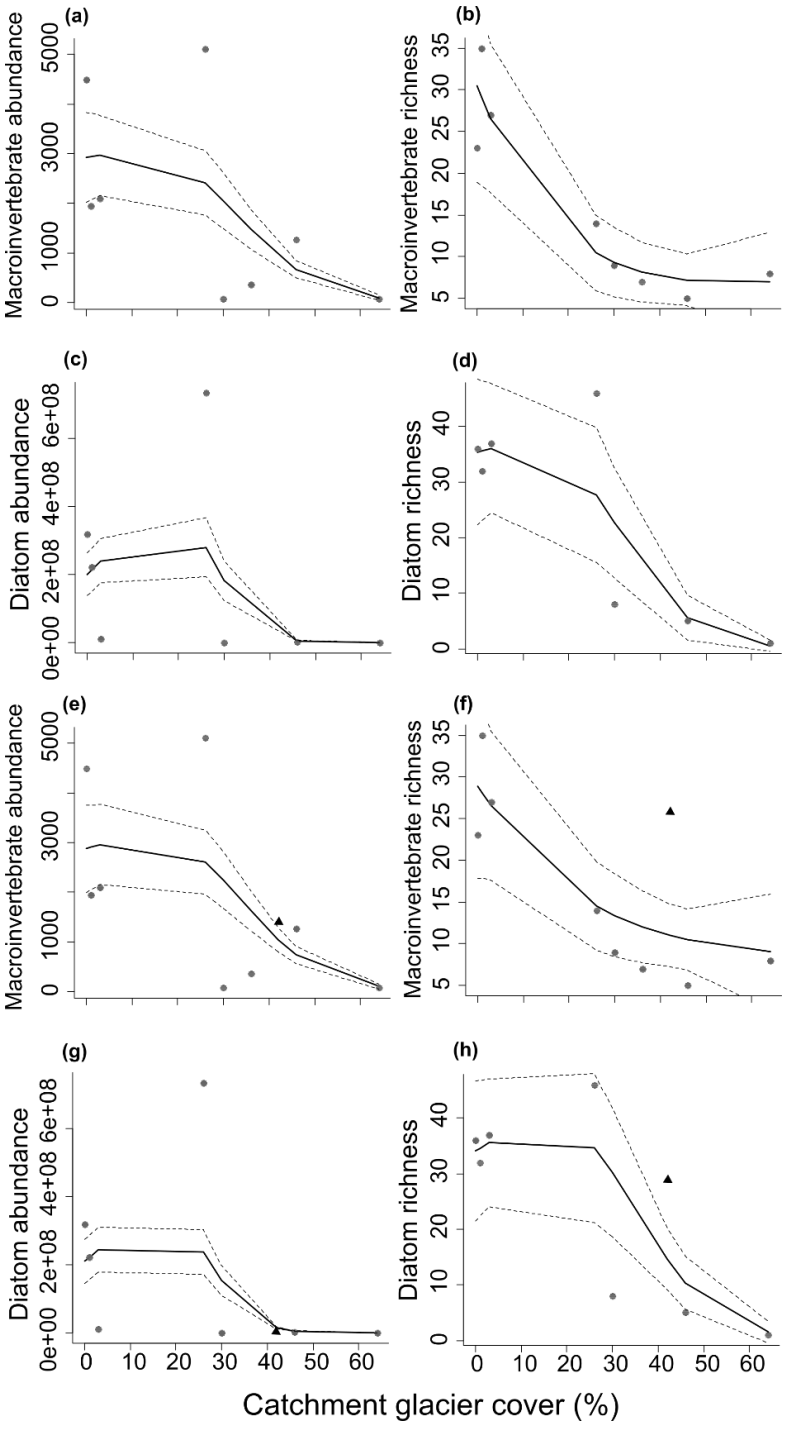

Figure A3.6 Significant relationships between taxonomic richness and abundance (m^{-2}) of macroinvertebrate and diatom valves for alpine rivers both excluding (a to d) and including (e to h) site O3 (black triangle), which was influenced by proglacial lake inputs. For diatom metrics, *n* = 8 as biofilm information was unavailable for site E5.

Table A3.6 GAM statistics relating to the relationships illustrated in Figure A3.6.

Dependent variable	Model (Distribution)	χ^2/ *F*	*p*-value	Deviance explained (%)
Figure A3.6 (a to d)				
Macroinvertebrate				
Density	GAM (Negative binomial)	129.60	< 0.001 ***	42.0
Taxonomic richness	GAM (Negative binomial)	21.78	< 0.001 ***	90.2
Diatom				
Density	GAM (Negative binomial)	1257	< 0.001 ***	56.2
Taxonomic richness	GAM (Negative binomial)	20.80	< 0.001 ***	80.7
Figure A3.6 (e to h)				
Macroinvertebrate				
Density	GAM (Negative binomial)	128.7	< 0.001 ***	41.3
Taxonomic richness	GAM (Negative binomial)	13.41	0.001 **	51.6
Diatom				
Density	GAM (Negative binomial)	1279	< 0.001 ***	58.9
Taxonomic richness	GAM (Negative binomial)	22.53	< 0.001 ***	63.8

Appendix 3.7: Food web nodes

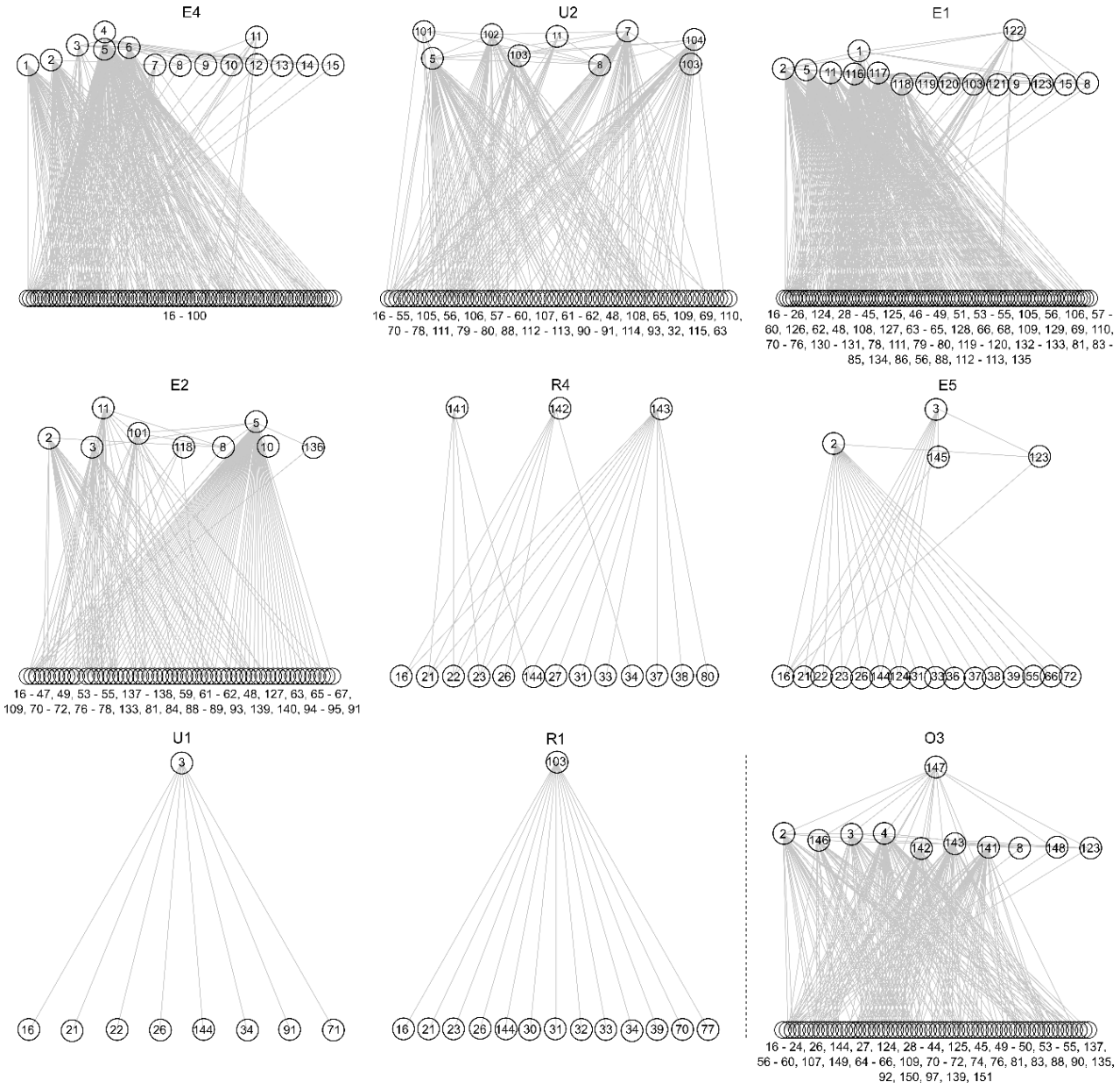

Figure A3.7 Numbered food web nodes. Numbers correspond to the Node column of Table A3.5 to identify the species representative of each node. Sites are displayed in order of increasing catchment glacier cover but the dotted line separates site O3 which was influenced by proglacial lake inputs.

Appendix 3.8: Connectance and trophic food web descriptors

Table A3.8 Connectance and trophic descriptors of food webs constructed for nine alpine rivers in the Austrian Alps. Sites are presented in order of reducing catchment glacier cover. B = basal nodes, I = intermediate nodes, T = top nodes, *SD* = standard deviation, L = trophic link length, A = trophic link angle, * = site downstream of a proglacial lake. Trophic similarity considered the number of node connections shared by two taxa as a fraction of their overall connections and the total similarity value was averaged per node (mean/maximum trophic similarity) (Hudson et al., 2016). The 2-span statistic represented the distance between pairs of consumers and resources. Link length statistics described differences in the orders of magnitude of *M* and *N* between nodes while link angles noted the rate of change in *M* between resources and consumers. Chain span represented difference in the orders of magnitude of *M* and *N* between basal and top nodes. Tritrophic statistics considered these parameters for the link lengths (L) and angles (A) between basal and intermediate nodes (lower), intermediate nodes and consumers (upper), and difference in angle between these two measures (A between) (Cohen et al., 2009). All other terms are defined in Section 4.2. Tritrophic statistics could not be calculated for sites E5 and U1 due to the absence of population density data. Sites R1 and R4 had insufficient nodes for tritrophic statistic calculation.

	R1	U1	O3*	E5	R4	E2	E1	U2	E4
Connectance descriptors									
Node properties									
Number of nodes (*S*)	14	9	73	20	16	72	109	70	95
Resource: consumer ratio	13.00	9.00	6.27	4.50	4.33	0.78	6.56	7.56	6.08
Fraction of B level nodes (%)	0.93	0.89	0.85	0.80	0.81	0.88	0.85	0.87	0.84
Fraction of I level nodes (%)	0.00	0.00	0.10	0.10	0.00	0.08	0.10	0.09	0.10
Fraction of T level nodes (%)	0.07	0.11	0.06	0.10	0.19	0.04	0.05	0.04	0.06
Link properties									
Number of trophic links (*L*)	13	9	232	28	23	153	375	198	280
Linkage density (*L/S*)	0.93	1.00	3.18	1.40	1.44	2.13	3.44	2.83	2.95
Directed connectance (L/S^2)	0.07	0.11	0.04	0.07	0.09	0.03	0.03	0.04	0.03
Proportion of links (I: B)	0.00	0.00	0.36	0.07	0.00	0.41	0.39	0.50	0.02
Proportion of links (I: I)	0.00	0.00	0.05	0.00	0.00	0.01	0.03	0.04	0.01
Proportion of links (T: B)	1.00	0.89	0.58	0.82	1.00	0.51	0.55	0.41	0.74
Proportion of links (T: I)	0.00	0.00	0.02	0.12	0.00	0.06	0.03	0.05	0.04
Chain properties									
Mean chain length	1.00	1.00	2.24	1.12	1.00	1.59	2.01	1.93	1.35
Median chain length	1	1	2	1	1	2	2	2	1
Maximum chain length	1	1	5	2	1	3	4	4	4
Chain length (*SD*)	0.00	0.00	1.18	0.33	0.00	0.53	0.87	0.68	0.59
Characteristic path length	1.72	1.58	2.26	1.85	1.93	2.02	2.14	2.12	2.18
Mean degree distribution	0.07	0.09	0.02	0.06	0.08	0.01	0.01	0.02	0.01

Table A3.8 - continued

	R1	U1	O3*	E5	R4	E2	E1	U2	E4
Feeding relationship properties									
Omnivory	0.00	0.00	0.08	0.10	0.00	0.06	0.06	0.10	0.06
Mean trophic generality	13.00	9.00	21.09	7.00	7.67	17.00	23.44	22.00	18.67
Normalised generality (*SD*)	3.74	3.00	2.95	2.99	2.36	4.26	3.90	3.40	3.87
Mean trophic vulnerability	1.00	1.00	3.36	1.56	1.77	2.19	3.57	2.91	3.08
Normalised vulnerability (*SD*)	0.29	0.00	0.74	0.63	0.76	0.78	0.73	0.67	0.82
Mean/max trophic similarity	0.93	0.90	0.81	0.89	0.84	0.93	0.90	0.88	0.91
Trophic descriptors									
Link statistics									
Number of food chains	13	8	323	26	23	183	588	297	291
Mean link length	11.42		10.90		12.66	10.99	11.36	12.01	12.78
Mean link angle	-14.41		-20.72		-14.43	-22.46	-17.62	-28.64	-19.77
Tritrophic statistics									
Number of three node chains			65			49	88	78	30
Mean 2-span			10.80			12.01	11.14	13.70	13.99
Mean L upper			0.82			1.28	1.61	1.65	1.12
Mean L lower			10.31			11.76	10.55	12.19	13.84
Mean A upper			-47.93			-127.00	-84.31	-64.79	29.10
Mean A lower			-20.11			-11.62	-10.56	-23.85	-22.89
Mean A between			-55.51			-115.40	-73.75	-40.95	-32.01
Multitrophic statistics									
Community span	11.42		16.13		12.66	16.83	16.55	17.12	17.30
Mean count chain length	1.00		2.15		1.00	1.65	1.91	1.89	1.37
Mean sum chain length	11.42		12.72		12.66	12.64	12.86	14.53	13.79
Mean chain span	11.42		11.95		12.66	11.97	12.29	14.44	13.40

Appendix 3.9: Influence of a proglacial lake on food web structure

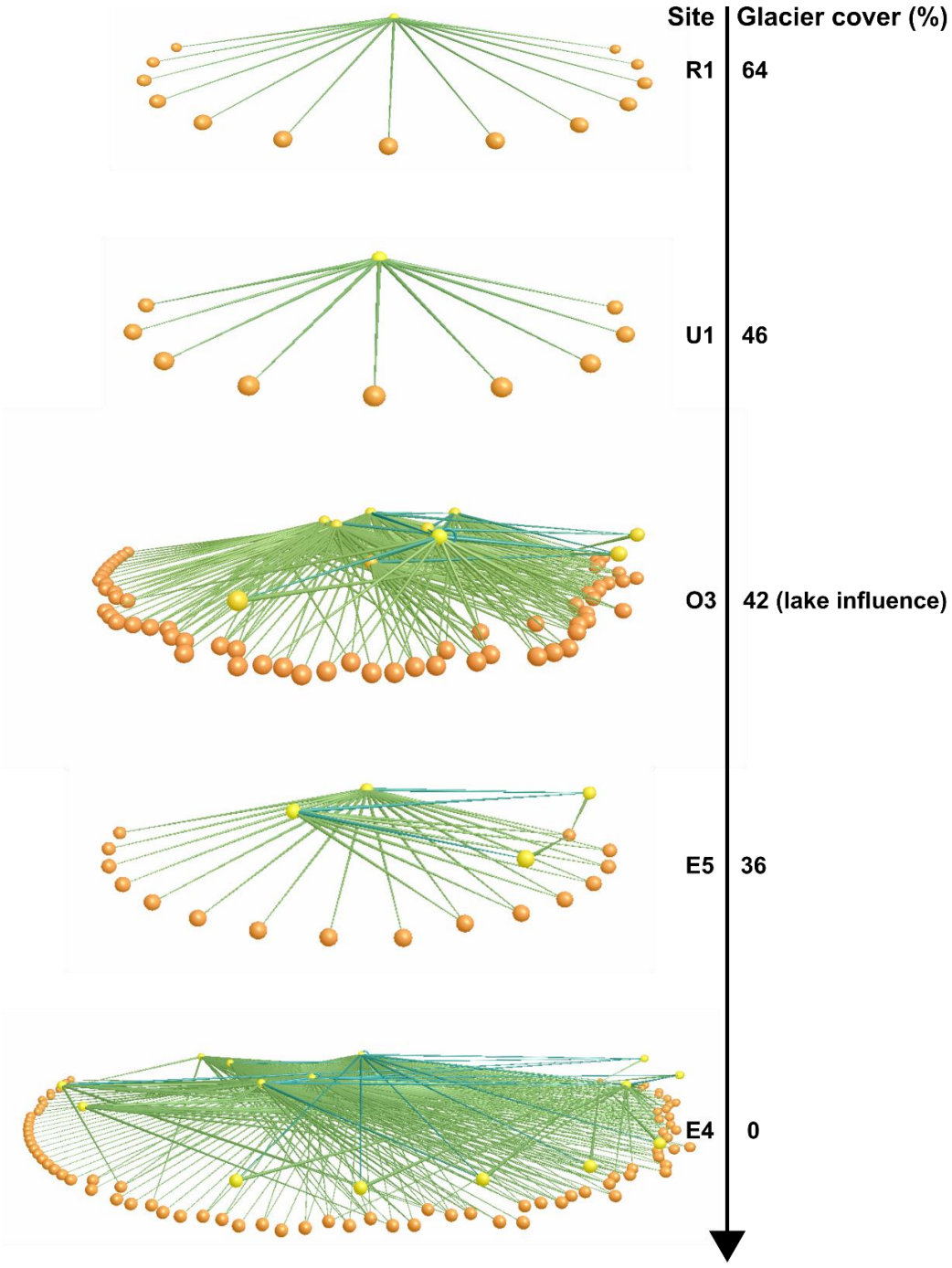

Figure A3.9.1 Food webs representative of river sites with variable catchment glacier cover in the Austrian Alps. Dramatic differences in food web structure at site O3 of the Obersulzbach valley, in comparison to other sites with similar catchment glacier cover, are potentially driven by the influence of an upstream proglacial lake. Colours represent basal (orange circles) and consumer (yellow circles) nodes, alongside linkages connecting basal and intermediate (green lines) and intermediate and top (blue lines) nodes.

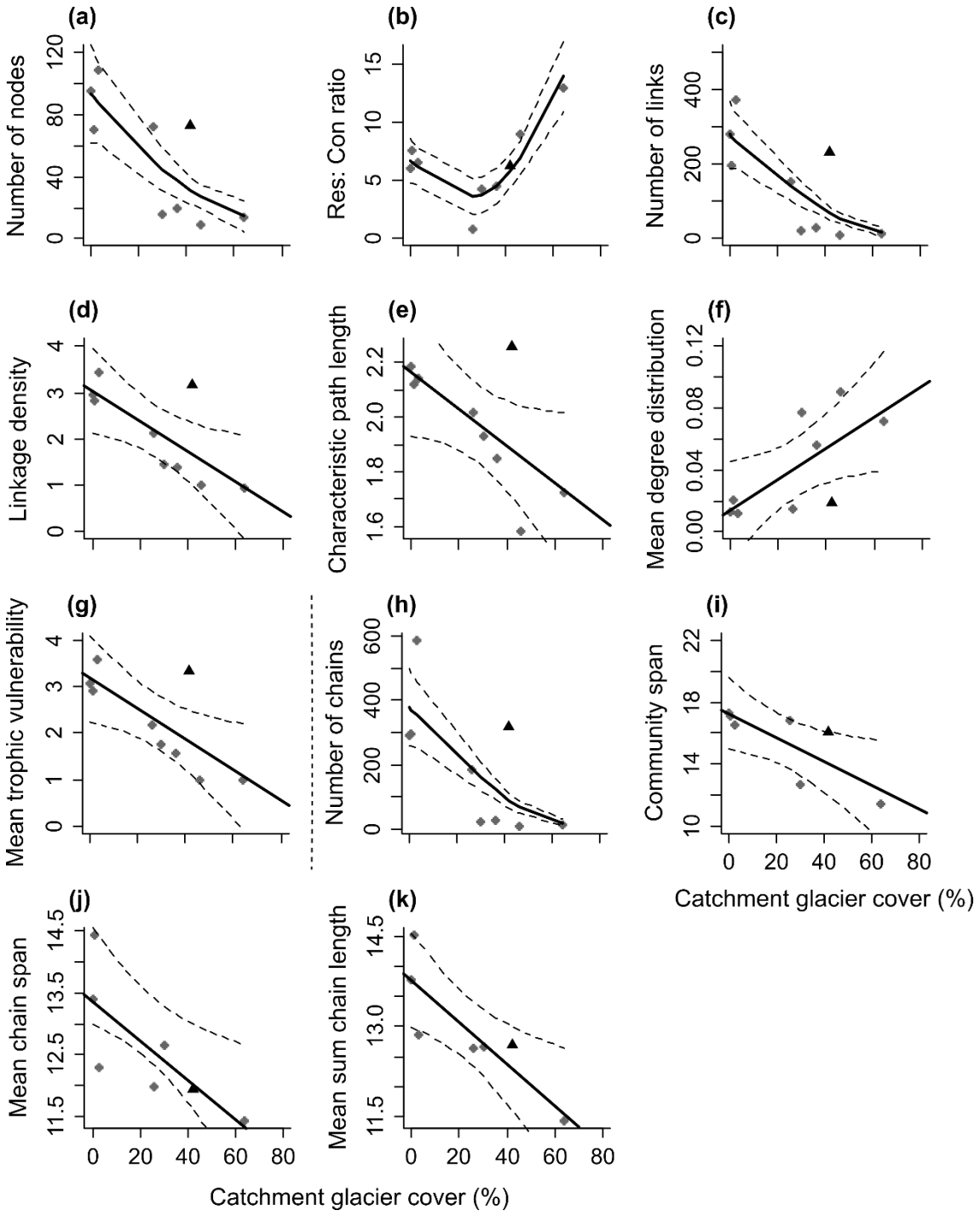

Figure A3.9.2 Significant GAM/GLM relationships between catchment glacier cover and both connectance and trophic food web descriptors for alpine river sites. These relationships include site O3 (black triangles) which is situated approximately 3.3 km downstream of the Obersulzbachkees proglacial lake (*n* = 9). Black lines illustrated lines of best fit and 95 % confidence intervals. Res = resource, Con = consumer. For the trophic descriptors, *n* = 7 as abundance information was absent for site E5 and U1.

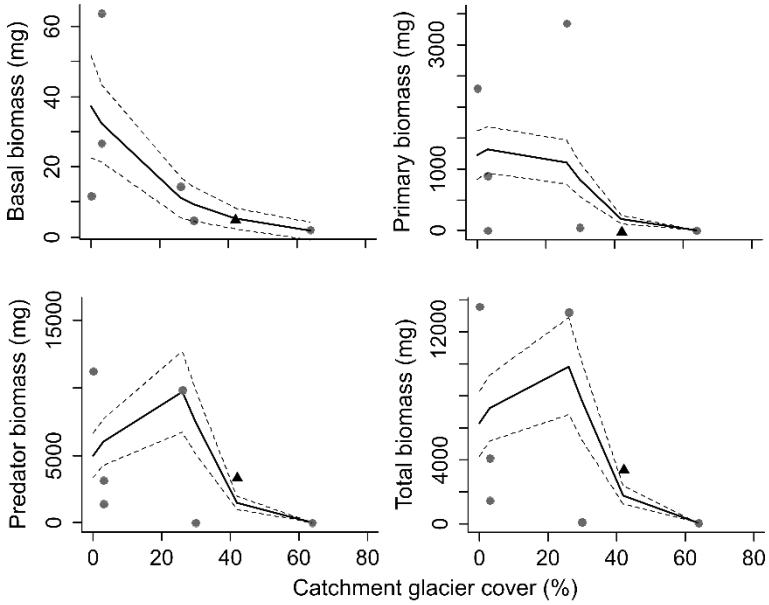

Figure A3.9.3 Significant increases in the total biomass (mg m^{-2}) of basal taxa, primary consumers, predators and all aquatic biota of alpine river food webs with declining catchment glacier cover in the Austrian Alps. Summary statistics are presented in Table A3.9.1. Black lines illustrate lines of best fit and 95 % confidence intervals. Basal biomass included biomass values for primary producers alongside AFDM of amorphous detritus. Biomass information was available for macroinvertebrate and periphyton species but *n* = 7 as diatom biomass estimates were unavailable for sites E5 and U1. Site O3 (black triangles), which was influenced by a proglacial lake, is included in these correlations.

Table A3.9.1 GLM/GAM summary statistics describing the relationships illustrated in Figure A3.9.2 and Figure A3.9.3. Res = resource, Con = consumer.

Dependent variable	Model (Distribution)	χ^2 / *F*	*p*-value	Deviance explained (%)
Connectance descriptors				
Node properties				
Number of nodes	GAM (Negative binomial)	32.03	< 0.001 ***	50.3
Res: Con ratio	GAM (Gaussian)	15.13	0.005 **	83.5
Link properties				
Number of links	GAM (Negative binomial)	69.62	< 0.001 ***	43.6
Linkage density	GLM (Gaussian)	8.54	< 0.022 *	55.0
Chain properties				
Characteristic path length	GLM (Gaussian)	5.68	0.049 *	44.8
Mean degree distribution	GLM (Gaussian)	6.71	0.036 *	48.9
Feeding relationship properties				
Mean trophic vulnerability	GLM (Gaussian)	8.49	< 0.023 *	54.8
Trophic descriptors				
Link statistics				
Number of chains	GAM (Negative binomial)	81.55	< 0.001 ***	39.4
Multitrophic statistics				
Community span	GLM (Gaussian)	7.80	0.038 *	60.9
Mean chain span	GLM (Gaussian)	7.28	0.043 *	59.3
Mean sum chain length	GLM (Gaussian)	14.02	0.013 *	73.7
Biomass				
Basal	GAM (Negative binomial)	30.57	< 0.001 ***	68.6
Primary consumer	GAM (Negative binomial)	106.1	< 0.001 ***	33.1
Predator	GAM (Negative binomial)	237	< 0.001 ***	35.1
Total	GAM (Negative binomial)	277.8	< 0.001 ***	45.7

Appendix 3.10: Additional food web descriptors

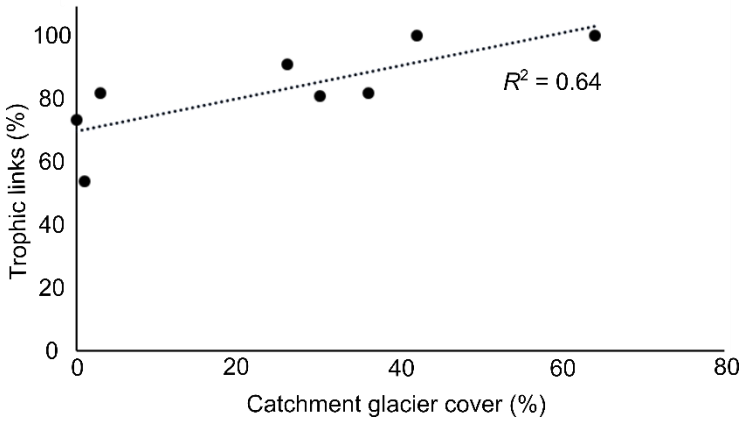

Figure A3.10.1 Significant linear relationship between the percentage of taxa connected by ≤ two trophic links and catchment glacier cover, for eight alpine river food webs.

Table A3.10.1 Comparison of global clustering coefficients computed for observed and randomly generated food webs. Values for random networks represent the average global clustering coefficient of 1000 randomly generated networks constructed to comprise the same number of nodes and links as each observed river food web, using the Erdos-Renyi model in the *igraph* package of R (Csardi and Nepusz, 2016).

		Global clustering coefficients		
Site	**Catchment glacier cover (%)**	**Observed network (O)**	**Random network (R)**	**O/R**
E1	36	0.714	0.148	5
E2	3	0.737	0.064	12
E4	26	0.737	0.060	12
E5	0	0.884	0.063	14
R1	64	0.000	0.135	0
R4	30	0.693	0.189	4
U1	46	0.000	0.236	0
U2	1	0.754	0.082	9

Appendix 3.11: Relationships between food web descriptors and environmental parameters

Table A3.11.1 Significant GLM/GAM relationships between both connectance and trophic descriptors for eight alpine river food webs and physicochemical variables. Tritrophic statistics were not correlated as following removal of site O3, data were only available for four sites.

Independentl **Dependent variables**	**Model (Distribution)**	χ^2 / ***F***	***p*-value**	**Deviance explained (%)**
Turbidity (NTU)				
Number of nodes	GAM (Negative binomial)	58.02	< 0.001 ***	96.0
Intermediate taxa	GAM (Gaussian)	49.58	< 0.001 ***	95.2
Number of links	GAM (Negative binomial)	136.00	< 0.001 ***	92.5
Linkage density	GAM (Gaussian)	9.40	0.020 *	79.0
Directed connectance	GAM (Gaussian)	69.98	< 0.001 ***	96.6
T: B taxa	GAM (Gaussian)	5.85	0.049 *	70.1
T: I taxa	GAM (Gaussian)	41.59	< 0.001 ***	94.5
I: B taxa	GAM (Gaussian)	8.83	0.023 *	77.9
Mean chain length	GAM (Gaussian)	6.23	0.044 *	71.4
Maximum chain length	GAM (Gaussian)	19.05	0.005 **	88.4
Characteristic path length	GAM (Gaussian)	11.64	0.013 *	82.3
Mean degree distribution	GAM (Gaussian)	247.50	< 0.001 ***	99.0
Omnivory	GAM (Gaussian)	16.87	0.006 **	87.1
Mean trophic generality	GAM (Gaussian)	14.80	0.009 **	85.6
Mean trophic vulnerability	GAM (Gaussian)	7.90	0.028 *	76.0
Number of chains	GAM (Negative binomial)	107.90	< 0.001 ***	91.4
Community span	GAM (Gaussian)	84.59	< 0.001 ***	98.3
Mean count chain length	GLM (Gaussian)	11.64	0.027 *	74.4
1/Pfankuch Index				
Number of nodes	GAM (Negative binomial)	57.80	< 0.001 ***	93.7
Number of links	GAM (Negative binomial)	139.60	< 0.001 ***	92.2
Linkage density	GAM (Gaussian)	16.49	0.005 **	86.8
Directed connectance	GLM (Gaussian)	9.02	0.024 *	60.0
T: B taxa	GLM (Gaussian)	36.25	< 0.001 ***	85.8
I: I taxa	GAM (Gaussian)	6.84	0.036 *	73.2
I: B taxa	GLM (Gaussian)	49.98	< 0.001 ***	89.3
Mean chain length	GAM (Gaussian)	7.35	0.032 *	74.6
Median chain length	GLM (Gaussian)	14.68	0.009 **	71.0
Maximum chain length	GAM (Gaussian)	16.55	0.005 **	86.9
Characteristic path length	GAM (Gaussian)	6.53	0.040 *	72.3
Mean degree distribution	GAM (Gaussian)	17.59	0.004 **	87.6
Mean trophic generality	GLM (Gaussian)	117.04	0.017 *	63.8
Mean trophic vulnerability	GAM (Gaussian)	11.88	0.012 *	82.6
Number of chains	GAM (Negative binomial)	177.80	< 0.001 ***	90.6
Mean link angle	GLM (Gaussian)	28.33	0.006 **	87.6
Community span	GAM (Gaussian)	62.46	0.004 **	97.7

Table A3.11.1 – continued

Independent/ Dependent variables	Model (Distribution)	χ^2 / *F*	*p*-value	Deviance explained (%)
Mean count chain length	GLM (Gaussian)	9.20	0.039 *	69.7
Water temperature (°C)				
Number of chains	GLM (Gaussian)	8.72	0.026 *	59.2
Electrical conductivity (µm cm^{-1})				
Number of nodes	GAM (Negative binomial)	17.86	< 0.001 ***	29.8
T: B taxa	GLM (Gaussian)	8.04	0.030 *	57.3
Mean link angle	GLM (Gaussian)	61.64	0.0014 **	93.9
pH				
Number of nodes	GAM (Negative binomial)	44.90	< 0.001 ***	76.8
Number of links	GAM (Negative binomial)	107.30	< 0.001 ***	78.3
Linkage density	GAM (Gaussian)	6.83	0.036 *	73.2
I: B taxa	GAM (Gaussian)	5.86	0.048 *	70.1
Characteristic path length	GAM (Gaussian)	11.06	0.014 *	81.6
Mean degree distribution	GAM (Gaussian)	6.49	0.040 *	72.2
Mean trophic vulnerability	GAM (Gaussian)	7.85	0.028 *	75.9
Number of chains	GAM (Negative binomial)	134.60	< 0.001 ***	80.1
Community span	GLM (Gaussian)	22.80	0.009 **	85.1
Mean sum chain length	GLM (Gaussian)	21.22	0.010 **	84.1

Table A3.11.2 Significant GAM/GLM relationships between connectance and trophic descriptors for eight alpine river food webs and nutrient concentrations. Tritrophic statistics were not correlated as following removal of site O3, influenced by a proglacial lake, data were only available for four sites. Correlations between PO_4^{3-} and descriptors were also tested but produced no significant results. Nutrient data were unavailable for some sites (Table A1.2).

***Independent*/ Dependent variables**	**Model (Distribution)**	**χ^2 / *F***	***p*-value**	**Deviance explained (%)**
DOC (mg L^{-1})				
Number of links	GAM (Negative binomial)	11.24	< 0.001 ***	19.9
Number of chains	GAM (Negative binomial)	16.51	< 0.001 ***	25.4
NO_3^- (mg L^{-1})				
Number of nodes	GAM (Negative binomial)	11.75	0.003 **	29.8
Number of links	GAM (Negative binomial)	22.34	< 0.001 ***	25.4
Number of chains	GAM (Negative binomial)	22.31	< 0.001 ***	21.3
TP (mg L^{-1})				
Mean count chain length	GLM (Gaussian)	18.12	0.024 *	85.8
TN (mg L^{-1})				
Number of nodes	GAM (Negative binomial)	60.09	< 0.001 ***	96.0
Intermediate taxa	GLM (Gaussian)	7.41	0.035 *	55.2
Number of links	GAM (Negative binomial)	146.50	< 0.001 ***	96.8
Linkage density	GLM (Gaussian)	217.40	< 0.001 **	97.3
Directed connectance	GLM (Gaussian)	15.08	0.008 *	71.5
T: B taxa	GLM (Gaussian)	11.63	0.014 *	66.0
I: I taxa	GLM (Gaussian)	23.94	0.003 *	80.0
I: B taxa	GLM (Gaussian)	14.60	0.009 **	70.9
Mean chain length	GLM (Gaussian)	23.94	0.003 **	80.0
Maximum chain length	GLM (Gaussian)	80.20	< 0.001 ***	93.0
Characteristic path length	GLM (Gaussian)	21.15	0.004 **	77.9
Mean degree distribution	GLM (Gaussian)	32.81	0.0012 **	84.5
Mean trophic generality	GLM (Gaussian)	41.21	< 0.001 ***	87.3
Mean trophic vulnerability	GAM (Gaussian)	39.36	< 0.001 ***	94.0
Number of chains	GAM (Negative binomial)	184.20	< 0.001 ***	97.0
Community span	GAM (Gaussian)	161.70	< 0.001 ***	99.1
Mean count chain length	GLM (Gaussian)	11.70	0.027 *	74.5

Appendix 3.12: Species-averaged and individual *MN* regressions

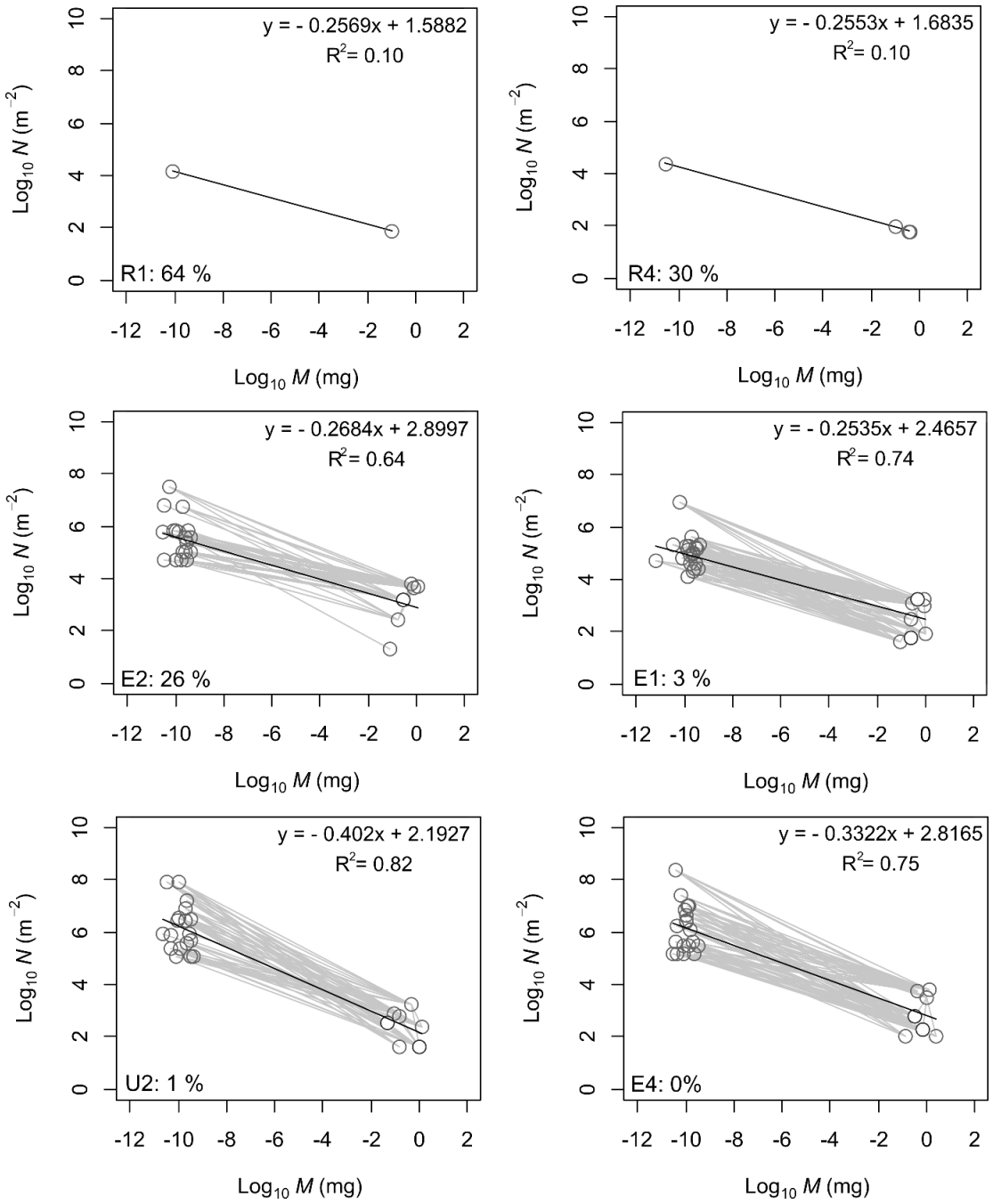

Figure A3.12.1 Linear regressions between species-averaged biomass (log_{10} *M*) and abundance (log_{10} *N*) for alpine river food webs. Lines of best fit are displayed in black. Site codes and percentage catchment glacier cover are shown for each river site. *MN* relationships could not be established for site E5 as biofilm samples were damaged during transport and site U1 as the biofilm species identified within the gut contents were not found in the biofilm samples, preventing estimates of their abundance. Absence of abundance or biomass data has resulted in certain taxa present in the connectance food webs being unrepresented in *MN* analysis.

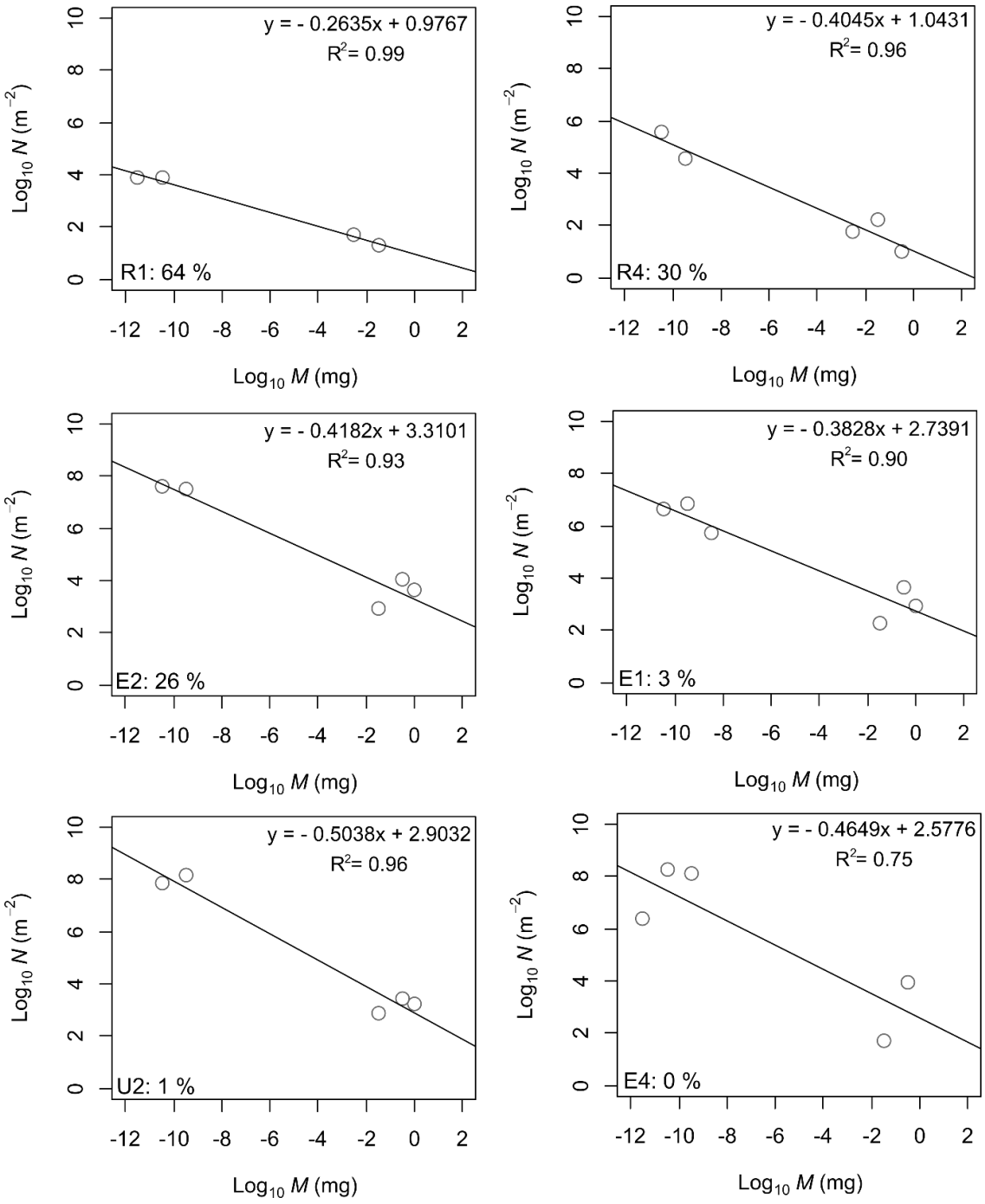

Figure A3.12.2 Linear regressions between the centre point of each biomass bin of 1 on the $\log_{10}$ scale and the $\log_{10}$ abundance of individual aquatic taxa found within each bin. Linear regressions are displayed and text defines the site code and percentage catchment glacier cover for each river site. Individual *MN* relationships could not be established for site E5 and U1 due to absence of biofilm abundance data.

Appendix 4: Supporting information for Chapter Five

Appendix 4.1: Arrhenius plot

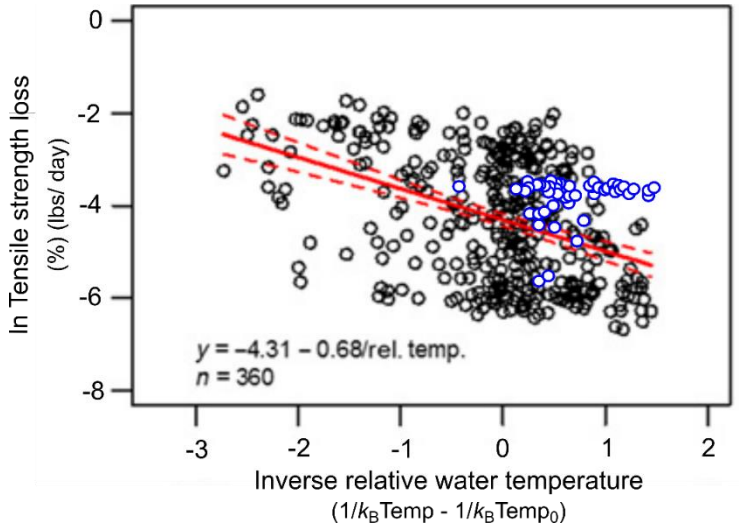

Figure A4.1 Relationship between inverse relative river water temperature and non-temperature-adjusted daily cellulose decomposition rates for glacierised mountain rivers (blue open circles) and rivers in eleven biomes (black open circles, red lines) recorded by Tiegs et al. (2019). There was no significant relationship between water temperature and tensile strength loss for sampled rivers (R^2 = 0.04). K_B = Boltzmann constant (0.0000862), Temp = mean river site water temperature (K), $Temp_0$ = 283.15 K. Normalisation of temperatures to the equivalent of 10 °C followed Tiegs et al. (2019).

Appendix 4.2: Microbial taxa responses to reducing glacier cover and tensile strength loss

Table A4.2 Wald statistics illustrating bacterial (16S) and fungal (ITS) OTUs whose abundance was associated significantly (Pr(>wald) = < 0.05) with either catchment glacier cover (%) or tensile strength loss (TS loss). Values were calculated following *manyglm* analysis using the *mvabund* package of R (Wang et al., 2018). Arrows indicate if OTU abundance increased or decreased with reductions in glacier cover and tensile strength loss across six glacierised regions.

OTU Identification	Wald value	Pr(>wald)	Glacier cover (%)	TS loss
Fungi (ITS)				
Lemonniera centrosphaera	110.28	0.002	↑	
Tetracladium sp.	38.22	0.010	↑	
Unclassified	30.84	0.031	↓	
Unclassified	40.89	0.003	↓	
Unclassified	45.21	0.002	↓	
Helotiales sp.	50.27	0.002	↑	
Unclassified	50.25	0.002	↓	
Unclassified	29.70	0.045	↓	
Unidentified	36.95	0.013	↓	
Tetracladium marchalianum	61.52	0.002	↑	
Unclassified	90.67	0.002	↓	
Unclassified	31.57	0.025	↓	
Leotiomycetes sp.	116.81	0.002	↓	
Unclassified	31.81	0.024	↓	
Tetracladium sp.	37.97	0.011	↑	
Ascomycota sp.	74.88	0.002	↓	
Tetracladium sp.	32.36	0.023	↑	
Ascomycota sp.	54.43	0.002	↑	
Tetracladium psychrophilum	94.84	0.045		↓
Bacteria (16S)				
Cytophagales sp.	59.74	0.001	↑	
Unclassified chloroplast	47.75	0.048	↑	
Hymenobacter sp.	49.63	0.043	↓	
Unclassified chloroplast	121.37	0.001	↓	
Cytophagales sp.	68.95	0.001		↓
Unclassified chloroplast	46.66	0.018		↓
Flavobacterium sp.	201.75	0.001		↓
Flavobacterium sp.	48.27	0.014		↓

Appendix 4.3: Influence of proglacial lake inputs on catchment glacier cover relationships

Table A4.3 GLM/GAM summary statistics as displayed in Table 5.1 following the removal of river sites influenced by proglacial lake inputs (grey bands). 16S = bacterial (16S) copy number, ITS = fungal (ITS) copy number, *cbhI* = *cbhI* gene copy number, Ascomycota, *Tetracladium* and saprotroph = OTU abundance.

***Independent* / Dependent variables**	**Model (Distribution)**	**χ^2/ *F***	***p*-value**	**Deviance explained (%)**
Catchment glacier cover (%)				
ITS	GLM (Gaussian)	11.47	0.003 **	37.6
		8.12	0.012 *	33.7
16S	GLM (Gaussian)	0.75	0.394	2.2
		3.17	0.085	9.9
Ascomycota	GAM (Negative binomial)	14.99	< 0.001 ***	13.5
		15.10	< 0.001 ***	15.2
Tetracladium	GAM (Negative binomial)	386.10	< 0.001 ***	23.1
		379.80	< 0.001 ***	22.6
Saprotroph	GAM (Negative binomial)	305.70	< 0.001 ***	28.9
		332.20	< 0.001 ***	35.5
cbhI	GLM (Gaussian)	18.88	< 0.001 ***	65.4
		11.84	< 0.001 ***	62.8
Tensile strength loss (%) (lbs/ degree-day)				
ITS	GLM (Gaussian)	7.66	0.014 *	32.4
		5.65	0.033	30.3
cbhI	GLM (Gaussian)	20.25	< 0.001 ***	65.4
		10.52	0.007 **	46.7

Appendix 4.4: Mixed effect models

Table A4.4 GLMM and GAMM summary statistics. The random effect of mean absolute latitude per region was tested alongside the fixed effect models displayed in Table 5.1. For GAMM relationships incorporating OTU abundances, data from France, New Zealand and Alaska were removed as low numbers of sites (n = < 5) hosting microbial amplification limited calculation of robust regressions. Removal of these sites resulted in the fixed effect of catchment glacier cover upon *Tetracladium* OTU abundance no longer being significant. Cover = catchment glacier cover (%), TS = tensile strength loss (%) (lbs/degree-days), Asco = Ascymycota OTU abundance, *Tetra* = *Tetracladium* OTU abundance, sapro = saprotroph OTU abundance, *cbhI* = cellobiohydrolase I gene copy number, ITS = fungal (ITS) copy number. Int. = Intercept and Res. = Residual. The AIC values are reported for the mixed effect models (AIC_m) and a comparative GLM or GAM run with an identical structure but fixed effects only (AIC_f). The lowest AIC value is highlighted in bold.

	Random effects		**Fixed effects**									
	Int.	**Res.**	**Intercept**				**Independent variable**					
Variables	***SD***	***SD***	**Value**	**SE**	***t***	***p*-value**	**Value**	**SE**	***t***	***p*-value**	**AIC_m**	**AIC_f**
GLMM												
ITS vs cover	1.26	1.90	22.62	0.85	26.51	< 0.001	-0.06	0.02	-3.20	0.005	110.92	**105.26**
TS vs ITS	< 0.001	0.09	-0.30	0.18	-1.66	0.117	0.02	0.01	2.54	0.023	-20.32	**-36.12**
TS vs *cbhI*	0.01	0.07	-0.25	0.08	-3.19	0.007	0.05	0.01	5.55	<0.001	-27.51	**-43.72**
GAMM												
Asco vs cover	0.11	2519.25	9598.45	887.43	10.82	< 0.001	-55.27	21.42	-2.58	0.021	359.52	**357.52**
Tetra vs cover	1141.84	1562.51	1517.86	939.66	1.62	0.127	-3.66	15.74	-0.23	0.819	345.73	**345.51**
sapro vs cover	0.37	3262.89	7283.67	1149.4	6.34	< 0.001	-71.66	27.74	-2.58	0.021	369.35	**367.35**
cbhI vs cover	< 0.001	1.26	9.11	0.27	33.18	< 0.001	-1.17	1.09	-1.07	0.300	91.41	**81.36**

Appendix 4.5: Significant relationships with environmental parameters

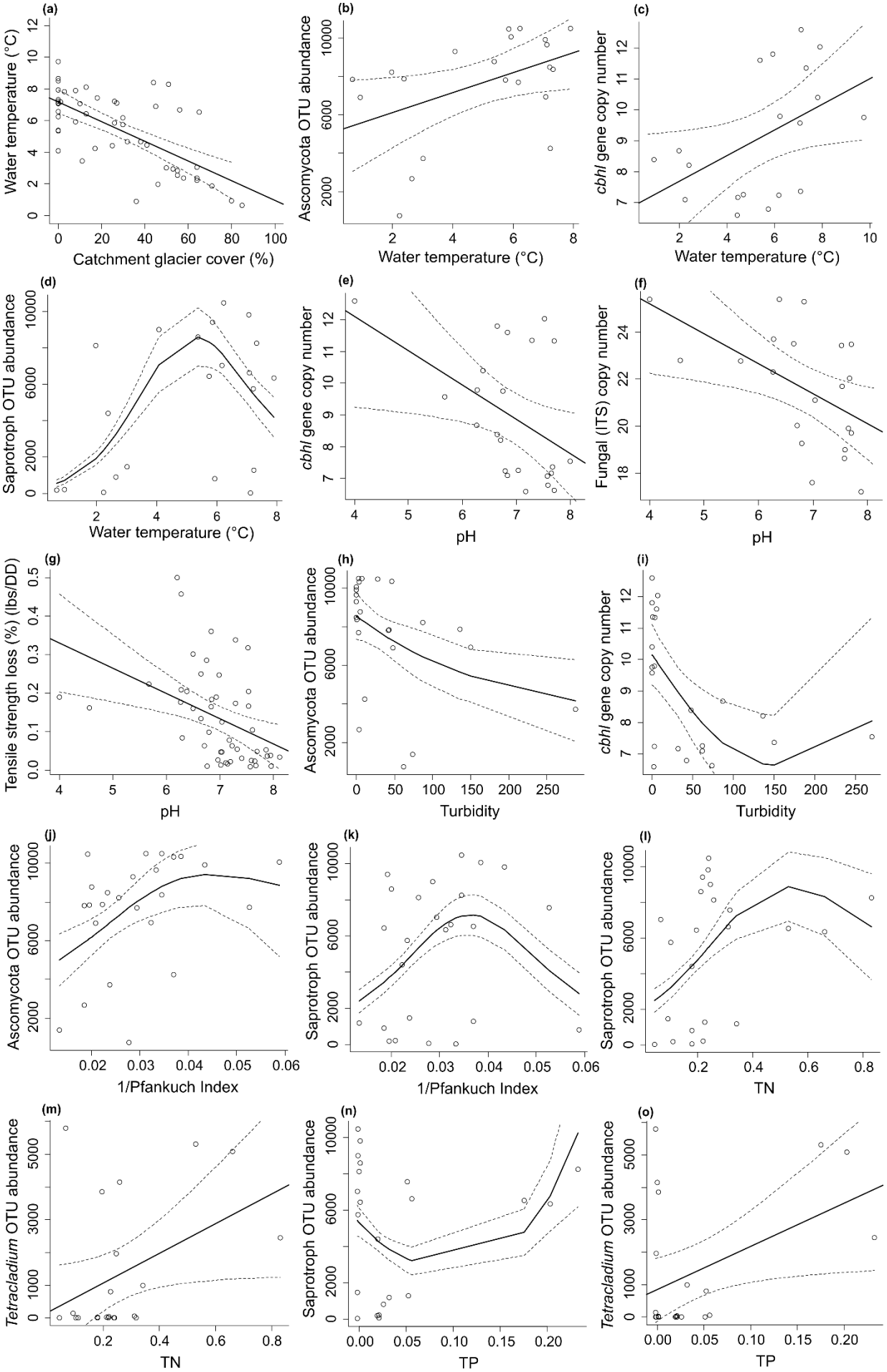

Figure A4.5 - continued

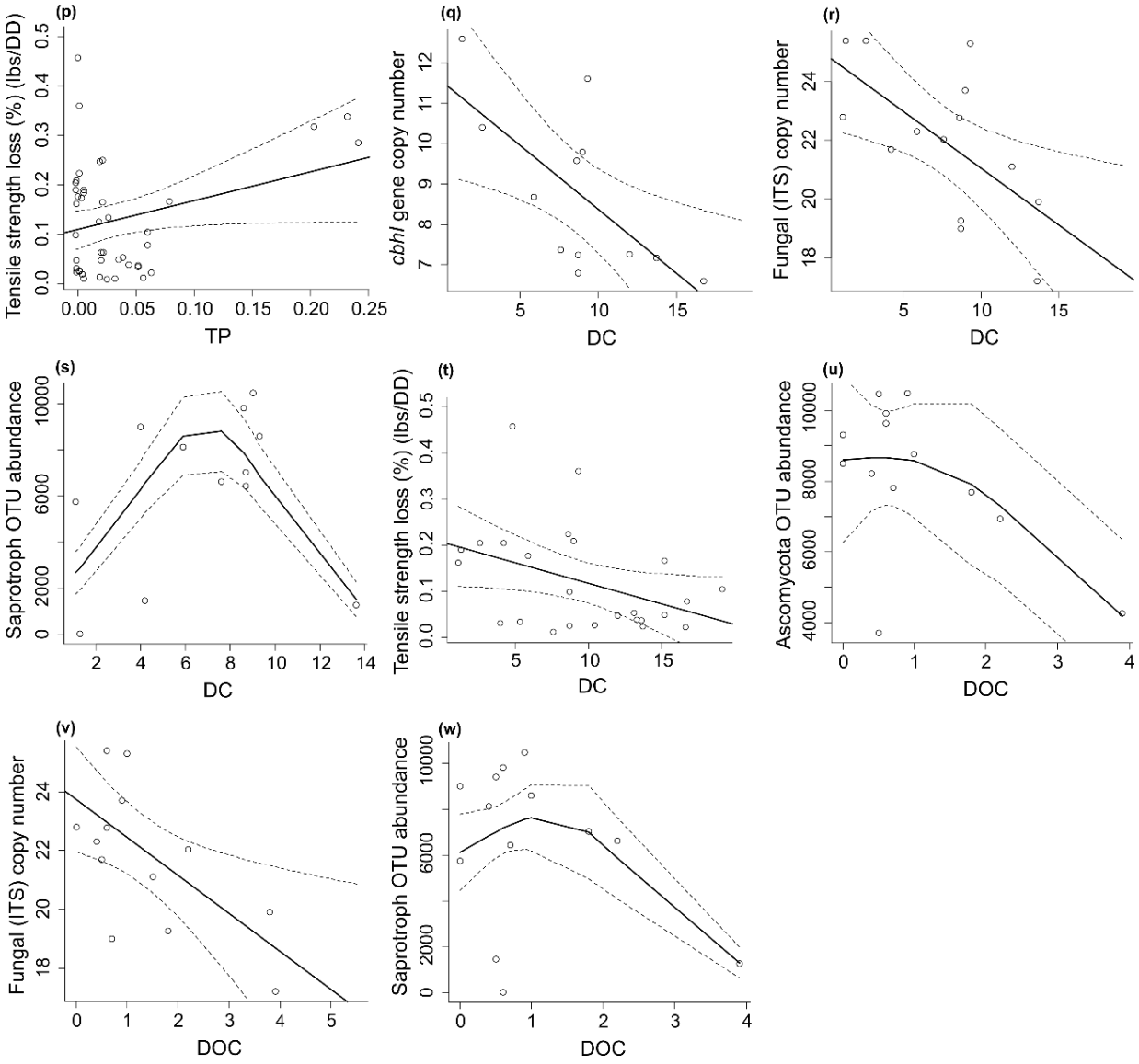

Figure A4.5 Significant GLM/GAM relationships between physicochemical parameters, nutrient concentrations (mg L^{-1}), catchment glacier cover, tensile strength loss, microbial copy numbers and fungal OTU abundance (Ascomycota, *Tetracladium,* saprotrophs) for river sites across six glacierised regions. There were no significant relationships regarding taxa of the order Saccharomycetales and all environmental parameters. Summary statistics are presented in Table 5.1.

Appendix 5: Supporting information for Chapter Six

Appendix 5.1: Taxa responses to declining catchment glacier cover at different levels of biological organisation

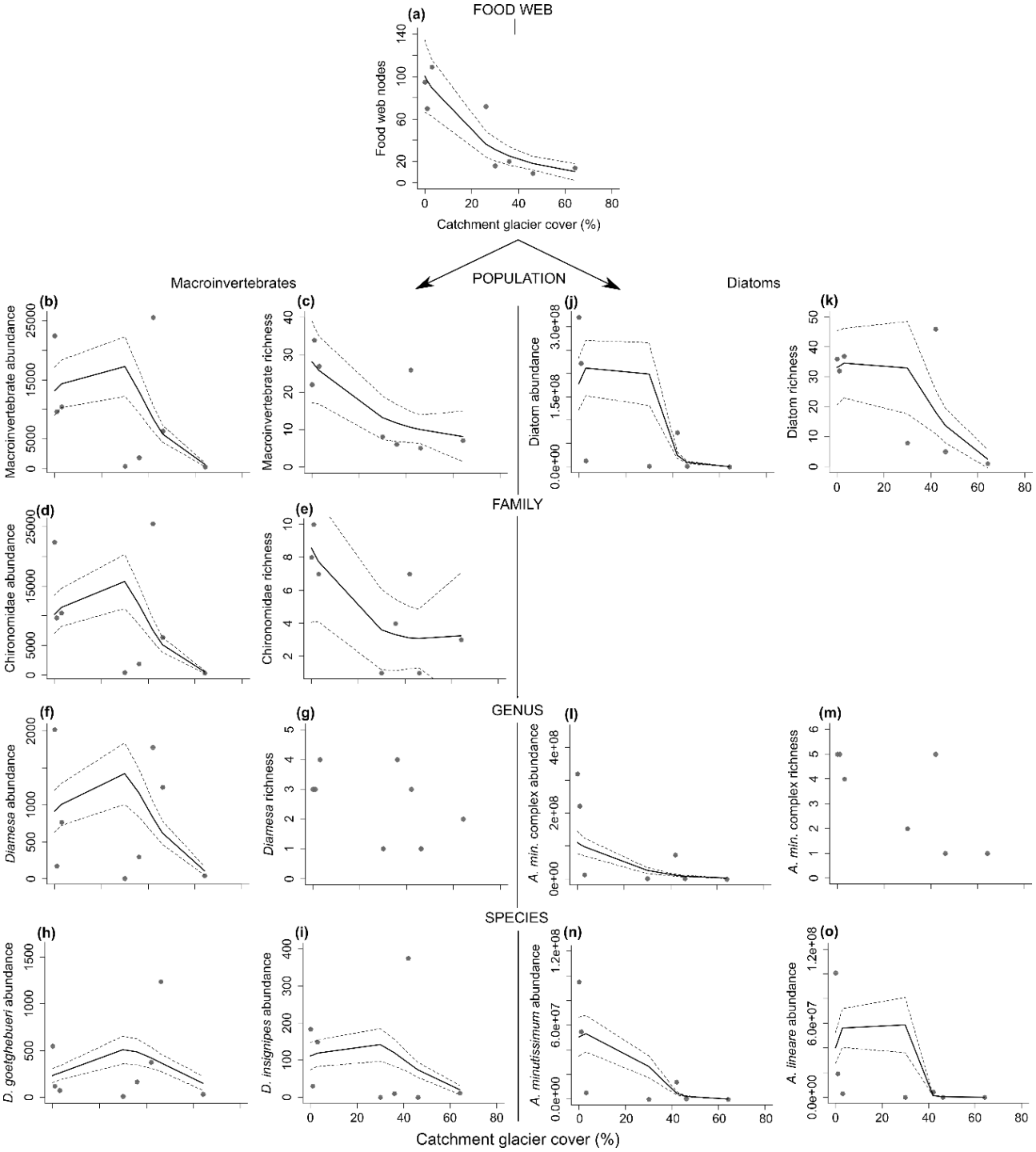

Figure A5.1 Variability in the response of macroinvertebrate (b to i) and diatom (j to o) taxonomic richness and abundance to a gradient of reducing catchment glacier cover at different levels of biological organisation (a to o). Significant GAM statistics are displayed in

Table A5.1. *D. goetghebueri* = *Diamesa goetghebueri*, *D. insignipes* = *Diamesa insignipes*, *A. min*. = *Achnanthidium minutissimum*, *A. lineare* = *Achnanthidium lineare*. Species were selected to exemplify that the significance and distribution of relationships between parameters altered with taxonomic classification.

Table A5.1 Summary statistics for the GLM/GAM relationships illustrated in Figure A5.1.

Dependent variable	Model (Distribution)	χ^2/ *F*	*p*-value	Deviance explained (%)
Food web				
Number of nodes	GAM (Negative binomial)	46.73	< 0.001 ***	74.9
Macroinvertebrates				
Macroinvertebrate abundance	GAM (Negative binomial)	116.1	< 0.001 ***	20.8
Macroinvertebrate richness	GAM (Negative binomial)	13.63	< 0.001 ***	49.3
Chironomidae abundance	GAM (Negative binomial)	124.6	< 0.001 ***	14.5
Chironomidae richness	GAM (Negative binomial)	6.23	0.045 *	47.6
Diamesa abundance	GAM (Negative binomial)	61.41	< 0.001 ***	9.4
Diamesa richness	GLM (Gaussian)	1.71	0.239	22.1
D. goetghebueri abundance	GAM (Negative binomial)	18.45	< 0.001 ***	5.41
D. insignipes abundance	GAM (Negative binomial)	26.39	< 0.001 ***	6.57
Diatoms				
Diatom abundance	GAM (Negative binomial)	1054	< 0.001 ***	43.0
Diatom richness	GAM (Negative binomial)	18.38	< 0.001 ***	44.6
A. min. complex abundance	GAM (Negative binomial)	224.4	< 0.001 ***	29.1
A. min. complex richness	GLM (Gaussian)	5.936	0.059	54.3
A. minutissimum abundance	GAM (Negative binomial)	765.9	< 0.001 ***	42.4
A. lineare abundance	GAM (Negative binomial)	1012	< 0.001 ***	45.3

Appendix 5.2: Relationships between catchment glacier cover and α-diversity

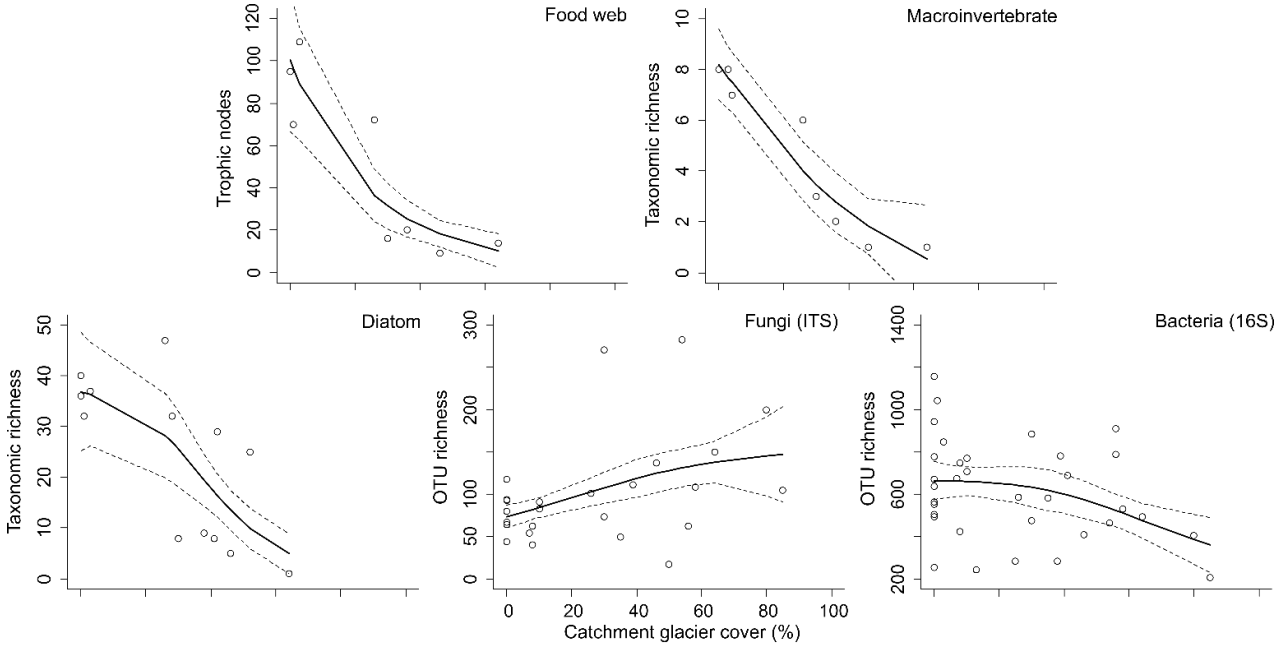

Figure A5.2 Significant GAM relationships between α-diversity (taxonomic richness, OTU richness) of taxonomic groups and reducing catchment glacier cover, determined from sampled river sites (food webs, macroinvertebrates, diatoms = Austrian Alps; Bacteria (16S) = Antisana Ecuador, Eastern Alps Austria, Finse Norway, Western Alps France; Fungi (ITS) = as for bacteria with the addition of Southern Alps New Zealand).

Table A5.2 GAM summary statistics pertaining to Figure A5.2.

Dependent variable	Model (Distribution)	χ^2/ *F*	*p*-value	Deviance explained (%)
α-diversity				
Food web	GAM (Negative binomial)	46.73	< 0.001 ***	74.9
Macroinvertebrate	GAM (Gaussian)	24.61	0.002 **	90.8
Diatom	GAM (Negative binomial)	26.71	< 0.001 ***	43.5
Fungi (ITS)	GAM (Negative binomial)	21.34	< 0.001 ***	19.6
Bacteria (16S)	GAM (Negative binomial)	11.35	0.003 **	11.6

Appendix 5.3: Comparison of observed food webs to those in published literature

Table A5.3 Comparison of connectance food web descriptors from this thesis and 241 river food webs derived from 37 published studies. Descriptors include species richness (*S*), number of links (*L*), linkage density (*L/S*), directed connectance (*C*) and mean chain length (MCL). Studies were identified using the Web of Science (15 March 2019) with a combination of search terms (river, food web, connectance). Food webs are collated for rivers from different landscapes, years, seasons and disturbance regimes, but may not be exhaustive. Those marked * pertain to meltwater-fed rivers in published studies. References are detailed in full below.

Reference	Country	River	*S*	*L*	*L/S*	*C*	MCL	Notes
Chapter Four	Austria	R1	14	13	0.93	0.07	1.0	
		U1	9	9	1.00	0.11	1.0	
		O3	73	232	3.18	0.04	2.24	lake inputs
		E5	20	28	1.40	0.07	1.12	
		R4	16	23	1.44	0.09	1.0	
		E2	72	153	2.13	0.03	1.59	
		E1	109	375	3.44	0.03	2.01	
		U2	70	198	2.83	0.04	1.93	
		E4	95	280	2.95	0.03	1.35	
Clitherow et al. (2013)	Austria	Eisboden river	13	16	1.23	0.05	2.0	2006 *
			19	51	2.68	0.14	2.36	2008 *
			19	67	3.53	0.19	2.32	2011 *
			23	85	3.70	0.16	2.28	Composite *
Ceneviva-Bastos et al. (2014)	Brazil	São José dos Dourados River tributary stream manipulation	106	261	2.46	0.05		Open
			74	185	2.50	0.07		Open (21 months later)
			107	261	2.44	0.05		Shaded
			63	109	1.73	0.06		Shaded (21 months later)
Ceneviva-Bastos et al. (2017)	Brazil	Headwater stream manipulation	82	181	2.11	0.05		Control
			98	240	2.44	0.05		Control
			86	191	2.19	0.05		Before wood debris
			109	294	2.67	0.05		After wood debris
			84	194	2.27	0.05		Before debris/ leaf packs
			114	323	2.83	0.05		After debris and leaf packs
Docile et al. (2016)	Brazil	Paquequer River Basin	39	70	1.79	0.19		Urban streams
			39	62	1.59	0.17		
			43	86	2.00	0.20		
			23	34	1.48	0.28		
			44	68	1.55	0.16		
			19	32	1.68	0.53		
			18	28	1.56	0.50		
			15	21	1.40	0.58		
			32	45	1.41	0.18		
			14	20	1.43	0.42		
			57	114	2.00	0.15		
			41	81	1.98	0.19		
			48	76	1.58	0.14		
			39	66	1.69	0.18		
			30	41	1.37	0.19		
			35	58	1.66	0.19		
			29	37	1.28	0.18		
			21	21	1.00	0.19		
			12	9	0.75	0.26		
			28	34	1.21	0.18		
Motta and Uieda (2005)	Brazil	Potreirinho Creek	117	345	3.00	0.05		Composite

Table A5.3 - continued

Reference	Country	River	*S*	*L*	*L/S*	*C*	MCL	Notes
Tavares-Cromar and Williams (1996)	Canada	Duffin Creek	39	146	3.74	0.10		October
			35	110	3.14	0.09		December
			32	107	3.34	0.11		February
			31	102	3.29	0.11		April
			37	120	3.24	0.09		June
			32	101	3.16	0.10		August
			33	104	3.15	0.10		October
			42	193	4.29	0.10		Composite
Tamaris-Turizo et al. (2018)	Colombia	San Lorenzo	17	39	1.77	0.08	1.81	Wet season
			31	77	2.48	0.08	1.95	Dry season
		La Victoria	24	75	3.12	0.13	1.92	Wet season
			32	87	2.71	0.08	1.93	Dry season
		Puerto Mosquito	22	42	2.47	0.14	1.84	Wet season
			33	123	4.33	0.13	2.03	Dry season
Lavandier and Decamps (1983)	France	l'Estaragne headwater	16	46	2.88	0.10		*
			30	93	3.72	0.18		*
Poepperl (2003)	Germany	Alte Schwentine	14	34	2.43	0.19		
Meyer and Poepperl (2004)	Germany	Steina mountain stream	18	90	5.00	0.29		
Mantel et al. (2004)	Hong Kong	Tai Po Kau Forest stream	28	157	5.61	0.21	2.04	
Canning et al. (2018)	New Zealand	Waipuku Stream	19	45				Forest
			24	61				Grassland
		Waipuku Stream tributary	23	62				Forest
			22	56				Grassland
		Mangatoki Stream	22	53				Forest
			20	46				Grassland
		Kaupokonui East Stream	27	73				Forest
		Tributary	24	61				Grassland
		Kaupokonui East Stream	29	42				Forest
			23	46				Grassland
		Dunns Creek	24	61				Forest
			33	84				Grassland
		Little Dunns Creek	21	48				Forest
			25	63				Grassland
		Ouri Stream	33	95				Forest
			39	127				Grassland
		Cold Stream	29	83				Forest
			25	69				Grassland
		Kapoaiaia Stream	22	42				Forest
			19	46				Grassland
		Composite (n = 10)	25	60	2.43	0.10	1.97	Forest
			25	66	2.59	0.60	1.94	Grassland
Jaarsma et al. (1998)	New Zealand	Healy Creek	96	589	6.14	0.14	3.02	
	New Zealand	Dempsters Creek	107	967	9.04	0.19	4.67	
Townsend et al. (1998)	New Zealand	Blackrock	87	859	9.87	0.13	2.24	
		Broad	95	1278	13.45	0.17	2.25	
		Canton	109	1455	13.35	0.14	2.45	
		Dempsters	107	1783	16.66	0.18	4.42	
		German	86	820	9.54	0.13	2.40	
		Healy	96	1131	11.78	0.15	2.99	
		Kye Burn	98	1503	15.34	0.18	2.35	
		Little Kye Burn	78	770	9.87	0.15	2.39	
		Stony	113	1880	16.64	0.17	2.38	
		Sutton	92	1144	12.44	0.17	1.79	

Table A5.3 – continued

Reference	Country	River	*S*	*L*	*L/S*	*C*	MCL	Notes
Thompson and Townsend (2003)	New Zealand	Venlaw	69	190	2.75	0.08	2.12	Forest streams
		Berwick	79	284	3.59	0.10	1.68	
		North Col	78	421	5.40	0.11	2.27	
		Powder	78	268	3.44	0.08	2.24	
		Trib C	98	626	6.42	0.18	2.35	
		Sutton	92	423	4.60	0.17	1.79	
Thompson and Townsend (2004)	New Zealand	South Island Streams	83	375	4.31	0.13	2.24	Pasture, forest, tussock
			89	656	5.95	0.17	2.25	
			100	708	6.50	0.14	2.45	
			70	421	5.40	0.11	2.27	
			77	268	3.44	0.08	2.24	
			82	224	2.67	0.07	1.61	
			58	117	2.02	0.08	1.72	
			75	240	3.04	0.08	1.56	
			45	440	2.24	0.07	1.57	
			76	155	2.18	0.06	1.69	
			66	187	2.71	0.08	2.12	
			96	966	9.03	0.18	4.42	
			79	353	4.10	0.13	2.40	
			90	589	6.14	0.14	3.02	
			93	629	6.42	0.18	2.35	
			67	375	4.81	0.15	2.39	
			104	832	7.36	0.17	2.38	
			89	423	4.60	0.17	1.79	
Thompson and Townsend (2005)	New Zealand	South Island Streams	87	375	4.31	0.13	2.24	Sites as above
			95	565	5.95	0.17	2.25	
			109	708	6.50	0.14	2.45	
			78	421	5.40	0.11	2.27	
			78	268	3.44	0.08	2.24	
			84	224	2.67	0.07	1.61	
			58	117	2.02	0.08	1.72	
			79	240	3.04	0.08	1.56	
			49	110	2.24	0.07	1.57	
			71	155	2.18	0.06	1.69	
			69	187	2.71	0.08	2.12	
			107	966	9.03	0.18	4.42	
			86	353	4.10	0.13	2.40	
			96	589	6.14	0.14	3.02	
			98	629	6.42	0.18	2.35	
			78	375	4.81	0.15	2.39	
			113	832	7.36	0.17	2.38	
López-Rodríguez et al. (2012)	Spain	Arroyo de las Perdices tributary	5	5	1.00	0.20		Intermittent streams
			2	3	1.50	0.75		
			2	2	1.00	0.50		
Mor et al. (2018)	Spain	Montsant River	41	170	4.15	0.10	2.30	Upstream of dam
			59	283	4.80	0.08	3.90	Downstream
			88	434	4.93	0.06	2.80	Downstream
			59	322	5.46	0.09	2.70	Downstream
Sánchez-Hernández (2016)	Spain	River Tormes	54	341	6.31	0.12	2.19	Different *Salmo trutta* ages
			54	346	6.41	0.12	2.20	
			54	341	6.31	0.12	2.24	

Table A5.3 – continued

Reference	Country	River	*S*	*L*	*L/S*	*C*	MCL	Notes
Vannucchi et al. (2017)	Spain	Cacín stream	27	64	2.37	0.09	1.70	November
			23	64	2.78	0.12	1.61	December
			19	52	2.74	0.14	1.74	January
			20	56	2.80	0.14	1.65	February
			24	73	3.04	0.13	1.67	March
			16	47	2.94	0.18	1.63	April
			26	83	3.19	0.12	1.69	May
			23	68	2.96	0.13	1.74	June
			25	75	3.00	0.12	1.72	July
			18	52	2.89	0.16	1.61	August
			27	77	2.85	0.11	1.71	September
			26	74	2.85	0.11	1.73	October
Baumgartner and Robinson (2017)	Switzerland	Mönchaltorfer Aa catchment	18	136	5.72	0.24		Influenced by a waste water treatment facility
			11	59	3.52	0.21		
			11	61	3.48	0.20		
Brown et al. (2011)	UK	Mill stream	61	320	5.25	0.09	2.09	Stream side mesocosms
	UK	Mill stream	71	390	5.49	0.08	2.06	
	UK	Mill stream	67	492	7.34	0.11	2.13	
	UK	Mill stream	68	437	6.43	0.09	2.16	
Hildrew et al. (1985)	UK	Broadstone stream	24	90	3.75	0.16		
Lancaster and Robertson (1995)	UK	Broadstone stream	35	122	3.49	0.11		
Layer et al. (2010)	UK	Multiple streams across UK	23	137	5.96	0.26		Streams along a pH gradient
			24	159	6.63	0.28		
			30	187	6.23	0.21		
			44	427	9.70	0.22		
			25	136	5.44	0.22		
			25	178	7.12	0.28		
			24	135	5.63	0.23		
			22	94	4.20	0.19		
			21	99	4.71	0.22		
			19	71	3.74	0.20		
			21	108	5.14	0.24		
			22	56	2.55	0.12		
			61	759	12.44	0.20		
			35	285	8.14	0.23		
			29	194	6.69	0.23		
			40	335	8.38	0.21		
			20	114	5.70	0.29		
			44	384	8.73	0.20		
			66	940	14.24	0.22		
			87	1653	19.00	0.22		
Ledger et al. (2013)	UK	Stream side mesocosm	61	376	5.96	0.09	1.49	Control
			48	248	4.94	0.10	1.09	Drought
Mathews (1993)	UK	River Thames	10	18	1.80	0.20		
Woodward and Hildrew (2001)	UK	Broadstone stream	24	109	4.50	0.19	4.91	Pre- and post-*Cordulegaster boltonii* invasion
			25	128	5.10	0.21	5.33	
			33	146	4.40	0.13	4.88	
			34	170	5.00	0.15	5.38	
Schmid-Araya et al. (2002)	UK	Broadstone stream	85	378	4.45	0.05		August
			86	352	4.09	0.05		November
			70	297	4.24	0.06		February
			54	229	4.24	0.08		May
			128	271	5.63	0.04		Composite

Table A5.3 – continued

Reference	Country	River	*S*	*L*	*L/S*	*C*	MCL	Notes
Schmid-Araya et al. (2016)	UK	River Lambourn	113	540	4.78	0.04	2.72	Spring
			133	824	6.20	0.05	2.89	Summer
Woodward et al. (2008)	UK	Bere stream	142	1383	9.70	0.07		
Woodward et al. (2010)	UK	Tadnoll Brook	59	170	2.88	0.05		
		Afon Hirnant	33	112	3.39	0.10		
Hernandez and Sukhdeo (2008)	USA	Muskingham Brook	46	146	3.17	0.08		Fall 2002
			39	126	3.23	0.10		Winter 2003
			48	171	3.56	0.09		Spring 2003
			42	120	2.86	0.08		Summer 2003
			39	127	3.26	0.10		Fall 2003
			33	97	2.94	0.11		Winter 2004
			48	159	3.31	0.10		Spring 2004
			38	116	3.05	0.11		Summer 2004
Parker and Huryn (2006)	USA	Alaska	33	93	2.82	0.17	2.98	Spring (spring)
			31	99	3.19	0.19	3.10	Spring (summer)
			28	79	2.82	0.19	2.01	Mountain stream (spring)
			28	81	2.89	0.21	1.65	Mountain stream (summer)
Parker and Huryn (2013)	USA (Alaska)	Gates	15	18	1.20	0.40	1.76	*
		Ribdon tributary	10	13	1.30	0.43	1.58	*
		Sagavanirktok tributary	21	40	1.90	0.24	1.15	*
		Echooka tributary	63	156	2.48	0.06	1.99	
		Holden Creek	43	88	2.05	0.08	1.87	
		Ivishak tributary	38	109	2.87	0.13	1.70	
		Trevor Creek	38	81	2.13	0.11	1.83	
		Cobblestone spring	47	124	2.64	0.09	1.93	
		Echooka spring	48	163	3.40	0.12	2.15	
		Ivishak spring	50	230	4.60	0.16	3.22	
		Ribdon True spring	55	193	3.51	0.11	2.13	
		Lower Kuparuk spring	63	271	4.30	0.11	1.81	
		Lower Toolik spring	44	219	4.98	0.24	1.20	
		May spring	50	148	2.96	0.10	1.90	
		Upper Kuparuk spring	39	165	4.23	0.24	1.17	
		Dan Creek	63	134	2.13	0.05	1.64	
		Hershey Creek	45	152	3.38	0.15	1.54	
		Oksrukuyik Creek	59	183	3.10	0.08	1.82	
		Upper Kuparuk River	52	184	3.54	0.12	2.09	
Thompson and Townsend (2003)	USA (Maine, North Carolina)	Troy	78	181	2.32	0.07	1.95	Forest streams
		Martins	105	343	3.27	0.07	3.13	
		Herlzler	71	148	2.08	0.08	1.52	
		Cooper	58	126	2.17	0.08	2.04	

References for Table A5.3

Baumgartner, S. D. and Robinson, C. T. 2017. Changes in macroinvertebrate trophic structure along a land-use gradient within a lowland stream network. *Aquatic Sciences.* **79**(2), pp. 407-418.

Brown, L. E., Edwards, F. K., Milner, A. M., Woodward, G. and Ledger, M. 2011. Food web complexity and allometric scaling relationships in stream mesocosms: implications for experimentation. *Journal of Animal Ecology.* **80**, pp. 884-895.

Canning, A. D., Death, R. G. and Gardner, E. M. 2018. The effects of forest canopy and flood disturbance on New Zealand stream food web structure and robustness. *Austral Ecology.* **43**(3), pp. 352-358.

Ceneviva-Bastos, M. and Casatti, L. 2014. Shading effects on community composition and food web structure of a deforested pasture stream: Evidences from a field experiment in Brazil. *Limnologica*. **46**, pp. 9-21.

Ceneviva-Bastos, M., Montaña, C. G., Schalk, C. M., Camargo, P. B. and Casatti, L. 2017. Responses of aquatic food webs to the addition of structural complexity and basal resource diversity in degraded Neotropical streams. *Austral Ecology*. **42**(8), pp. 908-919.

Clitherow, L. R., Carrivick, J. L. and Brown, L. E. 2013. Food web structure in a harsh glacier-fed river. *PLoS ONE.* **8**(4).

Docile, T., Rosa, D. C., Figueiró, R. and Nessimian, J. 2016. Urbanisation alters the flow of energy through stream food webs. *Insect Conservation and Diversity*. **9**(5), pp. 416-426.

Hernandez, A. D. and Sukhdeo, M. V. K. 2008. Parasites alter the topology of a stream food web across seasons. *Oecologia.* **156**(3), pp, 613-624.

Hildrew, A. G., Townsend, C. R. and Hasham, A. 1985. The predatory Chironomidae of an iron-rich stream: feeding ecology and food web structure. *Ecological Entomology.* **10**(4), pp. 403-413.

Jaarsma, N. G., De Boer, S. M., Townsend, C. R., Thompson, R. M. and Edwards, E. D. 1998. Characterising food-webs in two New Zealand streams. *New Zealand Journal of Marine and Freshwater Research.* **32**(2), pp. 271-286.

Lancaster, J. and Robertson, A. L. 1995. Microcrustacean prey and macroinvertebrate predators in a stream food web. *Freshwater Biology.* **34**(1), pp. 123-134.

Lavandier, P. and Décamps, H. 1983. Un torrent d'altitude dans les Pyrénées: L'Estaragne. In: Lamotte, M. and Bourlière, F. (eds.). *Ecosystèmes Limniques*. Paris: Masson, pp. 81–111.

Layer, K., Riede, J. O., Hildrew, A. G. and Woodward, G. 2010. Food web structure and stability in 20 streams across a wide pH gradient. *Advances in Ecological Research.* **42**, pp. 265-299.

Ledger, M. E., Brown, L. E., Edwards, F. K., Hudson, L. N., Milner, A. M. and Woodward, G. 2013. Extreme climatic events alter aquatic food webs: a synthesis of evidence from a mesocosm drought experiment. *Advances in Ecological Research.* **48**, pp. 343-395.

López-Rodríguez, M. J., Peralta-Maraver, I., Geatani, B., Sainz-Cantero, C. E., Fochetti, R. and Tierno de Figueroa, J. M. 2012. Diversity patterns and food web structure in a

Mediterranean intermittent stream. *International Review of Hydrobiology.* **97**(6), pp. 485-496.

Mantel, S. K., Salas, M. and Dudgeon, D. 2004. Foodweb structure in a tropical Asian forest stream. *Freshwater Science*. **23**(4), pp. 728-755.

Mathews, C. P. 1993. Productivity and energy flows at all trophic levels in the River Thames, England: Mark 2. In: Christensen, V and Pauly, D. (eds.). *Trophic Models of Aquatic Ecosystems*. ICLARM Conference Proceedings No 26, pp. 161-171.

Meyer, E. I. and Poepperl, R. 2004. Assessing food-web structure, matter fluxes, and system attributes of a Central European mountain stream by performing mass-balanced network analysis. *Canadian Journal of Fisheries and Aquatic Sciences.* **61**(9), pp. 1565-1581.

Mor, R., Ruhí, A., Tornés, E., Valcárcel, H., Muñoz, I. and Sabater, S. 2018. Dam regulation and riverine food-web structure in a Mediterranean river. *Science of The Total Environment.* **625**, pp. 301-310.

Motta, R. L. and Uieda, V. S. 2005. Food web structure in a tropical stream ecosystem. *Austral Ecology.* **30**(1), pp. 58-73.

Parker, S. M. and Huryn, A. D. 2006. Food web structure and function in two Arctic streams with contrasting disturbance regimes. *Freshwater Biology.* **51**(7), pp. 1249-1263.

Parker, S. M. and Huryn, A. D. 2013. Disturbance and productivity as codeterminants of stream food web complexity in the Arctic. *Limnology and Oceanography.* **58**(6), pp. 2158-2170.

Poepperl, R. 2003. A quantitative food web model for the macroinvertebrate community of a northern German lowland stream. *International Review of Hydrobiology*. **88**(5), pp. 433-452.

Sánchez-Hernández, J. 2016. Do age-related changes in feeding habits of brown trout alter structural properties of food webs? *Aquatic Ecology.* **50**(4), pp. 685-695.

Schmid-Araya, J. M., Hildrew, A. G., Robertson, A., Schmid, P. E. and Winterbottom, J. 2002. The importance of meiofauna in food webs: evidence from an acid stream. *Ecology.* **83**(8), pp. 1271-1285.

Schmid-Araya, J. M., Schmid, P. E., Tod, S. P. and Esteban, G. F. 2016. Trophic positioning of meiofauna revealed by stable isotopes and food web analyses. *Ecology.* **97**(11), pp. 3099-3109.

Tamaris-Turizo, C. E., Pinilla-A, G. A. and Muñoz, I. 2018. Trophic network of aquatic macroinvertebrates along an altitudinal gradient in a Neotropical mountain river. *Revista Brasileira de Entomologia*. **62**(3), pp. 180-187.

Tavares-Cromar, A. F. and Williams, D. D. 1996. The importance of temporal resolution in food web analysis: Evidence from a detritus-based stream. *Ecological Monographs*. **66**(1), pp. 91-113.

Thompson, R. M. and Townsend, C. R. 2003. Impacts on stream food webs of native and exotic forest: An intercontinental comparison. *Ecology*. **84**(1), pp. 145-161.

Thompson, R. M. and Townsend, C. R. 2004. Land-use influences on New Zealand stream communities: Effects on species composition, functional organisation, and food-web structure. *New Zealand Journal of Marine and Freshwater Research.* **38**(4), pp. 595-608.

Thompson, R. M. and Townsend, C. R. 2005. Energy availability, spatial heterogeneity and ecosystem size predict food-web structure in streams. *Oikos.* **108**(1), pp. 137-148.

Townsend, C. R., Thompson, R. M., McIntosh, A. R., Kilroy, C., Edwards, E. and Scarsbrook, M. R. 1998. Disturbance, resource supply, and food-web architecture in streams. *Ecology Letters.* **1**, pp. 200-209.

Vannucchi, P. E., Peralta-Maraver, I., Tierno de Figueroa, J. M. and López-Rodríguez, M. J. 2017. Dynamics of the macroinvertebrate community and food web of a Mediterranean stream. *Journal of Freshwater Ecology.* **32**(1), pp. 229-245.

Woodward, G. and Hildrew, A. G. 2001. Invasion of a stream food web by a new top predator. *Journal of Animal Ecology.* **70**(2), pp. 273-288.

Woodward, G., Papantoniou, G., Edwards, F. and Lauridsen, R. B. 2008. Trophic trickles and cascades in a complex food web: impacts of a keystone predator on stream community structure and ecosystem processes. *Oikos.* **117**(5), pp. 683-692.

Woodward, G., Blanchard, J., Lauridsen, R. B., Edwards, F. K., Jones, I., Figueroa, S., Warren, P. H. and Petchey, O. L. 2010. Individual-based food webs: species identity, body size and sampling effects. *Advances in Ecological Research.* **43**, pp. 211-266.

Appendix 5.4: Quantitative representations of glacier influence

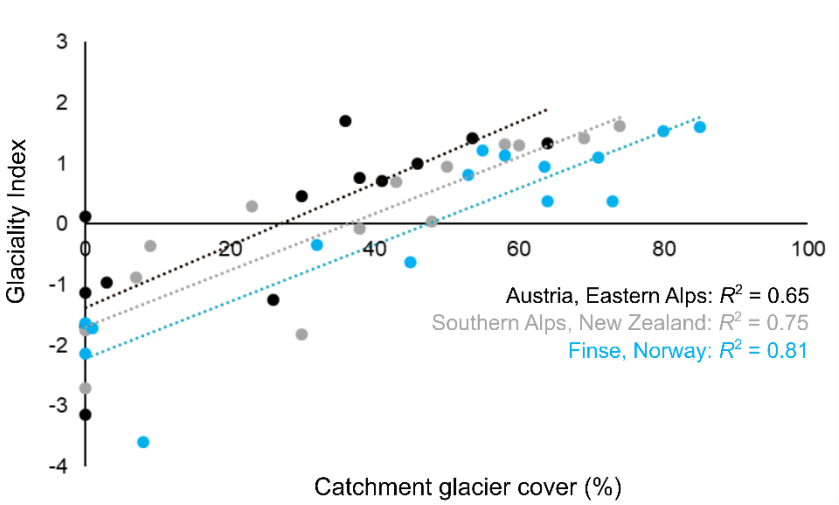

Figure A5.4 Significant linear relationships between the percentage of catchments covered permanently by glacier ice and a multivariate glaciality index (Ilg and Castella, 2006). Glacier cover was calculated remotely using the watershed analysis tools of ArcGIS. Calculation of the glaciality index followed Ilg and Castella (2006) and captured the intensity of ice melt influence in-situ by assessing the harshness of site physicochemical variables (water temperature, Pfankuch Index (Pfankuch, 1975), optical turbidity and electrical conductivity). More positive values represent greater glacial influence. Sites influenced by upstream proglacial lake flow were removed from this comparison as these inputs can disconnect glacier cover from predicted glacial influence.

Appendix: References

Banašek-Richter, C., Cattin, M.F. and Bersier, L.F. 2004. Sampling effects and the robustness of quantitative and qualitative food-web descriptors. *Journal of Theoretical Biology*. **226**(1), pp. 23–32.

Cohen, J. E., Schittler, D. N., Raffaelli, D. G. and Reuman, D. C. 2009. Food webs are more than the sum of their tritrophic parts. *Proceedings of the National Academy of Sciences of the United States of America*. **106**(22), pp. 335–340.

Comité European de Normalisation (CEN). 2015. *Water Quality - Guidance on the Estimation of Phytoplankton Biovolume, EN 16695, 2015*. Geneva: Comité European de Normalisation.

Csardi, G. and Nepusz, T. 2006. *The igraph Software Package for Complex Network Research*. [Online]. [Accessed 18 March 2019]. Available from: https://pdfs.semanticscholar.org/1d27/44b 83519657f5f2610698a8ddd177ced4f5c.pdf

Hudson, L. N., Reuman, D. and Emerson, R. 2016. *cheddar: Analysis and Visualisation of Ecological Communities. R Package Version 0.1 - 631.* [Online]. [Accessed 12 November 2018]. Available from: https://cran.r-project.org/package=cheddar

Ilg, C. and Castella, E. 2006. Patterns of macroinvertebrate traits along three glacial stream continuums. *Freshwater Biology*. **51**(5), pp. 840–853.

Menden-Deuer, S. and Lessard, E. J. 2000. Carbon to volume relationships for dinoflagellates, diatoms, and other protist plankton. *Limnology and Oceanography*. **45**(3), pp. 569–579.

Nolte, U. 1990. Chironomid biomass determination from larval shape. *Freshwater Biology*. **24**(3), pp. 443–451.

Pfankuch, D. J. 1975. *Stream Reach Inventory and Channel Stability Evaluation.* Northern Region, Montana: US Department Forest Service.

Smock, L. A. 1980. Relationships between body size and biomass of aquatic insects. *Freshwater Biology*. **10**(4), pp. 375–383.

Sun, J. and Lui, S. 2003. Geometric models for calculating cell biovolume and surface area for phytoplankton. *Journal of Plankton Research*. **25**(11), pp. 1331–1346.

Tiegs, S. D., Costello, D. M., Isken, M. W., Woodward, G., McIntyre, P. B., Gessner, M. O., Chauvet, E., Griffiths, N. A., Flecker, A. S., Acuña, V., Albariño, A., Allen, D. C., Alonso, C., Andino, P., Arango, C., Aroviita, J., Barbosa, M. V. M., Barmuta, L. A., Baxter, C., Bell, T. D. C., Bellinger, B., Boyero, L., Brown, L. E., Bruder, A., Bruesewitz, D. A., Burdon, F. J., Callisto, M., Canhoto, C., Capps, K. A., Castillo, M. M., Clapcott, J., Colas, F., Colón-Gaud, C., Cornut, J., Crespo-Pérez, V., Cross, W. F., Culp, J. M., Danger, M., Dangles, O., De Eyto, E., Derry, A. M., Díaz Villanueva, V., Douglas, M. M., Elosegi, A., Encalada, A. C., Entrekin, S., Espinosa, R., Ethaiya, D., Ferreira, V., Ferriol, C., Flanagan, K. M., Fleituch, T., Follstad Shah, J. J., Frainer, A., Friberg, N., Frost, P. C., Garcia, E. A., García Lago, L., García Soto, P. E., Ghate, S., Giling, D. P., Gilmer, A., Gonçalves Jr, J., F., Gonzales, R. K., Graça, M. A. S., Grace, M., Grossart, H-P.,

Guérold, F., Gulis V., Hepp, L. U., Higgins, S., Hishi, T., Huddart, J., Hudson, J., Imberger, S., Iñiguez-Armijos, C., Iwata, T., Janetski, D. J., Jennings, E., Kirkwood, A. E., Koning, A. A., Kosten, S., Kuehn, K. A., Laudon, H., Leavitt, P. R., Lemes da Silva, A. L., Leroux, S. J., LeRoy, C. J., Lisi, P. J., MacKenzie, R., Marcarelli, A. M., Masese, F. O., McKie, B. G., Medeiros, A. O., Meissner, K., Miliša, M., Mishra, S., Miyake, Y., Moerke, A., Mombrikotb, S., Mooney, R., Moulton, T., Muotka, T., Negishi, J. N., Neres-Lima, V., Nieminen, M. L., Nimptsch, J., Ondruch, J., Paavola, R., Pardo, I., Patrick, C. J., Peeters, E. T. H. M., Pozo, J., Pringle, C., Prussian, A., Quenta, E., Quesada, A., Reid, B., Richardson, J. S., Rigosi, A., Rincón, J., Risnoveanu, G., Robinson, C. T., Rodríguez-Gallego, L., Royer, T. V., Rusak, J. A., Santamans, A. C., Selmeczy, G. B., Simiyu, G., Skuja, A., Smykla, J., Sponseller, R., Stoler, A., Swan, C. M., Szlag, D., Teixeira-de Mello, F., Tonkin, J. D., Uusheimo, S., Veach, A. M., Vilbaste, S., Vought, L. B. M., Wang, C-P., Webster, J. R., Wilson, P. B., Woelfl, S., Xenopoulos, M. A., Yates, A. G., Yoshimura, C., Yule, C. M., Zhang, Y. X. and Zwart, J. A. 2019. Global patterns and drivers of ecosystem functioning in rivers and riparian zones. *Science Advances*. **5**(1)

Wang, Y., Maumann, U., Wright, S. and Warton, D. 2018. *mvabund: Statistical Methods for Analysing Multivariate Abundance Data.* [Online]. [Accessed 2 November 2018]. Available from: https://cran.r-project.org/package=mvabund